MATHEMATICAL AND NUMERICAL MODELING OF FLUID–POROELASTIC STRUCTURE INTERACTION

by

Ilona Ambartsumyan

B.Sc., Moscow Institute of Physics and Technology, 2011

M.Sc., Moscow Institute of Physics and Technology, 2013

Submitted to the Graduate Faculty of

the Kenneth P. Dietrich School of Arts and Sciences in partial fulfillment

of the requirements for the degree of

Doctor of Philosophy

University of Pittsburgh

2018

UNIVERSITY OF PITTSBURGH

DIETRICH SCHOOL OF ARTS AND SCIENCES

This dissertation was presented

by

Ilona Ambartsumyan

It was defended on

March 27th 2018

and approved by

Prof. Ivan Yotov, Dept. of Mathematics, University of Pittsburgh

Prof. William Layton, Dept. of Mathematics, University of Pittsburgh

Prof. Michael Neilan, Dept. of Mathematics, University of Pittsburgh

Prof. Paolo Zunino, Dept. of Mathematics, Politecnico di Milano

Dissertation Director: Prof. Ivan Yotov, Dept. of Mathematics, University of Pittsburgh

MATHEMATICAL AND NUMERICAL MODELING OF FLUID–POROELASTIC STRUCTURE INTERACTION

Ilona Ambartsumyan, PhD

University of Pittsburgh, 2018

The focus of this thesis is on finite element computational models for solving the coupled problem arising in the interaction between a free fluid and a fluid in a poroelastic medium. We assume that the free fluid is governed by the Stokes equations, while the flow in the poroelastic medium is modeled using the Biot poroelasticity system. We further impose equilibrium and kinematic conditions along the interface between two regions. As we employ the mixed Darcy formulation, continuity of flux condition becomes of the essential type and we use a Lagrange multiplier method to impose weakly this condition.

The thesis consists of three major parts. First, we investigate a Lagrange multiplier method for the linear Stokes–Biot model under the assumption of Newtonian fluid. We perform a stability and error analysis for the semi-discrete continuous-in-time and the fully discrete formulations, that indicate optimal order of convergence. We proceed with performing a series of numerical experiments, designed to confirm the theoretical convergence rates and to study the applicability of the method to modeling physical phenomena and the sensitivity of the model with respect to its parameters.

In the second part, we present a nonlinear extension of the model, applicable to modeling non-Newtonian fluids. More precisely, we focus on the quasi-Newtonian fluids that exhibit a shear-thinning property. We establish existence and uniqueness of the solution of two alternative formulations of the proposed method in both fully continuous and semi-discrete continuous-in-time settings, and derive the error bounds for the formulation that appears more appealing from the computational point of view. We conclude with numerical tests,

verifying theoretical findings and illustrating behavior of the method.

Lastly, we discuss coupling of the Stokes–Biot model with an advection–diffusion equation for modeling transport of chemical species within the fluid, which we discretize using the non-symmetric interior penalty Galerkin method. We discuss the stability and convergence properties of the scheme, and provide extensive numerical studies showing applicability of the method to modeling fluid flow in an irregularly shaped fractured reservoir with physical parameters.

Keywords: numerical methods, mixed finite element methods, FPSI, Stokes–Biot model, quasi-Newtonian fluids, coupled flow and transport, discontinuous Galerkin methods, NIPG.

TABLE OF CONTENTS

LIST OF TABLES

LIST OF FIGURES

ACKNOWLEDGEMENTS

First of all, I would like to deeply thank my advisor, Dr. Ivan Yotov, for his support and guidance throughout my PhD studies, and for giving me an opportunity to work on so many challenging and always interesting research projects.

I would also like to express my gratitude to Dr. Michael Neilan and Dr. William Layton for everything I've learned from their great courses and for serving in my thesis committee.

Big thank you to Dr. Paolo Zunino for his valuable suggestions and patience, and also for being a member of my thesis committee. I thank Dr. Jan Nordbotten, Dr. Vince Ervin and Dr. John Lee for their insights, feedbacks and comments. I want to also thank ChangQing Wang and Weitse Boon for the help and ideas in the projects we shared.

A very special thanks to Eldar without whom this work would have never been done. Finally I thank my parents who always believed in me and supported my decisions.

1.0 INTRODUCTION

1.1 MOTIVATION AND OVERVIEW OF EXISTING METHODS

In this work we develop methods and tools to model processes involving the interaction of a free incompressible viscous Newtonian fluid with a fluid within a poroelastic medium. This is a challenging multiphysics problem with applications to predicting and controlling processes arising in groundwater flow in fractured aquifers, oil and gas extraction, arterial flows, and industrial filters. In these applications, it is important to model properly the interaction between the free fluid with the fluid within the porous medium, and to take into account the effect of the deformation of the medium. For example, geomechanical effects play an important role in hydraulic fracturing, as well as in modeling phenomena such as subsidence and compaction.

The free fluid region can be modeled by the Stokes or the Navier-Stokes equations, while the flow through the deformable porous medium is modeled by the quasi-static Biot system of poroelasticity [13]. The two regions are coupled via dynamic and kinematic interface conditions, including balance of forces, continuity of normal velocity, and a no slip or slip with friction tangential velocity condition. These multiphysics models exhibit features of coupled Stokes-Darcy flows and fluid-structure interaction (FSI). There is extensive literature on modeling these separate couplings, see e.g. [39, 54, 64, 82, 94, 96] for Stokes-Darcy flows and [9, 11, 22, 46, 51, 78] for FSI. More recently there has been growing interest in modeling Stokes-Biot couplings, which can be referred to as fluid-poroelastic structure interaction (FPSI). The well-posedness of the mathematical model based on the Stokes-Biot system for the coupling between a fluid and a poroelastic structure is studied in [87]. A numerical study of the problem, using the Navier-Stokes equations for the fluid, is presented in [7], utilizing a

variational multiscale approach to stabilize the finite element spaces. The problem is solved using both a monolithic and a partitioned approach, with the latter requiring subiterations between the two problems. The reader is also referred to [20], where a non-iterative operator-splitting method for a coupled Navier-Stokes-Biot model is developed.

An alternative partitioned approach for the coupled Stokes-Biot problem based on the Nitsche's method is developed in [19]. The resulting method is loosely coupled and non-iterative with conditional stability. Unlike the method in [20], which is suitable for the pressure formulation of Darcy flow, the Nitsche's method can handle the mixed Darcy formulation. It does, however, suffer from a reduced convergence, due to the splitting across the interface. This is typical for Nitsche's splittings, see e.g. [23] for modeling of FSI. Possible approaches to alleviate this problem include iterative correction [24] and the use of the split method as a preconditioner for the monolithic scheme [19].

In applications to flow in fractured poroelastic media, an alternative modeling approach is based on a reduced-dimension fracture model. We mention recent work using the Reynolds lubrication equation [56, 70] as well as an averaged Brinkman equation [21]. Earlier works that do not account for elastic deformation of the media include averaged Darcy models [32,47,49,68,71], Forchheimer models [48], and Brinkman models [66], as well as an averaged Stokes flow that results in a Brinkman model for the fracture flow [72].

In this work we focus on the monolithic scheme for the full-dimensional Stokes-Biot problem with the approximation of the continuity of normal velocity condition through the use of a Lagrange multiplier. We consider the mixed formulation for Darcy flow in the Biot system, which provides a locally mass conservative flow approximation and an accurate Darcy velocity. However, this formulation results in the continuity of normal velocity condition being of essential type, which requires weak enforcement through either a penalty or a Lagrange multiplier formulation. Here we study the latter, as an alternative to the previously developed Nitsche formulation [19]. The advantage of the Lagrange multiplier method is that it does not involve a penalty parameter and it can enforce the continuity of normal velocity with machine precision accuracy on matching grids [2]. The method is also convergent on non-matching grids. After deriving a finite element based numerical approximation scheme for the Stokes-Biot problem, we provide a detailed theoretical analysis of stability and er-

ror estimates. A critical component of the analysis is the construction of a finite element interpolant into the space of velocities with weakly continuous normal components. This interpolant is shown to have optimal approximation properties, even for grids that do not match across the interface. The numerical tests confirm the theoretical convergence rates and illustrate that the method is applicable for simulating real world phenomena with a wide range of realistic physical parameters.

An additional advantage of the Lagrange multiplier formulation is that it is suitable for efficient parallel domain decomposition algorithms for the solution of the coupled problem, via its reduction to an interface problem, see, e.g. [94] for the Stokes-Darcy problem. It can also lead to multiscale approximations through the use of a coarse-scale Lagrange multiplier or mortar space [3, 53, 55].

We discuss the Stokes–Biot model in details in Chapter 2, which is organized as follows. In Section 2.1 we derive the weak formulation for the Stokes-Biot model. Section 2.2 is devoted to the semi-discrete continuous-in-time numerical scheme and the uniqueness and existence of its solution, as well as its stability and convergence analysis. A discussion of the fully discrete scheme is presented in Section 2.3. Finally, extensive numerical experiments are discussed in Section 2.4.

We note that in many applications the fluid exhibits properties that cannot be captured by a Newtonian fluid assumption. For instance, during water flooding in oil extraction, polymeric solutions are often added to the aqueous phase to increase its viscosity, resulting in a more stable displacement of oil by the injected water [67]. In hydraulic fracturing, proppant particles are mixed with polymers to maintain high permeability of the fractured media [65]. In blood flow simulations of small vessels or for patients with a cardiovascular disease, where the arterial geometry has been altered to include regions of recirculation, one needs to consider models that can capture the sheer-thinning property of the blood [62].

Motivated by such applications, we develop FPSI with non-Newtonian fluids, which, to the best of our knowledge, has not been studied in the literature. We focus on fluids that possess the sheer thinning property, i.e., the viscosity decreases under shear strain, which is typical for polymer solutions and blood. Viscosity models for such non-Newtonian fluids include the Power law, the Cross model and the Carreau model [28, 67, 75, 76]. The Power

law model is popular because it only contains two parameters, and it is possible to derive analytical solutions in various flow conditions [14]. On the other hand, it implies that in the flow region the viscosity goes to infinity if the deformation goes to zero, which may not be representative in certain applications and also significantly complicates the theoretical aspects of the problem. The Cross and Carreau models were deduced empirically as improvements of the Power law model. In both of these models the viscosity is strictly greater than zero and bounded, but knowledge of three parameters is required. We assume that the viscosity in each subdomain satisfies one such model, with dependence on the magnitude of the deformation tensor and the magnitude of Darcy velocity in the fluid and poroelastic regions, respectively. We further assume that along the interface the fluid viscosity is a function of the fluid and structure interface velocities.

Since we allow for unbounded viscosity models, such as the Power law, the analysis is performed in an appropriate Sobolev space setting, using spaces such as $W^{1,r}$, where $1 < r < 2$ is the viscosity shear thinning parameter. Nonlinear Stokes-Darcy models with bounded viscosity have been studied in [26, 40, 45], while the unbounded case is considered in [44]. The resulting weak formulation is a nonlinear time-dependent system, which is difficult to analyze, due to to the presence of the time derivative of the diplacement in some non-coercive terms. We consider an alternative mixed elasticity formulation with the structure velocity and elastic stress as primary variables, see also [87]. In this case we obtain a system with a degenerate evolution in time operator and a nonlinear saddle-point type spatial operator. The structure of the problem is similar to the one analyzed in [88], see also [16] in the linear case. However, the analysis in [88] is restricted to the Hilbert space setting and needs to be extended to the Sobolev space setting. Furthermore, the analysis in [88] is for monotone operators, see [89], and as a result requires certain right hand side terms to be zero, while in typical applications these terms may not be zero. Here we explore the coercivity of the operators to reformulate the problem as a parabolic-type system for the pressure and stress in the poroelastic region.

We present the analysis of the nonlinear Stokes–Biot model in Chapter 3. In Section 3.1 we describe the properties of quasi-Newtonian fluids that possess the shear–thinning property. Next, in Section 3.2 we state two weak formulations of the model and show

that both formulations are well-posed in Section 3.3. Section 3.4 presents the analysis for the semi-discrete continuous-in-time scheme. Numerical experiments, verifying convergence properties and illustrating the behavior of the method in the blood flow setting, are provided in Section 3.5.

Another topic of our interest is coupling FPSI with transport, as these are fundamental processes arising in many diversified fields such as petroleum engineering, groundwater hydrology, environmental engineering, soil mechanics, earth sciences, chemical and biomedical engineering. Realistic simulations for simultaneous flow, transport and chemical reaction present significant computational challenges. In particular, one area of applications includes simulating processes in subsurface waste repositories. This setting assumes a solid concrete matrix to seal the radioactive wastes underground, however, due to the erosion by water, acid solute or other undetermined elements during the long time periods as well as potential deformations the fractures are inevitable. This leads to necessity of consideration of how these radioactive wastes leak through the concrete matrix from these apertures since the convection in fractures is much faster than that in structure matrix. Other important applications include approximation to proppant modeling in hydraulic fracturing, groundwater contamination simulation and others.

For the modeling of transport, the discontinuous Galerkin (DG) methods [5,5,6,8,10,30, 31,33,74,80,81,91] are considered as being advantageous over the more conventional FEM methods for many attractive properties including local mass conservation, less numerical diffusion and more accurate local approximations for problems with rough and discontinuous coefficients. In addition to that, DG methods allow more general meshes with variable degrees of approximation, since the approximation spaces are localized on each element. This results in a substantially easier $h-p$ adaptive implementations for DG in comparison with the conventional approaches. The flexibility of the method also increases the efficiency in adaptivity, since the conformity of the mesh does not need to be maintained and, in turn, the unnecessary areas do not need to be refined. Furthermore, for time dependent problems, the non-conforming nature of DG allows for an easy and effective mesh modification dynamically with time [90], which is crucial for large transient problems involving a long period of simulation time, in particular, for problems where strong physics occurs in a small part of

the domain with a moving location.

Traditional algorithms for the coupled transport problem employ operator splitting to treat flow, advection, diffusion-dispersion and chemical reaction sequentially and separately. Characteristics methods [4,36] are popular for the advection-diffusion subproblem. While the operator splitting approach allows one to employ different algorithms to each subproblem as well as to implement complicated kinetics in a modular fashion [37,38], it can result in slow convergence and a loss of accuracy [37,38]. This brings our attention to the DG methods that have been applied for flow and transport problems in porous media [92]. Four versions of primal DG methods have been developed, namely, OBBDG (Oden-Babuska-Baumann [74] scheme), NIPG (non-symmetric interior penalty Galerkin) [81], SIPG (symmetric interior penalty Galerkin) [91, 95] and IIPG (incomplete interior penalty Galerkin) [35, 91], for solutions of flow and reactive transport problems. DG for miscible displacement has been investigated by numerical experiments and was reported to exhibit good numerical performance. However, to the best of our knowledge, the mathematical analysis on the convergence behavior of DG applied to coupled Stokes-Biot flow and transport problems has not been conducted. In this paper, we restrict ourselves to the primal DG method with interior penalty term (NIPG) for the transport equation.

Chapter 4 is devoted to the analysis of coupled FPSI–transport problem. We start by introducing the transport equation and its spacial discretization in Section 4.1 and Section 4.2. In Section 4.3 we discuss the stability and convergence properties of the method. Finally, Section 4.4 presents the convergence study and various numerical experiments, designed to study flow and concentration of the interested species in fractured poroelastic medium.

1.2 STOKES–BIOT MODEL PROBLEM

We consider a multiphysics model problem for free fluid's interaction with a flow in a deformable porous media, where the simulation domain $\Omega \subset \mathbf{R}^d$, $d = 2, 3$, is a union of non-overlapping regions Ω_f and Ω_p. Here Ω_f is a free fluid region with flow governed by the Stokes equations and Ω_p is a poroelastic material governed by the Biot system. For simplic-

ity of notation, we assume that each region is connected. The extension to non-connected regions is straightforward. Let $\Gamma_{fp} = \partial\Omega_f \cap \partial\Omega_p$. Let $(\mathbf{u}_\star, p_\star)$ be the velocity-pressure pair in $\Omega_\star$, $\star = f$, p, and let $\boldsymbol{\eta}_p$ be the displacement in Ω_p. Let $\nu > 0$ be the fluid viscosity, let $\mathbf{f}_\star$ be the body force terms, and let $q_\star$ be external source or sink terms. Let $\mathbf{D}(\mathbf{u}_f)$ and $\boldsymbol{\sigma}_f(\mathbf{u}_f, p_f)$ denote, respectively, the deformation rate tensor and the stress tensor:

$$\mathbf{D}(\mathbf{u}_f) = \frac{1}{2}(\nabla\mathbf{u}_f + \nabla\mathbf{u}_f^T), \qquad \boldsymbol{\sigma}_f(\mathbf{u}_f, p_f) = -p_f\mathbf{I} + 2\nu\mathbf{D}(\mathbf{u}_f). \tag{1.2.1}$$

In the free fluid region Ω_f, $(\mathbf{u}_f, p_f)$ satisfy the Stokes equations

$$-\nabla\cdot\boldsymbol{\sigma}_f(\mathbf{u}_f, p_f) = \mathbf{f}_f \quad \text{in } \Omega_f \times (0,T], \tag{1.2.2}$$

$$\nabla\cdot\mathbf{u}_f = q_f \quad \text{in } \Omega_f \times (0,T], \tag{1.2.3}$$

where $T > 0$ is the final time. Let $\boldsymbol{\sigma}_e(\boldsymbol{\eta}_p)$ and $\boldsymbol{\sigma}_p(\boldsymbol{\eta}_p, p_p)$ be the elastic and poroelastic stress tensors, respectively:

$$\boldsymbol{\sigma}_e(\boldsymbol{\eta}_p) = \lambda_p(\nabla\cdot\boldsymbol{\eta}_p)\mathbf{I} + 2\mu_p\mathbf{D}(\boldsymbol{\eta}_p), \qquad \boldsymbol{\sigma}_p(\boldsymbol{\eta}_p, p_p) = \boldsymbol{\sigma}_e(\boldsymbol{\eta}_p) - \alpha p_p\mathbf{I}, \tag{1.2.4}$$

where $0 < \lambda_{min} \le \lambda_p(\mathbf{x}) \le \lambda_{max}$ and $0 < \mu_{min} \le \mu_p(\mathbf{x}) \le \mu_{max}$ are the Lamé parameters and $0 \le \alpha \le 1$ is the Biot-Willis constant. The poroelasticity region Ω_p is governed by the quasi-static Biot system [13]

$$-\nabla\cdot\boldsymbol{\sigma}_p(\boldsymbol{\eta}_p, p_p) = \mathbf{f}_p, \quad \nu K^{-1}\mathbf{u}_p + \nabla p_p = 0, \qquad \text{in } \Omega_p \times (0,T], \tag{1.2.5}$$

$$\frac{\partial}{\partial t}\left(s_0 p_p + \alpha\nabla\cdot\boldsymbol{\eta}_p\right) + \nabla\cdot\mathbf{u}_p = q_p \qquad \text{in } \Omega_p \times (0,T], \tag{1.2.6}$$

where $s_0 \ge 0$ is a storage coefficient and K the symmetric and uniformly positive definite rock permeability tensor, satisfying, for some constants $0 < k_{min} \le k_{max}$,

$$\forall\,\boldsymbol{\xi} \in \mathbf{R}^d,\ k_{min}\boldsymbol{\xi}^T\boldsymbol{\xi} \le \boldsymbol{\xi}^T K(\mathbf{x})\boldsymbol{\xi} \le k_{max}\boldsymbol{\xi}^T\boldsymbol{\xi},\ \forall\,\mathbf{x} \in \Omega_p.$$

Following [7,87], the *interface conditions* on the fluid-poroelasticity interface Γ_{fp} are *mass conservation*, *balance of stresses*, and the Beavers-Joseph-Saffman (BJS) condition [12, 83] modeling *slip with friction*:

$$\mathbf{u}_f\cdot\mathbf{n}_f + \left(\frac{\partial\boldsymbol{\eta}_p}{\partial t} + \mathbf{u}_p\right)\cdot\mathbf{n}_p = 0, \qquad \text{on } \Gamma_{fp} \times (0,T], \tag{1.2.7}$$

$$-(\boldsymbol{\sigma}_f \mathbf{n}_f)\cdot\mathbf{n}_f = p_p, \qquad \boldsymbol{\sigma}_f\mathbf{n}_f + \boldsymbol{\sigma}_p\mathbf{n}_p = 0, \qquad \text{on } \Gamma_{fp}\times(0,T], \tag{1.2.8}$$

$$-(\boldsymbol{\sigma}_f \mathbf{n}_f)\cdot\mathbf{t}_{f,j} = \nu\alpha_{BJS}\sqrt{K_j^{-1}}\left(\mathbf{u}_f - \frac{\partial\boldsymbol{\eta}_p}{\partial t}\right)\cdot\mathbf{t}_{f,j}, \qquad \text{on } \Gamma_{fp}\times(0,T], \tag{1.2.9}$$

where $\mathbf{n}_f$ and $\mathbf{n}_p$ are the outward unit normal vectors to $\partial\Omega_f$, and $\partial\Omega_p$, respectively, $\boldsymbol{\tau}_{f,j}$, $1\le j\le d-1$, is an orthogonal system of unit tangent vectors on Γ_{fp}, $K_j = (K\mathbf{t}_{f,j})\cdot\mathbf{t}_{f,j}$, and $\alpha_{BJS}\ge 0$ is an experimentally determined friction coefficient. We note that the continuity of flux constrains the normal velocity of the solid skeleton, while the BJS condition accounts for its tangential velocity. The first equation in (1.2.8), along with the definition of $\boldsymbol{\sigma}_f$ in (1.2.1), implies the jump in pressure condition

$$p_f - 2\mu(\mathbf{D}(\mathbf{u}_f)\mathbf{n}_f)\cdot\mathbf{n}_f = p_p. \tag{1.2.10}$$

We note that a different pressure jump condition is obtained in [25,61] using asymptotic analysis.

The above system of equations needs to be complemented by a set of boundary and initial conditions. Let $\Gamma_f = \partial\Omega_f\cap\partial\Omega$ and $\Gamma_p = \partial\Omega_p\cap\partial\Omega$. Let $\Gamma_p = \Gamma_p^D\cup\Gamma_p^N$. We assume for simplicity homogeneous boundary conditions:

$$\mathbf{u}_f = 0 \text{ on } \Gamma_f\times(0,T], \quad \boldsymbol{\eta}_p = 0 \text{ on } \Gamma_p\times(0,T],$$
$$p_p = 0 \text{ on } \Gamma_p^D\times(0,T], \quad \mathbf{u}_p\cdot\mathbf{n}_p = 0 \text{ on } \Gamma_p^N\times(0,T].$$

For the uniqueness purposes we either assume that $|\Gamma_p^D|>0$ or restrict the mean value of the pressure. We also assume that Γ_p^D is not adjacent to the interface Γ_{fp}, i.e., $\operatorname{dist}(\Gamma_p^D,\Gamma_{fp})\ge s>0$. Non-homogeneous displacement and velocity conditions can be handled in a standard way by adding suitable extensions of the boundary data. The pressure boundary condition is natural in the mixed Darcy formulation, so non-homogeneous pressure data would lead to an additional boundary term. We further set the initial conditions

$$p_p(\mathbf{x},0) = p_{p,0}(\mathbf{x}), \ \boldsymbol{\eta}_p(\mathbf{x},0) = \boldsymbol{\eta}_{p,0}(\mathbf{x}) \text{ in } \Omega_p.$$

1.3 PRELIMINARIES

1.3.1 Notations

Throughout the thesis, we make use of the usual notation for the Lebesgue spaces $L^p(S)$, $S \subset \mathbf{R}^d$, equipped with the norm

$$\|\phi\|^p_{L^p(S)} = \int_S \phi^p \, dA.$$

Similarly, we consider the Sobolev space $W^{k,p}(S)$ with the norm and the seminorm

$$\|\phi\|^p_{W^{k,p}(S)} = \sum_{|\alpha|\le k} \int_S |\partial^\alpha \phi|^p \, dA, \quad |\phi|^p_{W^{k,p}(S)} = \sum_{|\alpha|=k} \int_S |\partial^\alpha \phi|^p \, dA.$$

We further define the space of $(L^p(\Omega_p))^d$-vectors with divergence in $L^p(\Omega_p)$, $L^p(\mathrm{div}; S) = \left\{\phi \in (L^p(S))^d : \nabla \cdot \phi \in L^p(S)\right\}$, with the norm

$$\|\phi\|^p_{L^p(\mathrm{div};S)} = \int_S \left(|\phi|^p + |\nabla \cdot \phi|^p\right) \, dA.$$

We note that with $p = 2$, the above spaces reduce to $L^2(S)$, $H^k(S)$ and $H(\mathrm{div}; S)$, respectively. We denote by $W^{-k,p'}(S)$ the dual space of $W^{k,p}(S)$, where p' is the conjugate of p, i.e., $1/p + 1/p' = 1$. For $0 < p < 1$, the fractional order Sobolev space $W^{k,p}(\partial S)$ is equipped with the norm

$$\|\phi\|^p_{W^{k,p}(\partial S)} = \|\phi\|^p_{L^p(\partial S)} + |\phi|^p_{W^{k,p}(\partial S)}, \quad |\phi|^p_{W^{k,p}(\partial S)} = \int_{\partial S}\int_{\partial S} \frac{|\phi(t) - \phi(s)|^p}{|t-s|^{d-1+kp}} \, ds \, dt.$$

The $L^2(S)$ inner product is denoted by $(\cdot,\cdot)_S$ for scalar, vector and tensor valued functions. For a section of a subdomain boundary G we write $\langle \cdot, \cdot \rangle_G$ for the $L^2(G)$ inner product (or duality pairing). We also denote by C a generic positive constant independent of the discretization parameters, and abuse notation by denoting ϵ as an arbitrary constant with different values at different occurrences.

For a time-dependent function ϕ, we introduce the Bochner spaces equipped with norms:

$$\|\phi\|^p_{L^p(0,T;X)} := \int_0^T \|\phi(t)\|^p_X \, ds, \qquad \|\phi\|_{L^\infty(0,T;X)} := \text{ess sup}_{t\in[0,T]} \|\phi(t)\|_X$$

$$\|\phi\|_{W^{1,\infty}(0,T;X)} := \text{ess sup}_{t\in[0,T]} \{\|\phi(t)\|_X, \|\partial_t \phi(t)\|_X\}. \tag{1.3.1}$$

We will make use of the following well-known inequalities:

• (Hölder/Cauchy-Schwarz) For any $\phi \in L^p(S)$, $\psi \in L^{p'}(S)$,

$$\|\phi\,\psi\|_{L^1(S)} \leq \|\phi\|_{L^p(S)}\|\psi\|_{L^{p'}(S)}, \tag{1.3.2}$$

• (Trace) For any $\phi \in W^{1,p}(S)$,

$$\|\phi\|_{W^{1/p',p}(\partial S)} \leq C\|v\|_{W^{1,p}(S)}, \tag{1.3.3}$$

• (Korn's) For any $\phi \in W^{1,p}(S)$,

$$\|\mathbf{D}(\phi)\|_{L^p(S)} \geq C\|\phi\|_{W^{1,p}(S)}, \tag{1.3.4}$$

• (Poincare) For any $\phi \in W_0^{1,p}(S)$,

$$\|\phi\|_{L^p(S)} \leq C\|\nabla\phi\|_{L^p(S)}, \tag{1.3.5}$$

• (Young's) For any real numbers a, b and $\epsilon > 0$,

$$ab \leq \frac{\epsilon^p a^p}{p} + \frac{b^{p'}}{\epsilon^{p'}p'}, \tag{1.3.6}$$

• (Gronwall's) Let $g(t) \geq 0$ and $\phi(t) \leq f(t) + \int_s^t g(\tau)\phi(\tau)d\tau$, then

$$\phi(t) \leq f(t) + \int_s^t f(\tau)g(\tau)\exp\left(\int_\tau^t g(r)dr\right)d\tau. \tag{1.3.7}$$

• (Discrete Gronwall's) Let $\tau > 0$, $B \geq 0$, and let a_n, b_n, c_n, d_n, $n \geq 0$, be non-negative sequences such that $a_0 \leq B$ and

$$a_n + \tau\sum_{l=1}^{n} b_l \leq \tau\sum_{l=1}^{n-1} d_l a_l + \tau\sum_{l=1}^{n} c_l + B, \quad n \geq 1.$$

Then,

$$a_n + \tau\sum_{l=1}^{n} b_l \leq \exp(\tau\sum_{l=1}^{n-1} d_l)\left(\tau\sum_{l=1}^{n} c_l + B\right), \quad n \geq 1. \tag{1.3.8}$$

1.3.2 Discretization of Stokes–Darcy problem

We also recall several fundamental results related to the discretization of Stokes and Darcy problems. Consider a shape-regular and quasi-uniform partitions [29] of Ω_f, $\mathcal{T}_h^f$, consisting of affine elements with maximal element diameter h. For the discretization of Stokes velocity and pressure variables we choose finite element spaces, which are assumed to be LBB-stable:

$$\begin{cases} \mathbf{V}_{f,h} \subset (H^1(\Omega_f))^d,\ W_{f,h} \subset L^2(\Omega_f), \text{ and} \\ \inf_{0\neq w_{f,h}\in W_{f,h}} \sup_{0\neq \mathbf{v}_{f,h}\in \mathbf{V}_{f,h}} \frac{-(\nabla\cdot\mathbf{v}_{f,h}, w_{f,h})_{\Omega_f}}{\|\mathbf{v}_{f,h}\|_{H^1(\Omega_f)}\|w_{f,h}\|_{L^2(\Omega_f)}} \geq \beta_f > 0. \end{cases} \tag{1.3.9}$$

Examples of such spaces include the MINI elements, the Taylor-Hood elements and the conforming Crouzeix-Raviart elements, [15]. We assume that the spaces $\mathbf{V}_{f,h}$ and $W_{f,h}$ contain at least polynomials of degree k_f and s_f, respectively.

We recall that there exists the Scott-Zhang interpolant, $S_{s,h}$, satisfying [85]:

$$\|\mathbf{v}_f - S_{f,h}\mathbf{v}_f\|_{L^p(\Omega_f)} + h\|\nabla(\mathbf{v}_f - S_{f,h}\mathbf{v}_f)\|_{L^p(\Omega_f)} \leq Ch^{r_{k_f}}\|\mathbf{v}_f\|_{W^{r_{k_f},p}(\Omega_f)}, \quad 1 \leq r_{k_f} \leq k_f + 1. \tag{1.3.10}$$

For the discretization of the Darcy problem we choose $\mathbf{V}_{p,h} \subset \mathbf{V}_p$ and $W_{p,h} \subset W_p$ to be any of well-known inf-sup stable mixed finite element spaces, such as the Raviart-Thomas or the Brezzi-Douglas-Marini spaces, [15], satisfying

$$\begin{cases} \mathbf{V}_{p,h} \subset H(\mathrm{div};\Omega_p),\ W_{p,h} \subset L^2(\Omega_p), \text{ and} \\ \inf_{0\neq w_{p,h}\in W_{p,h}} \sup_{0\neq \mathbf{v}_{p,h}\in \mathbf{V}_{p,h}} \frac{-(\nabla\cdot\mathbf{v}_{p,h}, w_{p,h})_{\Omega_f}}{\|\mathbf{v}_{p,h}\|_{H(\mathrm{div};\Omega_p)}\|w_{p,h}\|_{L^2(\Omega_p)}} \geq \beta_p > 0. \end{cases} \tag{1.3.11}$$

We will use the MFE interpolant, $\Pi_{p,h}$, satisfying for any $\theta > 0$ and for all $\mathbf{v}_p \in \mathbf{V}_p \cap H^\theta(\Omega_p)$,

$$(\nabla\cdot\Pi_{p,h}\mathbf{v}_p, w_{p,h}) = (\nabla\cdot\mathbf{v}_p, w_{p,h}), \qquad \forall w_{p,h} \in W_{p,h}, \tag{1.3.12}$$

$$\langle \Pi_{p,h}\mathbf{v}_p\cdot\mathbf{n}_p, \mathbf{v}_{p,h}\cdot\mathbf{n}_p\rangle_{\Gamma_{fp}} = \langle \mathbf{v}_p\cdot\mathbf{n}_p, \mathbf{v}_{p,h}\cdot\mathbf{n}_p\rangle_{\Gamma_{fp}}, \qquad \forall \mathbf{v}_{p,h} \in \mathbf{V}_{p,h}. \tag{1.3.13}$$

The following bounds on $\Pi_{p,h}$ hold [1, 29, 42, 69]:

$$\|\mathbf{v}_p - \Pi_{p,h}\mathbf{v}_p\|_{L^p(\Omega_p)} \leq Ch^{r_{k_p}}\|\mathbf{v}_p\|_{W^{r_{k_p},p}(\Omega_p)}, \quad 1 \leq r_{k_p} \leq k_p + 1, \tag{1.3.14}$$

$$\|\Pi_{p,h}\mathbf{v}_p\|_{L^p(\Omega_p)} \leq C\left(\|\mathbf{v}_p\|_{L^r(\Omega_p)} + h\|\nabla\mathbf{v}_p\|_{L^r(\Omega_p)}\right). \tag{1.3.15}$$

For the pressure variables we use the L^2-projection operators onto $W_{f,h}$ and $W_{p,h}$, $Q_{f,h}$ and $Q_{p,h}$, respectively:

$$(p_f - Q_{f,h}p_f, w_{f,h})_{\Omega_f} = 0, \qquad \forall\, w_{f,h} \in W_{f,h} \tag{1.3.16}$$

$$(p_p - Q_{p,h}p_p, w_{p,h})_{\Omega_p} = 0, \qquad \forall\, w_{p,h} \in W_{p,h} \tag{1.3.17}$$

These operators satisfy the approximation properties [29]:

$$\|p_f - Q_{f,h}p_f\|_{L^p(\Omega_f)} \leq Ch^{r_{s_f}} \|p_f\|_{W^{r_{s_f},p}(\Omega_f)}, \quad 0 \leq r_{s_f} \leq s_f + 1, \tag{1.3.18}$$

$$\|p_p - Q_{p,h}p_p\|_{L^p(\Omega_p)} \leq Ch^{r_{s_p}} \|p_p\|_{W^{r_{s_p},p}(\Omega_p)}, \quad 0 \leq r_{s_p} \leq s_p + 1. \tag{1.3.19}$$

2.0 A LAGRANGE MULTIPLIER METHOD FOR A STOKES-BIOT FLUID-POROELASTIC STRUCTURE INTERACTION MODEL

2.1 WEAK FORMULATION FOR STOKES–BIOT MODEL PROBLEM

We first introduce the following spaces:

$$\begin{aligned} \mathbf{V}_f &= \{\mathbf{v}_f \in H^1(\Omega_f)^d : \mathbf{v}_f = 0 \text{ on } \Gamma_f\}, & W_f &= L^2(\Omega_f), \\ \mathbf{V}_p &= \{\mathbf{v}_p \in H(\mathrm{div};\Omega_p) : \mathbf{v}_p \cdot \mathbf{n}_p = 0 \text{ on } \Gamma_p^N\}, & W_p &= L^2(\Omega_p), \\ \mathbf{X}_p &= \{\boldsymbol{\xi}_p \in H^1(\Omega_p)^d : \boldsymbol{\xi}_p = 0 \text{ on } \Gamma_p\}. \end{aligned} \tag{2.1.1}$$

We define the global velocity and pressure spaces as

$$\mathbf{V} = \{\mathbf{v} = (\mathbf{v}_f, \mathbf{v}_p) \in \mathbf{V}_f \times \mathbf{V}_p\}, \quad W = \{w = (w_f, w_p) \in W_f \times W_p\},$$

with norms

$$\|\mathbf{v}\|_{\mathbf{V}}^2 = \|\mathbf{v}_f\|_{H^1(\Omega_f)}^2 + \|\mathbf{v}_p\|_{H(\mathrm{div};\Omega_p)}^2, \quad \|w\|_W^2 = \|w_f\|_{L^2(\Omega_f)}^2 + \|w_p\|_{L^2(\Omega_p)}^2.$$

The weak formulation is obtained by multiplying the equations in each region by suitable test functions, integrating by parts the second order terms in space, and utilizing the interface and boundary conditions. Let

$$\begin{aligned} a_f(\mathbf{u}_f, \mathbf{v}_f) &= (2\nu \mathbf{D}(\mathbf{u}_f), \mathbf{D}(\mathbf{v}_f))_{\Omega_f}, \\ a_p^d(\mathbf{u}_p, \mathbf{v}_p) &= (\nu K^{-1}\mathbf{u}_p, \mathbf{v}_p)_{\Omega_p}, \\ a_p^e(\boldsymbol{\eta}_p, \boldsymbol{\xi}_p) &= (2\mu_p \mathbf{D}(\boldsymbol{\eta}_p), \mathbf{D}(\boldsymbol{\xi}_p))_{\Omega_p} + (\lambda_p \nabla \cdot \boldsymbol{\eta}_p, \nabla \cdot \boldsymbol{\xi}_p)_{\Omega_p} \end{aligned}$$

be the bilinear forms related to Stokes, Darcy and the elasticity operators, respectively. Let

$$b_\star(\mathbf{v}, w) = -(\nabla \cdot \mathbf{v}, w)_{\Omega_\star}.$$

Multiplying both sides of (1.2.2) by $\mathbf{v}_f \in \mathbf{V}_f$ and integrating over Ω_f, we obtain

$$\begin{aligned}\int_{\Omega_f} \mathbf{f}_f \cdot \mathbf{v}_f dA &= -\int_{\Omega_f} (\nabla \cdot (-p_f \mathbf{I} + 2\nu \mathbf{D}(\mathbf{u}_f))) \cdot \mathbf{v}_f \, dA \\ &= \int_{\Omega_f} 2\nu \mathbf{D}(\mathbf{u}_f) : \mathbf{D}(\mathbf{v}_f) dA - \int_{\Omega_f} p_f \nabla \cdot \mathbf{v}_f dA - \int_{\Gamma_{fp}} (\boldsymbol{\sigma}_f(\mathbf{u}_f, p_f) \cdot \mathbf{n}_f) \cdot \mathbf{v}_f ds \\ &= a_f(\mathbf{u}_f, v_f) + b_f(\mathbf{v}_f, p_f) - \int_{\Gamma_{fp}} (\boldsymbol{\sigma}_f(\mathbf{u}_f, p_f) \cdot \mathbf{n}_f) \cdot \mathbf{v}_f ds. \end{aligned} \tag{2.1.2}$$

Similarly, from the first equation in (1.2.5) multiplying both sides by $\boldsymbol{\xi}_p \in \mathbf{X}_p$ and integrating over Ω_p we have

$$\begin{aligned}\int_{\Omega_p} \mathbf{f}_p \cdot \boldsymbol{\xi}_p dA &= -\int_{\Omega_p} (\nabla \cdot (\boldsymbol{\sigma}_e(\boldsymbol{\eta}_p) - \alpha p_p \mathbf{I})) \cdot \boldsymbol{\xi}_p dA = \int_{\Omega_p} \boldsymbol{\sigma}_e(\boldsymbol{\eta}_p) : \mathbf{D}(\boldsymbol{\xi}_p) dA \\ &- \int_{\Gamma_{fp}} (\boldsymbol{\sigma}_e(\boldsymbol{\eta}_p) \cdot \mathbf{n}_p) \cdot \boldsymbol{\xi}_p ds - \alpha \int_{\Omega_p} p_p (\nabla \cdot \boldsymbol{\xi}_p) dA + \alpha \int_{\Gamma_{fp}} p_p (\mathbf{n}_p \cdot \boldsymbol{\xi}_p) ds \\ &= a_p^e(\boldsymbol{\eta}_p, \boldsymbol{\xi}_p) + \alpha b_p(\boldsymbol{\xi}_p, p_p) - \int_{\Gamma_{fp}} (\boldsymbol{\sigma}_e(\boldsymbol{\eta}_p) \cdot \mathbf{n}_p) \cdot \boldsymbol{\xi}_p ds + \alpha \int_{\Gamma_{fp}} p_p (\mathbf{n}_p \cdot \boldsymbol{\xi}_p) ds \\ &= a_p^e(\boldsymbol{\eta}_p, \boldsymbol{\xi}_p) + \alpha b_p(\boldsymbol{\xi}_p, p_p) - \int_{\Gamma_{fp}} (\boldsymbol{\sigma}_p(\boldsymbol{\eta}_p, p_p) \cdot \mathbf{n}_p) \cdot \boldsymbol{\xi}_p ds, \end{aligned} \tag{2.1.3}$$

and from the second equation in (1.2.6) , multiplying both sides by $\mathbf{v}_p \in \mathbf{V}_p$ and integrating yields

$$\begin{aligned} 0 &= \int_{\Omega_p} \nu K^{-1} \mathbf{u}_p \cdot \mathbf{v}_p dA - \int_{\Omega_p} p_p (\nabla \cdot \mathbf{v}_p) dA + \int_{\Gamma_{fp}} p_p (\mathbf{n}_p \cdot \mathbf{v}_p) ds \\ &= a_p^d(\mathbf{u}_p, \mathbf{v}_p) + b_p(\mathbf{v}_p, p_p) + \int_{\Gamma_{fp}} p_p (\mathbf{n}_p \cdot \mathbf{v}_p) ds. \end{aligned} \tag{2.1.4}$$

Using the fact that $\{\mathbf{n}_f, \mathbf{t}_{f,j}, j = 1, ..., n-1\}$ forms an orthonormal basis on Γ_{fp}, the first condition in (1.2.8) and (1.2.9), we have

$$\begin{aligned}\int_{\Gamma_{fp}} (\boldsymbol{\sigma}_f(\mathbf{u}_f, p_f) \cdot \mathbf{n}_f) \cdot \mathbf{v}_f ds &= \int_{\Gamma_{fp}} ((\boldsymbol{\sigma}_f(\mathbf{u}_f, p_f) \cdot \mathbf{n}_f) \cdot \mathbf{n}_f)(\mathbf{n}_f \cdot \mathbf{v}_f) ds \\ &+ \sum_{j=1}^{n-1} \int_{\Gamma_{fp}} ((\boldsymbol{\sigma}_f(\mathbf{u}_f, p_f) \cdot \mathbf{n}_f) \cdot \mathbf{t}_{f,j})(\mathbf{t}_{f,j} \cdot \mathbf{v}_f) ds = -\int_{\Gamma_{fp}} p_p \mathbf{n}_f \cdot \mathbf{v}_f ds \end{aligned}$$

$$-\sum_{j=1}^{n-1}\int_{\Gamma_{fp}}(\nu\alpha_{BJS}\sqrt{K_j^{-1}}(\mathbf{u}_f-\partial_t\boldsymbol{\eta}_p)\cdot\mathbf{t}_{f,j})(\mathbf{t}_{f,j}\cdot\mathbf{v}_f)ds, \tag{2.1.5}$$

where we used the notation $\partial_t\cdot=\partial\cdot/\partial_t$. Similarly, we use the fact that $\mathbf{t}_{p,j}=-\mathbf{t}_{f,j}$, the second condition in (1.2.8) and (1.2.9) to obtain

$$\begin{aligned}\int_{\Gamma_{fp}}(\boldsymbol{\sigma}_p(\boldsymbol{\eta}_p,p_p)\cdot\mathbf{n}_p)\cdot\boldsymbol{\xi}_p ds=&-\int_{\Gamma_{fp}}p_p\mathbf{n}_p\cdot\boldsymbol{\xi}_p ds\\&-\sum_{j=1}^{n-1}\int_{\Gamma_{fp}}(\nu\alpha_{BJS}\sqrt{K_j^{-1}}(\mathbf{u}_f-\partial_t\boldsymbol{\eta}_p)\cdot\mathbf{t}_{f,j})(-\mathbf{t}_{f,j}\cdot\boldsymbol{\xi}_p)ds.\end{aligned} \tag{2.1.6}$$

Next, we add (2.1.2)–(2.1.4) and use (2.1.5)–(2.1.6) to write

$$\begin{aligned}&a_f(\mathbf{u}_f,\mathbf{v}_f)+a_p^d(\mathbf{u}_p,\mathbf{v}_p)+a_p^e(\boldsymbol{\eta}_p,\boldsymbol{\xi}_p)+a_{BJS}(\mathbf{u}_f,\partial_t\boldsymbol{\eta};\mathbf{v}_f,\boldsymbol{\xi}_p)\\&\quad+b_f(\mathbf{v}_f,p_f)+b_p(\mathbf{v}_p,p_p)+\alpha b_p(\boldsymbol{\xi}_p,p_p)+\int_{\Gamma_{fp}}p_p(\mathbf{n}_f\cdot\mathbf{v}_f+(\mathbf{v}_p+\boldsymbol{\xi}_p)\cdot\mathbf{n}_p)ds\\&\qquad=(\mathbf{f}_f,\mathbf{v}_f)_{\Omega_f}+(\mathbf{f}_p,\boldsymbol{\xi}_p)_{\Omega_p},\end{aligned} \tag{2.1.7}$$

where

$$a_{BJS}(\mathbf{u}_f,\partial_t\boldsymbol{\eta}_p;\mathbf{v}_f,\boldsymbol{\xi}_p)=\sum_{j=1}^{d-1}\left\langle\nu\alpha_{BJS}\sqrt{K_j^{-1}}(\mathbf{u}_f-\partial_t\boldsymbol{\eta}_p)\cdot\mathbf{t}_{f,j},(\mathbf{v}_f-\boldsymbol{\xi}_p)\cdot\mathbf{t}_{f,j}\right\rangle_{\Gamma_{fp}}.$$

Multiplying both sides of (1.2.3) and (1.2.6) with $w_f\in W_f$, $w_p\in W_p$ and integrating over Ω_f and Ω_p, respectively, and then adding them up, we get

$$\int_{\Omega_p}s_0\partial_t p_p w_p dA-\alpha b_p(\partial_t\boldsymbol{\eta}_p,w_p)-b_p(\mathbf{u}_p,w_p)-b_f(\mathbf{u}_f,w_f)=(q_p,w_p)_{\Omega_p}+(q_f,w_f)_{\Omega_f}. \tag{2.1.8}$$

In order to incorporate the mass conservation interface condition (1.2.7), we introduce a Lagrange multiplier

$$\lambda=-(\boldsymbol{\sigma}_f\mathbf{n}_f)\cdot\mathbf{n}_f=p_p\ \in\Lambda\text{ on }\Gamma_{fp}.$$

Then (2.1.7) reads

$$\begin{aligned}&a_f(\mathbf{u}_f,\mathbf{v}_f)+a_p^d(\mathbf{u}_p,\mathbf{v}_p)+a_p^e(\boldsymbol{\eta}_p,\boldsymbol{\xi}_p)+a_{BJS}(\mathbf{u}_f,\partial_t\boldsymbol{\eta};\mathbf{v}_f,\boldsymbol{\xi}_p)+b_f(\mathbf{v}_f,p_f)+b_p(\mathbf{v}_p,p_p)\\&\qquad+\alpha b_p(\boldsymbol{\xi}_p,p_p)+b_\Gamma(\mathbf{v}_f,\mathbf{v}_p,\boldsymbol{\xi}_p,\lambda)=(\mathbf{f}_f,\mathbf{v}_f)_{\Omega_f}+(\mathbf{f}_p,\boldsymbol{\xi}_p)_{\Omega_p},\end{aligned} \tag{2.1.9}$$

and (1.2.7) can be enforced as

$$b_\Gamma(\mathbf{u}_f, \partial_t \boldsymbol{\eta}_p, \mathbf{u}_p; \mu) = 0, \quad \forall \mu \in \Lambda, \tag{2.1.10}$$

where

$$b_\Gamma(\mathbf{v}_f, \mathbf{v}_p, \boldsymbol{\xi}_p; \mu) = \langle \mathbf{v}_f \cdot \mathbf{n}_f + (\boldsymbol{\xi}_p + \mathbf{v}_p) \cdot \mathbf{n}_p, \mu \rangle_{\Gamma_{fp}}.$$

For the well-posedness of b_Γ we require that $\lambda \in \Lambda = (\mathbf{V}_p \cdot \mathbf{n}_p|_{\Gamma_{fp}})'$. According to the normal trace theorem, since $\mathbf{v}_p \in \mathbf{V}_p \subset H(\mathrm{div}; \Omega_p)$, then $\mathbf{v}_p \cdot \mathbf{n}_p \in H^{-1/2}(\partial\Omega_p)$. It is shown in [52] that, if $\mathbf{v}_p \cdot \mathbf{n}_p = $ on $\partial\Omega_p \setminus \Gamma_{fp}$, then $\mathbf{v}_p \cdot \mathbf{n}_p \in H^{-1/2}(\Gamma_{fp})$. The argument there uses the fact that, for any $\varphi \in H^{1/2}(\Gamma_{fp})$, $\langle \mathbf{v}_p \cdot \mathbf{n}_p, \varphi \rangle_{\Gamma_{fp}} = \langle \mathbf{v}_p \cdot \mathbf{n}_p, E\varphi \rangle_{\partial\Omega_p}$, where $E\varphi \in H^{1/2}(\partial\Omega_p)$ is a continuous extension. In our case, since $\mathbf{v}_p \cdot \mathbf{n}_p = 0$ on Γ_p^N and $\mathrm{dist}(\Gamma_p^D, \Gamma_{fp}) \geq s > 0$, the argument can be modified by first extending φ continuously to $H_{00}^{1/2}(\Gamma_{fp} \cup \Gamma_p^N)$, and then by zero to $H^{1/2}(\partial\Omega_p)$, again concluding that $\mathbf{v}_p \cdot \mathbf{n}_p \in H^{-1/2}(\Gamma_{fp})$. We note that $\|\mathbf{v}_p \cdot \mathbf{n}_p\|_{H^{-1/2}(\Gamma_{fp})}$ depends on s. Therefore we can take $\Lambda = H^{1/2}(\Gamma_{fp})$.

Combining (2.1.8)-(2.1.10) we obtain the Lagrange multiplier variational formulation: for $t \in (0, T]$, find $\mathbf{u}_f(t) \in \mathbf{V}_f$, $p_f(t) \in W_f$, $\mathbf{u}_p(t) \in \mathbf{V}_p$, $p_p(t) \in W_p$, $\boldsymbol{\eta}_p(t) \in \mathbf{X}_p$, and $\lambda(t) \in \Lambda$, such that $p_p(0) = p_{p,0}$, $\boldsymbol{\eta}_p(0) = \boldsymbol{\eta}_{p,0}$, and for all $\mathbf{v}_f \in \mathbf{V}_f$, $w_f \in W_f$, $\mathbf{v}_p \in \mathbf{V}_p$, $w_p \in W_p$, $\boldsymbol{\xi}_p \in \mathbf{X}_p$, and $\mu \in \Lambda$,

$$\begin{aligned} &a_f(\mathbf{u}_f, \mathbf{v}_f) + a_p^d(\mathbf{u}_p, \mathbf{v}_p) + a_p^e(\boldsymbol{\eta}_p, \boldsymbol{\xi}_p) + a_{BJS}(\mathbf{u}_f, \partial_t \boldsymbol{\eta}_p; \mathbf{v}_f, \boldsymbol{\xi}_p) + b_f(\mathbf{v}_f, p_f) + b_p(\mathbf{v}_p, p_p) \\ &\qquad + \alpha b_p(\boldsymbol{\xi}_p, p_p) + b_\Gamma(\mathbf{v}_f, \mathbf{v}_p, \boldsymbol{\xi}_p; \lambda) = (\mathbf{f}_f, \mathbf{v}_f)_{\Omega_f} + (\mathbf{f}_p, \boldsymbol{\xi}_p)_{\Omega_p}, \end{aligned} \tag{2.1.11}$$

$$\begin{aligned} &(s_0 \partial_t p_p, w_p)_{\Omega_p} - \alpha b_p\left(\partial_t \boldsymbol{\eta}_p, w_p\right) - b_p(\mathbf{u}_p, w_p) - b_f(\mathbf{u}_f, w_f) \\ &\qquad = (q_f, w_f)_{\Omega_f} + (q_p, w_p)_{\Omega_p}, \end{aligned} \tag{2.1.12}$$

$$b_\Gamma\left(\mathbf{u}_f, \mathbf{u}_p, \partial_t \boldsymbol{\eta}_p; \mu\right) = 0. \tag{2.1.13}$$

We note that the balance of normal stress, BJS, and conservation of momentum interface conditions (1.2.8)–(1.2.9) are natural and have been utilized in the derivation of the weak formulation, while the conservation of mass condition (1.2.7) is essential and it is imposed weakly in (2.1.13). The weak formulation (2.1.11)–(2.1.13) is suitable for multiscale numerical approximations and efficient parallel domain decomposition algorithms [3, 53, 55, 94].

2.2 SEMI-DISCRETE FORMULATION

Let $\mathcal{T}_h^f$ and $\mathcal{T}_h^p$ be shape-regular and quasi-uniform partitions [29] of Ω_f and Ω_p, respectively, both consisting of affine elements with maximal element diameter h. The two partitions may be non-matching at the interface Γ_{fp}. For the discretization of the fluid velocity and pressure we choose finite element spaces $\mathbf{V}_{f,h} \subset \mathbf{V}_f$ and $W_{f,h} \subset W_f$, which are assumed to be inf-sup stable and for the discretization of the porous medium problem we choose $\mathbf{V}_{p,h} \subset \mathbf{V}_p$ and $W_{p,h} \subset W_p$ to be any of well-known inf-sup stable mixed finite element spaces. The global spaces are

$$\mathbf{V}_h = \{\mathbf{v}_h = (\mathbf{v}_{f,h}, \mathbf{v}_{p,h}) \in \mathbf{V}_{f,h} \times \mathbf{V}_{p,h}\}, \quad W_h = \{w_h = (w_{f,h}, w_{p,h}) \in W_{f,h} \times W_{p,h}\}.$$

We employ a conforming Lagrangian finite element space $\mathbf{X}_{p,h} \subset \mathbf{X}_p$ to approximate the structure displacement. Note that the finite element spaces $\mathbf{V}_{f,h}$, $\mathbf{V}_{p,h}$, and $\mathbf{X}_{p,h}$ satisfy the prescribed homogeneous boundary conditions on the external boundaries. For the discrete Lagrange multiplier space we take

$$\Lambda_h = \mathbf{V}_{p,h} \cdot \mathbf{n}_p|_{\Gamma_{fp}}.$$

The semi-discrete continuous-in-time problem reads: given $p_{p,h}(0)$ and $\boldsymbol{\eta}_{p,h}(0)$, for $t \in (0, T]$, find $\mathbf{u}_{f,h}(t) \in \mathbf{V}_{f,h}$, $p_{f,h}(t) \in W_{f,h}$, $\mathbf{u}_{p,h}(t) \in \mathbf{V}_{p,h}$, $p_{p,h}(t) \in W_{p,h}$, $\boldsymbol{\eta}_{p,h}(t) \in \mathbf{X}_{p,h}$, and $\lambda_h(t) \in \Lambda_h$ such that for all $\mathbf{v}_{f,h} \in \mathbf{V}_{f,h}$, $w_{f,h} \in W_{f,h}$, $\mathbf{v}_{p,h} \in \mathbf{V}_{p,h}$, $w_{p,h} \in W_{p,h}$, $\boldsymbol{\xi}_{p,h} \in \mathbf{X}_{p,h}$, and $\mu_h \in \Lambda_h$,

$$\begin{aligned} &a_f(\mathbf{u}_{f,h}, \mathbf{v}_{f,h}) + a_p^d(\mathbf{u}_{p,h}, \mathbf{v}_{p,h}) + a_p^e(\boldsymbol{\eta}_{p,h}, \boldsymbol{\xi}_{p,h}) + a_{BJS}(\mathbf{u}_{f,h}, \partial_t \boldsymbol{\eta}_{p,h}; \mathbf{v}_{f,h}, \boldsymbol{\xi}_{p,h}) + b_f(\mathbf{v}_{f,h}, p_{f,h}) \\ &\quad + b_p(\mathbf{v}_{p,h}, p_{p,h}) + \alpha b_p(\boldsymbol{\xi}_{p,h}, p_{p,h}) + b_\Gamma(\mathbf{v}_{f,h}, \mathbf{v}_{p,h}, \boldsymbol{\xi}_{p,h}; \lambda_h) = (\mathbf{f}_f, \mathbf{v}_{f,h})_{\Omega_f} + (\mathbf{f}_p, \boldsymbol{\xi}_{p,h})_{\Omega_p}, \end{aligned} \tag{2.2.1}$$

$$\begin{aligned} &(s_0 \partial_t p_{p,h}, w_{p,h})_{\Omega_p} - \alpha b_p(\partial_t \boldsymbol{\eta}_{p,h}, w_{p,h}) - b_p(\mathbf{u}_{p,h}, w_{p,h}) - b_f(\mathbf{u}_{f,h}, w_{f,h}) \\ &\quad = (q_f, w_{f,h})_{\Omega_f} + (q_p, w_{p,h})_{\Omega_p}, \end{aligned} \tag{2.2.2}$$

$$b_\Gamma(\mathbf{u}_{f,h}, \mathbf{u}_{p,h}, \partial_t \boldsymbol{\eta}_{p,h}; \mu_h) = 0. \tag{2.2.3}$$

We will take $p_{p,h}(0)$ and $\boldsymbol{\eta}_{p,h}(0)$ to be suitable projections of the initial data $p_{p,0}$ and $\boldsymbol{\eta}_{p,0}$.

The assumptions on the fluid viscosity ν and the material coefficients K, λ_p, and μ_p imply that the bilinear forms $a_f(\cdot,\cdot)$, $a_p^d(\cdot,\cdot)$, and $a_p^e(\cdot,\cdot)$ are coercive and continuous in the appropriate norms. In particular, there exist positive constants c^f, c^p, c^e, C^f, C^p, C^e such that

$$c^f\|\mathbf{v}_f\|^2_{H^1(\Omega_f)} \le a_f(\mathbf{v}_f,\mathbf{v}_f), \quad a_f(\mathbf{v}_f,\mathbf{q}_f) \le C^f\|\mathbf{v}_f\|_{H^1(\Omega_f)}\|\mathbf{q}_f\|_{H^1(\Omega_f)}, \quad \forall \mathbf{v}_f,\mathbf{q}_f \in \mathbf{V}_f, \tag{2.2.4}$$

$$c^p\|\mathbf{v}_p\|^2_{L^2(\Omega_p)} \le a_p^d(\mathbf{v}_p,\mathbf{v}_p), \quad a_p^d(\mathbf{v}_p,\mathbf{q}_p) \le C^p\|\mathbf{v}_p\|_{L^2(\Omega_p)}\|\mathbf{q}_p\|_{L^2(\Omega_p)}, \quad \forall \mathbf{v}_p,\mathbf{q}_p \in \mathbf{V}_p, \tag{2.2.5}$$

$$c^e\|\boldsymbol{\xi}_p\|^2_{H^1(\Omega_p)} \le a_p^e(\boldsymbol{\xi}_p,\boldsymbol{\xi}_p), \quad a_p^e(\boldsymbol{\xi}_p,\boldsymbol{\zeta}_p) \le C^e\|\boldsymbol{\xi}_p\|_{H^1(\Omega_p)}\|\boldsymbol{\zeta}_p\|_{H^1(\Omega_p)}, \quad \forall \boldsymbol{\xi}_p,\boldsymbol{\zeta}_p \in \mathbf{X}_p, \tag{2.2.6}$$

where (2.2.4) and (2.2.6) hold true thanks to Poincare inequality (1.3.5) and (2.2.6) also relies on Korn's inequality (1.3.4), see [29] or [43] for more details. We further define, for $\mathbf{v}_f \in \mathbf{V}_f$, $\boldsymbol{\xi}_p \in \mathbf{X}_p$,

$$|\mathbf{v}_f - \boldsymbol{\xi}_p|^2_{a_{BJS}} = a_{BJS}(\mathbf{v}_f,\boldsymbol{\xi}_p;\mathbf{v}_f,\boldsymbol{\xi}_p) = \sum_{j=1}^{d-1} \nu\alpha_{BJS}\|K_j^{-1/4}(\mathbf{v}_f - \boldsymbol{\xi}_p)\cdot\mathbf{t}_{f,j}\|^2_{L^2(\Gamma_{fp})}.$$

We next state a discrete inf-sup condition, which will be utilized to control the pressure in the two regions and the Lagrange multiplier. Following [52], we define a seminorm in Λ_h,

$$|\mu_h|^2_{\Lambda_h} = a_p^d(\mathbf{u}^*_{p,h}(\mu_h),\mathbf{u}^*_{p,h}(\mu_h)), \tag{2.2.7}$$

where $(\mathbf{u}^*_{p,h}(\mu_h), p^*_{p,h}(\mu_h)) \in \mathbf{V}_{p,h}\times W_{p,h}$ is the mixed finite element solution to the Darcy problem with Dirichlet data μ_h on Γ_{fp}:

$$\begin{aligned} &a_p^d(\mathbf{u}^*_{p,h}(\mu_h),\mathbf{v}_{p,h}) + b_p(\mathbf{v}_{p,h},p^*_h(\mu_h)) = -\langle \mathbf{v}_{p,h}\cdot\mathbf{n}_p,\mu_h\rangle_{\Gamma_{fp}}, \quad \forall\, \mathbf{v}_{p,h}\in\mathbf{V}_{p,h},\\ &b_p(\mathbf{u}^*_{p,h}(\mu_h),w_{p,h}) = 0, \quad \forall\, w_{p,h}\in W_{p,h}. \end{aligned}$$

We equip Λ_h with the norm $\|\mu_h\|^2_{\Lambda_h} = \|\mu_h\|^2_{L^2(\Gamma_{fp})} + |\mu_h|^2_{\Lambda_h}$. This norm can be considered as a discrete version of the $H^{1/2}(\Gamma_{fp})$-norm [52]. For convenience of notation we define the composite norms

$$\|(\mathbf{v}_h,\boldsymbol{\xi}_{p,h})\|^2_{\mathbf{V}\times\mathbf{X}_p} = \|\mathbf{v}_h\|^2_{\mathbf{V}} + \|\boldsymbol{\xi}_{p,h}\|^2_{H^1(\Omega_p)}, \quad \|(w_h,\mu_h)\|^2_{W\times\Lambda_h} = \|w_h\|^2_W + \|\mu_h\|^2_{\Lambda_h},$$

as well as

$$b(\mathbf{v}_h,\boldsymbol{\xi}_{p,h};w_h) = b_f(\mathbf{v}_{f,h},w_{f,h}) + b_p(\mathbf{v}_{p,h},w_{p,h}) + \alpha b_p(\boldsymbol{\xi}_{p,h},w_{p,h}),$$

$$b_\Gamma(\mathbf{v}_h, \boldsymbol{\xi}_{p,h}; \mu_h) = b_\Gamma(\mathbf{v}_{f,h}, \mathbf{v}_{p,h}, \boldsymbol{\xi}_{p,h}; \mu_h).$$

The next result establishes the Ladyzhenskaya-Babuska-Brezzi (LBB) condition for the mixed Stokes-Darcy problem, where it is understood that the zero functions are excluded from the inf-sup.

Lemma 2.2.1. *There exists a constant $\beta > 0$ independent of h such that*

$$\inf_{(w_h,\mu_h)\in W_h\times\Lambda_h} \sup_{\mathbf{v}_h\in\mathbf{V}_h} \frac{b_f(\mathbf{v}_{f,h}; w_{f,h}) + b_p(\mathbf{v}_{p,h}; w_{p,h}) + \langle \mathbf{v}_{f,h}\cdot\mathbf{n}_f + \mathbf{v}_{p,h}\cdot\mathbf{n}_p, \mu_h\rangle}{\|\mathbf{v}_h\|_{\mathbf{V}}\|(w_h,\mu_h)\|_{W\times\Lambda_h}} \geq \beta. \quad (2.2.8)$$

Proof. The result is proven in [52] in the case of velocity boundary conditions on $\partial\Omega$ by restricting the mean value of W_h. It can be easily verified that, since $|\Gamma_p^D| > 0$, the result holds with no restriction on W_h. □

This result implies the inf-sup condition for the formulation (2.2.1)-(2.2.3).

Corollary 2.2.1. *There exists a constant $\beta > 0$ independent of h such that*

$$\inf_{(w_h,\mu_h)\in W_h\times\Lambda_h} \sup_{(\mathbf{v}_h,\boldsymbol{\xi}_{p,h})\in\mathbf{V}_h\times\mathbf{X}_{p,h}} \frac{b(\mathbf{v}_h, \boldsymbol{\xi}_{p,h}; w_h) + b_\Gamma(\mathbf{v}_h, \boldsymbol{\xi}_{p,h}; \mu_h)}{\|(\mathbf{v}_h, \boldsymbol{\xi}_{p,h})\|_{\mathbf{V}\times\mathbf{X}_p}\|(w_h,\mu_h)\|_{W\times\Lambda_h}} \geq \beta. \quad (2.2.9)$$

Proof. The statement follows from Lemma 2.2.1 by simply taking $\boldsymbol{\xi}_{p,h} = 0$. □

2.2.1 Existence and uniqueness of the solution

In this subsection we show that the semi-discrete Stokes-Biot system is well-posed. For the existence of the solution we adopt the theory of differential-algebraic equations (DAEs) [17].

Let $\{\boldsymbol{\phi}_{\mathbf{u}_f,i}\}, \{\boldsymbol{\phi}_{\mathbf{u}_p,i}\}, \{\boldsymbol{\phi}_{\boldsymbol{\eta}_p,i}\}, \{\phi_{p_f,i}\}, \{\phi_{p_p,i}\}$ and $\{\phi_{\lambda,i}\}$ be bases of $\mathbf{V}_{f,h}, \mathbf{V}_{p,h}, \mathbf{X}_{p,h}, W_{f,h}$, $W_{p,h}$ and Λ_h, respectively. Let $M_p, A_f, A_p, A_e, B_{ff}^T, B_{pp}^T$ and B_{ep}^T denote the matrices whose (i,j)-entries are, respectively, $(\phi_{p_p,j}, \phi_{p_p,i})_{\Omega_p}$, $a_f(\boldsymbol{\phi}_{\mathbf{u}_f,j}, \boldsymbol{\phi}_{\mathbf{u}_f,i})$, $a_p^d(\boldsymbol{\phi}_{\mathbf{u}_p,j}, \boldsymbol{\phi}_{\mathbf{u}_p,i})$, $a_p^e(\boldsymbol{\phi}_{\boldsymbol{\eta}_p,j}, \boldsymbol{\phi}_{\boldsymbol{\eta}_p,i})$, $b_f(\nabla\cdot\boldsymbol{\phi}_{\mathbf{u}_f,j}, \phi_{p_f,i})$, $b_p(\nabla\cdot\boldsymbol{\phi}_{\mathbf{u}_p,j}, \phi_{p_p,i})$, and $b_p(\nabla\cdot\boldsymbol{\phi}_{\boldsymbol{\eta}_p,j}, \phi_{p_p,i})$. We also introduce matrices $A_{ff}^{BJS}, A_{fe}^{BJS}$ and A_{ee}^{BJS} whose (i,j)-entries are, respectively, $a_{BJS}(\boldsymbol{\phi}_{\mathbf{u}_f,j}, 0;\ \boldsymbol{\phi}_{\mathbf{u}_f,i}, 0)$, $a_{BJS}(\boldsymbol{\phi}_{\mathbf{u}_f,j},\ 0; 0, \boldsymbol{\phi}_{\boldsymbol{\eta}_p,i})$, and $a_{BJS}(0, \boldsymbol{\phi}_{\boldsymbol{\eta}_p,j}; 0, \boldsymbol{\phi}_{\boldsymbol{\eta}_p,j})$. Finally, let $B_{f,\Gamma}^T$, $B_{p,\Gamma}^T$ and $B_{e,\Gamma}^T$ stand for the matrices with (i,j)-entries defined by $b_\Gamma(\boldsymbol{\phi}_{\mathbf{u}_f,j}, 0, 0; \phi_{\lambda,i})$, $b_\Gamma(0, \boldsymbol{\phi}_{\mathbf{u}_p,j}, 0; \phi_{\lambda,i})$, and $b_\Gamma(0, 0, \boldsymbol{\phi}_{\boldsymbol{\eta}_p,j}; \phi_{\lambda,i})$, respectively.

Taking in (2.2.1)-(2.2.3) $\mathbf{u}_{f,h}(t,\mathbf{x}) = \sum_i u_{f,i}(t)\phi_{\mathbf{u}_f,i}$, $\mathbf{u}_{p,h}(t,\mathbf{x}) = \sum_i u_{p,i}(t)\phi_{\mathbf{u}_p,i}$, $\boldsymbol{\eta}_{p,h}(t,\mathbf{x}) = \sum_i \eta_{p,i}(t)\phi_{\boldsymbol{\eta}_p,i}$, $p_{f,h}(t,\mathbf{x}) = \sum_i p_{f,i}(t)\phi_{p_f,i}$, $p_{p,h}(t,\mathbf{x}) = \sum_i p_{p,i}(t)\phi_{p_p,i}$ and $\lambda_h(t,\mathbf{x}) = \sum_i \lambda_i(t)\phi_{\lambda,i}$ with (time-dependent) coefficients $\overline{\mathbf{u}}_f, \overline{\mathbf{u}}_p, \overline{\boldsymbol{\eta}}_p, \overline{p}_f, \overline{p}_p, \overline{\lambda}$, leads to the matrix-vector system

$$A_f\,\overline{\mathbf{u}}_f + A_p\,\overline{\mathbf{u}}_p + A_e\,\overline{\boldsymbol{\eta}}_p + A_{ff}^{BJS}\,\overline{\mathbf{u}}_f + A_{fe}^{BJS}\,\partial_t\overline{\boldsymbol{\eta}}_p + B_{ff}^T\,\overline{p}_f + \left(B_{pp}^T + \alpha B_{ep}^T\right)\overline{p}_p + \left(B_{f,\Gamma}^T + B_{p,\Gamma}^T + B_{e,\Gamma}^T\right)\overline{\lambda} = \mathcal{F}_{\mathbf{u}_f} + \mathcal{F}_{\boldsymbol{\eta}_p} \tag{2.2.10}$$

$$M_p\,\partial_t\overline{p}_p - \alpha B_{ep}\,\partial_t\overline{\boldsymbol{\eta}}_p - B_{pp}\,\overline{\mathbf{u}}_p - B_{ff}\,\overline{\mathbf{u}}_f + A_{fe}^{BJS,T}\,\overline{\mathbf{u}}_f + A_{ee}^{BJS}\,\partial_t\overline{\boldsymbol{\eta}}_p = \mathcal{F}_{p_f} + \mathcal{F}_{p_p}, \tag{2.2.11}$$

$$B_{\mathbf{f},\Gamma}\overline{\mathbf{u}}_f + B_{p,\Gamma}\overline{\mathbf{u}}_p + B_{e,\Gamma}\partial_t\overline{\boldsymbol{\eta}}_p = 0, \tag{2.2.12}$$

which can be written in the DAE system form

$$\mathbf{E}\,\partial_t X(t) + \mathbf{H}\,X(t) = L(t), \tag{2.2.13}$$

where

$$X(t) = \begin{pmatrix} \overline{\mathbf{u}}_f(t) \\ \overline{\mathbf{u}}_p(t) \\ \overline{\boldsymbol{\eta}}_p(t) \\ \overline{p}_f(t) \\ \overline{p}_p(t) \\ \overline{\lambda}(t) \end{pmatrix}, \quad L(t) = \begin{pmatrix} \mathcal{F}_{\mathbf{u}_f} \\ 0 \\ \mathcal{F}_{\boldsymbol{\eta}_p} \\ \mathcal{F}_{p_f} \\ \mathcal{F}_{p_p} \\ 0 \end{pmatrix}, \quad \mathbf{E} = \begin{pmatrix} 0 & 0 & A_{fe}^{BJS} & 0 & 0 & 0 \\ 0 & 0 & 0 & 0 & 0 & 0 \\ 0 & 0 & A_{ee}^{BJS} & 0 & 0 & 0 \\ 0 & 0 & 0 & 0 & 0 & 0 \\ 0 & 0 & -\alpha B_{ep} & 0 & s_0 M_p & 0 \\ 0 & 0 & -B_{e,\Gamma} & 0 & 0 & 0 \end{pmatrix}, \tag{2.2.14}$$

$$\mathbf{H} = \begin{pmatrix} A_f + A_{ff}^{BJS} & 0 & 0 & B_{ff}^T & 0 & B_{f,\Gamma}^T \\ 0 & A_p & 0 & 0 & B_{pp}^T & B_{p,\Gamma}^T \\ A_{fe}^{BJS,T} & 0 & A_e & 0 & \alpha B_{ep}^T & B_{e,\Gamma}^T \\ -B_{ff} & 0 & 0 & 0 & 0 & 0 \\ 0 & -B_{pp} & 0 & 0 & 0 & 0 \\ -B_{f,\Gamma} & -B_{p,\Gamma} & 0 & 0 & 0 & 0 \end{pmatrix}. \tag{2.2.15}$$

We note that the matrix

$$\mathbf{E} + \mathbf{H} = \begin{pmatrix} A_f + A_{ff}^{BJS} & 0 & A_{fe}^{BJS} & B_{ff}^T & 0 & B_{f,\Gamma}^T \\ 0 & A_p & 0 & 0 & B_{pp}^T & B_{p,\Gamma}^T \\ A_{fe}^{BJS,T} & 0 & A_e + A_{ee}^{BJS} & 0 & \alpha B_{ep}^T & B_{e,\Gamma}^T \\ -B_{ff} & 0 & 0 & 0 & 0 & 0 \\ 0 & -B_{pp} & -\alpha B_{ep} & 0 & s_0 M_p & 0 \\ -B_{f,\Gamma} & -B_{p,\Gamma} & -B_{e,\Gamma} & 0 & 0 & 0 \end{pmatrix}$$

can be written as a block 2×2 matrix

$$\mathbf{E} + \mathbf{H} = \begin{pmatrix} \mathbf{A} & \mathbf{B}^T \\ -\mathbf{B} & \mathbf{C} \end{pmatrix},$$

where

$$\mathbf{A} = \begin{pmatrix} A_f + A_{ff}^{BJS} & 0 & A_{fe}^{BJS} \\ 0 & A_p & 0 \\ A_{fe}^{BJS,T} & 0 & A_e + A_{ee}^{BJS} \end{pmatrix}, \mathbf{B}^T = \begin{pmatrix} B_{ff}^T & 0 & B_{f,\Gamma}^T \\ 0 & B_{pp}^T & B_{p,\Gamma}^T \\ 0 & \alpha B_{ep}^T & B_{e,\Gamma}^T \end{pmatrix}, \mathbf{C} = \begin{pmatrix} 0 & 0 & 0 \\ 0 & s_0 M_p & 0 \\ 0 & 0 & 0 \end{pmatrix}.$$

The following result can be found in [97].

Lemma 2.2.2. *If* $\mathbf{A}$ *and* $\mathbf{C}$ *are positive semi-definite and* $\ker(\mathbf{A}) \cap \ker(\mathbf{B}) = \ker(\mathbf{C}) \cap \ker(\mathbf{B}^T) = \{0\}$*, then* $\mathbf{E} + \mathbf{H}$ *is invertible.*

It is convenient to associate with matrices $\mathbf{A}$, $\mathbf{B}$, and $\mathbf{C}$ the bilinear forms $\phi_{\mathbf{A}}(\cdot,\cdot)$, $\phi_{\mathbf{B}}(\cdot,\cdot)$ and $\phi_{\mathbf{C}}(\cdot,\cdot)$ on $(\mathbf{V}_h \times \mathbf{X}_h)\times(\mathbf{V}_h \times \mathbf{X}_h)$, $(\mathbf{V}_h \times \mathbf{X}_h)\times(W_h \times \Lambda_h)$ and $(W_h \times \Lambda_h)\times(W_h \times \Lambda_h)$, respectively:

$$\begin{aligned}
\phi_{\mathbf{A}}((\mathbf{u}_h, \boldsymbol{\eta}_{p,h}), (\mathbf{v}_h, \boldsymbol{\xi}_{p,h})) &= a_f(\mathbf{u}_{f,h}, \mathbf{v}_{f,h}) + a_p^d(\mathbf{u}_{p,h}, \mathbf{v}_{p,h}) + a_p^e(\boldsymbol{\eta}_{p,h}, \boldsymbol{\xi}_{p,h}) \\
&\quad + a_{BJS}(\mathbf{u}_{f,h}, \boldsymbol{\eta}_{p,h}; \mathbf{v}_{f,h}, \boldsymbol{\xi}_{p,h}) \\
\phi_{\mathbf{B}}((\mathbf{u}_h, \boldsymbol{\eta}_{p,h}), (w_h, \mu_h)) &= b_f(\mathbf{u}_{f,h}, w_{f,h}) + b_p(\mathbf{u}_{p,h}, w_{p,h}) \\
&\quad + \alpha b_p(\boldsymbol{\eta}_{p,h}, w_{p,h}) + b_\Gamma(\mathbf{u}_{f,h}, \mathbf{u}_{p,h}, \boldsymbol{\eta}_{p,h}; \mu_h) \\
\phi_{\mathbf{C}}((p_h, \lambda_h), (w_h, \mu_h)) &= (s_0 p_{p,h}, w_{p,h})_{\Omega_p}.
\end{aligned}$$

By identifying functions in the finite element spaces with algebraic vectors of their degrees of freedom, we note that $\ker(\phi_{\mathbf{A}}) = \ker(\mathbf{A})$, $\ker(\phi_{\mathbf{B}}) = \ker(\mathbf{B})$, and $\ker(\phi_{\mathbf{C}}) = \ker(\mathbf{C})$. Also, for $\phi_{\mathbf{B}^T}((w_h, \mu_h), (\mathbf{v}_h, \boldsymbol{\xi}_{p,h})) = \phi_{\mathbf{B}}((\mathbf{v}_h, \boldsymbol{\xi}_{p,h}), (w_h, \mu_h))$, we have that $\ker(\phi_{\mathbf{B}^T}) = \ker(\mathbf{B}^T)$. We next show that the conditions of the Lemma 2.2.2 are satisfied.

Lemma 2.2.3. *The bilinear forms* $\phi_{\mathbf{A}}$, $\phi_{\mathbf{B}}$ *and* $\phi_{\mathbf{C}}$ *satisfy*

$$\begin{aligned}
\ker(\phi_{\mathbf{A}}) \cap \ker(\phi_{\mathbf{B}}) &= \{(0,0)\}, \\
\ker(\phi_{\mathbf{C}}) \cap \ker(\phi_{\mathbf{B}^T}) &= \{(0,0)\}.
\end{aligned}$$

Moreover, $\phi_{\mathbf{A}}$ *and* $\phi_{\mathbf{C}}$ *are positive definite and semi-definite, respectively.*

Proof. The coercivity of $a_f(\cdot,\cdot)$, $a_p^d(\cdot,\cdot)$, and $a_p^e(\cdot,\cdot)$, (2.2.4)–(2.2.6), and the non-negativity of $a_{BJS}(\cdot,\cdot)$ imply that $\phi_{\mathbf{A}}(\cdot,\cdot)$ is coercive and $\ker(\phi_{\mathbf{A}}) = 0$, hence the first statement of the lemma follows. We next note that $\ker(\phi_{\mathbf{B}^T})$ consists of $(w_h, \mu_h) \in W_h \times \Lambda_h$ such that

$$\phi_{\mathbf{B}^T}((w_h, \mu_h), (\mathbf{v}_h, \boldsymbol{\xi}_{p,h})) = 0, \quad \forall\, (\mathbf{v}_h, \boldsymbol{\xi}_{p,h}) \in \mathbf{V}_h \times \mathbf{X}_{p,h},$$

therefore the inf-sup condition (2.2.9) implies that $\ker(\phi_{\mathbf{B}^T}) = \{(0,0)\}$, which gives the second statement of the lemma. The positive semi-definiteness of $\phi_{\mathbf{C}}(\cdot,\cdot)$ is straightforward. □

Theorem 2.2.1. *There exists a unique solution* $(\mathbf{u}_{f,h}, p_{f,h}, \mathbf{u}_{p,h}, p_{p,h}, \boldsymbol{\eta}_{p,h}, \lambda_h)$ *in* $L^\infty(0,T;\mathbf{V}_{f,h})\times\ L^\infty(0,T;W_{f,h}) \times L^\infty(0,T;\mathbf{V}_{p,h}) \times W^{1,\infty}(0,T;W_{p,h}) \times W^{1,\infty}(0,T;\mathbf{X}_{p,h}) \times L^\infty(0,T;\Lambda_h)$ *of the weak formulation* (2.2.1)-(2.2.3).

Proof. According to the DAE theory, see Theorem 2.3.1 in [17], if the matrix pencil $s\mathbf{E}+\mathbf{H}$ is nonsingular for some $s \neq 0$ and the initial data is consistent, then (2.2.13) has a solution. Lemma 2.2.3 guarantees that in our case the pencil with $s = 1$ is invertible. Also, the initial data $p_{p,h}(0)$ and $\boldsymbol{\eta}_{p,h}(0)$ does not lead to consistency issues. In particular, the only algebraic constraints in the DAE system (2.2.13) are the second and fourth equations, see the definition of $\mathbf{E}$ in (2.2.14). The second equation is the discretized Darcy's law, and the initial value $\mathbf{u}_{p,h}(0)$ can be chosen to satisfy it for any given $p_{p,h}(0)$, while the fourth equation is the discretized incompressibility constraint for Stokes, which does not involve the initial data. Furthermore, the initial data can be assumed to satisfy the boundary conditions. As a result, Theorem 2.3.1 in [17] implies existence of a solution of the weak semi-discrete formulation (2.2.1)-(2.2.3).

To show uniqueness, we assume that there are two solutions satisfying these equations with the same initial conditions. Then their difference $(\tilde{\mathbf{u}}_{f,h}, \tilde{p}_{f,h}, \tilde{\mathbf{u}}_{p,h}, \tilde{p}_{p,h}, \tilde{\boldsymbol{\eta}}_{p,h}, \tilde{\lambda}_h)$ satisfies (2.2.1)-(2.2.3) with zero data. By taking $(\mathbf{v}_{f,h}, w_{f,h}, \mathbf{v}_{p,h}, w_{p,h}, \boldsymbol{\xi}_{p,h}, \mu_h) = (\tilde{\mathbf{u}}_{f,h}, \tilde{p}_{f,h}, \tilde{\mathbf{u}}_{p,h}, \tilde{p}_{p,h}, \partial_t\tilde{\boldsymbol{\eta}}_{p,h}, \tilde{\lambda}_h)$ in (2.2.1)-(2.2.3), we obtain the energy equality

$$a_f(\tilde{\mathbf{u}}_{f,h}, \tilde{\mathbf{u}}_{f,h}) + a_p^d(\tilde{\mathbf{u}}_{p,h}, \tilde{\mathbf{u}}_{p,h}) + a_p^e\left(\tilde{\boldsymbol{\eta}}_{p,h}, \partial_t\tilde{\boldsymbol{\eta}}_{p,h}\right) + (s_0\partial_t\tilde{p}_{p,h}, \tilde{p}_{p,h}) + \left|\tilde{\mathbf{u}}_{f,h} - \partial_t\tilde{\boldsymbol{\eta}}_{p,h}\right|^2_{a_{BJS}} = 0$$

Using the following algebraic identity

$$\int_S \phi\frac{\partial\phi}{\partial t}\,dA = \frac{1}{2}\frac{\partial}{\partial t}\|\phi\|^2_{L^2(S)}, \tag{2.2.16}$$

we write the energy equality as

$$\frac{1}{2}\partial_t\left(s_0\|\tilde{p}_{p,h}\|^2_{L^2(\Omega_p)} + a_p^e(\tilde{\boldsymbol{\eta}}_{p,h}, \tilde{\boldsymbol{\eta}}_{p,h})\right) + a_f(\tilde{\mathbf{u}}_{f,h}, \tilde{\mathbf{u}}_{f,h}) + a_p^d(\tilde{\mathbf{u}}_{p,h}, \tilde{\mathbf{u}}_{p,h}) + \left|\tilde{\mathbf{u}}_{f,h} - \partial_t\tilde{\boldsymbol{\eta}}_{p,h}\right|^2_{a_{BJS}} = 0$$

Integrating in time over $[0,t]$ for arbitrary $t \in (0,T]$, we obtain

$$\frac{1}{2}\left(s_0\|\tilde{p}_{p,h}(t)\|^2_{L^2(\Omega_p)} + a_p^e(\tilde{\boldsymbol{\eta}}_{p,h}(t), \tilde{\boldsymbol{\eta}}_{p,h}(t))\right)$$

$$+\int_0^t \left[\left| \tilde{\mathbf{u}}_{f,h} - \partial_t \tilde{\boldsymbol{\eta}}_{p,h} \right|^2_{a_{BJS}} + a_f(\tilde{\mathbf{u}}_{f,h}, \tilde{\mathbf{u}}_{f,h}) + a_p^d(\tilde{\mathbf{u}}_{p,h}, \tilde{\mathbf{u}}_{p,h}) \right] ds = 0. \tag{2.2.17}$$

Due to the coercivity of bilinear forms, we conclude that $\tilde{\mathbf{u}}_{f,h}(t) = 0$, $\tilde{\mathbf{u}}_{p,h}(t) = 0$, $\tilde{\boldsymbol{\eta}}_{p,h}(t) = 0$, $\forall t \in [0, T]$. If $s_0 \neq 0$, we also have that $\tilde{p}_{p,h}(t) = 0$, but we can also obtain uniqueness for both pressure variables and the Lagrange multiplier simultaneously and independently of parameters. In particular, from the inf-sup condition (2.2.9) and (2.2.1), we have for $(\tilde{p}_h, \tilde{\lambda}_h)$

$$\begin{aligned}
&\beta \|(\tilde{p}_h, \tilde{\lambda}_h)\|_{W \times \Lambda_h} \\
&\leq \sup_{(\mathbf{v}_h, \boldsymbol{\xi}_{p,h}) \in \mathbf{V}_h \times \mathbf{X}_{p,h}} \frac{b_f(\mathbf{v}_{f,h}, \tilde{p}_{f,h}) + b_p(\mathbf{v}_{p,h}, \tilde{p}_{p,h}) + \alpha b_p(\boldsymbol{\xi}_{p,h}, \tilde{p}_{p,h}) + b_\Gamma(\mathbf{v}_{f,h}, \mathbf{v}_{p,h}, \boldsymbol{\xi}_{p,h}; \tilde{\lambda}_h)}{\|(\mathbf{v}_h, \boldsymbol{\xi}_h)\|_{\mathbf{V} \times \mathbf{X}_p}} \\
&= \sup_{(\mathbf{v}_h, \boldsymbol{\xi}_{p,h}) \in \mathbf{V}_h \times \mathbf{X}_{p,h}} \left[\frac{-a_f(\tilde{\mathbf{u}}_{f,h}, \mathbf{v}_{f,h}) - a_p^d(\tilde{\mathbf{u}}_{p,h}, \mathbf{v}_{p,h}) - a_p^e(\tilde{\boldsymbol{\eta}}_{p,h}, \boldsymbol{\xi}_{p,h})}{\|(\mathbf{v}_h, \boldsymbol{\xi}_h)\|_{\mathbf{V} \times \mathbf{X}_p}} \right. \\
&\qquad \left. \frac{-a_{BJS}(\tilde{\mathbf{u}}_{f,h}, \partial_t \tilde{\boldsymbol{\eta}}_{p,h}; \mathbf{v}_{f,h}, \boldsymbol{\xi}_{p,h})}{\|(\mathbf{v}_h, \boldsymbol{\xi}_h)\|_{\mathbf{V} \times \mathbf{X}_p}} \right] = 0.
\end{aligned}$$

Therefore, we conclude that $\tilde{p}_{f,h}(t) = 0$, $\tilde{p}_{p,h}(t) = 0$, $\tilde{\lambda}_h(t) = 0$, $\forall t \in (0, T]$ and the solution of (2.2.1)-(2.2.3) is unique. □

The next two subsections are devoted to the stability and error analysis of the semi-discrete problem.

2.2.2 Stability analysis of the semi-discrete formulation

By taking $(\mathbf{v}_{f,h}, w_{f,h}, \mathbf{v}_{p,h}, w_{p,h}, \boldsymbol{\xi}_{p,h}, \mu_h) = \left(\mathbf{u}_{f,h}, p_{f,h}, \mathbf{u}_{p,h}, p_{p,h}, \partial_t \boldsymbol{\eta}_{p,h}, \lambda_h\right)$ in (2.2.1)–(2.2.3) and proceeding as in the uniqueness proof, Theorem 2.2.1, we obtain

$$\begin{aligned}
&\frac{1}{2}\left(s_0 \|p_{p,h}(t)\|^2_{L^2(\Omega_p)} + a_p^e(\boldsymbol{\eta}_{p,h}(t), \boldsymbol{\eta}_{p,h}(t)) \right) \\
&\quad + \int_0^t \left[\left| \mathbf{u}_{f,h} - \partial_t \boldsymbol{\eta}_{p,h} \right|^2_{a_{BJS}} + a_f(\mathbf{u}_{f,h}, \mathbf{u}_{f,h}) + a_p^d(\mathbf{u}_{p,h}, \mathbf{u}_{p,h}) \right] ds \\
&\quad = \frac{1}{2}\left(s_0 \|p_{p,h}(0)\|^2_{L^2(\Omega_p)} + a_p^e(\boldsymbol{\eta}_{p,h}(0), \boldsymbol{\eta}_{p,h}(0)) \right) + \int_0^t \mathcal{F}\left(t; \mathbf{u}_{f,h}, \partial_t \boldsymbol{\eta}_{p,h}, p_{f,h}, p_{p,h}\right) ds,
\end{aligned} \tag{2.2.18}$$

where $\mathcal{F}\left(t; \mathbf{u}_{f,h}, \partial_t \boldsymbol{\eta}_{p,h}, p_{f,h}, p_{p,h}\right)$ denotes the total forcing term:

$$\mathcal{F}\left(t; \mathbf{u}_{f,h}, \partial_t \boldsymbol{\eta}_{p,h}, p_{f,h}, p_{p,h}\right) = (\mathbf{f}_f, \mathbf{u}_{f,h})_{\Omega_f} + \left(\mathbf{f}_p, \partial_t \boldsymbol{\eta}_{p,h}\right)_{\Omega_p} + (q_f, p_{f,h})_{\Omega_f} + (q_p, p_{p,h})_{\Omega_p}$$

Using integration by parts in time, we write the forcing term as

$$\mathcal{F}\left(t;\mathbf{u}_{f,h},\partial_t\boldsymbol{\eta}_{p,h},p_{f,h},p_{p,h}\right)=(\mathbf{f}_f,\mathbf{u}_{f,h})_{\Omega_f}+\partial_t\left(\mathbf{f}_p,\boldsymbol{\eta}_{p,h}\right)_{\Omega_p}-\left(\partial_t\mathbf{f}_p,\boldsymbol{\eta}_{p,h}\right)_{\Omega_p}$$
$$+(q_f,p_{f,h})_{\Omega_f}+(q_p,p_{p,h})_{\Omega_p}.$$

Therefore, for any $\epsilon_1>0$, we have

$$\begin{aligned}
&\int_0^t\mathcal{F}\left(t;\mathbf{u}_{f,h},\partial_t\boldsymbol{\eta}_{p,h},p_{f,h},p_{p,h}\right)ds\\
&\quad\le\frac{1}{2}\|\boldsymbol{\eta}_{p,h}(0)\|^2_{L^2(\Omega_p)}+\frac{1}{2}\|\mathbf{f}_p(0)\|^2_{L^2(\Omega_p)}+\frac{1}{2}\int_0^t\left(\|\boldsymbol{\eta}_{p,h}\|^2_{L^2(\Omega_p)}+\|\partial_t\mathbf{f}_p\|^2_{L^2(\Omega_p)}\right)ds\\
&\qquad+\frac{\epsilon_1}{2}\left(\|\boldsymbol{\eta}_{p,h}(t)\|^2_{L^2(\Omega_p)}+\int_0^t\left(\|\mathbf{u}_{f,h}\|^2_{L^2(\Omega_f)}+\|p_{f,h}\|^2_{L^2(\Omega_f)}+\|p_{p,h}\|^2_{L^2(\Omega_p)}\right)ds\right)\\
&\qquad+\frac{1}{2\epsilon_1}\left(\|\mathbf{f}_p(t)\|^2_{L^2(\Omega_p)}+\int_0^t\left(\|\mathbf{f}_f\|^2_{L^2(\Omega_f)}+\|q_f\|^2_{L^2(\Omega_f)}+\|q_p\|^2_{L^2(\Omega_p)}\right)ds\right).
\end{aligned}\tag{2.2.19}$$

Combining (2.2.18), (2.2.19) and (2.2.4)–(2.2.6), and taking ϵ_1 small enough, we obtain

$$\begin{aligned}
&s_0\|p_{p,h}(t)\|^2_{L^2(\Omega_p)}+\|\boldsymbol{\eta}_{p,h}(t)\|^2_{H^1(\Omega_p)}+\int_0^t\left(\left|\mathbf{u}_{f,h}-\partial_t\boldsymbol{\eta}_{p,h}\right|^2_{a_{BJS}}+\|\mathbf{u}_{f,h}|^2_{H^1(\Omega_f)}+\|\mathbf{u}_{p,h}\|^2_{L^2(\Omega_p)}\right)ds\\
&\le C\epsilon_1\int_0^t\left(\|p_{f,h}\|^2_{L^2(\Omega_f)}+\|p_{p,h}\|^2_{L^2(\Omega_p)}\right)ds+C\int_0^t\|\boldsymbol{\eta}_{p,h}\|^2_{L^2(\Omega_p)}ds\\
&\quad+C\left(s_0\|p_{p,h}(0)\|^2_{L^2(\Omega_p)}+\|\boldsymbol{\eta}_{p,h}(0)\|^2_{H^1(\Omega_p)}+\|\mathbf{f}_p(0)\|^2_{L^2(\Omega_p)}+\int_0^t\|\partial_t\mathbf{f}_p\|^2_{L^2(\Omega_p)}\,ds\right)\\
&\quad+C\epsilon_1^{-1}\left(\|\mathbf{f}_p(t)\|^2_{L^2(\Omega_p)}+\int_0^t\left(\|\mathbf{f}_f\|^2_{L^2(\Omega_f)}+\|q_f\|^2_{L^2(\Omega_f)}+\|q_p\|^2_{L^2(\Omega_p)}\right)ds\right).
\end{aligned}\tag{2.2.20}$$

Finally, from the inf-sup condition (2.2.9) and (2.2.1), we have

$$\begin{aligned}
&\|(p_h,\lambda_h)\|_{W\times\Lambda_h}\\
&\quad\le C\sup_{(\mathbf{v}_h,\boldsymbol{\xi}_{p,h})\in\mathbf{V}_h\times\mathbf{X}_{p,h}}\frac{b_f(\mathbf{v}_{f,h},p_{f,h})+b_p(\mathbf{v}_{p,h},p_{p,h})+\alpha b_p(\boldsymbol{\xi}_{p,h},p_{p,h})+b_\Gamma(\mathbf{v}_{f,h},\mathbf{v}_{p,h},\boldsymbol{\xi}_{p,h};\lambda_h)}{\|(\mathbf{v}_h,\boldsymbol{\xi}_{p,h})\|_{\mathbf{V}\times\mathbf{X}_p}}\\
&\quad=C\sup_{(\mathbf{v}_h,\boldsymbol{\xi}_{p,h})\in\mathbf{V}_h\times\mathbf{X}_{p,h}}\left[\frac{-a_f(\mathbf{u}_{f,h},\mathbf{v}_{f,h})-a_p^d(\mathbf{u}_{p,h},\mathbf{v}_{p,h})-a_p^e(\boldsymbol{\eta}_{p,h},\boldsymbol{\xi}_{p,h})}{\|(\mathbf{v}_h,\boldsymbol{\xi}_{p,h})\|_{\mathbf{V}\times\mathbf{X}_p}}\right.\\
&\qquad\left.+\frac{-a_{BJS}(\mathbf{u}_{f,h},\partial_t\boldsymbol{\eta}_{p,h};\mathbf{v}_{f,h},\boldsymbol{\xi}_{p,h})+(\mathbf{f}_f,\mathbf{v}_{f,h})+(\mathbf{f}_p,\boldsymbol{\xi}_{p,h})}{\|(\mathbf{v}_h,\boldsymbol{\xi}_{p,h})\|_{\mathbf{V}\times\mathbf{X}_p}}\right],
\end{aligned}$$

which, combined with (2.2.4)–(2.2.6), gives

$$\epsilon_2\int_0^t\left(\|p_{f,h}\|^2_{L^2(\Omega_f)}+\|p_{p,h}\|^2_{L^2(\Omega_p)}+\|\lambda\|^2_{\Lambda_h}\right)ds\le C\epsilon_2\int_0^t\left(\|\mathbf{u}_{f,h}\|^2_{H^1(\Omega_f)}+\|\mathbf{u}_{p,h}\|^2_{L^2(\Omega_p)}\right.$$

$$+\left\|\boldsymbol{\eta}_{p,h}\right\|^2_{H^1(\Omega_p)}+|\mathbf{u}_{f,h}-\partial_t\boldsymbol{\eta}_{p,h}|^2_{a_{BJS}}+\|\mathbf{f}_f\|^2_{L^2(\Omega_f)}+\|\mathbf{f}_p\|^2_{L^2(\Omega_p)}\Big)\,ds. \tag{2.2.21}$$

Adding (2.2.20) and (2.2.21) and taking ϵ_2 small enough, and then ϵ_1 small enough, implies

$$\begin{aligned}
&s_0\|p_{p,h}(t)\|^2_{L^2(\Omega_p)}+\|\boldsymbol{\eta}_{p,h}(t)\|^2_{H^1(\Omega_p)}+\int_0^t\Big(\left|\mathbf{u}_{f,h}-\partial_t\boldsymbol{\eta}_{p,h}\right|^2_{a_{BJS}}\\
&\quad+\|\lambda_h\|^2_{\Lambda_h}+\|p_{f,h}\|^2_{L^2(\Omega_f)}+\|p_{p,h}\|^2_{L^2(\Omega_p)}+\|\mathbf{u}_{f,h}\|^2_{H^1(\Omega_f)}+\|\mathbf{u}_{p,h}\|^2_{L^2(\Omega_p)}\Big)\,ds\\
&\le C\Big(\int_0^t\|\boldsymbol{\eta}_{p,h}\|^2_{H^1(\Omega_p)}\,ds+s_0\|p_{p,h}(0)\|^2_{L^2(\Omega_p)}+\|\boldsymbol{\eta}_{p,h}(0)\|^2_{H^1(\Omega_p)}+\|\mathbf{f}_p(0)\|^2_{L^2(\Omega_p)}\\
&\quad+\int_0^t\Big(\|\mathbf{f}_f\|^2_{L^2(\Omega_f)}+\|\mathbf{f}_p\|^2_{L^2(\Omega_p)}+\|\partial_t\mathbf{f}_p\|^2_{L^2(\Omega_p)}+\|q_f\|^2_{L^2(\Omega_f)}+\|q_p\|^2_{L^2(\Omega_p)}\Big)\,ds\Big).
\end{aligned}\tag{2.2.22}$$

The use of the Gronwall's inequality (1.3.7) implies the following stability result.

Theorem 2.2.2. *The solution of the semi-discrete problem (2.2.1)–(2.2.3) satisfies*

$$\begin{aligned}
&\sqrt{s_0}\|p_{p,h}\|_{L^\infty(0,T;L^2(\Omega_p))}+\|\boldsymbol{\eta}_{p,h}\|_{L^\infty(0,T;H^1(\Omega_p))}+\|\mathbf{u}_{f,h}\|_{L^2(0,T;H^1(\Omega_f))}+\|\mathbf{u}_{p,h}\|_{L^2(0,T;L^2(\Omega_p))}\\
&\quad+\|p_{f,h}\|_{L^2(0,T;L^2(\Omega_f))}+\|p_{p,h}\|_{L^2(0,T;L^2(\Omega_p))}+\|\lambda_h\|_{L^2(0,T;\Lambda_h)}+\left|\mathbf{u}_{f,h}-\partial_t\boldsymbol{\eta}_{p,h}\right|_{L^2(0,T;a_{BJS})}\\
&\le C\sqrt{\exp(T)}\Big(\sqrt{s_0}\|p_{p,h}(0)\|_{L^2(\Omega_p)}+\|\boldsymbol{\eta}_{p,h}(0)\|_{H^2(\Omega_p)}+\|\mathbf{f}_p\|_{L^\infty(0,T;L^2(\Omega_p))}+\|\mathbf{f}_p\|_{L^2(0,T;L^2(\Omega_p))}\\
&\quad+\|\mathbf{f}_f\|_{L^2(0,T;L^2(\Omega_f))}+\|\partial_t\mathbf{f}_p\|_{L^2(0,T;L^2(\Omega_p))}+\|q_f\|_{L^2(0,T;L^2(\Omega_f))}+\|q_p\|_{L^2(0,T;L^2(\Omega_p))}\Big).
\end{aligned}\tag{2.2.23}$$

2.2.3 Error analysis

2.2.3.1 Construction of a weakly-continuous interpolant Let $Q_{\lambda,h}$ be the L^2 -projection operator onto Λ_h, satisfying:

$$\langle\lambda-Q_{\lambda,h}\lambda,\mu_h\rangle_{\Gamma_{fp}}=0, \qquad \forall\,\mu_h\in\Lambda_h \tag{2.2.24}$$

$$\|\lambda-Q_{\lambda,h}\lambda\|_{L^2(\Gamma_{fp})}\le Ch^{\tilde{r}_{k_p}}\|\lambda\|_{H^{\tilde{r}_{k_p}}(\Gamma_{fp})}, \qquad 0\le\tilde{r}_{k_p}\le k_p+1. \tag{2.2.25}$$

Since the discrete Lagrange multiplier space is chosen as $\Lambda_h=\mathbf{V}_{p,h}\cdot\mathbf{n}_p|_{\Gamma_{fp}}$, we have

$$\langle\lambda-Q_{\lambda,h}\lambda,\mathbf{v}_{p,h}\cdot\mathbf{n}_p\rangle_{\Gamma_{fp}}=0, \qquad \forall\,\mathbf{v}_{p,h}\in\mathbf{V}_{p,h}.$$

We note that the discrete seminorm (2.2.7) in Λ_h is well defined for any function in $L^2(\Gamma_{fp})$. It is easy to see that $|\lambda-Q_{\lambda,h}\lambda|_{\Lambda_h}=0$, hence

$$\|\lambda-Q_{\lambda,h}\lambda\|_{\Lambda_h}=\|\lambda-Q_{\lambda,h}\lambda\|_{L^2(\Gamma_{fp})}. \tag{2.2.26}$$

We use the operators defined in Chapter 1 to build an operator onto the space that satisfies the weak continuity of normal velocity condition (2.2.3). Let

$$\mathbf{U} = \{(\mathbf{v}_f, \mathbf{v}_p, \boldsymbol{\xi}_p) \in \mathbf{V}_f \times \mathbf{V}_p \cap H^\theta(\Omega_p) \times \mathbf{X}_p : \mathbf{v}_f \cdot \mathbf{n}_f + \mathbf{v}_p \cdot \mathbf{n}_p + \boldsymbol{\xi}_p \cdot \mathbf{n}_p = 0\}.$$

Consider its discrete analog

$$\mathbf{U}_h = \left\{(\mathbf{v}_{f,h}, \mathbf{v}_{p,h}, \boldsymbol{\xi}_{p,h}) \in \mathbf{V}_{f,h} \times \mathbf{V}_{p,h} \times \mathbf{X}_{p,h} : b_\Gamma\left(\mathbf{v}_{f,h}, \mathbf{v}_{p,h}, \boldsymbol{\xi}_{p,h}; \mu_h\right) = 0, \forall \mu_h \in \Lambda_h\right\}.$$

We will construct an interpolation operator $I_h : \mathbf{U} \to \mathbf{U}_h$ as a triple

$$I_h(\mathbf{v}_f, \mathbf{v}_p, \boldsymbol{\xi}_p) = \left(I_{f,h}\mathbf{v}_f, I_{p,h}\mathbf{v}_p, I_{s,h}\boldsymbol{\xi}_p\right),$$

with the following properties:

$$b_\Gamma\left(I_{f,h}\mathbf{v}_f, I_{p,h}\mathbf{v}_p, I_{s,h}\boldsymbol{\xi}_p; \mu_h\right) = 0, \qquad \forall \mu_h \in \Lambda_h, \tag{2.2.27}$$

$$b_p(I_{p,h}\mathbf{v}_p - \mathbf{v}_p, w_{p,h}) = 0, \qquad \forall w_{p,h} \in W_{p,h}. \tag{2.2.28}$$

We let $I_{f,h} := S_{f,h}$ and $I_{s,h} := S_{s,h}$. To construct $I_{p,h}$, we first consider an auxiliary problem:

$$\begin{cases} \nabla \cdot \nabla \phi = 0 & \text{in } \Omega_p, \\ \phi = 0 & \text{on } \Gamma_p^D, \\ \nabla \phi \cdot \mathbf{n}_p = 0 & \text{on } \Gamma_p^N, \\ \nabla \phi \cdot \mathbf{n}_p = (\mathbf{v}_f - I_{f,h}\mathbf{v}_f) \cdot \mathbf{n}_f + (\boldsymbol{\xi}_p - I_{s,h}\boldsymbol{\xi}_p) \cdot \mathbf{n}_p & \text{on } \Gamma_{fp}. \end{cases} \tag{2.2.29}$$

Let $\mathbf{z} = \nabla \phi$ and define $\mathbf{w} = \mathbf{z} + \mathbf{v}_p$. From (2.2.29) we have

$$\nabla \cdot \mathbf{w} = \nabla \cdot \mathbf{z} + \nabla \cdot \mathbf{v}_p = \nabla \cdot \mathbf{v}_p \text{ in } \Omega_p, \tag{2.2.30}$$

and

$$\begin{aligned} \mathbf{w} \cdot \mathbf{n}_p &= \mathbf{z}_p \cdot \mathbf{n}_p + \mathbf{v}_p \cdot \mathbf{n}_p = \mathbf{v}_f \cdot \mathbf{n}_f - I_{f,h}\mathbf{v}_f \cdot \mathbf{n}_f + \boldsymbol{\xi}_p \cdot \mathbf{n}_p - I_{s,h}\boldsymbol{\xi}_p \cdot \mathbf{n}_p + \mathbf{v}_p \cdot \mathbf{n}_p \\ &= -I_{f,h}\mathbf{v}_f \cdot \mathbf{n}_f - I_{s,h}\boldsymbol{\xi}_p \cdot \mathbf{n}_p \quad \text{on } \Gamma_{fp}. \end{aligned} \tag{2.2.31}$$

We now let

$$I_{p,h}\mathbf{v}_p = \Pi_{p,h}\mathbf{w}. \tag{2.2.32}$$

Next, we verify that the operator $I_h = (I_{f,h}, I_{p,h}, I_{s,h})$ satisfies (2.2.27)–(2.2.28). Using (1.3.12) and (2.2.30), property (2.2.28) follows from

$$(\nabla \cdot I_{p,h}\mathbf{v}_p, w_{p,h})_{\Omega_p} = (\nabla \cdot \Pi_{p,h}\mathbf{w}, w_{p,h})_{\Omega_p} = (\nabla \cdot \mathbf{w}, w_{p,h})_{\Omega_p} = (\nabla \cdot \mathbf{v}_p, w_{p,h})_{\Omega_p}, \quad \forall\, w_{p,h} \in W_{p,h}.$$

Using (2.2.31) and (1.3.13), we have for all $\mu_h \in \Lambda_h$,

$$\begin{aligned}\langle I_{p,h}\mathbf{v}_p \cdot \mathbf{n}_p, \mu_h\rangle_{\Gamma_{fp}} = \langle \Pi_{p,h}\mathbf{w} \cdot \mathbf{n}_p, \mu_h\rangle_{\Gamma_{fp}} &= \langle \mathbf{w} \cdot \mathbf{n}_p, \mu_h\rangle_{\Gamma_{fp}} \\ &= \langle -I_{f,h}\mathbf{v}_f \cdot \mathbf{n}_f - I_{s,h}\boldsymbol{\xi}_p \cdot \mathbf{n}_p, \mu_h\rangle_{\Gamma_{fp}},\end{aligned}$$

which implies (2.2.27).

The approximation properties of the components of I_h are the following.

Lemma 2.2.4. *For all sufficiently smooth $\mathbf{v}_f$, $\mathbf{v}_p$, and $\boldsymbol{\xi}_p$,*

$$\|\mathbf{v}_f - I_{f,h}\mathbf{v}_f\|_{H^1(\Omega_f)} \le Ch^{r_{k_f}} \|\mathbf{v}_f\|_{H^{r_{k_f}+1}(\Omega_f)}, \quad 0 \le r_{k_f} \le k_f, \tag{2.2.33}$$

$$\|\boldsymbol{\xi}_p - I_h^s\boldsymbol{\xi}_p\|_{L^2(\Omega_p)} + h|\boldsymbol{\xi}_p - I_h^s\boldsymbol{\xi}_p|_{H^1(\Omega_p)} \le Ch^{r_{k_s}} \|\boldsymbol{\xi}_p\|_{H^{r_{k_s}}(\Omega_p)}, \quad 1 \le r_{k_s} \le k_s + 1, \tag{2.2.34}$$

$$\begin{aligned}\|\mathbf{v}_p - I_{p,h}\mathbf{v}_p\|_{L^2(\Omega_p)} \le C\left(h^{r_{k_p}} \|\mathbf{v}_p\|_{H^{r_{k_p}}(\Omega_p)} + h^{r_{k_f}} \|\mathbf{v}_f\|_{H^{r_{k_f}+1}(\Omega_f)} + h^{r_{k_s}} \|\boldsymbol{\xi}_p\|_{H^{r_{k_s}+1}(\Omega_p)}\right), \\ 1 \le r_{k_p} \le k_p + 1,\ 0 \le r_{k_f} \le k_f,\ 0 \le r_{k_s} \le k_s.\end{aligned} \tag{2.2.35}$$

Proof. The bounds (2.2.33) and (2.2.34) follow immediately from (1.3.10). Next, using (2.2.32), we have

$$\|\mathbf{v}_p - I_{p,h}\mathbf{v}_p\|_{L^2(\Omega_p)} = \|\mathbf{v}_p - \Pi_{p,h}\mathbf{v}_p - \Pi_{p,h}\mathbf{z}\|_{L^2(\Omega_p)} \le \|\mathbf{v}_p - \Pi_{p,h}\mathbf{v}_p\|_{L^2(\Omega_p)} + \|\Pi_{p,h}\mathbf{z}\|_{L^2(\Omega_p)}. \tag{2.2.36}$$

Elliptic regularity for (2.2.29) [34] implies, for some $0 < \theta \le 1/2$,

$$\|\mathbf{z}\|_{H^\theta(\Omega_p)} \le C\left(\|(\mathbf{v}_f - I_{f,h}\mathbf{v}_f) \cdot \mathbf{n}_f\|_{H^{\theta-1/2}(\Gamma_{fp})} + \|\left(\boldsymbol{\xi}_p - I_{s,h}\boldsymbol{\xi}_p\right) \cdot \mathbf{n}_p\|_{H^{\theta-1/2}(\Gamma_{fp})}\right). \tag{2.2.37}$$

Since $\nabla \cdot \mathbf{z} = 0$ by construction, using (1.3.15), (2.2.37), and (1.3.3), we get

$$\begin{aligned}\|\Pi_{p,h}\mathbf{z}\|_{L^2(\Omega_p)} &\le C\|\mathbf{z}\|_{H^\theta(\Omega_p)} \\ &\le C\left(\|(\mathbf{v}_f - I_{f,h}\mathbf{v}_f) \cdot \mathbf{n}_f\|_{H^{\theta-1/2}(\Gamma_{fp})} + \|\left(\boldsymbol{\xi}_p - I_{s,h}\boldsymbol{\xi}_p\right) \cdot \mathbf{n}_p\|_{H^{\theta-1/2}(\Gamma_{fp})}\right) \\ &\le C\left(\|\mathbf{v}_f - I_{f,h}\mathbf{v}_f\|_{H^1(\Omega_f)} + \|\boldsymbol{\xi}_p - I_{s,h}\boldsymbol{\xi}_p\|_{H^1(\Omega_p)}\right).\end{aligned} \tag{2.2.38}$$

A combination of (2.2.36), (2.2.38), (1.3.14), (2.2.33), and (2.2.34) implies (2.2.35). □

2.2.3.2 Error estimates In this section we derive a priori error estimate for the semi-discrete formulation (2.2.1)-(2.2.3). We recall that, due to (2.1.13), $(\mathbf{u}_f, \mathbf{u}_p, \partial_t \boldsymbol{\eta}_p) \in \mathbf{U}$ and we can apply the interpolant $I_h(\mathbf{u}_f, \mathbf{u}_p, \partial_t \boldsymbol{\eta}_p) = (I_{f,h}\mathbf{u}_f, I_{p,h}\mathbf{u}_p, I_{s,h}\partial_t \boldsymbol{\eta}_p) \in \mathbf{U}_h$ for any $t \in (0, T]$. We introduce the errors for all variables and split them into approximation and discretization errors:

$$
\begin{aligned}
\mathbf{e}_f &:= \mathbf{u}_f - \mathbf{u}_{f,h} = (\mathbf{u}_f - I_{f,h}\mathbf{u}_f) + (I_{f,h}\mathbf{u}_f - \mathbf{u}_{f,h}) := \boldsymbol{\chi}_f + \boldsymbol{\phi}_{f,h},\\
\mathbf{e}_p &:= \mathbf{u}_p - \mathbf{u}_{p,h} = (\mathbf{u}_p - I_{p,h}\mathbf{u}_p) + (I_{p,h}\mathbf{u}_p - \mathbf{u}_{p,h}) := \boldsymbol{\chi}_p + \boldsymbol{\phi}_{p,h},\\
\mathbf{e}_s &:= \boldsymbol{\eta}_p - \boldsymbol{\eta}_{p,h} = (\boldsymbol{\eta}_p - I_{s,h}\boldsymbol{\eta}_p) + (I_{s,h}\boldsymbol{\eta}_p - \boldsymbol{\eta}_{p,h}) := \boldsymbol{\chi}_s + \boldsymbol{\phi}_{s,h},\\
e_{fp} &:= p_f - p_{f,h} = (p_f - Q_{f,h}p_f) + (Q_{f,h}p_f - p_{f,h}) := \chi_{fp} + \phi_{fp,h},\\
e_{pp} &:= p_p - p_{p,h} = (p_p - Q_{p,h}p_p) + (Q_{p,h}p_p - p_{p,h}) := \chi_{pp} + \phi_{pp,h},\\
e_\lambda &:= \lambda - \lambda_h = (\lambda - Q_{\lambda,h}\lambda) + (Q_{\lambda,h}\lambda - \lambda_h) := \chi_\lambda + \phi_{\lambda,h}.
\end{aligned}
\tag{2.2.39}
$$

Subtracting (2.2.1)–(2.2.2) from (2.1.11)–(2.1.12) and summing the two equations, we obtain the error equation

$$
\begin{aligned}
&a_f(\mathbf{e}_f, \mathbf{v}_{f,h}) + a_p^d(\mathbf{e}_p, \mathbf{v}_{p,h}) + a_p^e(\mathbf{e}_s, \boldsymbol{\xi}_{p,h}) + a_{BJS}(\mathbf{e}_f, \partial_t \mathbf{e}_s; \mathbf{v}_{f,h}, \boldsymbol{\xi}_{p,h}) + b_f(\mathbf{v}_{f,h}, e_{fp})\\
&\quad + b_p(\mathbf{v}_{p,h}, e_{pp}) + \alpha b_p(\boldsymbol{\xi}_{p,h}, e_{pp}) + b_\Gamma(\mathbf{v}_{f,h}, \mathbf{v}_{p,h}, \boldsymbol{\xi}_{p,h}; e_\lambda) + (s_0\, \partial_t e_{pp}, w_{p,h})\\
&\quad - \alpha b_p(\partial_t e_s, w_{p,h}) - b_p(\mathbf{e}_p, w_{p,h}) - b_f(\mathbf{e}_f, w_{f,h}) = 0,
\end{aligned}
\tag{2.2.40}
$$

Setting $\mathbf{v}_{f,h} = \boldsymbol{\phi}_{f,h}, \mathbf{v}_{p,h} = \boldsymbol{\phi}_{p,h}, \boldsymbol{\xi}_{p,h} = \partial_t \boldsymbol{\phi}_{s,h}, w_{f,h} = \phi_{fp,h}$, and $w_{p,h} = \phi_{pp,h}$, we have

$$
\begin{aligned}
&a_f(\boldsymbol{\chi}_f, \boldsymbol{\phi}_{f,h}) + a_f(\boldsymbol{\phi}_{f,h}, \boldsymbol{\phi}_{f,h}) + a_p^d(\boldsymbol{\chi}_p, \boldsymbol{\phi}_{p,h}) + a_p^d(\boldsymbol{\phi}_{p,h}, \boldsymbol{\phi}_{p,h}) + a_p^e\left(\boldsymbol{\chi}_s, \partial_t \boldsymbol{\phi}_{s,h}\right)\\
&+ a_p^e\left(\boldsymbol{\phi}_{s,h}, \partial_t \boldsymbol{\phi}_{s,h}\right) + a_{BJS}\left(\boldsymbol{\chi}_f, \partial_t \boldsymbol{\chi}_s; \boldsymbol{\phi}_{f,h}, \partial_t \boldsymbol{\phi}_{s,h}\right) + a_{BJS}\left(\boldsymbol{\phi}_{f,h}, \partial_t \boldsymbol{\phi}_{s,h}; \boldsymbol{\phi}_{f,h}, \partial_t \boldsymbol{\phi}_{s,h}\right)\\
&+ b_f(\boldsymbol{\phi}_{f,h}, \chi_{fp}) + b_f(\boldsymbol{\phi}_{f,h}, \phi_{fp,h}) + b_p(\boldsymbol{\phi}_{p,h}, \chi_{pp}) + b_p(\boldsymbol{\phi}_{p,h}, \phi_{pp,h}) + \alpha b_p\left(\partial_t \boldsymbol{\phi}_{s,h}, \chi_{pp}\right)\\
&+ \alpha b_p\left(\partial_t \boldsymbol{\phi}_{s,h}, \phi_{pp,h}\right) + b_\Gamma\left(\boldsymbol{\phi}_{f,h}, \boldsymbol{\phi}_{p,h}, \partial_t \boldsymbol{\phi}_{s,h}; \chi_\lambda\right) + b_\Gamma\left(\boldsymbol{\phi}_{f,h}, \boldsymbol{\phi}_{p,h}, \partial_t \boldsymbol{\phi}_{s,h}; \phi_{\lambda,h}\right)\\
&+ (s_0\, \partial_t \chi_{pp}, \phi_{pp,h}) + (s_0\, \partial_t \phi_{pp,h}, \phi_{pp,h}) - \alpha b_p\left(\partial_t \boldsymbol{\chi}_s, \phi_{pp,h}\right) - \alpha b_p\left(\partial_t \boldsymbol{\phi}_{s,h}, \phi_{pp,h}\right) - b_p(\boldsymbol{\chi}_p, \phi_{pp,h})\\
&- b_p(\boldsymbol{\phi}_{p,h}, \phi_{pp,h}) - b_f(\boldsymbol{\chi}_f, \phi_{fp,h}) - b_f(\boldsymbol{\phi}_{f,h}, \phi_{fp,h}) = 0.
\end{aligned}
\tag{2.2.41}
$$

The following terms simplify, due to the properties of projection operators (1.3.17),(2.2.24) and (2.2.28):

$$b_p(\boldsymbol{\chi}_p, \phi_{pp,h}) = b_p(\boldsymbol{\phi}_{p,h}, \chi_{pp}) = 0, \quad (s_0\, \partial_t \chi_{pp}, \phi_{pp,h}) = \langle \boldsymbol{\phi}_{p,h} \cdot \mathbf{n}_p, \chi_\lambda \rangle_{\Gamma_{fp}} = 0, \tag{2.2.42}$$

where we also used that $\Lambda_h = \mathbf{V}_{p,h} \cdot \mathbf{n}_p|_{\Gamma_{fp}}$ for the last equality. We also have

$$b_\Gamma\left(\boldsymbol{\phi}_{f,h}, \boldsymbol{\phi}_{p,h}, \partial_t \boldsymbol{\phi}_{s,h}; \phi_{\lambda,h}\right) = 0, \quad b_\Gamma\left(\boldsymbol{\phi}_{f,h}, \boldsymbol{\phi}_{p,h}, \partial_t \boldsymbol{\phi}_{s,h}; \chi_\lambda\right) = \left\langle \boldsymbol{\phi}_{f,h} \cdot \mathbf{n}_f + \partial_t \boldsymbol{\phi}_{s,h} \cdot \mathbf{n}_p, \chi_\lambda \right\rangle_{\Gamma_{fp}},$$

where we have used (2.2.27) and (2.2.3) for the first equality and the last equality in (2.2.42) for the second equality. Using (2.2.16), we write

$$(s_0\, \partial_t \phi_{pp,h}, \phi_{pp,h}) = \frac{1}{2} s_0\, \partial_t \|\phi_{pp,h}\|^2_{L^2(\Omega_p)}, \quad a_p^e\left(\boldsymbol{\phi}_{s,h}, \partial_t \boldsymbol{\phi}_{s,h}\right) = \frac{1}{2} \partial_t a_p^e\left(\boldsymbol{\phi}_{s,h}, \boldsymbol{\phi}_{s,h}\right).$$

Rearranging terms and using the results above, the error equation (2.2.41) becomes

$$\begin{aligned}
&a_f(\boldsymbol{\phi}_{f,h}, \boldsymbol{\phi}_{f,h}) + a_p^d(\boldsymbol{\phi}_{p,h}, \boldsymbol{\phi}_{p,h}) + \frac{1}{2}\partial_t \left(a_p^e(\boldsymbol{\phi}_{s,h}, \boldsymbol{\phi}_{s,h}) + s_0 \|\phi_{pp,h}\|^2_{L^2(\Omega_p)} \right) + \left| \boldsymbol{\phi}_{f,h} - \partial_t \boldsymbol{\phi}_{s,h} \right|^2_{a_{BJS}} \\
&\quad = a_f(\boldsymbol{\chi}_f, \boldsymbol{\phi}_{f,h}) + a_p^d(\boldsymbol{\chi}_p, \boldsymbol{\phi}_{p,h}) + a_p^e\left(\boldsymbol{\chi}_s, \partial_t \boldsymbol{\phi}_{s,h}\right) \\
&\quad + \sum_{j=1}^{d-1} \left\langle \nu \alpha_{BJS} \sqrt{K_j^{-1}} (\boldsymbol{\chi}_f - \partial_t \boldsymbol{\chi}_s) \cdot \mathbf{t}_{f,j}, (\boldsymbol{\phi}_{f,h} - \partial_t \boldsymbol{\phi}_{s,h}) \cdot \mathbf{t}_{f,j} \right\rangle_{\Gamma_{fp}} + b_f(\boldsymbol{\phi}_{f,h}, \chi_{fp}) \\
&\quad + b_f(\boldsymbol{\chi}_f, \phi_{fp,h}) + \alpha b_p(\partial_t \boldsymbol{\phi}_{s,h}, \chi_{pp}) + \alpha b_p(\partial_t \boldsymbol{\chi}_s, \phi_{pp,h}) + \langle \boldsymbol{\phi}_{f,h} \cdot \mathbf{n}_f + \partial_t \boldsymbol{\phi}_{s,h} \cdot \mathbf{n}_p, \chi_\lambda \rangle_{\Gamma_{fp}}.
\end{aligned} \tag{2.2.43}$$

We proceed with bounding the terms on the right-hand side in (2.2.43). Using the continuity of the bilinear forms (2.2.4) and (2.2.5) and inequalities (1.3.2) and (1.3.6), we have

$$\begin{aligned}
a_f(\boldsymbol{\chi}_f, \boldsymbol{\phi}_{f,h}) + a_p^d(\boldsymbol{\chi}_p, \boldsymbol{\phi}_{p,h}) \leq\ & C\epsilon_1^{-1} \left(\|\boldsymbol{\chi}_f\|^2_{H^1(\Omega_f)} + \|\boldsymbol{\chi}_p\|^2_{L^2(\Omega_p)} \right) \\
& + \epsilon_1 \left(\|\boldsymbol{\phi}_{f,h}\|^2_{H^1(\Omega_f)} + \|\boldsymbol{\phi}_{p,h}\|^2_{L^2(\Omega_p)} \right).
\end{aligned} \tag{2.2.44}$$

Similarly, using inequalities (1.3.2), (1.3.3) and (1.3.6), we obtain

$$\begin{aligned}
&\sum_{j=1}^{d-1} \left\langle \nu \alpha_{BJS} \sqrt{K_j^{-1}} (\boldsymbol{\chi}_f - \partial_t \boldsymbol{\chi}_s) \cdot \mathbf{t}_{f,j}, (\boldsymbol{\phi}_{f,h} - \partial_t \boldsymbol{\phi}_{s,h}) \cdot \mathbf{t}_{f,j} \right\rangle_{\Gamma_{fp}} \\
&\qquad \leq \epsilon_1 \left| \boldsymbol{\phi}_{f,h} - \partial_t \boldsymbol{\phi}_{s,h} \right|^2_{a_{BJS}} + C\epsilon_1^{-1} \left(\|\boldsymbol{\chi}_f\|^2_{H^1(\Omega_f)} + \|\partial_t \boldsymbol{\chi}_s\|^2_{H^1(\Omega_p)} \right).
\end{aligned} \tag{2.2.45}$$

Finally, using (1.3.2),(1.3.3) and (1.3.6), we bound the rest of the terms that do not involve $\partial_t \boldsymbol{\phi}_{s,h}$:

$$
\begin{aligned}
&b_f(\boldsymbol{\phi}_{f,h}, \chi_{fp}) + b_f(\boldsymbol{\chi}_f, \phi_{fp,h}) + \alpha b_p\left(\partial_t \boldsymbol{\chi}_s, \phi_{pp,h}\right) + \langle \boldsymbol{\phi}_{f,h} \cdot \mathbf{n}_f, \chi_\lambda \rangle_{\Gamma_{fp}} \leq C\epsilon_2^{-1} \|\boldsymbol{\chi}_f\|^2_{L^2(\Omega_f)} \\
&+ \epsilon_2 \|\phi_{fp,h}\|^2_{L^2(\Omega_f)} + C\epsilon_1^{-1} \left(\|\chi_{fp}\|^2_{L^2(\Omega_f)} + \|\nabla \cdot \partial_t \boldsymbol{\chi}_s\|^2_{L^2(\Omega_p)} + \|\chi_\lambda\|^2_{L^2(\Gamma_{fp})} \right) \\
&+ \epsilon_1 \left(\|\nabla \cdot \boldsymbol{\phi}_{f,h}\|^2_{L^2(\Omega_f)} + \|\phi_{pp,h}\|^2_{L^2(\Omega_p)} + \|\boldsymbol{\phi}_{f,h} \cdot \mathbf{n}_f\|^2_{L^2(\Gamma_{fp})} \right) \\
&\leq \epsilon_1 \left(\|\boldsymbol{\phi}_{f,h}\|^2_{H^1(\Omega_f)} + \|\phi_{pp,h}\|^2_{L^2(\Omega_p)} \right) + C\epsilon_1^{-1} \left(\|\chi_{fp}\|^2_{L^2(\Omega_f)} + \|\partial_t \boldsymbol{\chi}_s\|^2_{H^1(\Omega_p)} + \|\chi_\lambda\|^2_{L^2(\Gamma_{fp})} \right) \\
&+ \epsilon_2 \|\phi_{fp,h}\|^2_{L^2(\Omega_f)} + C\epsilon_2^{-1} \|\boldsymbol{\chi}_f\|^2_{L^2(\Omega_f)}. \qquad (2.2.46)
\end{aligned}
$$

Combining (2.2.43)–(2.2.46), integrating over $[0, t]$, where $0 < t \leq T$, using the coercivity of the bilinear forms (2.2.4)–(2.2.6), and taking ϵ_1 small enough, we obtain

$$
\begin{aligned}
&\|\boldsymbol{\phi}_{s,h}(t)\|^2_{H^1(\Omega_f)} + s_0 \|\phi_{pp,h}(t)\|^2_{L^2(\Omega_p)} + \|\boldsymbol{\phi}_{f,h}\|^2_{L^2(0,t;H^1(\Omega_f))} \\
&\qquad + \|\boldsymbol{\phi}_{p,h}\|^2_{L^2(0,t;L^2(\Omega_p))} + \left|\boldsymbol{\phi}_{f,h} - \partial_t \boldsymbol{\phi}_{s,h}\right|^2_{L^2(0,t;a_{BJS})} \\
&\leq \epsilon_1 \|\phi_{pp,h}\|^2_{L^2(0,t;L^2(\Omega_p))} + C\epsilon_1^{-1} \left(\|\partial_t \boldsymbol{\chi}_s\|^2_{L^2(0,t;H^1(\Omega_p))} + \|\chi_{fp}\|^2_{L^2(0,t;L^2(\Omega_f))} \right. \\
&\qquad \left. + \|\boldsymbol{\chi}_f\|^2_{L^2(0,t;H^1(\Omega_f))} + \|\boldsymbol{\chi}_p\|^2_{L^2(0,t;L^2(\Omega_p))} + \|\chi_\lambda\|^2_{L^2(0,t;L^2(\Gamma_{fp}))} \right) \\
&\qquad + C \int_0^t \left(a_p^e(\boldsymbol{\chi}_s, \partial_t \boldsymbol{\phi}_{s,h}) + \alpha b_p(\partial_t \boldsymbol{\phi}_{s,h}, \chi_{pp}) + \langle \partial_t \boldsymbol{\phi}_{s,h} \cdot \mathbf{n}_p, \chi_\lambda \rangle_{\Gamma_{fp}} \right) ds \\
&+ C \left(\|\boldsymbol{\phi}_{s,h}(0)\|^2_{H^1(\Omega_f)} + s_0 \|\phi_{pp,h}(0)\|^2_{L^2(\Omega_p)} \right) + \epsilon_2 \|\phi_{fp,h}\|^2_{L^2(\Omega_f)} + C\epsilon_2^{-1} \|\boldsymbol{\chi}_f\|^2_{L^2(\Omega_f)}. \qquad (2.2.47)
\end{aligned}
$$

For the initial conditions, we set $p_{p,h}(0) = Q_{p,h} p_{p,0}$ and $\boldsymbol{\eta}_{p,h}(0) = I_{s,h} \boldsymbol{\eta}_{p,0}$, implying

$$
\boldsymbol{\phi}_{s,h}(0) = 0, \qquad \phi_{pp,h}(0) = 0 \qquad (2.2.48)
$$

We next bound the terms on the right involving $\partial_t \boldsymbol{\phi}_{s,h}$. Using integration by parts in time, (1.3.2), (1.3.6), (2.2.6) and (2.2.48), we obtain

$$
\begin{aligned}
&\int_0^t a_p^e \left(\boldsymbol{\chi}_s, \partial_t \boldsymbol{\phi}_{s,h} \right) ds = a_p^e(\boldsymbol{\chi}_s, \boldsymbol{\phi}_{s,h})\big|_0^t - \int_0^t a_p^e \left(\partial_t \boldsymbol{\chi}_s, \boldsymbol{\phi}_{s,h} \right) ds \\
&\quad \leq C \left(\epsilon_1^{-1} \|\boldsymbol{\chi}_s(t)\|^2_{H^1(\Omega_p)} + \|\partial_t \boldsymbol{\chi}_s\|^2_{L^2(0,t;H^1(\Omega_p))} \right) + \epsilon_1 \|\boldsymbol{\phi}_{s,h}(t)\|^2_{H^1(\Omega_p)} + \|\boldsymbol{\phi}_{s,h}\|^2_{L^2(0,t;H^1(\Omega_p))}. \\
&\qquad (2.2.49)
\end{aligned}
$$

Similarly, using (1.3.2), (1.3.3), (1.3.6) and (2.2.48), we have

$$\begin{aligned}
&\int_0^t \left\langle \partial_t \boldsymbol{\phi}_{s,h}\cdot\mathbf{n}_p, \chi_\lambda\right\rangle_{\Gamma_{fp}} ds + \int_0^t \alpha b_p\left(\partial_t\boldsymbol{\phi}_{s,h}, \chi_{pp}\right) ds = \langle \boldsymbol{\phi}_{s,h}\cdot\mathbf{n}_p, \chi_\lambda\rangle_{\Gamma_{fp}}\big|_0^t + \alpha b_p\left(\boldsymbol{\phi}_{s,h}, \partial_t\chi_{pp}\right)\big|_0^t \\
&\quad - \int_0^t \left\langle \boldsymbol{\phi}_{s,h}\cdot\mathbf{n}_p, \partial_t\chi_\lambda\right\rangle_{\Gamma_{fp}} ds - \int_0^t \alpha b_p\left(\boldsymbol{\phi}_{s,h}, \partial_t\chi_{pp}\right) ds \le \epsilon_1 \|\boldsymbol{\phi}_{s,h}(t)\cdot\mathbf{n}_p\|^2_{L^2(\Gamma_{fp})} \\
&\quad + \|\boldsymbol{\phi}_{s,h}\cdot\mathbf{n}_p\|^2_{L^2(0,t;L^2(\Gamma_{fp}))} + \epsilon_1\|\nabla\cdot\boldsymbol{\phi}_{s,h}(t)\|^2_{L^2(\Omega_p)} + \|\nabla\cdot\boldsymbol{\phi}_{s,h}\|^2_{L^2(0,t;L^2(\Omega_p))} \\
&\quad + C\left(\epsilon_1^{-1}\|\chi_\lambda(t)\|^2_{L^2(\Gamma_{fp})} + \|\partial_t\chi_\lambda\|^2_{L^2(0,t;L^2(\Gamma_{fp}))} + \epsilon_1^{-1}\|\chi_{pp}(t)\|^2_{L^2(\Omega_p)} + \|\partial_t\chi_{pp}\|^2_{L^2(0,t;L^2(\Omega_p))}\right) \\
&\le \epsilon_1\|\boldsymbol{\phi}_{s,h}(t)\|^2_{H^1(\Omega_p)} + \|\boldsymbol{\phi}_{s,h}\|^2_{L^2(0,t;H^1(\Omega_p))} \\
&\quad + C\left(\epsilon_1^{-1}\|\chi_\lambda(t)\|^2_{L^2(\Gamma_{fp})} + \|\partial_t\chi_\lambda\|^2_{L^2(0,t;L^2(\Gamma_{fp}))} + \epsilon_1^{-1}\|\chi_{pp}(t)\|^2_{L^2(\Omega_p)} + \|\partial_t\chi_{pp}\|^2_{L^2(0,t;L^2(\Omega_p))}\right).
\end{aligned} \tag{2.2.50}$$

Using (2.2.48)–(2.2.50) and taking ϵ_1 small enough, we obtain from (2.2.47),

$$\begin{aligned}
&\|\boldsymbol{\phi}_{s,h}(t)\|^2_{H^1(\Omega_p)} + s_0\|\phi_{pp,h}(t)\|^2_{L^2(\Omega_p)} + \|\boldsymbol{\phi}_{f,h}\|^2_{L^2(0,t;H^1(\Omega_f))} \\
&\qquad + \|\boldsymbol{\phi}_{p,h}\|^2_{L^2(0,t;L^2(\Omega_p))} + \left|\boldsymbol{\phi}_{f,h} - \partial_t\boldsymbol{\phi}_{s,h}\right|^2_{L^2(0,t;a_{BJS})} \\
&\quad \le \epsilon_1\|\phi_{pp,h}\|^2_{L^2(0,t;L^2(\Omega_p))} + \epsilon_2\|\phi_{fp,h}\|^2_{L^2(0,t;L^2(\Omega_f))} + \|\boldsymbol{\phi}_{s,h}\|^2_{L^2(0,t;H^1(\Omega_p))} \\
&\qquad + C\epsilon_1^{-1}\Big(\|\chi_{fp}\|^2_{L^2(0,t;L^2(\Omega_f))} + \|\boldsymbol{\chi}_f\|^2_{L^2(0,t;H^1(\Omega_f))} + \|\boldsymbol{\chi}_p\|^2_{L^2(0,t;L^2(\Omega_p))} \\
&\qquad\quad + \|\chi_\lambda(t)\|^2_{L^2(\Gamma_{fp})} + \|\chi_{pp}(t)\|^2_{L^2(\Omega_p)} + \|\chi_\lambda\|^2_{L^2(0,t;L^2(\Gamma_{fp}))} + \|\boldsymbol{\chi}_s(t)\|^2_{H^1(\Omega_p)}\Big) \\
&\qquad + C\left(\|\partial_t\boldsymbol{\chi}_s\|^2_{L^2(0,t;H^1(\Omega_p))} + \|\partial_t\chi_\lambda\|^2_{L^2(0,t;L^2(\Gamma_{fp}))} + \|\partial_t\chi_{pp}\|^2_{L^2(0,t;L^2(\Omega_p))}\right).
\end{aligned} \tag{2.2.51}$$

Next, we use the inf-sup condition (2.2.9) with the choice $(w_h, \mu_h) = ((\phi_{fp,h}, \phi_{pp,h}), \phi_{\lambda,h})$ and the error equation obtained by subtracting (2.2.1) from (2.1.11):

$$\begin{aligned}
&C\|((\phi_{fp,h}, \phi_{pp,h}), \phi_{\lambda,h})\|_{W\times\Lambda_h} \\
&\le \sup_{(\mathbf{v}_h,\boldsymbol{\xi}_{p,h})\in\mathbf{V}_h\times\mathbf{X}_{p,h}} \frac{b_f(\mathbf{v}_{f,h},\phi_{fp,h}) + b_p(\mathbf{v}_{p,h},\phi_{pp,h}) + \alpha b_p(\boldsymbol{\xi}_{p,h},\phi_{pp,h}) + b_\Gamma(\mathbf{v}_{f,h},\mathbf{v}_{p,h},\boldsymbol{\xi}_{p,h};\phi_{\lambda,h})}{\|(\mathbf{v}_h,\boldsymbol{\xi}_{p,h})\|_{\mathbf{V}\times\mathbf{X}_p}} \\
&= \sup_{(\mathbf{v}_h,\boldsymbol{\xi}_{p,h})\in\mathbf{V}_h\times\mathbf{X}_{p,h}} \left(\frac{-a_f(\mathbf{e}_f,\mathbf{v}_{f,h}) - a_p^d(\mathbf{e}_p,\mathbf{v}_{p,h}) - a_p^e(\mathbf{e}_s,\boldsymbol{\xi}_{p,h}) - a_{BJS}(\mathbf{e}_f,\partial_t\mathbf{e}_s;\mathbf{v}_{f,h},\boldsymbol{\xi}_{p,h})}{\|(\mathbf{v}_h,\boldsymbol{\xi}_{p,h})\|_{\mathbf{V}\times\mathbf{X}_p}}\right. \\
&\qquad \left. + \frac{-b_f(\mathbf{v}_{f,h},\chi_{fp}) - b_p(\mathbf{v}_{p,h},\chi_{pp}) - \alpha b_p(\boldsymbol{\xi}_{p,h},\chi_{pp}) - b_\Gamma(\mathbf{v}_{f,h},\mathbf{v}_{p,h},\boldsymbol{\xi}_{p,h};\chi_\lambda)}{\|(\mathbf{v}_h,\boldsymbol{\xi}_{p,h})\|_{\mathbf{V}\times\mathbf{X}_p}}\right).
\end{aligned}$$

Due to (1.3.17) and (2.2.24), $b_p(\mathbf{v}_{p,h}, \chi_{pp}) = \langle \mathbf{v}_{p,h} \cdot \mathbf{n}_p, \chi_\lambda \rangle_{\Gamma_{fp}} = 0$. Then, integrating over $[0,t]$ and using the continuity of the bilinear forms (2.2.4)–(2.2.6) and the trace inequality (1.3.3), we get

$$\begin{aligned}
&\epsilon_2(\|\phi_{fp,h}\|^2_{L^2(0,t;L^2(\Omega_f))} + \|\phi_{pp,h}\|^2_{L^2(0,t;L^2(\Omega_p))} + \|\phi_{\lambda,h}\|^2_{L^2(0,t;L^2(\Gamma_{fp}))}) \\
&\quad \le C\epsilon_2 \Big(\|\boldsymbol{\phi}_{f,h}\|^2_{L^2(0,t;H^1(\Omega_f))} + \|\boldsymbol{\phi}_{p,h}\|^2_{L^2(0,t;L^2(\Omega_p))} + \|\boldsymbol{\phi}_{s,h}\|^2_{L^2(0,t;H^1(\Omega_p))} \\
&+ \left|\boldsymbol{\phi}_{f,h} - \partial_t \boldsymbol{\phi}_{s,h}\right|^2_{L^2(0,t;a_{BJS})} + \|\boldsymbol{\chi}_f\|^2_{L^2(0,t;H^1(\Omega_f))} + \|\boldsymbol{\chi}_p\|^2_{L^2(0,t;L^2(\Omega_p))} + \|\partial_t \boldsymbol{\chi}_s\|^2_{L^2(0,t;H^1(\Omega_p))} \\
&\qquad + \|\chi_{fp}\|^2_{L^2(0,t;L^2(\Omega_f))} + \|\chi_{pp}\|^2_{L^2(0,t;L^2(\Omega_p))} + \|\chi_\lambda\|_{L^2(0,t;L^2(\Gamma_{fp}))} \Big). \qquad (2.2.52)
\end{aligned}$$

Adding (2.2.51) and (2.2.52) and taking ϵ_2 small enough, and then ϵ_1 small enough, gives

$$\begin{aligned}
&\|\boldsymbol{\phi}_{s,h}(t)\|^2_{H^1(\Omega_p)} + s_0\|\phi_{pp,h}(t)\|^2_{L^2(\Omega_p)} + \|\boldsymbol{\phi}_{f,h}\|^2_{L^2(0,t;H^1(\Omega_f))} + \|\boldsymbol{\phi}_{p,h}\|^2_{L^2(0,t;L^2(\Omega_p))} \\
&\quad + \left|\boldsymbol{\phi}_{f,h} - \partial_t \boldsymbol{\phi}_{s,h}\right|^2_{L^2(0,t;a_{BJS})} + \|\phi_{fp,h}\|^2_{L^2(0,t;L^2(\Omega_f))} + \|\phi_{pp,h}\|^2_{L^2(0,t;L^2(\Omega_p))} + \|\phi_{\lambda,h}\|^2_{L^2(0,t;\Lambda_h)} \\
&\le C\Big(\|\boldsymbol{\phi}_{s,h}\|^2_{L^2(0,t;H^1(\Omega_p))} + \|\partial_t \boldsymbol{\chi}_s\|^2_{L^2(0,t;H^1(\Omega_p))} + \|\chi_{fp}\|^2_{L^2(0,t;L^2(\Omega_f))} + \|\boldsymbol{\chi}_f\|^2_{L^2(0,t;H^1(\Omega_f))} \\
&\quad + \|\boldsymbol{\chi}_p\|^2_{L^2(0,t;L^2(\Omega_p))} + \|\chi_\lambda(t)\|^2_{L^2(\Gamma_{fp})} + \|\chi_{pp}(t)\|^2_{L^2(\Omega_p)} + \|\chi_\lambda\|^2_{L^2(0,t;L^2(\Gamma_{fp}))} \\
&\quad + \|\partial_t \chi_\lambda\|^2_{L^2(0,t;L^2(\Gamma_{fp}))} + \|d_t \chi_{pp}\|^2_{L^2(0,t;L^2(\Omega_p))} + \|\partial_t \boldsymbol{\chi}_s(t)\|^2_{H^1(\Omega_p)} \Big). \qquad (2.2.53)
\end{aligned}$$

Applying Gronwall's inequality (1.3.7) and using the triangle inequality and the approximation properties (1.3.18)–(1.3.19), (2.2.26) and (2.2.33)–(2.2.35), results in the following theorem.

Theorem 2.2.3. *Assuming sufficient smoothness for the solution of* (2.1.11)–(2.1.13)*, the solution of the semi-discrete problem* (2.2.1)–(2.2.3) *with* $p_{p,h}(0) = Q_{p,h}p_{p,0}$ *and* $\boldsymbol{\eta}_{p,h}(0) = I_{s,h}\boldsymbol{\eta}_{p,0}$ *satisfies*

$$\begin{aligned}
&\|\boldsymbol{\eta}_p - \boldsymbol{\eta}_{p,h}\|_{L^\infty(0,T;H^1(\Omega_p))} + \sqrt{s_0}\|p_p - p_{p,h}\|_{L^\infty(0,T;L^2(\Omega_p))} + \|\mathbf{u}_f - \mathbf{u}_{f,h}\|_{L^2(0,T;H^1(\Omega_f))} \\
&\quad + \|\mathbf{u}_p - \mathbf{u}_{p,h}\|_{L^2(0,T;L^2(\Omega_p))} + \left|(\mathbf{u}_f - \partial_t \boldsymbol{\eta}_p) - (\mathbf{u}_{f,h} - \partial_t \boldsymbol{\eta}_{p,h})\right|_{L^2(0,T;a_{BJS})} \\
&\quad + \|p_f - p_{f,h}\|_{L^2(0,T;L^2(\Omega_f))} + \|p_p - p_{p,h}\|_{L^2(0,T;L^2(\Omega_p))} + \|\lambda - \lambda_h\|_{L^2(0,T;\Lambda_h)} \\
&\le C\sqrt{e^T}\Big(h^{r_{k_f}} \|\mathbf{u}_f\|_{L^2(0,T;H^{r_{k_f}+1}(\Omega_f))} + h^{r_{s_f}} \|p_f\|_{L^2(0,T;H^{r_{s_f}}(\Omega_f))} + h^{r_{k_p}} \|\mathbf{u}_p\|_{L^2(0,T;H^{r_{k_p}}(\Omega_p))} \\
&\quad + h^{\tilde{r}_{k_p}} \left(\|\lambda\|_{L^2(0,T;H^{\tilde{r}_{k_p}}(\Gamma_{fp}))} + \|\lambda\|_{L^\infty(0,T;H^{\tilde{r}_{k_p}}(\Gamma_{fp}))} + \|\partial_t \lambda\|_{L^2(0,T;H^{\tilde{r}_{k_p}}(\Gamma_{fp}))} \right)
\end{aligned}$$

$$+ h^{r_{s_p}} \left(\|p_p\|_{L^\infty(0,T;H^{r_{s_p}}(\Omega_p))} + \|p_p\|_{L^2(0,T;H^{r_{s_p}}(\Omega_p))} + \|\partial_t p_p\|_{L^2(0,T;H^{r_{s_p}}(\Omega_p))} \right)$$
$$+ h^{r_{k_s}} \left(\|\boldsymbol{\eta}_p\|_{L^\infty(0,T;H^{r_{k_s}+1}(\Omega_p))} + \left\|\boldsymbol{\eta}_p\right\|_{L^2(0,T;H^{r_{k_s}+1}(\Omega_p))} + \left\|\partial_t \boldsymbol{\eta}_p\right\|_{L^2(0,T;H^{r_{k_s}+1}(\Omega_p))} \right) \Bigg),$$
$$0 \le r_{k_f} \le k_f,\ 0 \le r_{s_f} \le s_f + 1,\ 1 \le \{r_{k_p},\, \tilde{r}_{k_p}\} \le k_p + 1,\ 0 \le r_{s_p} \le s_p + 1,\ 0 \le r_{k_s} \le k_s.$$

2.3 FULLY DISCRETE FORMULATION

For the time discretization we employ the backward Euler method. Let τ be the time step, $T = N\tau$, and let $t_n = n\tau$, $0 \le n \le N$. Let $d_\tau u^n := \tau^{-1}(u^n - u^{n-1})$ be the first order (backward) discrete time derivative, where $u^n := u(t_n)$. Then the fully discrete model reads: given $p^0_{p,h} = p_{p,h}(0)$ and $\boldsymbol{\eta}^0_{p,h} = \boldsymbol{\eta}_{p,h}(0)$, find $\mathbf{u}^n_{f,h} \in \mathbf{V}_{f,h}$, $p^n_{f,h} \in W_{f,h}$, $\mathbf{u}^n_{p,h} \in \mathbf{V}_{p,h}$, $p^n_{p,h} \in W_{p,h}$, $\boldsymbol{\eta}^n_{p,h} \in \mathbf{X}_{p,h}$, and $\lambda^n_h \in \Lambda_h$, $1 \le n \le N$, such that for all $\mathbf{v}_{f,h} \in \mathbf{V}_{f,h}$, $w_{f,h} \in W_{f,h}$, $\mathbf{v}_{p,h} \in \mathbf{V}_{p,h}$, $w_{p,h} \in W_{p,h}$, $\boldsymbol{\xi}_{p,h} \in \mathbf{X}_{p,h}$, and $\mu_h \in \Lambda_h$,

$$a_f(\mathbf{u}^n_{f,h}, \mathbf{v}_{f,h}) + a^d_p(\mathbf{u}^n_{p,h}, \mathbf{v}_{p,h}) + a^e_p(\boldsymbol{\eta}^n_{p,h}, \boldsymbol{\xi}_{p,h}) + a_{BJS}(\mathbf{u}^n_{f,h}, d_\tau \boldsymbol{\eta}^n_{p,h}; \mathbf{v}_{f,h}, \boldsymbol{\xi}_{p,h}) + b_f(\mathbf{v}_{f,h}, p^n_{f,h})$$
$$+ b_p(\mathbf{v}_{p,h}, p^n_{p,h}) + \alpha b_p(\boldsymbol{\xi}_{p,h}, p^n_{p,h}) + b_\Gamma(\mathbf{v}_{f,h}, \mathbf{v}_{p,h}, \boldsymbol{\xi}_{p,h}; \lambda^n_h) = (\mathbf{f}^n_f, \mathbf{v}_{f,h})_{\Omega_f} + (\mathbf{f}^n_p, \boldsymbol{\xi}_{p,h})_{\Omega_p}, \tag{2.3.1}$$

$$(s_0 d_\tau p^n_{p,h}, w_{p,h})_{\Omega_p} - \alpha b_p(d_\tau \boldsymbol{\eta}^n_{p,h}, w_{p,h}) - b_p(\mathbf{u}^n_{p,h}, w_{p,h}) - b_f(\mathbf{u}^n_{f,h}, w_{f,h})$$
$$= (q^n_f, w_{f,h})_{\Omega_f} + (q^n_p, w_{p,h})_{\Omega_p}, \tag{2.3.2}$$

$$b_\Gamma(\mathbf{u}^n_{f,h}, \mathbf{u}^n_{p,h}, d_\tau \boldsymbol{\eta}^n_{p,h}; \mu_h) = 0. \tag{2.3.3}$$

We will need the discrete-in-time norms, defined as follows:

$$\|\phi\|^2_{l^2(0,T;X)} := \left(\tau \sum_{n=1}^{N} \|\phi^n\|^2_X \right)^{1/2}, \qquad \|\phi\|^2_{l^\infty(0,T;X)} := \max_{0 \le n \le N} \|\phi^n\|_X.$$

Next, we state the main results for the formulation (2.3.1)-(2.3.3).

Theorem 2.3.1. *The solution of fully discrete problem (2.3.1)-(2.3.3) satisfies*

$$\begin{aligned}
&\sqrt{s_0}\|p_{p,h}\|_{l^\infty(0,T;L^2(\Omega_p))} + \|\boldsymbol{\eta}_{p,h}\|_{l^\infty(0,T;H^1(\Omega_p))} + \|\mathbf{u}_{f,h}\|_{l^2(0,T;H^1(\Omega_f))} + \|\mathbf{u}_{p,h}\|_{l^2(0,T;L^2(\Omega_p))} \\
&\quad + |\mathbf{u}_{f,h} - d_\tau\boldsymbol{\eta}_{p,h}|_{l^2(0,T;a_{BJS})} + \|p_{p,h}\|_{l^2(0,T;L^2(\Omega_p))} + \|p_{f,h}\|_{l^2(0,T;L^2(\Omega_f))} + \|\lambda_h\|_{l^2(0,T;\Lambda_h)} \\
&\quad + \tau\left(\sqrt{s_0}\|d_\tau p_{p,h}\|_{l^2(0,T;L^2(\Omega_p))} + \|d_\tau\boldsymbol{\eta}_{p,h}\|_{l^2(0,T;H^1(\Omega_p))}\right) \\
&\leq C\sqrt{\exp(T)}\Big(\sqrt{s_0}\|p^0_{p,h}\|_{L^2(\Omega_p)} + \|\boldsymbol{\eta}^0_{p,h}\|_{H^1(\Omega_p)} + \|\mathbf{f}_p\|_{l^\infty(0,T;L^2(\Omega_p))} + \|\partial_t\mathbf{f}_p\|_{L^2(0,T;L^2(\Omega_p))} \\
&\quad + \|\mathbf{f}_f\|_{l^2(0,T;L^2(\Omega_f))} + \|q_f\|_{l^2(0,T;L^2(\Omega_f))} + \|q_p\|_{l^2(0,T;L^2(\Omega_p))} + \|\mathbf{f}_p\|_{l^2(0,T;L^2(\Omega_p))}\Big).
\end{aligned}$$

Proof. We choose

$$(\mathbf{v}_{f,h}, w_{f,h}, \mathbf{v}_{p,h}, w_{p,h}, \boldsymbol{\xi}_{p,h}, \mu_h) = (\mathbf{u}^n_{f,h}, p^n_{f,h}, \mathbf{u}^n_{p,h}, p^n_{p,h}, d_\tau\boldsymbol{\eta}^n_{p,h}, \lambda_h)$$

in (2.3.1)–(2.3.3) and use the discrete analog of (2.2.16)

$$\int_S u^n d_\tau\phi^n\, dA = \frac{1}{2}d_\tau\|\phi^n\|^2_{L^2(S)} + \frac{1}{2}\tau\|d_\tau\phi^n\|^2_{L^2(S)}. \tag{2.3.4}$$

to obtain the energy equality

$$\begin{aligned}
&\frac{1}{2}d_\tau\left(s_0\|p^n_{p,h}\|^2_{L^2(\Omega_p)} + a^e_p(\boldsymbol{\eta}^n_{p,h}, \boldsymbol{\eta}^n_{p,h})\right) + \frac{\tau}{2}\left(s_0\|d_\tau p^n_{p,h}\|^2_{L^2(\Omega_p)} + a^e_p(d_\tau\boldsymbol{\eta}^n_{p,h}, d_\tau\boldsymbol{\eta}^n_{p,h})\right) \\
&\quad + a_f(\mathbf{u}^n_{f,h}, \mathbf{u}^n_{f,h}) + a^d_p(\mathbf{u}^n_{p,h}, \mathbf{u}^n_{p,h}) + |\mathbf{u}^n_{f,h} - d_\tau\boldsymbol{\eta}^n_{p,h}|^2_{a_{BJS}} = \mathcal{F}(t_n).
\end{aligned} \tag{2.3.5}$$

The right-hand side can be bounded as follows, using inequalities (1.3.2) and (1.3.6),

$$\begin{aligned}
\mathcal{F}(t_n) &= (\mathbf{f}_f(t_n), \mathbf{u}^n_{f,h}) + (\mathbf{f}_p(t_n), d_\tau\boldsymbol{\eta}^n_{p,h}) + (q_f(t_n), p^n_{f,h}) + (q_p(t_n), p^n_{p,h}) \\
&\leq (\mathbf{f}_p(t_n), d_\tau\boldsymbol{\eta}^n_{p,h}) + \frac{\epsilon_1}{2}\left(\|\mathbf{u}^n_{f,h}\|^2_{L^2(\Omega_f)} + \|p^n_{f,h}\|^2_{L^2(\Omega_f)} + \|p^n_{p,h}\|^2_{L^2(\Omega_p)}\right) \\
&\quad + C\frac{1}{2\epsilon_1}\left(\|\mathbf{f}_f(t_n)\|^2_{L^2(\Omega_f)} + \|q_f(t_n)\|^2_{L^2(\Omega_f)} + \|q_p(t_n)\|^2_{L^2(\Omega_p)}\right).
\end{aligned} \tag{2.3.6}$$

Combining (2.3.5) and (2.3.6), summing up over the time index $n = 1, ..., N$, multiplying by τ and using the coercivity of the bilinear forms (2.2.4)–(2.2.6), we obtain

$$\begin{aligned}
&s_0\|p^N_{p,h}\|^2_{L^2(\Omega_p)} + \|\boldsymbol{\eta}^N_{p,h}\|^2_{H^1(\Omega_p)} + \tau\sum_{n=1}^{N}\left(\|\mathbf{u}^n_{f,h}\|^2_{H^1(\Omega_f)} + \|\mathbf{u}^n_{p,h}\|^2_{L^2(\Omega_p)} + |\mathbf{u}^n_{f,h} - d_\tau\boldsymbol{\eta}^n_{p,h}|^2_{a_{BJS}}\right) \\
&+ \tau^2\sum_{n=1}^{N}\left(s_0\|d_\tau p^n_{p,h}\|^2_{L^2(\Omega_p)} + \|d_\tau\boldsymbol{\eta}^n_{p,h}\|^2_{H^1(\Omega_p)}\right) \leq C\left(s_0\|p^0_{p,h}\|^2_{L^2(\Omega_p)} + \|\boldsymbol{\eta}^0_{p,h}\|^2_{H^1(\Omega_p)}\right.
\end{aligned}$$

$$+\epsilon_1\tau\sum_{n=1}^{N}\Big(\|\mathbf{u}_{f,h}^n\|^2_{L^2(\Omega_f)}+\|p_{f,h}^n\|^2_{L^2(\Omega_f)}+\|p_{p,h}^n\|^2_{L^2(\Omega_p)}\Big)+\tau\sum_{n=1}^{N}(\mathbf{f}_p(t_n),d_\tau\boldsymbol{\eta}_{p,h}^n)$$
$$+\epsilon_1^{-1}\tau\sum_{n=1}^{N}\Big(\|\mathbf{f}_f(t_n)\|^2_{L^2(\Omega_f)}+\|q_f(t_n)\|^2_{L^2(\Omega_f)}+\|q_p(t_n)\|^2_{L^2(\Omega_p)}\Big)\Big). \tag{2.3.7}$$

To bound the last term on the right we use summation by parts:

$$\begin{aligned}\tau\sum_{n=1}^{N}(\mathbf{f}_p(t_n),d_\tau\boldsymbol{\eta}_{p,h}^n)&=(\mathbf{f}_p(t_N),\boldsymbol{\eta}_{p,h}^N)-(\mathbf{f}_p(0),\boldsymbol{\eta}_{p,h}^0)-\tau\sum_{n=1}^{N-1}(d_\tau\mathbf{f}_p^n,\boldsymbol{\eta}_{p,h}^n)\\&\le\frac{\epsilon_1}{2}\|\boldsymbol{\eta}_{p,h}^N\|^2_{L^2(\Omega_p)}+\frac{1}{2\epsilon_1}\|\mathbf{f}_p(t_N)\|^2_{L^2(\Omega_p)}+\frac{\tau}{2}\sum_{n=1}^{N-1}\|\boldsymbol{\eta}_{p,h}^n\|^2_{L^2(\Omega_p)}\\&\quad+\frac{1}{2}\left(\|\boldsymbol{\eta}_{p,h}^0\|^2_{L^2(\Omega_p)}+\|\mathbf{f}_p(0)\|^2_{L^2(\Omega_p)}+\tau\sum_{n=1}^{N-1}\|d_\tau\mathbf{f}_p^n\|^2_{L^2(\Omega_p)}\right).\end{aligned} \tag{2.3.8}$$

Next using the inf-sup condition (2.2.9) for $(p_{f,h}^n,p_{p,h}^n,\lambda_h^n)$ we obtain, in a similar way to (2.2.21),

$$\begin{aligned}&\epsilon_2\tau\sum_{n=1}^{N}\Big(\|p_{f,h}^n\|^2_{L^2(\Omega_f)}+\|p_{p,h}^n\|^2_{L^2(\Omega_p)}+\|\lambda_h^n\|^2_{\Lambda_h}\Big)\\&\quad\le C\epsilon_2\tau\sum_{n=1}^{N}\Big(\|\mathbf{f}_f(t_n)\|^2_{L^2(\Omega_f)}+\|\mathbf{f}_p(t_n)\|^2_{L^2(\Omega_p)}+\|\mathbf{u}_{f,h}^n\|^2_{H^1(\Omega_f)}+\|\mathbf{u}_{p,h}^n\|^2_{L^2(\Omega_p)}\\&\qquad+\|\boldsymbol{\eta}_{p,h}^n\|^2_{H^1(\Omega_p)}+|\mathbf{u}_{f,h}^n-d_\tau\boldsymbol{\eta}_{p,h}^n|^2_{a_{BJS}}\Big).\end{aligned} \tag{2.3.9}$$

Combining (2.3.7)–(2.3.9), and taking ϵ_2 small enough, and then ϵ_1 small enough, and using discrete Gronwall's (1.3.8) with $a_n=\|\boldsymbol{\eta}_{p,h}^n\|^2_{H^1(\Omega_p)}$, gives

$$\begin{aligned}&s_0\|p_{p,h}^N\|^2_{L^2(\Omega_p)}+\|\boldsymbol{\eta}_{p,h}^N\|^2_{H^1(\Omega_p)}+\tau\sum_{n=1}^{N}\Big[\|\mathbf{u}_{f,h}^n\|^2_{H^1(\Omega_f)}+\|\mathbf{u}_{p,h}^n\|^2_{L^2(\Omega_p)}+|\mathbf{u}_{f,h}^n-d_\tau\boldsymbol{\eta}_{p,h}^n|^2_{a_{BJS}}\Big]\\&\quad+\tau^2\sum_{n=1}^{N}\Big[s_0\|d_\tau p_{p,h}^n\|^2_{L^2(\Omega_p)}+\|d_\tau\boldsymbol{\eta}_{p,h}^n\|^2_{H^1(\Omega_p)}\Big]+\tau\sum_{n=1}^{N}\Big[\|p_{p,h}^n\|^2_{L^2(\Omega_p)}+\|p_{f,h}^n\|^2_{L^2(\Omega_f)}+\|\lambda_h^n\|^2_{\Lambda_h}\Big]\\&\le C\exp(T)\Big(s_0\|p_{p,h}^0\|^2_{L^2(\Omega_p)}+\|\boldsymbol{\eta}_{p,h}^0\|^2_{H^1(\Omega_p)}+\|\mathbf{f}_p(0)\|^2_{L^2(\Omega_p)}\\&\quad+\tau\sum_{n=1}^{N}\Big[\|\mathbf{f}_f(t_n)\|^2_{L^2(\Omega_f)}+\|\mathbf{f}_p(t_n)\|^2_{L^2(\Omega_p)}+\|q_f(t_n)\|^2_{L^2(\Omega_f)}+\|q_p(t_n)\|^2_{L^2(\Omega_p)}+\|d_\tau\mathbf{f}_p\|^2_{L^2(\Omega_p)}\Big]\Big),\end{aligned}$$

which implies the statement of the theorem using the appropriate space-time norms. □

Theorem 2.3.2. *Assuming sufficient smoothness for the solution of (2.1.11)–(2.1.13), the solution of the fully discrete problem (2.3.1)-(2.3.3) satisfies*

$$
\begin{aligned}
&\sqrt{s_0}\|p_p - p_{p,h}\|_{l^\infty(0,T;L^2(\Omega_p))} + \|\boldsymbol{\eta} - \boldsymbol{\eta}_{p,h}\|_{l^\infty(0,T;H^1(\Omega_p))} + \|\mathbf{u}_f - \mathbf{u}_{f,h}\|_{l^2(0,T;H^1(\Omega_f))} \\
&\quad + \|\mathbf{u}_p - \mathbf{u}_{p,h}\|_{l^2(0,T;L^2(\Omega_p))} + |\mathbf{u}_f - d_\tau\boldsymbol{\eta}_p - (\mathbf{u}_{f,h} - d_\tau\boldsymbol{\eta}_{p,h})|_{l^2(0,T;a_{BJS})} \\
&\quad + \|p_f - p_{f,h}\|_{l^2(0,T;L^2(\Omega_f))} + \|p_p - p_{p,h}\|_{l^2(0,T;L^2(\Omega_p))} + \|\lambda - \lambda_h\|_{l^2(0,T;\Lambda_h)} \\
&\quad + \sqrt{\tau}\Big(\sqrt{s_0}\|d_\tau(p_p - p_{p,h})\|_{l^2(0,T;L^2(\Omega_p))} + \|d_\tau(\boldsymbol{\eta}_p - \boldsymbol{\eta}_{p,h})\|_{l^2(0,T;H^1(\Omega_p))}\Big) \\
&\leq C\sqrt{\exp(T)}\Big(h^{r_{k_f}}\|\mathbf{u}_f\|_{l^2(0,T;H^{r_{k_f}+1}(\Omega_f))} + h^{r_{s_f}}\|p_f\|_{l^2(0,T;H^{r_{s_f}}(\Omega_f))} + h^{r_{k_p}}\|\mathbf{u}_p\|_{l^2(0,T;H^{r_{k_p}}(\Omega_p))} \\
&\quad + h^{\tilde{r}_{k_p}}\left(\|\lambda\|_{l^2(0,T;H^{\tilde{r}_{k_p}}(\Gamma_{fp}))} + \|\lambda\|_{l^\infty(0,T;H^{\tilde{r}_{k_p}}(\Gamma_{fp}))} + \|\partial_t\lambda\|_{L^2(0,T;H^{\tilde{r}_{k_p}}(\Gamma_{fp}))}\right) \\
&\quad + h^{r_{s_p}}\left(\|p_p\|_{l^\infty(0,T;H^{r_{s_p}}(\Omega_p))} + \|p_p\|_{l^2(0,T;H^{r_{s_p}}(\Omega_p))} + \|\partial_t p_p\|_{L^2(0,T;H^{r_{s_p}}(\Omega_p))}\right) \\
&\quad + h^{r_{k_s}}\left(\|\boldsymbol{\eta}_p\|_{l^\infty(0,T;H^{r_{k_s}+1}(\Omega_p))} + \|\boldsymbol{\eta}_p\|_{l^2(0,T;H^{r_{k_s}+1}(\Omega_p))} + \|\partial_t\boldsymbol{\eta}_p\|_{L^2(0,T;H^{r_{k_s}+1}(\Omega_p))}\right) \\
&\quad + \tau\left(\sqrt{s_0}\|\partial_{tt}p_p\|_{L^2(0,T;L^2(\Omega_p))} + \|\partial_{tt}\boldsymbol{\eta}_p\|_{L^2(0,T;H^1(\Omega_p))}\right)\Big),
\end{aligned}
$$

$$
0 \leq r_{k_f} \leq k_f,\ 0 \leq r_{s_f} \leq s_f + 1,\ 1 \leq \{r_{k_p}, \tilde{r}_{k_p}\} \leq k_p + 1,\ 0 \leq r_{s_p} \leq s_p + 1,\ 0 \leq r_{k_s} \leq k_s.
$$

For the sake of space, we do not present the proof of Theorem 2.3.2. The error equations are obtained by subtracting the first two equations of the fully discrete formulation (2.3.1)–(2.3.2) from the their continuous counterparts (2.1.11)–(2.1.12):

$$
\begin{aligned}
&a_f(\mathbf{e}_f^n, \mathbf{v}_{f,h}) + a_p^d(\mathbf{e}_p^n, \mathbf{v}_{p,h}) + a_p^e(\mathbf{e}_s^n, \boldsymbol{\xi}_{p,h}) + a_{BJS}(\mathbf{e}_f^n, d_\tau\mathbf{e}_s^n; \mathbf{v}_{f,h}, \boldsymbol{\xi}_{p,h}) + b_f(\mathbf{v}_{f,h}, e_{fp}^n) \\
&\quad + b_p(\mathbf{v}_{p,h}, e_{pp}^n) + \alpha b_p(\boldsymbol{\xi}_{p,h}, e_{pp}^n) + b_\Gamma(\mathbf{v}_{f,h}, \mathbf{v}_{p,h}, \boldsymbol{\xi}_{p,h}; e_\lambda^n) + \left(s_0\, d_\tau e_{pp}^n, w_{p,h}\right) - \alpha b_p(d_\tau e_s^n, w_{p,h}) \\
&\quad - b_p(\mathbf{e}_p^n, w_{p,h}) - b_f(\mathbf{e}_f^n, w_{f,h}) = (s_0 r_n(p_p), w_{p,h}) + a_{BJS}(0, r_n(\boldsymbol{\eta}_p); \mathbf{v}_{f,h}, \boldsymbol{\xi}_{p,h}) \\
&\quad - \alpha b_p(r_n(\boldsymbol{\eta}_p), w_{p,h}),
\end{aligned}
\tag{2.3.10}
$$

where r_n denotes the difference between the time derivative and its discrete analog:

$$
r_n(\theta) = \partial_t\theta(t_n) - d_\tau\theta^n.
$$

It is easy to see that [20, Lemma 4] for sufficiently smooth θ,

$$
\tau\sum_{n=1}^{N}\|r_n(\theta)\|_{H^k(S)}^2 \leq C\tau^2\|\partial_{tt}\theta\|_{L^2(0,T;H^k(S))}^2.
$$

The proof of Theorem 2.3.2 follows the structure of the proof of Theorem 2.2.3, using discrete-in-time arguments as in the proof of Theorem 2.3.1.

2.4 NUMERICAL RESULTS

In this subsection, we present results from several computational experiments in two dimensions. The fully discrete method (2.3.1)–(2.3.3) has been implemented using the finite element package FreeFem++ [59]. The first test confirms the theoretical convergence rates for the problem using an analytical solution. The second and third examples show the applicability of the method to modeling fluid flow in an irregularly shaped fractured reservoir with physical parameters, while the last one performs an analysis for the robustness of the method with respect to various parameters.

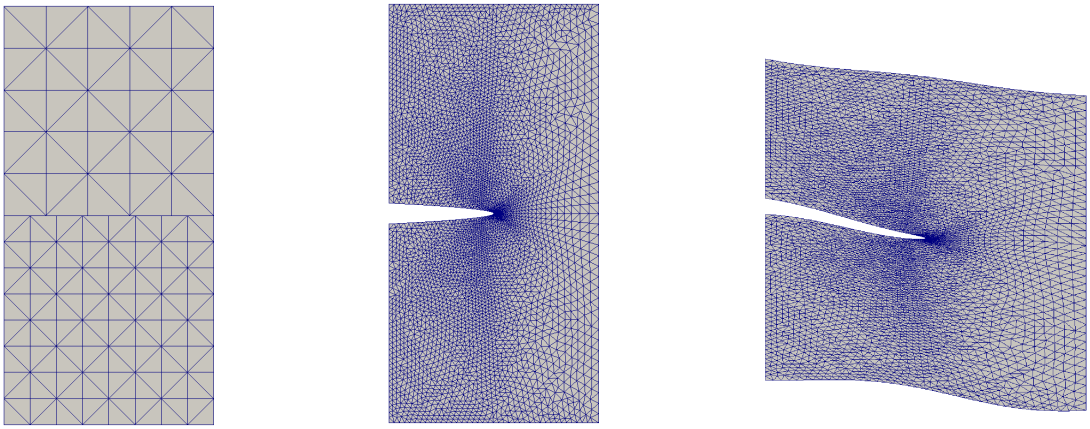

(a) Computational domain Ω in Ex. 1, non-matching grids

(b) Reference domain $\hat{\Omega}$ in Ex. 2, 3, and 4

(c) Physical domain Ω in Ex. 2 and 4

Figure 1: Computational domains.

2.4.1 Convergence test

In this test we study the convergence for the space discretization using an analytical solution. The domain is $\Omega = [0,1] \times [-1,1]$, see Figure 1a. We associate the upper half with the Stokes flow, while the lower half represents the flow in the poroelastic structure governed by the Biot system. The appropriate interface conditions are enforced along the interface $y = 0$.

The solution in the Stokes region is

$$\mathbf{u}_f = \pi \cos(\pi t) \begin{pmatrix} -3x + \cos(y) \\ y + 1 \end{pmatrix}, \quad p_f = \mathbf{e}^t \sin(\pi x) \cos(\frac{\pi y}{2}) + 2\pi \cos(\pi t).$$

The Biot solution is chosen accordingly to satisfy the interface conditions (1.2.7)-(1.2.9):

$$\mathbf{u}_p = \pi \mathbf{e}^t \begin{pmatrix} \cos(\pi x) \cos(\frac{\pi y}{2}) \\ \frac{1}{2} \sin(\pi x) \sin(\frac{\pi y}{2}) \end{pmatrix}, \quad p_p = \mathbf{e}^t \sin(\pi x) \cos(\frac{\pi y}{2}), \quad \boldsymbol{\eta}_p = \sin(\pi t) \begin{pmatrix} -3x + \cos(y) \\ y + 1 \end{pmatrix}.$$

The right hand side functions $\mathbf{f}_f$, q_f, $\mathbf{f}_p$ and q_p are computed from (1.2.2)–(1.2.6) using the above solution. The model problem is then complemented with the appropriate Dirichlet boundary conditions and initial data. The total simulation time for this test case is $T = 0.01$s and the time step is $\Delta t = 10^{-3}$s. The time step is sufficiently small, so that the time discretization error does not affect the convergence rates.

We study the convergence for two choices of finite element spaces. The lower order choice is the MINI elements $\mathcal{P}_1^b - \mathcal{P}_1$ for Stokes, the Raviart-Thomas $\mathcal{RT}_0 - \mathcal{P}_0$ and continuous Lagrangian $\mathcal{P}_1$ elements for the Biot system, and piecewise constant Lagrange multiplier $\mathcal{P}_0$. In this case $k_f = 1$, $s_f = 1$, $k_p = 0$, $s_p = 0$, and $k_s = 1$, so Theorem 2.3.2 implies first order of convergence for all variables. The higher order choice is the Taylor-Hood $\mathcal{P}_2 - \mathcal{P}_1$ for Stokes, the Raviart-Thomas $\mathcal{RT}_1 - \mathcal{P}_1^{dc}$ and $\mathcal{P}_2$ for Biot, and $\mathcal{P}_1^{dc}$ for the Lagrange multiplier, with $k_f = 2$, $s_f = 1$, $k_p = 1$, $s_p = 1$, and $k_s = 2$, in which case second order convergence rate for all variables is expected. These theoretical results are verified by the rates shown in the Table 1, where the errors were computed on a sequence of refined meshes, which are matching along the interface.

We also perform a convergence test with the lower order choice of finite elements on non-matching grids along the interface. We prescribe the ratio between mesh characteristic sizes to be $h_{Stokes} = \frac{5}{8} h_{Biot}$ as shown in Figure 1a. According to the results shown in Table 2, first order convergence is observed for all variables, which agrees with Theorem 2.3.2.

$\mathcal{P}_1^b - \mathcal{P}_1$, $\mathcal{RT}_0 - \mathcal{P}_0$, $\mathcal{P}_1$ and $\mathcal{P}_0$										
	$\|\mathbf{e}_f\|_{l^2(H^1(\Omega_f))}$		$\|e_{fp}\|_{l^2(L^2(\Omega_f))}$		$\|\mathbf{e}_p\|_{l^2(L^2(\Omega_p))}$		$\|e_{pp}\|_{l^\infty(L^2(\Omega_p))}$		$\|\mathbf{e}_s\|_{l^\infty(H_1(\Omega_p))}$	
h	error	rate	error	rate	error	rate	error	rate	error	rate
1/8	8.96E-03	–	2.61E-03	–	1.05E-01	–	1.03E-01	–	5.09E-02	–
1/16	4.47E-03	1.0	8.33E-04	1.6	5.23E-02	1.0	5.17E-02	1.0	1.34E-02	1.9
1/32	2.24E-03	1.0	2.76E-04	1.6	2.61E-02	1.0	2.59E-02	1.0	3.94E-03	1.8
1/64	1.12E-03	1.0	9.43E-05	1.6	1.31E-02	1.0	1.29E-02	1.0	1.43E-03	1.5
1/128	5.59E-04	1.0	3.28E-05	1.5	6.53E-03	1.0	6.47E-03	1.0	6.32E-04	1.2
$\mathcal{P}_2 - \mathcal{P}_1$, $\mathcal{RT}_1 - \mathcal{P}_1^{dc}$, $\mathcal{P}_2$ and $\mathcal{P}_1^{dc}$										
	$\|\mathbf{e}_f\|_{l^2(H^1(\Omega_f))}$		$\|e_{fp}\|_{l^2(L^2(\Omega_f))}$		$\|\mathbf{e}_p\|_{l^2(L^2(\Omega_p))}$		$\|e_{pp}\|_{l^\infty(L^2(\Omega_p))}$		$\|\mathbf{e}_s\|_{l^\infty(H_1(\Omega_p))}$	
h	error	rate	error	rate	error	rate	error	rate	error	rate
1/8	1.25E-04	–	1.31E-03	–	1.82E-02	–	1.60E-02	–	1.54E-01	–
1/16	2.90E-05	2.1	3.25E-04	2.0	4.38E-03	2.1	4.01E-03	2.0	3.82E-02	2.0
1/32	7.06E-06	2.0	8.07E-05	2.0	1.08E-03	2.0	1.00E-03	2.0	9.51E-03	2.0
1/64	1.77E-06	2.0	1.97E-05	2.0	2.67E-04	2.0	2.51E-04	2.0	2.37E-03	2.0
1/128	4.73E-07	1.9	4.51E-06	2.1	6.47E-05	2.0	6.23E-05	2.0	5.89E-04	2.0

Table 1: Example 1: relative numerical errors and convergence rates on matching grids.

$\mathcal{P}_1^b - \mathcal{P}_1$, $\mathcal{RT}_0 - \mathcal{P}_0$, $\mathcal{P}_1$ and $\mathcal{P}_0$										
	$\|\mathbf{e}_f\|_{l^2(H^1(\Omega_f))}$		$\|e_{fp}\|_{l^2(L^2(\Omega_f))}$		$\|\mathbf{e}_p\|_{l^2(L^2(\Omega_p))}$		$\|e_{pp}\|_{l^\infty(L^2(\Omega_p))}$		$\|\mathbf{e}_s\|_{l^\infty(H_1(\Omega_p))}$	
h_{Biot}	error	rate	error	rate	error	rate	error	rate	error	rate
1/8	1.43E-02	–	6.06E-03	–	1.05E-01	–	1.03E-01	–	5.09E-02	–
1/16	7.16E-03	1.0	1.79E-03	1.8	5.23E-02	1.0	5.17E-02	1.0	1.34E-02	1.9
1/32	3.58E-03	1.0	5.81E-04	1.6	2.61E-02	1.0	2.59E-02	1.0	3.94E-03	1.8
1/64	1.79E-03	1.0	1.95E-04	1.6	1.31E-02	1.0	1.29E-02	1.0	1.43E-03	1.5
1/128	8.94E-04	1.0	6.77E-05	1.5	6.53E-03	1.0	6.47E-03	1.0	6.32E-04	1.2

Table 2: Example 1: relative numerical errors and convergence rates on non-matching grids.

2.4.2 Application to flow through fractured reservoirs

For the rest of the cases, we introduce the reference domain $\hat{\Omega}$ given by the rectangle $[0, 1]\text{m} \times [-1, 1]\text{m}$, see Figure 1b. A fracture, which represents the reference fluid domain $\hat{\Omega}_f$ is then

positioned in the middle of the rectangle, with the boundary defined by

$$\hat{x}^2 = 200(0.05 - \hat{y})(0.05 + \hat{y}), \quad \hat{y} \in [-0.05, 0.05].$$

Furthermore, the physical domain Ω, see Figure 1c, with more realistic geometry, is defined as a transformation of the reference domain $\hat{\Omega}$ by the mapping [19]

$$\begin{bmatrix} x \\ y \end{bmatrix} = \begin{bmatrix} \hat{x} \\ 5\cos(\frac{\hat{x}+\hat{y}}{100})\cos(\frac{\pi\hat{x}+\hat{y}}{100})^2 + \hat{y}/2 - \hat{x}/10 \end{bmatrix}.$$

The external boundary of Ω_f is denoted as $\Gamma_{f,inflow}$, while the external boundary of Ω_p is split into $\Gamma_{p,\star}$, where $\star \in \{left,\ right,\ top,\ bottom\}$.

The next example is focused on modeling the interaction between a stationary fracture filled with fluid and the surrounding poroelastic reservoir. We are interested in the solution on the physical domain Ω. The physical units are meters for length, seconds for time, and KPa for pressure. The boundary conditions are chosen to be

Injection:	$\mathbf{u}_f \cdot \mathbf{n}_f = 10, \quad \mathbf{u}_f \cdot \boldsymbol{\tau}_f = 0$	on $\Gamma_{f,inflow}$,
No flow:	$\mathbf{u}_p \cdot \mathbf{n}_p = 0$	on $\Gamma_{p,left}$,
Pressure:	$p_p = 1000$	on $\Gamma_{p,bottom} \cup \Gamma_{p,right} \cup \Gamma_{p,top}$,
Normal displacement:	$\boldsymbol{\eta}_p \cdot \mathbf{n}_p = 0$	on $\Gamma_{p,top} \cup \Gamma_{p,right} \cup \Gamma_{p,bottom}$,
Shear traction:	$(\boldsymbol{\sigma}_p \mathbf{n}_p) \cdot \boldsymbol{\tau}_p = 0$	on $\Gamma_{p,top} \cup \Gamma_{p,right} \cup \Gamma_{p,bottom}$,
Normal stress:	$\boldsymbol{\sigma}_p \mathbf{n}_p = 0$	on $\Gamma_{p,left.}$

The initial conditions are set accordingly to $\boldsymbol{\eta}_p(0) = 0$ m and $p_p(0) = 10^3$ KPa. The total simulation time is $T = 300$ s and the time step is $\Delta t = 1$ s. The model parameters are given in Table 3. These parameters are realistic for hydraulic fracturing and are similar to the ones used in [56]. The Lamé coefficients are determined from the Young's modulus E and the Poisson's ratio ν_p via the relationships $\lambda_p = E\nu_p/[(1+\nu_p)(1-2\nu_p)]$, $\mu_p = E/[2(1+\nu_p)]$. We note that this is a challenging computational test due to the large variation in parameter values.

For this and the rest of the test cases we use the Taylor-Hood $\mathcal{P}_2 - \mathcal{P}_1$ [93] elements for the fluid velocity and pressure in the fracture region, the Raviart–Thomas $\mathcal{RT}_1 - \mathcal{P}_1^{dc}$

Parameter	Symbol	Units	Values
Young's modulus	E	(KPa)	10^7
Poisson's ratio	ν_p		0.2
Lamé coefficient	λ_p	(KPa)	$5/18 \times 10^7$
Lamé coefficient	μ_p	(KPa)	$5/12 \times 10^7$
Dynamic viscosity	ν	(KPa s)	10^{-6}
Permeability	K	(m^2)	$diag(200, 50) \times 10^{-12}$
Mass storativity	s_0	(KPa^{-1})	6.89×10^{-2}
Biot-Willis constant	α		1.0
Beavers-Joseph-Saffman coefficient	α_{BJS}		1.0
Total time	T	(s)	300

Table 3: Poroelasticity and fluid parameters in Example 2.

elements for the Darcy velocity and pressure, the continuous Lagrangian $\mathcal{P}_1$ elements for the displacement, and the $\mathcal{P}_1^{dc}$ elements for the Lagrange multiplier.

Figure 3 shows the computed solution in the reservoir (top and middle) and fracture (bottom) regions at the final time $T = 300$ s. The grayscale velocity legend in Figure 2a is included to show the range of the Darcy velocity magnitude. We observe channel-like flow in the fracture region, which concentrates at the tip. There is also leak-off into the reservoir. The fluid pressure in the reservoir has increased in the vicinity of the fracture from the initial value of 1000 KPa to approximately 2450 KPa, which is close to the pressure in the fracture. A relatively small pressure jump is observed, consistent with (1.2.10). In particular, the magnitude of $\mathbf{D}(\mathbf{u}_f)$ is in the order of 10^4, which, together with $\nu = 10^{-6}$, results in a pressure jump of order $10^{-1} - 10^{-2}$ KPa. The pressure drop in the reservoir in the direction away from the fracture is significant, but the resulting Darcy velocity is relatively small, due to the very low permeability. The displacement field shows that the fracture tends to open as the fluid is being injected, with the deformation of the rock being largest around the fracture and quickly approaching zero away from the it, which is expected due to large stiffness of the rock. The stress, which is computed by postrpocessing from the displacement, exhibits singularity at the tip of the fracture and some of the corners of the

poroelastic domain. This example demonstrates the ability of the proposed method to handle irregularly shaped domains with a computationally challenging set of parameters, which are realistic for hydraulic fracturing in tight rock formations.

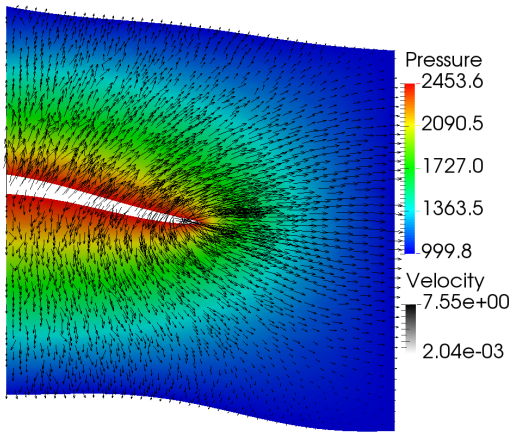

(a) Darcy velocity field (m/s) over pressure (KPa)

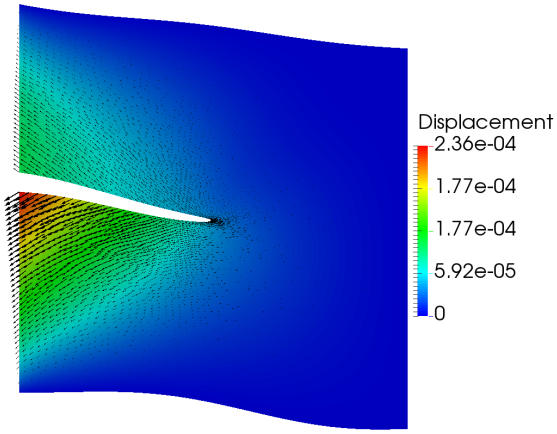

(b) Displacement field (m)

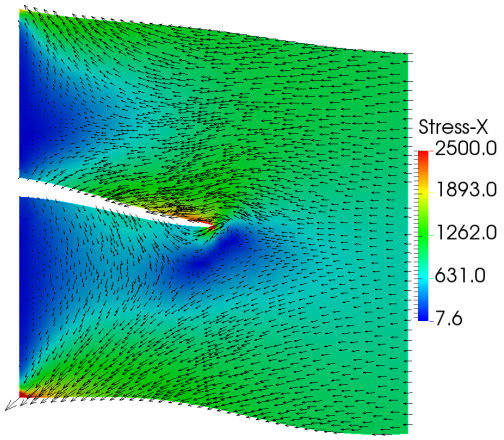

(c) Poroelastic stress, x-component (KPa)

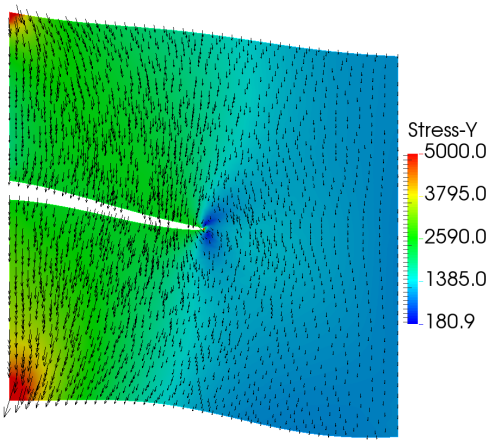

(d) Poroelastic stress, y-component (KPa)

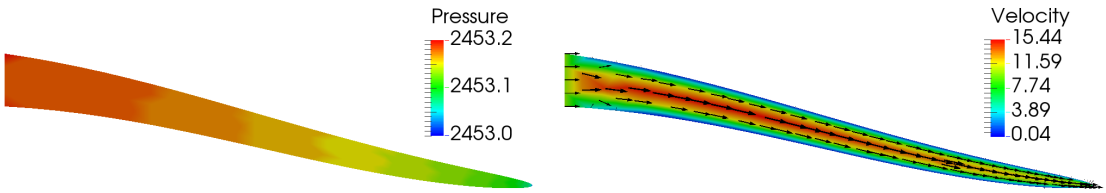

(a) Fluid pressure (KPa) in the fracture (b) Fluid velocity field (m/s) in the fracture

Figure 3: Computed solution in Example 2, fluid flow in a fractured reservoir, $t = 300$ s.

2.4.3 Flow through fractured reservoir with heterogeneous permeability

In this example we illustrate the ability of the method to handle heterogeneous permeability and Young's modulus. For this simulation we use the reference domain $\hat{\Omega}$, see Figure 1b. The same boundary and initial conditions as in the previous test case are specified, and the same physical parameters from Table 3 are used, except for the permeability K and the Young's modulus E. The permeability and porosity data is taken from a two-dimensional cross-section of the data provided by the Society of Petroleum Engineers (SPE) Comparative Solution Project[1]. The SPE data, which is given on a rectangular 60×220 grid is projected onto the triangular grid on the reference domain $\hat{\Omega}$, and visualized in Figure 4. We note that the permeability tensor is isotropic in this example. Given the porosity ϕ the Young's modulus is determined from the law

$$E = 10^7 \left(1 - \frac{\phi}{c}\right)^{2.1},$$

where the constant $c = 0.5$ refers to the porosity at which the effective Young's modulus becomes zero. This constant is chosen in general based on the properties of the porous medium. The justification for this law can be found in [63].

The simulation results at the final time $T = 300s$ are shown in Figure 5. Figures 5a and 5b show that the propagation of the fluid in the Darcy region, as evidenced by the variation in the velocity and pressure, follows the contours of regions of higher permeability

[1] www.spe.org/web/csp

seen in Figure 4b). As in the previous test case, the highest velocity in the reservoir is near the fracture tip. However, the leak-off along the fracture is less uniform, with a significant leak-off near the middle-top of the fracture due to the region of relatively high permeability located there. The last Figure 5c depicts the nonuniform displacement field in the reservoir caused by the heterogeneous Young's modulus. We note that the effect of heterogeneity of the elastic coefficients is less pronounced due to the large stiffness of the rock. The general displacement profile is similar to the homogeneous case.

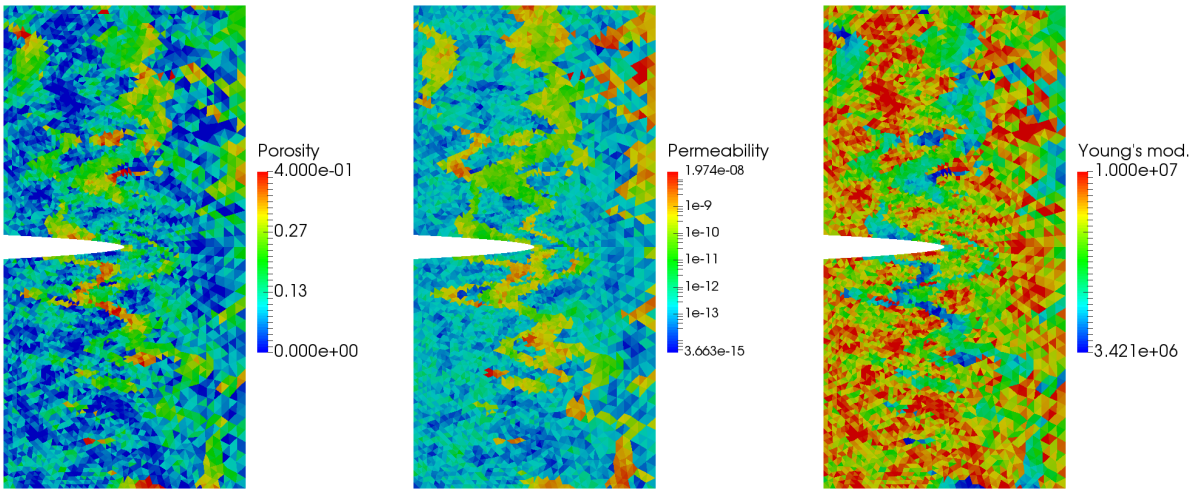

(a) Porosity (b) Permeabiltiy (c) Young's modulus

Figure 4: Heterogeneous material coefficients in Example 3.

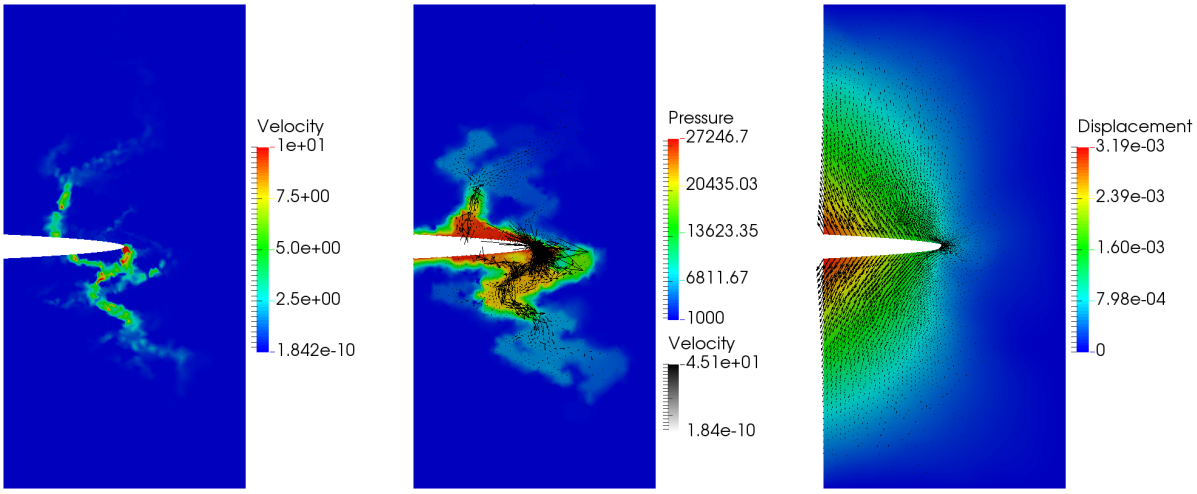

(a) Darcy velocity magnitude (m/s) (b) Velocity over pressure (KPa) (c) Displacement field (m)

Figure 5: Example 3: fluid flow in a fractured reservoir with heterogeneous permeability and Young's modulus, $t = 300$ s.

2.4.4 Robustness analysis

The goal of this section is to investigate how the developed model behaves when the parameters are modified, moving from mild non-physical values towards more realistic values that resemble the ones used in the hydraulic fracturing examples. We progressively update the parameters K, s_0 and E as shown in Table 4, while the rest of the parameters are taken from Table 3. All test cases in this section are governed by the same boundary and initial conditions as in the previous two examples.

Case A: The pressure gradient is small as seen from the contour plot, this is due to the large permeability. Also, from continuity of flux across the interface, one would expect to see that the magnitude of the Darcy velocity is close to the magnitude of the Stokes velocity, which we indeed observe in all the simulations.

Case B: The permeability now is 4 orders of magnitude smaller, resulting in a larger pressure gradient, which is consistent with Darcy's law (1.2.5). Also, more flow is going

	K (m^2)	s_0 (KPa^{-1})	E (KPa)
A	$\mathbf{I} \times 10^{-6}$	1.0	10^3
B	$diag(200, 50) \times 10^{-12}$	1.0	10^3
C	$diag(200, 50) \times 10^{-12}$	10^{-2}	10^3
D	$diag(200, 50) \times 10^{-12}$	10^{-2}	10^{10}

Table 4: Set of parameters for the sensitivity analysis in Example 4.

toward the tip of the fracture, since its walls are now much less permeable. The displacement magnitude is also larger, while keeping the same profile.

Case C: This case shows how the model reacts to decrease in mass storativity - which is by exhibiting larger pressure gradient and displacement magnitude while keeping the overall behavior as in case B.

Case D: The last case is to show the effect of a significant change in Young's modulus. Increasing it by 7 orders of magnitude, which makes the material much stiffer, results in the displacement being decreased by 7 orders of magnitude as expected.

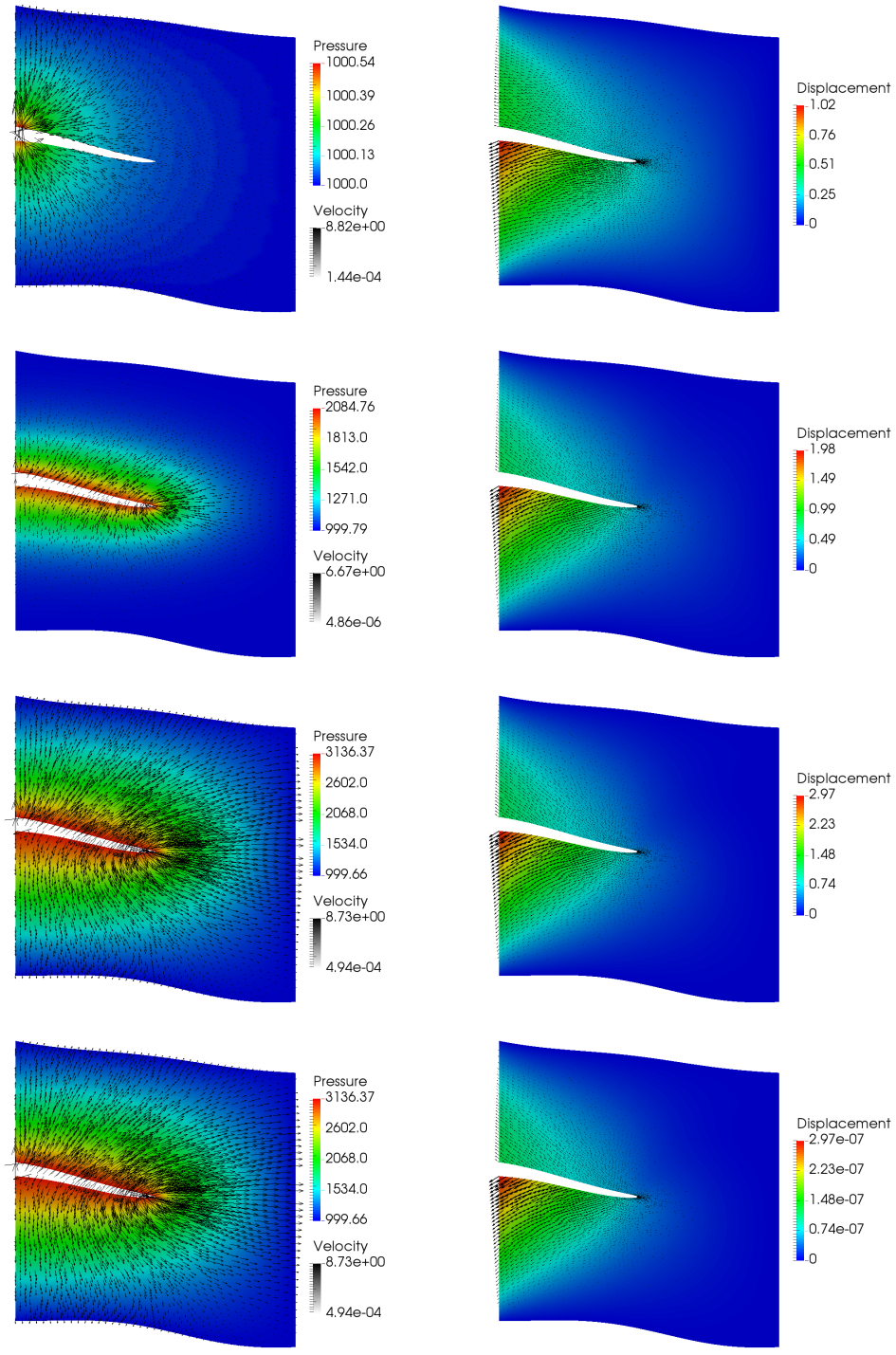

Figure 6: Robustness analysis simulations, $t = 300$ s. Cases A–D are shown from top to bottom. The left figures show the Darcy velocity superimposed with contour plot for the pressure. The right figures show the structure displacement field over the displacement magnitude contour plot. The grayscale velocity legend shows the range of velocity magnitude.

The above results show that the displacement magnitude directly increases with the magnitude of the pressure, while the profile of the displacement field stays the same. This is consistent with the dependence of the poroelastic stress on the fluid pressure, see (1.2.4). In addition, the displacement magnitude is inversely proportional to the Youngs modulus, which is consistent with the constitutive law for the elastic stress in (1.2.4).

3.0 A NONLINEAR STOKES-BIOT MODEL FOR THE INTERACTION OF A NON-NEWTONIAN FLUID WITH POROELASTIC MEDIA

3.1 QUASI-NEWTONIAN FLUIDS

In the fluid domain Ω_f we consider a generalized Newtonian fluid with the viscosity ν dependent on the magnitude of the deformation tensor, in particular shear-thinning fluids with ν a decreasing function of $|\mathbf{D}(\mathbf{u}_f)|$. We consider the following models [28,75], where $1 < r < 2$, $0 \leq \nu_\infty < \nu_0$, and $K_f > 0$ are constants:

Carreau model:

$$\nu(\mathbf{D}(\mathbf{u}_f)) = \nu_\infty + (\nu_0 - \nu_\infty)/(1 + K_f|\mathbf{D}(\mathbf{u}_f)|^2)^{(2-r)/2}, \tag{3.1.1}$$

Cross model:

$$\nu(\mathbf{D}(\mathbf{u}_f)) = \nu_\infty + (\nu_0 - \nu_\infty)/(1 + K_f|\mathbf{D}(\mathbf{u}_f)|^{2-r}), \tag{3.1.2}$$

Power law model:

$$\nu(\mathbf{D}(\mathbf{u}_f)) = K_f|\mathbf{D}(\mathbf{u}_f)|^{r-2}. \tag{3.1.3}$$

In turn, in Ω_p we consider the following two models for the effective viscosity ν_{eff} in Ω_p [67,76], where $1 < r < 2$, $0 \leq \nu_\infty < \nu_0$, and $K_p > 0$ are constants:

Cross model:

$$\nu_{eff}(\mathbf{u}_p) = \nu_\infty + (\nu_0 - \nu_\infty)/(1 + K_p|\mathbf{u}_p|^{2-r}), \tag{3.1.4}$$

Power law model:

$$\nu_{eff}(\mathbf{u}_p) = K_p(|\mathbf{u}_p|/(\sqrt{\kappa}m_c))^{r-2}, \tag{3.1.5}$$

where m_c is a constant that depends on the internal structure of the porous media. We note that even though the analysis of our formulation is valid for a symmetric and positive definite permeability tensor, we restrict it to $\kappa\mathbf{I}$, due to assumptions made in the derivations of some of the viscosity functions suitable for modeling non-Newtonian flow in porous media.

We assume that along the interface the fluid viscosity ν_I is a function of the magnitude of the tangential component of the slip velocity $\left|\sum_{j=1}^{d-1}((\mathbf{u}_f - \partial_t\boldsymbol{\eta}_p)\cdot\mathbf{t}_{f,j})\mathbf{t}_{f,j}\right|$ given by the Cross model (3.1.4) or the Power law model (3.1.5). For the rest of the chapter we will write ν, ν_{eff} or ν_I keeping in mind that these are nonlinear functions as defined above.

Adopting the approach from [44, 45], we assume that the viscosity functions satisfy one of the two sets of assumptions (A1)–(A2) or (B1)–(B2) below. Let $g(\mathbf{x}) : \mathbf{R}^d \to \mathbf{R}^+ \cup \{0\}$ and let $\mathbf{G}(\mathbf{x}) : \mathbf{R}^d \to \mathbf{R}^d$ be given by $\mathbf{G}(\mathbf{x}) = g(\mathbf{x})\mathbf{x}$. For $\mathbf{x}, \mathbf{h} \in \mathbf{R}^d$, let $\mathbf{G}(\mathbf{x})$ satisfy, for constants $C_1, \ldots, C_4 > 0$ and $c \geq 0$,

$$(\mathbf{G}(\mathbf{x}+\mathbf{h}) - \mathbf{G}(\mathbf{x}))\cdot\mathbf{h} \geq C_1|\mathbf{h}|^2, \tag{A1}$$

$$|\mathbf{G}(\mathbf{x}+\mathbf{h}) - \mathbf{G}(\mathbf{x})| \leq C_2|\mathbf{h}|, \tag{A2}$$

or

$$(\mathbf{G}(\mathbf{x}+\mathbf{h}) - \mathbf{G}(\mathbf{x}))\cdot\mathbf{h} \geq C_3\frac{|\mathbf{h}|^2}{c + |\mathbf{x}|^{2-r} + |\mathbf{x}+\mathbf{h}|^{2-r}}, \tag{B1}$$

$$|\mathbf{G}(\mathbf{x}+\mathbf{h}) - \mathbf{G}(\mathbf{x})| \leq C_4\frac{|\mathbf{h}|}{c + |\mathbf{x}|^{2-r} + |\mathbf{x}+\mathbf{h}|^{2-r}}, \tag{B2}$$

with the convention that $\mathbf{G}(\mathbf{x}) = \mathbf{0}$ if $\mathbf{x} = \mathbf{0}$, and $|\mathbf{h}|/(c + |\mathbf{x}| + |\mathbf{h}|) = 0$ if $c = 0$ and $\mathbf{x} = \mathbf{h} = \mathbf{0}$. From (B1)–(B2) it follows that there exist constants $C_5, C_6 > 0$ such that for $\mathbf{s}, \mathbf{t}, \mathbf{w} \in (L^r(G))^d$ [84]

$$(\mathbf{G}(\mathbf{s}) - \mathbf{G}(\mathbf{t}), \mathbf{s}-\mathbf{t})_G \geq C_5\left(\int_\Omega |\mathbf{G}(\mathbf{s}) - \mathbf{G}(\mathbf{t})|\,|\mathbf{s}-\mathbf{t}|\,d\mathbf{x} + \frac{\|\mathbf{s}-\mathbf{t}\|^2_{L^r(G)}}{c + \|\mathbf{s}\|^{2-r}_{L^r(G)} + \|\mathbf{t}\|^{2-r}_{L^r(G)}}\right), \tag{3.1.6}$$

$$(\mathbf{G}(\mathbf{s}) - \mathbf{G}(\mathbf{t}), \mathbf{w})_G \leq C_6\left\|\frac{|\mathbf{s}-\mathbf{t}|}{c + |\mathbf{s}| + |\mathbf{t}|}\right\|^{\frac{2-r}{r}}_{L^\infty(G)} (|\mathbf{G}(\mathbf{s}) - \mathbf{G}(\mathbf{t})|, |\mathbf{s}-\mathbf{t}|)^{1/r'}_G \|\mathbf{w}\|_{L^r(G)}. \tag{3.1.7}$$

Remark 3.1.1. *It is shown in [40] that conditions* (A1)–(A2) *are satisfied for* $g(\mathbf{D}(\mathbf{u}_f)) = \nu(\mathbf{D}(\mathbf{u}_f))$ *given in the Carreau model* (3.1.1) *with* $\nu_\infty > 0$*, in which case* $\nu_\infty \leq g(\mathbf{x}) \leq \nu_0$*. A similar argument can be applied to show that* (A1)–(A2) *hold for the Cross model, with* $g(\mathbf{D}(\mathbf{u}_f)) = \nu(\mathbf{D}(\mathbf{u}_f))$ *given in* (3.1.2) *for Stokes and* $g(\mathbf{u}_p) = \nu_{eff}(\mathbf{u}_p)$ *given in* (3.1.4) *for Darcy, in the case of* $\nu_\infty > 0$*. Furthurmore, it is shown in [84] that conditions* (B1)–(B2) *with* $c > 0$ *hold in the case of the Carreau model* (3.1.1) *with* $\nu_\infty = 0$*, and that conditions* (B1)–(B2) *with* $c = 0$ *hold for the Power law model* (3.1.3) *and* (3.1.5)*.*

3.2 VARIATIONAL FORMULATION

We will consider two cases when defining the functional spaces, depending on which set of assumptions holds. In the case (B1)–(B2), we consider Sobolev spaces:

$$\mathbf{V}_f = \{\mathbf{v}_f \in W^{1,r}(\Omega_f)^d : \mathbf{v}_f = \mathbf{0} \text{ on } \Gamma_f\}, \qquad W_f = L^{r'}(\Omega_f), \tag{3.2.1}$$

and

$$\begin{aligned} \mathbf{V}_p &= \{\mathbf{v}_p \in L^r(\mathrm{div};\Omega_p) : \mathbf{v}_p \cdot \mathbf{n}_p = 0 \text{ on } \Gamma_p^N\}, \qquad W_p = L^{r'}(\Omega_p), \\ \mathbf{X}_p &= \{\boldsymbol{\xi}_p \in H^1(\Omega_p)^d : \boldsymbol{\xi}_p = \mathbf{0} \text{ on } \Gamma_p\}. \end{aligned} \tag{3.2.2}$$

In the case of (A1)–(A2), we consider Hilbert spaces, with the above definitions replaced by

$$\mathbf{V}_f = \{\mathbf{v}_f \in H^1(\Omega_f)^d : \mathbf{v}_f = \mathbf{0} \text{ on } \Gamma_f\}, \qquad W_f = L^2(\Omega_f), \tag{3.2.3}$$

$$\mathbf{V}_p = \{\mathbf{v}_p \in H(\mathrm{div};\Omega_p) : \mathbf{v}_p \cdot \mathbf{n}_p = 0 \text{ on } \Gamma_p^N\}, \qquad W_p = L^2(\Omega_p). \tag{3.2.4}$$

The global spaces are products of the subdomain spaces. For simplicity we assume that each region consists of a single subdomain.

Remark 3.2.1. *For simplicity of the presentation, for the rest of the paper we focus on the case* (B1)–(B2)*, which is the technically more challenging case. The arguments apply directly to the case* (A1)–(A2)*.*

3.2.1 Lagrange multiplier formulation

We consider the variational formulation reads: *given* $\mathbf{f}_f \in W^{1,1}(0,T;\mathbf{V}_f')$, $\mathbf{f}_p \in W^{1,1}(0,T;\mathbf{X}_p')$, $q_f \in W^{1,1}(0,T;W_f')$, $q_p \in W^{1,1}(0,T;W_p')$, *and* $p_p(0) = p_{p,0} \in W_p$, $\boldsymbol{\eta}_p(0) = \boldsymbol{\eta}_{p,0} \in \mathbf{X}_p$, *find, for* $t \in (0,T]$, $(\mathbf{u}_f(t), p_f(t), \mathbf{u}_p(t), p_p(t), \boldsymbol{\eta}_p(t), \lambda(t)) \in L^\infty(0,T;\mathbf{V}_f) \times L^\infty(0,T;W_f) \times L^\infty(0,T;\mathbf{V}_p) \times W^{1,\infty}(0,T;W_p) \times W^{1,\infty}(0,T;\mathbf{X}_p) \times L^\infty(0,T;\Lambda)$, *such that for all* $\mathbf{v}_f \in \mathbf{V}_f$, $w_f \in W_f$, $\mathbf{v}_p \in \mathbf{V}_p$, $w_p \in W_p$, $\boldsymbol{\xi}_p \in \mathbf{X}_p$, *and* $\mu \in \Lambda$,

$$a_f(\mathbf{u}_f,\mathbf{v}_f) + a_p^d(\mathbf{u}_p,\mathbf{v}_p) + a_p^e(\boldsymbol{\eta}_p,\boldsymbol{\xi}_p) + a_{BJS}(\mathbf{u}_f,\partial_t\boldsymbol{\eta}_p;\mathbf{v}_f,\boldsymbol{\xi}_p) + b_f(\mathbf{v}_f,p_f) + b_p(\mathbf{v}_p,p_p) + \alpha_p b_p(\boldsymbol{\xi}_p,p_p) + b_\Gamma(\mathbf{v}_f,\mathbf{v}_p,\boldsymbol{\xi}_p;\lambda) = (\mathbf{f}_f,\mathbf{v}_f)_{\Omega_f} + (\mathbf{f}_p,\boldsymbol{\xi}_p)_{\Omega_p}, \tag{3.2.5}$$

$$(s_0\partial_t p_p, w_p)_{\Omega_p} - \alpha_p b_p\left(\partial_t\boldsymbol{\eta}_p, w_p\right) - b_p(\mathbf{u}_p,w_p) - b_f(\mathbf{u}_f,w_f) = (q_f,w_f)_{\Omega_f} + (q_p,w_p)_{\Omega_p}, \tag{3.2.6}$$

$$b_\Gamma\left(\mathbf{u}_f,\mathbf{u}_p,\partial_t\boldsymbol{\eta}_p;\mu\right) = 0. \tag{3.2.7}$$

Although (3.2.5)-(3.2.7) look very similar to (2.1.11)-(2.1.13), we keep in mind that the Stokes and Darcy functionals, $a_f(\cdot,\cdot)$, $a_p^d(\cdot,\cdot)$ as well as the functional corresponding to the BJS condition, $a_{BJS}(\cdot,\cdot;\cdot,\cdot)$, are now nonlinear.

For the term b_Γ to be well-defined, we choose the Lagrange multiplier space as $\Lambda = W^{1/r,r'}(\Gamma_{fp})$. It is shown in [44] that in the case $\mathrm{dist}(\Gamma_p^D,\Gamma_{fp}) \geq s > 0$, if $\mathbf{v}_p \in L^r(\mathrm{div};\Omega_p)$, then $\mathbf{v}_p\cdot\mathbf{n}_p|_{\Gamma_{fp}}$ can be identified with a functional in $W^{-1/r,r}(\Gamma_{fp})$. Furthermore, for $\mathbf{v}_f \in W^{1,r}(\Omega_f)$, $\mathbf{v}_f\cdot\mathbf{n}_f \in W^{1/r',r}(\partial\Omega_f)$, and for $\boldsymbol{\xi}_p \in H^1(\Omega_p) \subset W^{1,r}(\Omega_p)$, $\boldsymbol{\xi}_p\cdot\mathbf{n}_p \in W^{1/r',r}(\partial\Omega_p)$. Therefore, with $\mu \in W^{1/r,r'}(\Gamma_{fp})$, the integrals in $b_\Gamma(\mathbf{v}_f,\mathbf{v}_p,\boldsymbol{\xi}_p;\lambda)$ are well-defined.

Note that $(s_0\partial_t p_p, w_p)_{\Omega_p}$ is well-defined, since for $r < 2$, we have that $r' > 2$ and $L^{r'}(\Omega_p) \subset L^2(\Omega_p)$.

Although related models have been analyzed previously, e.g. the non-Newtonian Stokes-Darcy model was investigated in [44] and the Newtonian dynamic Stokes-Biot model was studied in [87], the well posedness of (3.2.5)–(3.2.7) has not been established in the literature. Analyzing this formulation directly is difficult, due to the presence of $\partial_t\boldsymbol{\eta}_p$ in several non-coercive terms. Instead, we analyze an alternative formulation and show that the two formulations are equivalent.

3.2.2 Alternative formulation

Our goal is to obtain a system of evolutionary saddle point type, which fits the general framework studied in [88]. Following the approach from [87], we do this by considering a mixed elasticity formulation with the structure velocity and elastic stress as primary variables. Recall that the elasticity stress tensor $\boldsymbol{\sigma}_e$ is connected to the displacement $\boldsymbol{\eta}_p$ through the relation [18]:

$$A\boldsymbol{\sigma}_e = \mathbf{D}(\boldsymbol{\eta}_p), \tag{3.2.8}$$

where A is a symmetric and positive definite compliance tensor. In the isotropic case A has the form

$$A\boldsymbol{\sigma}_e = \frac{1}{2\mu_p}\left(\boldsymbol{\sigma}_e - \frac{\lambda_p}{2\mu_p + d\lambda_p}\mathrm{tr}(\boldsymbol{\sigma}_e)\mathbf{I}\right), \quad \text{with} \quad A^{-1}\boldsymbol{\sigma}_e = 2\mu_p\,\boldsymbol{\sigma}_e + \lambda_p \mathrm{tr}(\boldsymbol{\sigma}_e)\mathbf{I}. \tag{3.2.9}$$

To derive a new variational formulation, we start by multiplying (1.2.2) and the second equation in (1.2.5) by test functions $\mathbf{v}_f \in \mathbf{V}_f$ and $\mathbf{v}_p \in \mathbf{V}_p$, respectively, and integrating by parts to obtain:

$$\int_{\Omega_f} (2\nu\mathbf{D}(\mathbf{u}_f) : \mathbf{D}(\mathbf{v}_f) - p_f \nabla\cdot\mathbf{v}_f)\, dA + \int_{\Omega_p} \left(\nu_{eff} K^{-1}\mathbf{u}_p\cdot\mathbf{v}_p - p_p\nabla\cdot\mathbf{v}_p\right) dA$$
$$+ \int_{\Gamma_{fp}} (-\boldsymbol{\sigma}_f\mathbf{n}_f\cdot\mathbf{v}_f + p_p\mathbf{v}_p\cdot\mathbf{n}_p)\, ds = \int_{\Omega_f}\mathbf{f}_f\cdot\mathbf{v}_f\, dA. \tag{3.2.10}$$

Decomposing the stress term into its normal and tangential components, and using the balance of normal stress condition (1.2.9), we obtain:

$$\int_{\Gamma_{fp}} -\boldsymbol{\sigma}_f\mathbf{n}_f\cdot\mathbf{v}_f\, ds = \int_{\Gamma_{fp}} -(\boldsymbol{\sigma}_f\mathbf{n}_f)\cdot\mathbf{n}_f\mathbf{v}_f\cdot\mathbf{n}_f\, ds - \sum_{j=1}^{n-1}\int_{\Gamma_{fp}} ((\boldsymbol{\sigma}_f\cdot\mathbf{n}_f)\cdot\mathbf{t}_{f,j})(\mathbf{v}_f\cdot\mathbf{t}_{f,j})\, ds$$
$$= \int_{\Gamma_{fp}} p_p\mathbf{v}_f\cdot\mathbf{n}_f\, ds + \sum_{j=1}^{n-1}\int_{\Gamma_{fp}} (\nu_I\alpha_{BJS}\sqrt{K_j^{-1}}(\mathbf{u}_f - \partial_t\boldsymbol{\eta}_p)\cdot\mathbf{t}_{f,j})(\mathbf{v}_f\cdot\mathbf{t}_{f,j})\, ds. \tag{3.2.11}$$

We multiply the first equation in (1.2.5) by $\mathbf{v}_s \in \mathbf{X}_p$ and integrate by parts, using the fact that $\boldsymbol{\sigma}_e = \boldsymbol{\sigma}_p + \alpha_p p_p\mathbf{I}$:

$$\int_{\Omega_p} ((\boldsymbol{\sigma}_e - \alpha_p p_p\mathbf{I}) : \mathbf{D}(\mathbf{v}_s))\, dA + \int_{\Gamma_{fp}} (\alpha_p p_p\mathbf{v}_s\cdot\mathbf{n}_p - \boldsymbol{\sigma}_e\mathbf{n}_p\cdot\mathbf{v}_s)\, ds = \int_{\Omega_p}\mathbf{f}_p\cdot\mathbf{v}_s\, dA. \tag{3.2.12}$$

For the elastic stress, conservation of momentum (1.2.9) reads:

$$(\boldsymbol{\sigma}_f \mathbf{n}_f)\cdot\mathbf{n}_f = (\boldsymbol{\sigma}_e \mathbf{n}_p)\cdot\mathbf{n}_p - \alpha_p p_p, \quad (\boldsymbol{\sigma}_f \mathbf{n}_f)\cdot\mathbf{t}_{f,j} = -(\boldsymbol{\sigma}_e \mathbf{n}_p)\cdot\mathbf{t}_{f,j} \quad \text{on } \Gamma_{fp}.$$

We use this modified condition to rewrite the interface terms in (3.2.12), similarly to how it was done for the fluid stress in (3.2.11)

$$\begin{aligned}
\int_{\Gamma_{fp}} -(\boldsymbol{\sigma}_e \mathbf{n}_p)\cdot\mathbf{v}_s\, ds &= \int_{\Gamma_{fp}} \left(-(\boldsymbol{\sigma}_f \mathbf{n}_f)\cdot\mathbf{n}_f \mathbf{v}_s\cdot\mathbf{n}_p - \alpha_p p_p \mathbf{v}_s\cdot\mathbf{n}_p\right) ds \\
&- \sum_{j=1}^{n-1}\int_{\Gamma_{fp}} ((\boldsymbol{\sigma}_e\cdot\mathbf{n}_p)\cdot\mathbf{t}_{f,j})(\mathbf{v}_s\cdot\mathbf{t}_{f,j})\, ds = \int_{\Gamma_{fp}} (1-\alpha_p) p_p \mathbf{v}_s\cdot\mathbf{n}_p\, ds \\
&+ \sum_{j=1}^{n-1}\int_{\Gamma_{fp}} (-\nu_I\, \alpha_{BJS}\sqrt{K_j^{-1}}(\mathbf{u}_f - \partial_t\boldsymbol{\eta}_p)\cdot\mathbf{t}_{f,j})(\mathbf{v}_s\cdot\mathbf{t}_{f,j})\, ds. \qquad (3.2.13)
\end{aligned}$$

Therefore, (3.2.10)-(3.2.13) can be combined as follows:

$$\begin{aligned}
&\int_{\Omega_f} (2\nu \mathbf{D}(\mathbf{u}_f) : \mathbf{D}(\mathbf{v}_f) - p_f \nabla\cdot\mathbf{v}_f)\, dA \\
&+ \int_{\Omega_p} \left(\nu_{eff}\kappa^{-1}\mathbf{u}_p\cdot\mathbf{v}_p - p_p\nabla\cdot\mathbf{v}_p + (\boldsymbol{\sigma}_e - \alpha_p p_p) : \mathbf{D}(\mathbf{v}_s)\right) dA \\
&+ \sum_{j=1}^{n-1}\int_{\Gamma_{fp}} (\nu_I \alpha_{BJS}\sqrt{K_j^{-1}}(\mathbf{u}_f - \partial_t\boldsymbol{\eta}_p)\cdot\mathbf{t}_{f,j})((\mathbf{v}_f - \mathbf{v}_s)\cdot\mathbf{t}_{f,j})\, ds \\
&+ \int_{\Gamma_{fp}} \left((\mathbf{v}_f\cdot\mathbf{n}_f + \mathbf{v}_s\cdot\mathbf{n}_p + \mathbf{v}_p\cdot\mathbf{n}_p)\, p_p\right) ds = \int_{\Omega_f} \mathbf{f}_f\cdot\mathbf{v}_f\, dA + \int_{\Omega_p} \mathbf{f}_p\cdot\mathbf{v}_s\, dA. \qquad (3.2.14)
\end{aligned}$$

We note that we can eliminate the displacement, $\boldsymbol{\eta}_p$, from the system by differentiating (3.2.8) and introducing a new variable $\mathbf{u}_s := \partial_t\boldsymbol{\eta}_p \in \mathbf{X}_p$, which has a meaning of structure velocity. Now, multiplying (1.2.3), (3.2.8) and (1.2.6) by corresponding test functions and adding the result, we obtain:

$$\begin{aligned}
&\int_{\Omega_p} (A\partial_t\boldsymbol{\sigma}_e : \boldsymbol{\tau}_e - \mathbf{D}(\mathbf{u}_s) : \boldsymbol{\tau}_e + s_0\partial_t p_p w_p + \alpha_p\nabla\cdot\mathbf{u}_s w_p + \nabla\cdot\mathbf{u}_p w_p)\, dA \\
&+ \int_{\Omega_f} (\nabla\cdot\mathbf{u}_f w_f)\, dA = \int_{\Omega_p} q_p w_p\, dA + \int_{\Omega_f} q_f w_f\, dA. \qquad (3.2.15)
\end{aligned}$$

As in the first formulation, we use a Lagrange multiplier to impose the mass conservation interface condition (1.2.7). Finally, we introduce the space for the elastic stress $\mathbf{\Sigma}_e = L^2_{sym}(\Omega_p)^{d\times d}$ with the norm

$$\|\boldsymbol{\sigma}_e\|^2_{\mathbf{\Sigma}_e} := \sum_{i,j=1}^{d} \|(\boldsymbol{\sigma}_e)_{i,j}\|^2_{L^2(\Omega_p)}.$$

Then, the weak formulation is: *Given* $f_f \in W^{1,1}(0,T;\mathbf{V}'_f)$, $f_p \in W^{1,1}(0,T;\mathbf{V}'_p)$, *and* $p_p(0) = p_{p,0} \in W_p$, $\boldsymbol{\sigma}_e(0) = A^{-1}\mathbf{D}(\boldsymbol{\eta}_{p,0}) \in \mathbf{\Sigma}_e$, *for* $t \in (0,T]$, *find* $(\mathbf{u}_f(t), p_f(t), \mathbf{u}_p(t), p_p(t), \mathbf{u}_s(t), \boldsymbol{\sigma}_e(t), \lambda(t)) \in L^\infty(0,T;\mathbf{V}_f) \times L^\infty(0,T;W_f) \times L^\infty(0,T;\mathbf{V}_p) \times W^{1,\infty}(0,T;W_p) \times L^\infty(0,T;\mathbf{X}_p) \times W^{1,\infty}(0,T;\Sigma_e) \times L^\infty(0,T;\Lambda)$, *such that for all* $\mathbf{v}_f \in \mathbf{V}_f$, $w_f \in W_f$, $\mathbf{v}_p \in \mathbf{V}_p$, $w_p \in W_p$, $\mathbf{v}_s \in \mathbf{X}_p$, $\boldsymbol{\tau}_e \in \mathbf{\Sigma}_e$, *and* $\mu \in \Lambda$,

$$\begin{aligned}
\int_{\Omega_p} \left(\boldsymbol{\sigma}_e : \mathbf{D}(\mathbf{v}_s) - \alpha_p p_p \nabla\cdot\mathbf{v}_s + \nu_{eff} K^{-1}\mathbf{u}_p\cdot\mathbf{v}_p - p_p\nabla\cdot\mathbf{v}_p + A\partial_t\boldsymbol{\sigma}_e : \boldsymbol{\tau}_e - \mathbf{D}(\mathbf{u}_s) : \boldsymbol{\tau}_e\right) dA \\
+ \int_{\Omega_p} \left(s_0\partial_t p_p w_p + \alpha_p \nabla\cdot\mathbf{u}_s w_p + \nabla\cdot\mathbf{u}_p w_p\right) dA \\
+ \int_{\Omega_f} \left(2\nu\mathbf{D}(\mathbf{u}_f) : \mathbf{D}(\mathbf{v}_f) - p_f\nabla\cdot\mathbf{v}_f + \nabla\cdot\mathbf{u}_f w_f\right) dA \\
+ \sum_{j=1}^{n-1} \int_{\Gamma_{fp}} (\nu_I\, \alpha_{BJS}\sqrt{K_j^{-1}}(\mathbf{u}_f - \mathbf{u}_s)\cdot\mathbf{t}_{f,j})((\mathbf{v}_f - \mathbf{v}_s)\cdot\mathbf{t}_{f,j})\, ds \\
+ \int_{\Gamma_{fp}} \left((\mathbf{v}_f\cdot\mathbf{n}_f + \mathbf{v}_s\cdot\mathbf{n}_p + \mathbf{v}_p\cdot\mathbf{n}_p)\,\lambda\right) ds - \int_{\Gamma_{fp}} \left((\mathbf{u}_f\cdot\mathbf{n}_f + \mathbf{u}_s\cdot\mathbf{n}_p + \mathbf{u}_p\cdot\mathbf{n}_p)\,\mu\right) ds \\
= \int_{\Omega_p} (\mathbf{f}_p\cdot\mathbf{v}_s + q_p w_p)\, dA + \int_{\Omega_f} (\mathbf{f}_f\cdot\mathbf{v}_f + q_f w_f)\, dA.
\end{aligned} \tag{3.2.16}$$

We introduce the functionals $b_s(\cdot,\cdot) : \mathbf{X}_p \times \mathbf{\Sigma}_e \longrightarrow \mathbf{R}$ and $a^s_p(\cdot,\cdot) : \mathbf{\Sigma}_e \times \mathbf{\Sigma}_e \longrightarrow \mathbf{R}$ defined by

$$b_s(\mathbf{v}_s, \boldsymbol{\tau}_e) := (\mathbf{D}(\mathbf{v}_s), \boldsymbol{\tau}_e)_{\Omega_p}, \qquad a^s_p(\boldsymbol{\sigma}_e, \boldsymbol{\tau}_e) := (A\boldsymbol{\sigma}_e, \boldsymbol{\tau}_e)_{\Omega_p}.$$

Hence, we can rewrite (3.2.16) in a more compact form:

$$\begin{aligned}
&a_f(\mathbf{u}_f, \mathbf{v}_f) + a^d_p(\mathbf{u}_p, \mathbf{v}_p) + a_{BJS}(\mathbf{u}_f, \mathbf{u}_s; \mathbf{v}_f, \mathbf{v}_s) + b_f(\mathbf{v}_f, p_f) + b_p(\mathbf{v}_p, p_p) \\
&\quad + \alpha_p b_p(\mathbf{v}_s, p_p) + b_s(\mathbf{v}_s, \boldsymbol{\sigma}_e) + b_\Gamma(\mathbf{v}_f, \mathbf{v}_p, \mathbf{v}_s; \lambda) = (\mathbf{f}_f, \mathbf{v}_f)_{\Omega_f} + (\mathbf{f}_p, \mathbf{v}_s)_{\Omega_p},
\end{aligned} \tag{3.2.17}$$

$$(s_0\partial_t p_p, w_p)_{\Omega_p} + a_p^s(\partial_t \boldsymbol{\sigma}_e, \boldsymbol{\tau}_e) - \alpha_p b_p(\mathbf{u}_s, w_p) - b_p(\mathbf{u}_p, w_p) - b_s(\mathbf{u}_s, \boldsymbol{\tau}_e) - b_f(\mathbf{u}_f, w_f)$$
$$= (q_f, w_f)_{\Omega_f} + (q_p, w_p)_{\Omega_p}, \tag{3.2.18}$$
$$b_\Gamma(\mathbf{u}_f, \mathbf{u}_p, \mathbf{u}_s; \mu) = 0. \tag{3.2.19}$$

We can also write (3.2.17)–(3.2.19) in an operator notation as a degenerate evolution problem in a mixed form:

$$\frac{\partial}{\partial t}\mathcal{E}_1 \mathbf{q}(t) + \mathcal{A}\mathbf{q}(t) + \mathcal{B}' s(t) = \mathbf{f}(t), \qquad \text{in } \mathcal{Q}', \tag{3.2.20}$$
$$\frac{\partial}{\partial t}\mathcal{E}_2 s(t) - \mathcal{B}\mathbf{q}(t) + \mathcal{C}s(t) = g(t), \qquad \text{in } S', \tag{3.2.21}$$

where we define $\mathcal{Q}$, the space of generalized displacement variables, as

$$\mathcal{Q} = \left\{ \mathbf{q} = (\mathbf{v}_p, \mathbf{v}_s, \mathbf{v}_f) \in \mathbf{V}_p \times \mathbf{X}_p \times \mathbf{V}_f \right\},$$

and, similarly, the space S, consisting of generalized stress variables, as

$$S = \{ s = (w_p, \boldsymbol{\tau}_e, w_f, \mu) \in W_p \times \boldsymbol{\Sigma}_e \times W_f \times \Lambda \}.$$

The spaces $\mathcal{Q}$ and S are equipped with norms:

$$\|\mathbf{q}\|_{\mathcal{Q}} = \|\mathbf{v}_p\|_{L^r(\mathrm{div};\Omega_p)} + \|\mathbf{v}_s\|_{H^1(\Omega_p)} + \|\mathbf{v}_f\|_{W^{1,r}(\Omega_f)},$$
$$\|s\|_S = \|w_p\|_{L^{r'}(\Omega_p)} + \|\boldsymbol{\tau}_e\|_{L^2(\Omega_p)} + \|w_f\|_{L^{r'}(\Omega_f)} + \|\mu\|_{W^{1/r,r'}(\Gamma_{fp})}.$$

The operators $\mathcal{A} : \mathcal{Q} \to \mathcal{Q}'$, $\mathcal{B} : \mathcal{Q} \to S'$, $\mathcal{C} : S \to S'$, and the functionals $\mathbf{f} \in \mathcal{Q}'$, $g \in S'$ are defined as follows:

$$\mathcal{A} = \begin{pmatrix} \nu_{eff}\kappa^{-1} & 0 & 0 \\ 0 & \alpha_{BJS}\,\gamma_t'\,\nu_I\,\sqrt{\kappa^{-1}}\,\gamma_t & -\alpha_{BJS}\,\gamma_t'\,\nu_I\,\sqrt{\kappa^{-1}}\,\gamma_t \\ 0 & -\alpha_{BJS}\,\gamma_t'\,\nu_I\,\sqrt{\kappa^{-1}}\,\gamma_t & 2\nu\mathbf{D}:\mathbf{D} + \alpha_{BJS}\,\gamma_t'\,\nu_I\,\sqrt{\kappa^{-1}}\,\gamma_t \end{pmatrix},$$

$$\mathcal{B} = \begin{pmatrix} \nabla\cdot & \alpha_p \nabla\cdot & 0 \\ 0 & -\mathbf{D} & 0 \\ 0 & 0 & \nabla\cdot \\ \gamma_n & \gamma_n & \gamma_n \end{pmatrix}, \quad \mathcal{C} = \begin{pmatrix} 0 & 0 & 0 & 0 \\ 0 & 0 & 0 & 0 \\ 0 & 0 & 0 & 0 \\ 0 & 0 & 0 & 0 \end{pmatrix}, \quad \mathbf{f} = \begin{pmatrix} \mathbf{0} \\ \mathbf{f}_p \\ \mathbf{f}_f \end{pmatrix}, \quad g = \begin{pmatrix} q_p \\ 0 \\ q_f \\ 0 \end{pmatrix},$$

where γ_t and γ_n denote the tangential and normal trace operators, respectively, and γ_t' is the adjoint operator of γ_t. The operators $\mathcal{E}_1 : \mathcal{Q} \to \mathcal{Q}'$, $\mathcal{E}_2 : S \to S'$ are given by:

$$\mathcal{E}_1 = \begin{pmatrix} 0 & 0 & 0 \\ 0 & 0 & 0 \\ 0 & 0 & 0 \end{pmatrix}, \quad \mathcal{E}_2 = \begin{pmatrix} s_0 & 0 & 0 & 0 \\ 0 & A & 0 & 0 \\ 0 & 0 & 0 & 0 \\ 0 & 0 & 0 & 0 \end{pmatrix}.$$

3.3 WELL-POSEDNESS OF THE MODEL

In this section we establish the solvability of (3.2.5)-(3.2.7). We start with the analysis of the alternative formulation (3.2.17)–(3.2.19).

3.3.1 Existence and uniqueness of a solution of the alternative formulation

We first explore important properties of the operators introduced at the end of Section 3.2.

Lemma 3.3.1. *The operator $\mathcal{B}$ and its adjoint $\mathcal{B}'$ are bounded and continuous. Moreover, there exist constants β_1, $\beta_2 > 0$ such that*

$$\inf_{\mathbf{0}\neq(\mathbf{0},\mathbf{v}_s,\mathbf{0})\in\mathcal{Q}} \sup_{(0,\boldsymbol{\tau}_e,0,0)\in S} \frac{b_s(\mathbf{v}_s,\boldsymbol{\tau}_e)}{\|(\mathbf{0},\mathbf{v}_s,\mathbf{0})\|_{\mathcal{Q}}\|(0,\boldsymbol{\tau}_e,0,0)\|_S} \geq \beta_1, \tag{3.3.1}$$

$$\inf_{0\neq(w_p,0,w_f,\mu)\in S} \sup_{(\mathbf{v}_p,\mathbf{0},\mathbf{v}_f)\in\mathcal{Q}} \frac{b_f(\mathbf{v}_f,w_f) + b_p(\mathbf{v}_p,w_p) + b_\Gamma(\mathbf{v}_f,\mathbf{v}_p,\mathbf{0};\mu)}{\|(\mathbf{v}_p,\mathbf{0},\mathbf{v}_f)\|_{\mathcal{Q}}\|(w_p,\mathbf{0},w_f,\mu)\|_S} \geq \beta_2. \tag{3.3.2}$$

Proof. The operator $\mathcal{B}$ is linear and satisfies for all $\mathbf{q} = (\mathbf{v}_p, \mathbf{v}_s, \mathbf{v}_f) \in \mathcal{Q}$ and $s = (w_p, \boldsymbol{\tau}_e, w_f, \mu) \in S$,

$$\begin{aligned}
&\mathcal{B}(\mathbf{q})(s) = b_f(\mathbf{v}_f, w_f) + b_p(\mathbf{v}_p, w_p) + \alpha_p b_p(\mathbf{v}_s, w_p) + b_s(\mathbf{v}_s, \boldsymbol{\tau}_e) + b_\Gamma(\mathbf{v}_f, \mathbf{v}_p, \mathbf{v}_s; \mu) \\
&\leq \|\nabla \cdot \mathbf{v}_f\|_{L^r(\Omega_f)} \|w_f\|_{L^{r'}(\Omega_f)} + \|\nabla \cdot \mathbf{v}_p\|_{L^r(\Omega_p)} \|w_p\|_{L^{r'}(\Omega_p)} + \alpha_p \|\nabla \cdot \mathbf{v}_s\|_{L^r(\Omega_p)} \|w_p\|_{L^{r'}(\Omega_p)} \\
&\quad + \|\mathbf{D}(\mathbf{v}_s)\|_{L^2(\Omega_p)} \|\boldsymbol{\tau}_e\|_{L^2(\Omega_p)} + \|\mathbf{v}_f \cdot \mathbf{n}_f + (\mathbf{v}_p + \mathbf{v}_s) \cdot \mathbf{n}_p\|_{W^{-1/r,r}(\Gamma_{fp})} \|\mu\|_{W^{1/r,r'}(\Gamma_{fp})} \\
&\leq C \Big(\|\mathbf{v}_f\|_{W^{1,r}(\Omega_f)} \|w_f\|_{L^{r'}(\Omega_f)} + \|\mathbf{v}_p\|_{L^r(\mathrm{div};\Omega_p)} \|w_p\|_{L^{r'}(\Omega_p)} + \|\mathbf{v}_s\|_{H^1(\Omega_p)} \|w_p\|_{L^{r'}(\Omega_p)} \\
&\quad + \|\mathbf{v}_s\|_{H^1(\Omega_p)} \|\boldsymbol{\tau}_e\|_{L^2(\Omega_p)} + \|\mathbf{v}_f\|_{W^{1,r}(\Omega_f)} \|\mu\|_{W^{1/r,r'}(\Gamma_{fp})} + \|\mathbf{v}_p\|_{L^r(\mathrm{div};\Omega_p)} \|\mu\|_{W^{1/r,r'}(\Gamma_{fp})} \\
&\quad + \|\mathbf{v}_s\|_{H^1(\Omega_p)} \|\mu\|_{W^{1/r,r'}(\Gamma_{fp})} \Big) \leq C \|\mathbf{q}\|_{\mathcal{Q}} \|s\|_S,
\end{aligned}$$

which implies that $\mathcal{B}$ and $\mathcal{B}'$ are bounded and continuous.

Next, let $\mathbf{0} \neq (\mathbf{0}, \mathbf{v}_s, \mathbf{0}) \in \mathcal{Q}$ be given. We choose $\boldsymbol{\tau}_e = \mathbf{D}(\mathbf{v}_s)$ and, using Korn's inequality (1.3.4) for $\mathbf{w} \in \mathbf{X}_p$, we obtain

$$\frac{b_s(\mathbf{v}_s, \boldsymbol{\tau}_e)}{\|\boldsymbol{\tau}_e\|_{L^2(\Omega_p)}} = \frac{\|\mathbf{D}(\mathbf{v}_s)\|^2_{L^2(\Omega_p)}}{\|\mathbf{D}(\mathbf{v}_s)\|_{L^2(\Omega_p)}} = \|\mathbf{D}(\mathbf{v}_s)\|_{L^2(\Omega_p)} \geq C_{K,p} \|\mathbf{v}_s\|_{H^1(\Omega_p)}.$$

Therefore, (3.3.1) holds.

Finally, we note that (3.3.2) was proven in [44] in the case of velocity boundary conditions with restricted mean value of $W_f \times W_p$. However, it can be shown that the result holds with no restriction on $W_f \times W_p$ since $|\Gamma_D| > 0$. □

Slightly abusing the notation from Chapter 1, we denote for $\mathbf{v}_f \in \mathbf{V}_f$ and $\mathbf{v}_s \in \mathbf{X}_p$,

$$|\mathbf{v}_f - \mathbf{v}_s|_{BJS} = \sum_{j=1}^{d-1} |\mathbf{v}_f - \mathbf{v}_s|_{BJS,j}, \quad |\mathbf{v}_f - \mathbf{v}_s|_{BJS,j} = \alpha_{BJS} \|K_j^{-1/4} (\mathbf{v}_f - \mathbf{v}_s) \cdot \mathbf{t}_{f,j}\|_{L^r(\Gamma_{fp})}.$$

Lemma 3.3.2. *The operators $\mathcal{A}$ and $\mathcal{E}_2$ are bounded, continuous, and monotone. In addition, the following continuity and coercivity estimates hold with constants c_f, $\bar{c}_f$, C_f, c_p, $\bar{c}_p$, C_p, c_I, $\bar{c}_I$, $C_I > 0$ for all $\mathbf{u}_f, \mathbf{v}_f \in \mathbf{V}_f$, $\mathbf{u}_p, \mathbf{v}_p \in \mathbf{V}_p$ and $\mathbf{u}_s, \mathbf{v}_s \in \mathbf{X}_p$,*

$$c_f \|\mathbf{v}_f\|^r_{W^{1,r}(\Omega_f)} - c * \bar{c}_f \leq a_f(\mathbf{v}_f, \mathbf{v}_f), \quad a_f(\mathbf{u}_f, \mathbf{v}_f) \leq C_f \|\mathbf{u}_f\|^{r/r'}_{W^{1,r}(\Omega_f)} \|\mathbf{v}_f\|_{W^{1,r}(\Omega_f)}, \tag{3.3.3}$$

$$c_p \|\mathbf{v}_p\|^r_{W^{1,r}(\Omega_p)} - c * \bar{c}_p \leq a^d_p(\mathbf{v}_p, \mathbf{v}_p), \quad a^d_p(\mathbf{u}_p, \mathbf{v}_p) \leq C_p \|\mathbf{u}_p\|^{r/r'}_{L^r(\Omega_p)} \|\mathbf{v}_p\|_{L^r(\Omega_p)}, \tag{3.3.4}$$

$$c_I |\mathbf{v}_f - \mathbf{v}_s|^r_{BJS} - c * \bar{c}_I \leq a_{BJS}(\mathbf{v}_f, \mathbf{v}_s; \mathbf{v}_f, \mathbf{v}_s),$$

$$a_{BJS}(\mathbf{u}_f,\mathbf{u}_s;\mathbf{v}_f,\mathbf{v}_s) \le C_I|\mathbf{u}_f-\mathbf{u}_s|_{BJS}^{r/r'}\|\mathbf{v}_f-\mathbf{v}_s\|_{L^r(\Gamma_{fp})}, \tag{3.3.5}$$

where c is the constant from (B1)–(B2).

Proof. The operator $\mathcal{E}_2$ is linear and, using (3.2.9), it satisfies

$$\mathcal{E}_2(s)(t) = (s_0p_p,w_p)_{\Omega_p} + (A\boldsymbol{\sigma}_e,\boldsymbol{\tau}_e)_{\Omega_p} \le C\left(\|p_p\|_{L^2(\Omega_p)}\|w_p\|_{L^2(\Omega_p)} + \|\boldsymbol{\sigma}_e\|_{L^2(\Omega_p)}\|\boldsymbol{\tau}_e\|_{L^2(\Omega_p)}\right),$$
$$\mathcal{E}_2(s)(s) = (s_0p_p,p_p)_{\Omega_p} + (A\boldsymbol{\sigma}_e,\boldsymbol{\sigma}_e)_{\Omega_p} \ge C\left(\|p_p\|^2_{L^2(\Omega_p)} + \|\boldsymbol{\sigma}_e\|^2_{L^2(\Omega_p)}\right), \quad \forall s,t\in S,$$

which imply that $\mathcal{E}_2$ is bounded, continuous and monotone. The continuity and monotonicity of the operator $\mathcal{A}$ follow from (B1)–(B2), see [44] and [89, Example 5.a, p.59].

For the continuity of $a_f(\cdot,\cdot)$, we apply (3.1.7) with $\mathbf{G}(\mathbf{x})=\nu(\mathbf{x})\mathbf{x}$, $\mathbf{s}=\mathbf{D}(\mathbf{u}_f)$, $\mathbf{t}=\mathbf{0}$ and $\mathbf{w}=\mathbf{D}(\mathbf{v}_f)$:

$$a_f(\mathbf{u}_f,\mathbf{v}_f) \le 2\,C_6\left\|\frac{|\mathbf{D}(\mathbf{u}_f)|}{c+|\mathbf{D}(\mathbf{u}_f)|}\right\|^{\frac{2-r}{r}}_{L^\infty(\Omega_f)}(|\nu(\mathbf{D}(\mathbf{u}_f))\mathbf{D}(\mathbf{u}_f)|,|\mathbf{D}(\mathbf{u}_f)|)^{1/r'}_{\Omega_f}\|\mathbf{D}(\mathbf{v}_f)\|_{L^r(\Omega_f)}.$$

Using (B2) with $\mathbf{x}=\mathbf{0}$, $\mathbf{h}=\mathbf{D}(\mathbf{u}_f)$, we also have

$$|\nu(\mathbf{D}(\mathbf{u}_f))\mathbf{D}(\mathbf{u}_f)| \le C_4\frac{|\mathbf{D}(\mathbf{u}_f)|}{c+|\mathbf{D}(\mathbf{u}_f)|^{2-r}} \le C_4\frac{|\mathbf{D}(\mathbf{u}_f)|^{r-1}}{c|\mathbf{D}(\mathbf{u}_f)|^{r-2}+1} \le C_4|\mathbf{D}(\mathbf{u}_f)|^{r-1}.$$

Combining the above two estimates, we obtain

$$a_f(\mathbf{u}_f,\mathbf{v}_f) \le C\|\mathbf{D}(\mathbf{u}_f)\|^{r/r'}_{L^r(\Omega_f)}\|\mathbf{D}(\mathbf{v}_f)\|_{L^r(\Omega_f)} \le C_f\|\mathbf{u}_f\|^{r/r'}_{W^{1,r}(\Omega_f)}\|\mathbf{v}_f\|_{W^{1,r}(\Omega_f)}.$$

To establish the coercivity bound for $a_f(\cdot,\cdot)$ given in (3.3.3) we consider three cases.

(i) $c=0$. From (3.1.6) we have

$$a_f(\mathbf{v}_f,\mathbf{v}_f) \ge 2\,C_5\frac{\|\mathbf{D}(\mathbf{v}_f)\|^2_{L^r(\Omega_f)}}{\|\mathbf{D}(\mathbf{v}_f)\|^{2-r}_{L^r(\Omega_f)}} = 2\,C_5\|\mathbf{D}(\mathbf{v}_f)\|^r_{L^r(\Omega_f)} \ge 2\,C_5C^r_{K,f}\,\|\mathbf{v}_f\|^r_{W^{1,r}(\Omega_f)}, \tag{3.3.6}$$

where $C_{K,f}$ is the constant arising in Korn's inequality (1.3.4).

(ii) $c\neq 0$ and $\mathbf{v}_f\in\mathbf{V}_f$ with $\|\mathbf{D}(\mathbf{v}_f)\|^{2-r}_{L^r(\Omega_f)} \ge c$. Then from (3.1.6) we have

$$a_f(\mathbf{v}_f,\mathbf{v}_f) \ge 2\,C_5\frac{\|\mathbf{D}(\mathbf{v}_f)\|^2_{L^r(\Omega_f)}}{c+\|\mathbf{D}(\mathbf{v}_f)\|^{2-r}_{L^r(\Omega_f)}} \ge C_5\|\mathbf{D}(\mathbf{v}_f)\|^r_{L^r(\Omega_f)} \ge C_5C^r_K\,\|\mathbf{v}_f\|^r_{W^{1,r}(\Omega_f)}. \tag{3.3.7}$$

(iii) $c \neq 0$ and $\mathbf{v}_f \in \mathbf{V}_f$ with $\|\mathbf{D}(\mathbf{v}_f)\|_{L^r(\Omega_f)}^{2-r} < c$. Then $C_K^r \|\mathbf{v}_f\|_{W^{1,r}(\Omega_f)}^r \leq \|\mathbf{D}(\mathbf{v}_f)\|_{L^r(\Omega_f)}^r \leq c^{r/(2-r)}$. Denote the coercivity constant from (3.3.7) as $c_f = C_5 C_K^r$ and let $\bar{c}_f = C_5 c^{(2r-2)/(2-r)}$. Now,

$$c_f \|\mathbf{v}_f\|_{W^{1,r}(\Omega_f)}^r \leq C_5 \|\mathbf{D}(\mathbf{v}_f)\|_{L^r(\Omega_f)}^r \leq C_5 c^{r/(2-r)} = c\bar{c}_f,$$

hence

$$c_f \|\mathbf{v}_f\|_{W^{1,r}(\Omega_f)}^r - c\bar{c}_f \leq 0 \leq a_f(\mathbf{v}_f, \mathbf{v}_f). \tag{3.3.8}$$

Combining (3.3.6)-(3.3.8) yields the coercivity estimate given in (3.3.3). The reader is also referred to [73], where a similar result is proven under slightly different assumptions, which are satisfied by the Carreau model with $\nu_\infty = 0$.

The continuity and coercivity bounds (3.3.4) and (3.3.5) follow in the same way. □

Remark 3.3.1. *The system (3.2.20)–(3.2.21) is a degenerate evolution problem in a mixed form, which fits the structure of the problems studied in [88]. However, the analysis in [88] is restricted to the Hilbert space setting and needs to be extended to the Sobolev space setting. Furthermore, the analysis in [88] is for monotone operators, see [89], and it is restricted to $\mathbf{f} \in \mathcal{Q}_1'$ and $g \in S_2'$, where $\mathcal{Q}_1'$ and S_2' are the spaces $\mathcal{Q}$ and S with semiscalar products arising from $\mathcal{E}_1$ and $\mathcal{E}_2$, respectively. In our case this translates to $\mathbf{f}_p = \mathbf{f}_f = \mathbf{0}$ and $q_f = 0$. To avoid this restriction, we take a different approach, based on reformulating the problem as a parabolic problem for p_p and $\boldsymbol{\sigma}_e$. The well-posedness of the resulting problem is established using the coercivity of the functionals established in Lemma 3.3.2.*

Denote by $W_{p,2}$ and $\boldsymbol{\Sigma}_{e,2}$ the closure of the spaces W_p and $\boldsymbol{\Sigma}_e$ with respect to the norms

$$\|w_p\|_{W_{p,2}}^2 := (s_0 w_p, w_p)_{L^2(\Omega_p)}, \quad \|\boldsymbol{\tau}_e\|_{\boldsymbol{\Sigma}_{e,2}}^2 := (A\boldsymbol{\tau}_e, \boldsymbol{\tau}_e)_{L^2(\Omega_p)}.$$

Note that $W_{p,2} = L^2(\Omega_p)$, and $\boldsymbol{\Sigma}_{e,2} = \boldsymbol{\Sigma}_e$. Let $S_2 = W_{p,2} \times \boldsymbol{\Sigma}_{e,2}$. We introduce the inner product $(\cdot,\cdot)_{S_2}$ defined by $((w_1, \boldsymbol{\tau}_1), (w_2, \boldsymbol{\tau}_2))_{S_2} := (s_0 w_1, w_2)_{L^2(\Omega_p)} + (A\boldsymbol{\tau}_1, \boldsymbol{\tau}_2)_{L^2(\Omega_p)}$.

Define the domain

$$\begin{aligned} D := \big\{ &(p_p, \boldsymbol{\sigma}_e) \in W_p \times \boldsymbol{\Sigma}_e : \text{ for given } (\mathbf{f}_f, \mathbf{f}_p, q_f) \in \mathbf{V}_f' \times \mathbf{X}_p' \times W_f' \\ &\exists\, ((\mathbf{u}_p, \mathbf{u}_s, \mathbf{u}_f), p_f, \lambda) \in \mathcal{Q} \times W_f \times \Lambda \text{ such that } \forall ((\mathbf{v}_p, \mathbf{v}_s, \mathbf{v}_f), (w_p, \boldsymbol{\tau}_e, w_f, \mu)) \in \mathcal{Q} \times S: \\ &a_f(\mathbf{u}_f, \mathbf{v}_f) + a_p^d(\mathbf{u}_p, \mathbf{v}_p) + a_{BJS}(\mathbf{u}_f, \mathbf{u}_s; \mathbf{v}_f, \mathbf{v}_s) + b_f(\mathbf{v}_f, p_f) + b_p(\mathbf{v}_p, p_p) \end{aligned}$$

$$+ \alpha_p b_p(\mathbf{v}_s, p_p) + b_s(\mathbf{v}_s, \boldsymbol{\sigma}_e) + b_\Gamma(\mathbf{v}_f, \mathbf{v}_p, \mathbf{v}_s; \lambda) = (\mathbf{f}_f, \mathbf{v}_f)_{\Omega_f} + (\mathbf{f}_p, \mathbf{v}_s)_{\Omega_p}, \quad (3.3.9)$$

$$(s_0 p_p, w_p)_{\Omega_p} + a_p^s(\boldsymbol{\sigma}_e, \boldsymbol{\tau}_e) - \alpha_p b_p(\mathbf{u}_s, w_p) - b_p(\mathbf{u}_p, w_p) - b_s(\mathbf{u}_s, \boldsymbol{\tau}_e) - b_f(\mathbf{u}_f, w_f)$$
$$= (q_f, w_f)_{\Omega_f} + (s_0 \bar{g}_p, w_p)_{\Omega_p} + (A\bar{g}_e, \boldsymbol{\tau}_e)_{\Omega_p}, \quad (3.3.10)$$

$$b_\Gamma(\mathbf{u}_f, \mathbf{u}_p, \mathbf{u}_s; \mu) = 0, \quad (3.3.11)$$

$$\text{for some } (\bar{g}_p, \bar{g}_e) \in W'_{p,2} \times \boldsymbol{\Sigma}'_{e,2} \Big\} \subset W_{p,2} \times \boldsymbol{\Sigma}_{e,2}\,. \quad (3.3.12)$$

We note that (3.3.9)–(3.3.11) can be written in an operator form as

$$\mathcal{A}\mathbf{q} + \mathcal{B}'s = \mathbf{f} \quad \text{in } \mathcal{Q}',$$
$$-\mathcal{B}\mathbf{q} + \mathcal{E}_2 s = \bar{g} \quad \text{in } S',$$

where $\bar{g} \in S'$ is the functional on the right hand side of (3.3.10).

Next, define operator $L : D \longrightarrow W'_{p,2} \times \boldsymbol{\Sigma}'_{e,2}$ as

$$L \begin{pmatrix} p_p \\ \boldsymbol{\sigma}_e \end{pmatrix} = \begin{pmatrix} \bar{g}_p \\ \bar{g}_e \end{pmatrix} - \begin{pmatrix} p_p \\ \boldsymbol{\sigma}_e \end{pmatrix}, \quad (3.3.13)$$

and consider the following problem: given $h_p \in W^{1,1}(0,T; W'_{p,2})$ and $h_e \in W^{1,1}(0,T; \boldsymbol{\Sigma}'_{e,2})$, find $(p_p, \boldsymbol{\sigma}_e) \in D$ satisfying

$$\frac{d}{dt} \begin{pmatrix} p_p(t) \\ \boldsymbol{\sigma}_e(t) \end{pmatrix} + L \begin{pmatrix} p_p(t) \\ \boldsymbol{\sigma}_e(t) \end{pmatrix} = \begin{pmatrix} h_p(t) \\ h_e(t) \end{pmatrix}. \quad (3.3.14)$$

A key result that we use to establish the existence of a solution to (3.2.17)–(3.2.19) is the following theorem; for details see [89, Theorem 6.1(b)].

Theorem 3.3.1. *Let the linear, symmetric and monotone operator $\mathcal{N}$ be given for the real vector space E to its algebraic dual E^*, and let E_b' be the Hilbert space which is the dual of E with the seminorm*

$$|x|_b \;=\; (\mathcal{N}x\,(x))^{1/2}\,, \quad x \in E\,.$$

Let $\mathcal{M} \subset E \times E_b'$ be a relation with domain $D = \{x \in E \,:\, \mathcal{M}(x) \neq \emptyset\}$.
Assume $\mathcal{M}$ is monotone and $Rg(\mathcal{N} + \mathcal{M}) = E_b'$. Then, for each $u_0 \in D$ and for each $f \in W^{1,1}(0,T;E_b')$, there is a solution u of

$$\frac{d}{dt}\left(\mathcal{N}u(t)\right) \;+\; \mathcal{M}\left(u(t)\right) \ni f(t)\,, \quad 0 < t < T\,,$$

with

$$\mathcal{N}u \in W^{1,\infty}(0,T;E_b')\,, \quad u(t) \in D\,, \quad \text{for all } 0 \le t \le T\,, \quad \text{and } \mathcal{N}u(0) \;= \mathcal{N}u_0\,.$$

Using Theorem 3.3.1, we can show that the problem (3.2.17)–(3.2.19) is well-posed.

Theorem 3.3.2. *For each $\mathbf{f}_f \in W^{1,1}(0,T;\mathbf{V}_f')$, $\mathbf{f}_p \in W^{1,1}(0,T;\mathbf{X}_p')$, $q_f \in W^{1,1}(0,T;W_f')$, $q_p \in W^{1,1}(0,T;W_p')$, and $p_p(0) = p_{p,0} \in W_p$, $\boldsymbol{\sigma}_e(0) = A^{-1}\mathbf{D}(\boldsymbol{\eta}_{p,0}) \in \boldsymbol{\Sigma}_e$, there exists a solution of (3.2.17)–(3.2.19) with $(\mathbf{u}_f, p_f, \mathbf{u}_p, p_p, \mathbf{u}_s, \boldsymbol{\sigma}_e, \lambda) \in L^\infty(0,T;\mathbf{V}_f) \times L^\infty(0,T;W_f) \times L^\infty(0,T;\mathbf{V}_p) \times W^{1,\infty}(0,T;W_p) \times L^\infty(0,T;\mathbf{X}_p) \times W^{1,\infty}(0,T;\boldsymbol{\Sigma}_e) \times L^\infty(0,T;\Lambda)$.*

To prove Theorem 3.3.2 we proceed in the following manner.

Step 1. (Section 3.3.1.1) Establish that the domain D given by (3.3.12) is nonempty.

Step 2. (Section 3.3.1.2) Show solvability of the parabolic problem (3.3.14).

Step 3. (Section 3.3.1.3) Show that the original problem (3.2.17)–(3.2.19) is a special case of (3.3.14).

Each of the steps will be covered in details in the corresponding subsection.

3.3.1.1 Step 1: The Domain D is nonempty We begin with a number of preliminary results used in the proof. We first introduce operators that will be used to regularize the problem. Let $R_s : X_p \longrightarrow X_p'$, $R_p : V_p \longrightarrow V_p'$, $L_f : W_f \longrightarrow W_f'$, $L_p : W_p \longrightarrow W_p'$ be defined by

$$R_s(\mathbf{u}_s)(\mathbf{v}_s) := r_s(\mathbf{u}_s, \mathbf{v}_s) = (\mathbf{D}(\mathbf{u}_s), \mathbf{D}(\mathbf{v}_s))_{\Omega_p}, \tag{3.3.15}$$

$$R_p(\mathbf{u}_p)(\mathbf{v}_p) := r_p(\mathbf{u}_p, \mathbf{v}_p) = (|\nabla \cdot \mathbf{u}_p|^{r-2}\nabla \cdot \mathbf{u}_p, \nabla \cdot \mathbf{v}_p)_{\Omega_p}, \tag{3.3.16}$$

$$L_f(p_f)(w_f) := l_f(p_f, w_f) = (|p_f|^{r'-2}p_f, w_f)_{\Omega_f}, \tag{3.3.17}$$

$$L_p(p_p)(w_p) := l_p(p_p, w_p) = (|p_p|^{r'-2}p_p, w_p)_{\Omega_p}. \tag{3.3.18}$$

Lemma 3.3.3. *The operators R_s, R_p, L_f, and L_p are bounded, continuous, coercive, and monotone.*

Proof. The operators satisfy the following continuity and coercivity bounds:

$$\begin{aligned}
&R_s(\mathbf{u}_s)(\mathbf{v}_s) \le \|\mathbf{u}_s\|_{H^1(\Omega_p)}\|\mathbf{v}_s\|_{H^1(\Omega_p)}, && R_s(\mathbf{u}_s)(\mathbf{u}_s) \ge C_{K,p}\|\mathbf{u}_s\|^2_{H^1(\Omega_p)}, && \forall \mathbf{u}_s, \mathbf{v}_s \in \mathbf{X}_p,\\
&R_p(\mathbf{u}_p)(\mathbf{v}_p) \le \|\nabla \cdot \mathbf{u}_p\|^{r/r'}_{L^r(\Omega_p)}\|\nabla \cdot \mathbf{v}_p\|_{L^r(\Omega_p)}, && R_p(\mathbf{u}_p)(\mathbf{u}_p) \ge \|\nabla \cdot \mathbf{u}_p\|^{r}_{L^r(\Omega_p)}, && \forall \mathbf{u}_p, \mathbf{v}_p \in \mathbf{V}_p,\\
&L_f(p_f)(w_f) \le \|p_f\|^{r'/r}_{L^{r'}(\Omega_f)}\|w_f\|_{L^{r'}(\Omega_f)}, && L_f(p_f)(p_f) \ge \|p_f\|^{r'}_{L^{r'}(\Omega_f)}, && \forall p_f, w_f \in W_f,\\
&L_p(p_p)(w_p) \le \|p_p\|^{r'/r}_{L^{r'}(\Omega_p)}\|w_p\|_{L^{r'}(\Omega_p)}, && L_p(p_p)(p_p) \ge \|p_p\|^{r'}_{L^{r'}(\Omega_p)}, && \forall p_p, w_p \in W_p.
\end{aligned}$$

The coercivity bounds follow directly from the definitions, using Korn's inequality (1.3.4) for R_s. The continuity bounds follow from the Cauchy-Schwarz or Hölder's inequalities, (1.3.2). The above bounds imply that the operators are bounded, continuous, and coercive. Monotonicity follows from bounds similar to (3.1.6), which can be established in a way similar to the Power law model [84]. □

It was shown in [44] that there exists a bounded extension of λ from $W^{1/r,r'}(\Gamma_{fp})$ to $W^{1/r,r'}(\partial\Omega_p)$, defined as $E_\Gamma\lambda = \gamma\phi(\lambda)$, where γ is the trace operator from $W^{1,r}(\Omega_p)$ to $W^{1/r,r'}(\partial\Omega_p)$ and $\phi(\lambda) \in W^{1,r'}(\Omega_p)$ is the weak solution of

$$-\nabla \cdot |\nabla\phi(\lambda)|^{r'-2}\nabla\phi(\lambda) = 0, \quad \text{in } \Omega_p, \tag{3.3.19}$$

$$\phi(\lambda) = \lambda, \quad \text{on } \Gamma_{fp}, \tag{3.3.20}$$

$$|\nabla\phi(\lambda)|^{r'-2}\nabla\phi(\lambda)\cdot\mathbf{n}=0,\quad \text{on } \partial\Omega_p\setminus\Gamma_{fp}\,. \tag{3.3.21}$$

We have the following equivalence of norms statement.

Lemma 3.3.4. *For $\lambda\in W^{1/r,r'}(\Gamma_{fp})$ and $\phi(\lambda)$ defined by (3.3.19)–(3.3.21), there exists c_1, $c_2>0$ such that*

$$c_1\|\phi(\lambda)\|_{W^{1,r'}(\Omega_p)}\le\|\lambda\|_{W^{1/r,r'}(\Gamma_{fp})}\le c_2\|\phi(\lambda)\|_{W^{1,r'}(\Omega_p)}. \tag{3.3.22}$$

Proof. For $\phi\in W^{1,r'}(\Omega)$, $|\nabla\phi(\lambda)|^{r'-2}\nabla\phi(\lambda)\in L^{r'}(\mathrm{div};\Omega)$ and, therefore, from (3.3.19)–(3.3.21), we have

$$\begin{aligned}(|\nabla\phi(\lambda)|^{r'-2}\nabla\phi(\lambda),\nabla\phi(\lambda))_{\Omega_p}&=\langle|\nabla\phi(\lambda)|^{r'-2}\nabla\phi(\lambda)\cdot\mathbf{n},E_\Gamma\lambda\rangle_{\partial\Omega_p}\\&\le\||\nabla\phi(\lambda)|^{r'-2}\nabla\phi(\lambda)\cdot\mathbf{n}\|_{W^{-1/r,r}(\partial\Omega_p)}\|E_\Gamma\lambda\|_{W^{1/r,r'}(\partial\Omega_p)}\\&\le C\,\||\nabla\phi(\lambda)|^{r'-2}\nabla\phi(\lambda)\cdot\mathbf{n}\|_{W^{-1/r,r}(\partial\Omega_p)}\|\lambda\|_{W^{1/r,r'}(\Gamma_{fp})}.\end{aligned} \tag{3.3.23}$$

Now, for $\psi\in W^{1,r'}(\Omega_p)$,

$$\begin{aligned}\int_{\partial\Omega_p}|\nabla\phi(\lambda)|^{r'-2}\nabla\phi(\lambda)\cdot\mathbf{n}\,\psi\,ds&=\int_{\Omega_p}\nabla\cdot|\nabla\phi(\lambda)|^{r'-2}\nabla\phi(\lambda)\,\psi\,d\mathbf{x}\\+\int_{\Omega_p}|\nabla\phi(\lambda)|^{r'-2}\nabla\phi(\lambda)\cdot\nabla\psi\,d\mathbf{x}&\le\||\nabla\phi(\lambda)|^{r'-2}\nabla\phi(\lambda)\|_{L^r(\Omega_p)}\,\|\psi\|_{W^{1,r'}(\Omega_p)}\quad\text{(using (3.3.19))}\\&=\|\nabla\phi\|^{r'/r}_{L^{r'}(\Omega_p)}\,\|\psi\|_{W^{1,r'}(\Omega_p)}\,.\end{aligned} \tag{3.3.24}$$

Using the fact the trace operator, $\gamma(\cdot)$, is a bounded, linear, bijective operator for the quotient space $W^{1,q}(\Omega_p)/W^{1,q}_0(\Omega_p)$ onto $W^{1-\frac{1}{q},q}(\partial\Omega_p)$ [50], we have

$$\begin{aligned}&\||\nabla\phi(\lambda)|^{r'-2}\nabla\phi(\lambda)\cdot\mathbf{n}\|_{W^{-1/r,r}(\partial\Omega_p)}\\&\qquad=\sup_{\xi\in W^{1/r,r'}(\partial\Omega_p)}\frac{\langle|\nabla\phi(\lambda)|^{r'-2}\nabla\phi(\lambda)\cdot\mathbf{n}\,,\xi\rangle_{W^{-1/r,r}(\partial\Omega_p),W^{1/r,r'}(\partial\Omega_p)}}{\|\xi\|_{W^{1/r,r'}(\partial\Omega_p)}}\\&\qquad\le C\sup_{\psi\in W^{1,r'}(\Omega_p)}\frac{\int_{\partial\Omega_p}|\nabla\phi(\lambda)|^{r'-2}\nabla\phi(\lambda)\cdot\mathbf{n}\,\gamma(\psi)\,ds}{\|\psi\|_{W^{1,r'}(\Omega_p)}}\\&\qquad\le C\,\|\nabla\phi\|^{r'/r}_{L^{r'}(\Omega_p)},\ \text{(using (3.3.24))}.\end{aligned} \tag{3.3.25}$$

Combining (3.3.23) and (3.3.25) with the Poincare inequality (1.3.5) implies that

$$\|\phi(\lambda)\|_{W^{1,r'}(\Omega)} \leq C\|\lambda\|_{W^{1/r,r'}(\Gamma_{fp})}. \tag{3.3.26}$$

On the other hand, due to (3.3.20) and the trace inequality (1.3.3), we have

$$\|\lambda\|_{W^{1/r,r'}(\Gamma_{fp})} \leq C\|\phi(\lambda)\|_{W^{1,r'}(\Omega)}. \tag{3.3.27}$$

Combining (3.3.26) and (3.3.27), we obtain (3.3.22). □

Introduce $L_\Gamma : \Lambda \longrightarrow \Lambda'$ defined by

$$L_\Gamma(\lambda)(\mu) := l_\Gamma(\lambda,\mu) = \left(|\nabla\phi(\lambda)|^{r-2}\nabla\phi(\lambda), \nabla\phi(\mu)\right)_{\Omega_p}. \tag{3.3.28}$$

Lemma 3.3.5. *The operator L_Γ is bounded, continuous, coercive, and monotone.*

Proof. The result can be obtained in a similar manner to the proof of Lemma 3.3.3, using the equivalence of norms proved in Lemma 3.3.4. □

To establish that the domain D is nonempty we first show that there exists a solution to a regularization of (3.3.9)–(3.3.11). Then a solution to (3.3.9)–(3.3.11) is established by analyzing the regularized solutions as the regularization parameter goes to zero.

Lemma 3.3.6. *The domain D specified by (3.3.12) is nonempty.*

Proof. We will focus on the case (B1)–(B2) with $c = 0$, which holds for the Power law model. The argument for the case $c > 0$ is similar, with an extra constant term on the right-hand side of the energy bound (3.3.33), due to coercivity estimates (3.3.3)–(3.3.5).

For $\mathbf{q}^{(i)} = (\mathbf{v}_{p,i}, \mathbf{v}_{s,i}, \mathbf{v}_{f,i}) \in \mathcal{Q}$, $s^{(i)} = (w_{p,i}, \boldsymbol{\tau}_{e,i}, w_{f,i}, \mu_i) \in S$, $i = 1, 2$, define the operators $\mathcal{R} : \mathcal{Q} \to \mathcal{Q}'$ and $\mathcal{L} : S \to S'$ as

$$\begin{aligned}
\mathcal{R}(\mathbf{q}^{(1)})(\mathbf{q}^{(2)}) &:= R_s(\mathbf{v}_{s,1})(\mathbf{v}_{s,2}) + R_p(\mathbf{v}_{p,1})(\mathbf{v}_{p,2}) = r_s(\mathbf{v}_{s,1}, \mathbf{v}_{s,2}) + r_p(\mathbf{v}_{p,1}, \mathbf{v}_{p,2}),\\
\text{and } \mathcal{L}(s^{(1)})(s^{(2)}) &:= L_f(w_{f,1})(w_{f,2}) + L_p(w_{p,1})(w_{p,2}) + L_\Gamma(\mu_1)(\mu_2)\\
&= l_f(w_{f,1}, w_{f,2}) + l_p(w_{p,1}, w_{p,2}) + l_\Gamma(\mu_1, \mu_2).
\end{aligned}$$

For $\epsilon > 0$, consider a regularization of (3.3.9)–(3.3.11) defined by: *Given* $\mathbf{f} \in \mathcal{Q}'$, $\bar{g} \in S'$, *determine* $\mathbf{q}_\epsilon \in \mathcal{Q}$, $s_\epsilon \in S$ *satisfying*

$$(\epsilon\mathcal{R} + \mathcal{A})\mathbf{q}_\epsilon + \mathcal{B}' s_\epsilon = \mathbf{f} \quad \text{in } \mathcal{Q}', \tag{3.3.29}$$

$$-\mathcal{B}\mathbf{q}_\epsilon + (\epsilon\mathcal{L} + \mathcal{E}_2)s_\epsilon = \bar{g} \quad \text{in } S'. \tag{3.3.30}$$

Introduce the operator $\mathcal{O} : \mathcal{Q} \times S \to (\mathcal{Q} \times S)'$ defined as

$$\mathcal{O}\begin{pmatrix} \mathbf{q} \\ s \end{pmatrix} = \begin{pmatrix} \epsilon\mathcal{R} + \mathcal{A} & \mathcal{B}' \\ -\mathcal{B} & \epsilon\mathcal{L} + \mathcal{E}_2 \end{pmatrix} \begin{bmatrix} \mathbf{q} \\ s \end{bmatrix}.$$

Note that

$$\begin{aligned} \mathcal{O}\begin{pmatrix} \mathbf{q}^{(1)} \\ s^{(1)} \end{pmatrix} \left(\begin{pmatrix} \mathbf{q}^{(2)} \\ s^{(2)} \end{pmatrix} \right) &= (\epsilon\mathcal{R} + \mathcal{A})(\mathbf{q}^{(1)})(\mathbf{q}^{(2)}) + \mathcal{B}'(s^{(1)})(\mathbf{q}^{(2)}) - \mathcal{B}(\mathbf{q}^{(1)})(s^{(2)}) \\ &\quad + (\epsilon\mathcal{L} + \mathcal{E}_2)(s^{(1)})(s^{(2)}), \end{aligned} \tag{3.3.31}$$

and

$$\begin{aligned} &\left(\mathcal{O}\begin{pmatrix} \mathbf{q}^{(1)} \\ s^{(1)} \end{pmatrix} - \mathcal{O}\begin{pmatrix} \mathbf{q}^{(2)} \\ s^{(2)} \end{pmatrix} \right) \left(\begin{pmatrix} \mathbf{q}^{(1)} \\ s^{(1)} \end{pmatrix} - \begin{pmatrix} \mathbf{q}^{(2)} \\ s^{(2)} \end{pmatrix} \right) \\ &= ((\epsilon\mathcal{R} + \mathcal{A})\mathbf{q}^{(1)} - (\epsilon\mathcal{R} + \mathcal{A})\mathbf{q}^{(2)})(\mathbf{q}^{(1)} - \mathbf{q}^{(2)}) + ((\epsilon\mathcal{L} + \mathcal{E}_2)s^{(1)} - (\epsilon\mathcal{L} + \mathcal{E}_2)s^{(2)})(s^{(1)} - s^{(2)}). \end{aligned}$$

From Lemmas 3.3.1, 3.3.2, 3.3.3, and 3.3.5 we have that $\mathcal{O}$ is a bounded, continuous, and monotone operator. Moreover, using the coercivity bounds from (3.3.3)–(3.3.5), we also have

$$\begin{aligned} \mathcal{O}\begin{pmatrix} \mathbf{q} \\ s \end{pmatrix} \left(\begin{pmatrix} \mathbf{q} \\ s \end{pmatrix} \right) &= (\epsilon\mathcal{R} + \mathcal{A})\mathbf{q}(\mathbf{q}) + (\mathcal{E}_2 + \epsilon\mathcal{L})s(s) \\ &= \epsilon r_s(\mathbf{v}_s, \mathbf{v}_s) + \epsilon r_p(\mathbf{v}_p, \mathbf{v}_p) + a_f(\mathbf{v}_f, \mathbf{v}_f) + a_p^d(\mathbf{v}_p, \mathbf{v}_p) + a_{BJS}(\mathbf{v}_f, \mathbf{v}_s; \mathbf{v}_f, \mathbf{v}_s) \\ &\quad + (s_0 w_p, w_p)_{\Omega_p} + a_p^s(\boldsymbol{\tau}_e, \boldsymbol{\tau}_e) + \epsilon l_f(w_f, w_f) + \epsilon l_p(w_p, w_p) + \epsilon l_\Gamma(\mu, \mu) \end{aligned}$$

$$\geq C\Big(\epsilon\|\mathbf{D}(\mathbf{v}_s)\|^2_{L^2(\Omega_p)} + \epsilon\|\nabla\cdot\mathbf{v}_p\|^r_{L^r(\Omega_p)} + \|\mathbf{D}(\mathbf{v}_f)\|^r_{L^r(\Omega_f)} + \|\mathbf{v}_p\|^r_{L^r(\Omega_p)} + |\mathbf{v}_f-\mathbf{v}_s|^r_{BJS}$$
$$+ s_0\|w_p\|^2_{L^2(\Omega_p)} + \|\boldsymbol{\tau}_e\|^2_{L^2(\Omega_p)} + \epsilon\|w_f\|^{r'}_{L^{r'}(\Omega_f)} + \epsilon\|w_p\|^{r'}_{L^{r'}(\Omega_p)} + \epsilon\|\mu\|^{r'}_{W^{1/r,r'}(\Gamma_{fp})}\Big). \quad (3.3.32)$$

In the case of (B1)–(B2) with $c>0$, we have an extra term $-c(\bar{c}_f+\bar{c}_p+\bar{c}_I)$ on the right-hand side of (3.3.32) due to the coercivity estimates from (3.3.3)–(3.3.5). The argument in this case doesn't change and we omit this term for simplicity. It follows from (3.3.32) that $\mathcal{O}$ is coercive. Thus, an application of the Browder-Minty theorem [77] establishes the existence of a solution $(\mathbf{q}_\epsilon, s_\epsilon)\in\mathcal{Q}\times S$ of (3.3.29)–(3.3.30), where $\mathbf{q}_\epsilon=(\mathbf{u}_{p,\epsilon},\mathbf{u}_{s,\epsilon},\mathbf{u}_{f,\epsilon})$ and $s_\epsilon=(p_{p,\epsilon},\boldsymbol{\sigma}_{e,\epsilon},p_{f,\epsilon},\lambda_\epsilon)$.

Now, from (3.3.32) and (3.3.29)–(3.3.30), we have

$$\epsilon\|\mathbf{u}_{s,\epsilon}\|^2_{H^1(\Omega_p)} + \epsilon\|\nabla\cdot\mathbf{u}_{p,\epsilon}\|^r_{L^r(\Omega_p)} + \|\mathbf{u}_{f,\epsilon}\|^r_{W^{1,r}(\Omega_f)} + \|\mathbf{u}_{p,\epsilon}\|^r_{L^r(\Omega_p)} + |\mathbf{u}_{f,\epsilon}-\mathbf{u}_{s,\epsilon}|^r_{BJS}$$
$$+ s_0\|p_{p,\epsilon}\|^2_{L^2(\Omega_p)} + \|\boldsymbol{\sigma}_{e,\epsilon}\|^2_{L^2(\Omega_p)} + \epsilon\|p_{f,\epsilon}\|^{r'}_{L^{r'}(\Omega_f)} + \epsilon\|p_{p,\epsilon}\|^{r'}_{L^{r'}(\Omega_p)} + \epsilon\|\lambda_\epsilon\|^{r'}_{W^{1/r,r'}(\Gamma_{fp})}$$
$$\leq C\Big(\|\mathbf{f}_p\|_{H^{-1}(\Omega_p)}\|\mathbf{u}_{s,\epsilon}\|_{H^1(\Omega_p)} + \|\mathbf{f}_f\|_{W^{-1,r'}(\Omega_f)}\|\mathbf{u}_{f,\epsilon}\|_{W^{1,r}(\Omega_f)}$$
$$+ \|q_f\|_{L^r(\Omega_f)}\|p_{f,\epsilon}\|_{L^{r'}(\Omega_f)} + \|\bar{g}_p\|_{L^r(\Omega_p)}\|p_{p,\epsilon}\|_{L^{r'}(\Omega_p)} + \|\bar{g}_e\|_{L^2(\Omega_p)}\|\boldsymbol{\sigma}_{e,\epsilon}\|_{L^2(\Omega_p)}\Big). \quad (3.3.33)$$

From (3.3.10), $\boldsymbol{\sigma}_{e,\epsilon}$ and $\mathbf{u}_{s,\epsilon}$ satisfy

$$a^s_p(\boldsymbol{\sigma}_{e,\epsilon},\boldsymbol{\tau}_e) - b_s(\mathbf{u}_{s,\epsilon},\boldsymbol{\tau}_e) = (A\bar{g}_e,\boldsymbol{\tau}_e)_{\Omega_p}, \quad \forall\boldsymbol{\tau}_e\in\boldsymbol{\Sigma}_e.$$

Therefore, applying the inf-sup condition (3.3.1), we obtain:

$$\|\mathbf{u}_{s,\epsilon}\|_{H^1(\Omega_p)} \leq C\sup_{0\neq(0,\boldsymbol{\tau}_e,0,0)\in S}\frac{b_s(\mathbf{u}_{s,\epsilon},\boldsymbol{\tau}_e)}{\|(0,\boldsymbol{\tau}_e,0,0)\|_S} = C\sup_{0\neq(0,\boldsymbol{\tau}_e,0,0)\in S}\frac{a^s_p(\boldsymbol{\sigma}_{e,\epsilon},\boldsymbol{\tau}_e)-(A\bar{g}_e,\boldsymbol{\tau}_e)_{\Omega_p}}{\|(0,\boldsymbol{\tau}_e,0,0)\|_S}$$
$$\leq C\left(\|\boldsymbol{\sigma}_{e,\epsilon}\|_{L^2(\Omega_p)} + \|\bar{g}_e\|_{L^2(\Omega_p)}\right). \quad (3.3.34)$$

Combining (3.3.34) and (3.3.33), and using Young's inequality, we obtain

$$\|\mathbf{u}_{s,\epsilon}\|^2_{H^1(\Omega_p)} + \epsilon\|\nabla\cdot\mathbf{u}_{p,\epsilon}\|^r_{L^r(\Omega_p)} + \|\mathbf{u}_{f,\epsilon}\|^r_{W^{1,r}(\Omega_f)} + \|\mathbf{u}_{p,\epsilon}\|^r_{L^r(\Omega_p)} + |\mathbf{u}_{f,\epsilon}-\mathbf{u}_{s,\epsilon}|^r_{BJS}$$
$$+ \epsilon\|\mathbf{u}_{s,\epsilon}\|^2_{H^1(\Omega_p)} + s_0\|p_{p,\epsilon}\|^2_{L^2(\Omega_p)} + \|\boldsymbol{\sigma}_{e,\epsilon}\|^2_{L^2(\Omega_p)} + \epsilon\|p_{f,\epsilon}\|^{r'}_{L^{r'}(\Omega_f)} + \epsilon\|p_{p,\epsilon}\|^{r'}_{L^{r'}(\Omega_p)}$$
$$+ \epsilon\|\lambda_\epsilon\|^{r'}_{W^{1/r,r'}(\Gamma_{fp})} \leq C\Big(\|q_f\|_{L^r(\Omega_f)}\|p_{f,\epsilon}\|_{L^{r'}(\Omega_f)} + \|\bar{g}_p\|_{L^r(\Omega_p)}\|p_{p,\epsilon}\|_{L^{r'}(\Omega_p)} + \|\mathbf{f}_p\|^2_{H^{-1}(\Omega_p)}$$
$$+ \|\mathbf{f}_f\|^{r'}_{W^{-1,r'}(\Omega_f)} + \|\bar{g}_e\|^2_{L^2(\Omega_p)}\Big) + \frac{1}{2}\left(\|\mathbf{u}_{s,\epsilon}\|^2_{H^1(\Omega_p)} + \|\mathbf{u}_{f,\epsilon}\|^r_{W^{1,r}(\Omega_f)} + \|\boldsymbol{\sigma}_{e,\epsilon}\|^2_{L^2(\Omega_p)}\right), \quad (3.3.35)$$

from which it follows that

$$\|\mathbf{u}_{s,\epsilon}\|^2_{H^1(\Omega_p)} + \epsilon\|\nabla\cdot\mathbf{u}_{p,\epsilon}\|^r_{L^r(\Omega_p)} + \|\mathbf{u}_{f,\epsilon}\|^r_{W^{1,r}(\Omega_f)} + \|\mathbf{u}_{p,\epsilon}\|^r_{L^r(\Omega_p)} + \|\boldsymbol{\sigma}_{e,\epsilon}\|^2_{L^2(\Omega_p)} + |\mathbf{u}_{f,\epsilon}-\mathbf{u}_{s,\epsilon}|^r_{BJS}$$
$$\leq C\left(\|\mathbf{f}_p\|^2_{H^{-1}(\Omega_p)} + \|\mathbf{f}_f\|^{r'}_{W^{-1,r'}(\Omega_f)} + \|q_f\|_{L^r(\Omega_f)}\|p_{f,\epsilon}\|_{L^{r'}(\Omega_f)}\right.$$
$$\left.+\|\bar{g}_e\|^2_{L^2(\Omega_p)} + \|\bar{g}_p\|_{L^r(\Omega_p)}\|p_{p,\epsilon}\|_{L^{r'}(\Omega_p)}\right). \tag{3.3.36}$$

To obtain bounds for $p_{p,\epsilon}$, $p_{f,\epsilon}$, and λ_ϵ we use (3.3.2). With $s=(p_{p,\epsilon},\mathbf{0},p_{f,\epsilon},\lambda_\epsilon)\in S$, we have

$$\begin{aligned}
&\|p_{f,\epsilon}\|_{L^{r'}(\Omega_f)} + \|p_{p,\epsilon}\|_{L^{r'}(\Omega_p)} + \|\lambda_\epsilon\|_{W^{1/r,r'}(\Gamma_{fp})}\\
&\quad\leq C\sup_{(\mathbf{v}_p,\mathbf{0},\mathbf{v}_f)\in\mathcal{Q}}\frac{b_f(\mathbf{v}_f,p_{f,\epsilon})+b_p(\mathbf{v}_p,p_{p,\epsilon})+b_\Gamma(\mathbf{v}_f,\mathbf{v}_p,\mathbf{0};\lambda_\epsilon)}{\|(\mathbf{v}_p,\mathbf{0},\mathbf{v}_f)\|_{\mathcal{Q}}}\\
&\quad\leq C\sup_{\mathbf{q}\in\mathcal{Q}}\frac{-\epsilon\, r_p(\mathbf{u}_{p,\epsilon},\mathbf{v}_p)-a_f(\mathbf{u}_{f,\epsilon},\mathbf{v}_f)-a_p^d(\mathbf{u}_{p,\epsilon},\mathbf{v}_p)-a_{BJS}(\mathbf{u}_{f,\epsilon},\mathbf{u}_{s,\epsilon};\mathbf{v}_f,\mathbf{0})+(\mathbf{f}_f,\mathbf{v}_f)_{\Omega_f}}{\|(\mathbf{v}_p,\mathbf{0},\mathbf{v}_f)\|_{\mathcal{Q}}}\\
&\quad\leq C\left(\epsilon\|\nabla\cdot\mathbf{u}_{p,\epsilon}\|^{r/r'}_{L^r(\Omega_p)} + \|\mathbf{u}_{f,\epsilon}\|^{r/r'}_{W^{1,r}(\Omega_f)} + \|\mathbf{u}_{p,\epsilon}\|^{r/r'}_{L^r(\Omega_p)} + |\mathbf{u}_{f,\epsilon}-\mathbf{u}_{s,\epsilon}|^{r/r'}_{BJS} + \|\mathbf{f}_f\|_{W^{-1,r'}(\Omega_f)}\right).
\end{aligned} \tag{3.3.37}$$

Using Young's inequality (1.3.6), (3.3.36) and (3.3.37), we obtain

$$\begin{aligned}
&\|\mathbf{u}_{s,\epsilon}\|^2_{H^1(\Omega_p)} + \epsilon\|\nabla\cdot\mathbf{u}_{p,\epsilon}\|^r_{L^r(\Omega_p)} + \|\mathbf{u}_{f,\epsilon}\|^r_{W^{1,r}(\Omega_f)} + \|\mathbf{u}_{p,\epsilon}\|^r_{L^r(\Omega_p)} + \|\boldsymbol{\sigma}_{e,\epsilon}\|^2_{L^2(\Omega_p)} + |\mathbf{u}_{f,\epsilon}-\mathbf{u}_{s,\epsilon}|^r_{BJS}\\
&\qquad + \|p_{f,\epsilon}\|^{r'}_{L^{r'}(\Omega_f)} + \|p_{p,\epsilon}\|^{r'}_{L^{r'}(\Omega_p)} + \|\lambda_\epsilon\|^{r'}_{W^{1/r,r'}(\Gamma_{fp})}\\
&\qquad\leq C\left(\|\mathbf{f}_p\|^2_{H^{-1}(\Omega_p)} + \|\mathbf{f}_f\|^{r'}_{W^{-1,r'}(\Omega_f)} + \|\bar{g}_p\|^r_{L^r(\Omega_p)} + \|\bar{g}_e\|^2_{L^2(\Omega_p)} + \|q_f\|^r_{L^r(\Omega_f)}\right),
\end{aligned} \tag{3.3.38}$$

which implies that $\|\mathbf{u}_{s,\epsilon}\|_{H^1(\Omega_p)}$, $\|\mathbf{u}_{f,\epsilon}\|_{W^{1,r}(\Omega_f)}$, $\|\boldsymbol{\sigma}_{e,\epsilon}\|_{L^2(\Omega_p)}$, $\|p_{f,\epsilon}\|_{L^{r'}(\Omega_f)}$, $\|p_{p,\epsilon}\|_{L^{r'}(\Omega_p)}$ and $\|\lambda_\epsilon\|_{W^{1/r,r'}(\Gamma_{fp})}$ are bounded independently of ϵ.

Also, as $\nabla\cdot\mathbf{V}_p=(W_p)'$, we have from (3.3.30), (3.3.10), and the continuity of L_p stated in Lemma 3.3.3:

$$\begin{aligned}
\|\nabla\cdot\mathbf{u}_{p,\epsilon}\|_{L^r(\Omega_p)} &\leq s_0\|\bar{g}_p\|_{L^r(\Omega_p)} + s_0\|p_{p,\epsilon}\|_{L^r(\Omega_p)} + \alpha_p\|\nabla\cdot\mathbf{u}_{s,\epsilon}\|_{L^r(\Omega_p)} + \epsilon\|p_{p,\epsilon}\|_{L^{r'}(\Omega_p)}\\
&\leq s_0\|\bar{g}_p\|_{L^r(\Omega_p)} + s_0\|p_{p,\epsilon}\|_{L^{r'}(\Omega_p)} + \alpha_p\|\mathbf{u}_{s,\epsilon}\|_{H^1(\Omega_p)} + \epsilon\|p_{p,\epsilon}\|_{L^{r'}(\Omega_p)}.
\end{aligned}$$

Therefore $\|\mathbf{u}_{p,\epsilon}\|_{L^r(\mathrm{div};\Omega_p)}$ is also bounded independently of ϵ.

Since $\mathcal{Q}$ and S are reflexive Banach spaces, as $\epsilon \to 0$ we can extract weakly convergent subsequences $\{\mathbf{q}_{\epsilon,n}\}_{n=1}^{\infty}$, $\{s_{\epsilon,n}\}_{n=1}^{\infty}$, and $\{\mathcal{A}\mathbf{q}_{\epsilon,n}\}_{n=1}^{\infty}$, such that $\mathbf{q}_{\epsilon,n} \rightharpoonup \mathbf{q}$ in $\mathcal{Q}$, $s_{\epsilon,n} \rightharpoonup s$ in S, $\mathcal{A}\mathbf{q}_{\epsilon,n} \rightharpoonup \zeta$ in $\mathcal{Q}'$, and

$$\begin{aligned} \zeta + \mathcal{B}'s &= \mathbf{f} \quad \text{in } \mathcal{Q}', \\ \mathcal{E}_2 s - \mathcal{B}\mathbf{q} &= \bar{g} \quad \text{in } S'. \end{aligned}$$

Moreover, from (3.3.29)–(3.3.30) we have

$$\begin{aligned} \limsup_{\epsilon\to 0} \left(\mathcal{A}(\mathbf{q}_\epsilon)(\mathbf{q}_\epsilon) + \mathcal{E}_2(s_\epsilon)(s_\epsilon)\right) &= \limsup_{\epsilon\to 0}(-\epsilon\mathcal{R}(\mathbf{q}_\epsilon)(\mathbf{q}_\epsilon) - \epsilon\mathcal{L}(s_\epsilon)(s_\epsilon) + \mathbf{f}(\mathbf{q}_\epsilon) + \bar{g}(s_\epsilon)) \\ &\leq \mathbf{f}(\mathbf{q}) + \bar{g}(s) = \zeta(\mathbf{q}) + \mathcal{E}_2(s)(s). \end{aligned}$$

Since $\mathcal{A} + \mathcal{E}_2$ is monotone and continuous, it follows, see [89, p. 38], that $\mathcal{A}\mathbf{q} = \zeta$. Hence, $\mathbf{q}$ and s solve (3.3.9)–(3.3.11), which establishes that D is nonempty. □

Corollary 3.3.1. *For L defined by (3.3.13) we have that $Rg(I + L) = W'_{p,2} \times \mathbf{\Sigma}'_{e,2}$.*

Proof. Note that for $(p_p, \boldsymbol{\sigma}_e) \in D$, $(w_p, \boldsymbol{\tau}_e) \in S_2$,

$$\begin{aligned} \left((I+L) \begin{pmatrix} p_p \\ \boldsymbol{\sigma}_e \end{pmatrix}, \begin{pmatrix} w_p \\ \boldsymbol{\tau}_e \end{pmatrix} \right)_{S_2} &= (s_0 p_p, w_p) + a_p^e(\boldsymbol{\sigma}_e, \boldsymbol{\tau}_e) - \alpha_p b_p(\mathbf{u}_s, w_p) \\ &\quad - b_p(\mathbf{u}_p, w_p) - b_s(\mathbf{u}_s, \boldsymbol{\tau}_e). \end{aligned}$$

Therefore, the problem $(I+L)\begin{pmatrix} p_p \\ \boldsymbol{\sigma}_e \end{pmatrix} = \begin{pmatrix} \bar{g}_p \\ \bar{g}_e \end{pmatrix}$ in S_2' is equivalent to (3.3.9)–(3.3.11), which, from Lemma 3.3.6, has a solution $(p_p, \boldsymbol{\sigma}_e) \in D$ for for arbitrary $(\bar{g}_p, \bar{g}_e) \in W'_{p,2} \times \mathbf{\Sigma}'_{e,2}$. □

3.3.1.2 Step 2: Solvability of the parabolic problem (3.3.14) In this section we establish the existence of a solution to (3.3.14). We begin by showing that L defined by (3.3.13) is a monotone operator.

Lemma 3.3.7. *The operator L defined by (3.3.14) is monotone.*

Proof. Let $(p_p, \boldsymbol{\sigma}_e) \in D$, $(w_p, \boldsymbol{\tau}_e) \in S_2$ be given. Then we have from (3.3.10)

$$\left(L \begin{pmatrix} p_p \\ \boldsymbol{\sigma}_e \end{pmatrix}, \begin{pmatrix} w_p \\ \boldsymbol{\tau}_e \end{pmatrix} \right)_{S_2} = (s_0 \bar{g}_p, w_p) + (A\bar{g}_e, \boldsymbol{\tau}_e) - (s_0 p_p, w_p) - a_p^s(\boldsymbol{\sigma}_e, \boldsymbol{\tau}_e)$$

$$= -\alpha_p b_p(\mathbf{u}_s, w_p) - b_p(\mathbf{u}_p, w_p) - b_s(\mathbf{u}_s, \boldsymbol{\tau}_e).$$

Suppose we are given $(p_p, \boldsymbol{\sigma}_e), (\tilde{p}_p, \tilde{\boldsymbol{\sigma}}_e) \in D$. Then, from (3.3.9)–(3.3.11), the corresponding $(\mathbf{u}_f, p_f, \mathbf{u}_p, \mathbf{u}_s, \lambda)$ and $(\tilde{\mathbf{u}}_f, \tilde{p}_f, \tilde{\mathbf{u}}_p, \tilde{\mathbf{u}}_s, \tilde{\lambda})$ satisfy

$$a_f(\mathbf{u}_f, \mathbf{v}_f) + a_p^d(\mathbf{u}_p, \mathbf{v}_p) + a_{BJS}(\mathbf{u}_f, \mathbf{u}_s; \mathbf{v}_f, \mathbf{v}_s) + b_f(\mathbf{v}_f, p_f) + b_p(\mathbf{v}_p, p_p)$$
$$+ \alpha_p b_p(\mathbf{v}_s, p_p) + b_s(\mathbf{v}_s, \boldsymbol{\sigma}_e) + b_\Gamma(\mathbf{v}_f, \mathbf{v}_p, \mathbf{v}_s; \lambda) = (\mathbf{f}_f, \mathbf{v}_f)_{\Omega_f} + (\mathbf{f}_p, \mathbf{v}_s)_{\Omega_p}, \tag{3.3.39}$$

$$(s_0 p_p, w_p)_{\Omega_p} + a_p^s(\boldsymbol{\sigma}_e, \boldsymbol{\tau}_e) - \alpha_p b_p(\mathbf{u}_s, w_p) - b_p(\mathbf{u}_p, w_p) - b_s(\mathbf{u}_s, \boldsymbol{\tau}_e) - b_f(\mathbf{u}_f, w_f)$$
$$= (s_0 \bar{g}_{p,1}, w_p)_{\Omega_p} + (A\bar{g}_{e,1}, \boldsymbol{\tau}_e)_{\Omega_p} + (q_f, w_f)_{\Omega_f}, \tag{3.3.40}$$

$$b_\Gamma(\mathbf{u}_f, \mathbf{u}_p, \mathbf{u}_s; \mu) = 0, \tag{3.3.41}$$

and

$$a_f(\tilde{\mathbf{u}}_f, \mathbf{v}_f) + a_p^d(\tilde{\mathbf{u}}_p, \mathbf{v}_p) + a_{BJS}(\tilde{\mathbf{u}}_f, \tilde{\mathbf{u}}_s; \mathbf{v}_f, \mathbf{v}_s) + b_f(\mathbf{v}_f, \tilde{p}_f) + b_p(\mathbf{v}_p, \tilde{p}_p)$$
$$+ \alpha_p b_p(\mathbf{v}_s, \tilde{p}_p) + b_s(\mathbf{v}_s, \tilde{\boldsymbol{\sigma}}_e) + b_\Gamma(\mathbf{v}_f, \mathbf{v}_p, \mathbf{v}_s; \tilde{\lambda}) = (\mathbf{f}_f, \mathbf{v}_f)_{\Omega_f} + (\mathbf{f}_p, \mathbf{v}_s)_{\Omega_p}, , \tag{3.3.42}$$

$$(s_0 \tilde{p}_p, w_p)_{\Omega_p} + a_p^s(\tilde{\boldsymbol{\sigma}}_e, \boldsymbol{\tau}_e) - \alpha_p b_p(\tilde{\mathbf{u}}_s, w_p) - b_p(\tilde{\mathbf{u}}_p, w_p) - b_s(\tilde{\mathbf{u}}_s, \boldsymbol{\tau}_e) - b_f(\tilde{\mathbf{u}}_f, w_f)$$
$$= (s_0 \bar{g}_{p,2}, w_p)_{\Omega_p} + (A\bar{g}_{e,2}, \boldsymbol{\tau}_e)_{\Omega_p} + (q_f, w_f)_{\Omega_f}, \tag{3.3.43}$$

$$b_\Gamma(\tilde{\mathbf{u}}_f, \tilde{\mathbf{u}}_p, \tilde{\mathbf{u}}_s; \mu) = 0. \tag{3.3.44}$$

Then we compute

$$\left(L\begin{pmatrix} p_p \\ \\ \boldsymbol{\sigma}_e \end{pmatrix} - L\begin{pmatrix} \tilde{p}_p \\ \\ \tilde{\boldsymbol{\sigma}}_e \end{pmatrix}, \begin{pmatrix} p_p - \tilde{p}_p \\ \\ \boldsymbol{\sigma}_e - \tilde{\boldsymbol{\sigma}}_e \end{pmatrix} \right)_{S_2} = -\alpha_p b_p\left(\mathbf{u}_s, p_p - \tilde{p}_p\right) - b_p(\mathbf{u}_p, p_p - \tilde{p}_p)$$
$$- b_s(\mathbf{u}_s, \boldsymbol{\sigma}_e - \tilde{\boldsymbol{\sigma}}_e) + \alpha_p b_p\left(\tilde{\mathbf{u}}_s, p_p - \tilde{p}_p\right)$$
$$+ b_p(\tilde{\mathbf{u}}_p, p_p - \tilde{p}_p) + b_s(\tilde{\mathbf{u}}_s, \boldsymbol{\sigma}_e - \tilde{\boldsymbol{\sigma}}_e).$$

Testing equation (3.3.39) with $(\mathbf{v}_f, \mathbf{v}_p, \mathbf{v}_s) = (\mathbf{u}_f, \mathbf{u}_p, \mathbf{u}_s)$, we obtain

$$a_f(\mathbf{u}_f, \mathbf{u}_f) + a_p^d(\mathbf{u}_p, \mathbf{u}_p) + a_{BJS}(\mathbf{u}_f, \mathbf{u}_s; \mathbf{u}_f, \mathbf{u}_s) + b_f(\mathbf{u}_f, p_f) + b_p(\mathbf{u}_p, p_p)$$
$$+ \alpha_p b_p(\mathbf{u}_s, p_p) + b_s(\mathbf{u}_s, \boldsymbol{\sigma}_e) + b_\Gamma(\mathbf{u}_f, \mathbf{u}_p, \mathbf{u}_s; \lambda) = (\mathbf{f}_f, \mathbf{u}_f)_{\Omega_f} + (\mathbf{f}_p, \mathbf{u}_s)_{\Omega_p}.$$

On the other hand, choosing $w_f = p_f$ and $\mu = \lambda$ in (3.3.40) and (3.3.41), we get

$$-b_f(\mathbf{u}_f, p_f) - b_\Gamma(\mathbf{u}_f, \mathbf{u}_p, \mathbf{u}_s; \lambda) = (q_f, p_f)_{\Omega_f}.$$

Hence,

$$a_f(\mathbf{u}_f, \mathbf{u}_f) + a_p^d(\mathbf{u}_p, \mathbf{u}_p) + a_{BJS}(\mathbf{u}_f, \mathbf{u}_s; \mathbf{u}_f, \mathbf{u}_s) + b_p(\mathbf{u}_p, p_p) + \alpha_p b_p(\mathbf{u}_s, p_p)$$
$$+ b_s(\mathbf{u}_s, \boldsymbol{\sigma}_e) = (\mathbf{f}_f, \mathbf{u}_f)_{\Omega_f} + (\mathbf{f}_p, \mathbf{u}_s)_{\Omega_p} + (q_f, p_f)_{\Omega_f}. \tag{3.3.45}$$

Repeating the same argument for problem (3.3.42)–(3.3.44), we obtain

$$a_f(\tilde{\mathbf{u}}_f, \tilde{\mathbf{u}}_f) + a_p^d(\tilde{\mathbf{u}}_p, \tilde{\mathbf{u}}_p) + a_{BJS}(\tilde{\mathbf{u}}_f, \tilde{\mathbf{u}}_s; \tilde{\mathbf{u}}_f, \tilde{\mathbf{u}}_s) + b_p(\tilde{\mathbf{u}}_p, \tilde{p}_p) + \alpha_p b_p(\tilde{\mathbf{u}}_s, \tilde{p}_p)$$
$$+ b_s(\tilde{\mathbf{u}}_s, \tilde{\boldsymbol{\sigma}}_e) = (\mathbf{f}_f, \tilde{\mathbf{u}}_f)_{\Omega_f} + (\mathbf{f}_p, \tilde{\mathbf{u}}_s)_{\Omega_p} + (q_f, \tilde{p}_f)_{\Omega_f}. \tag{3.3.46}$$

Next, we test (3.3.39) with $(\mathbf{v}_f, \mathbf{v}_p, \mathbf{v}_s) = (\tilde{\mathbf{u}}_f, \tilde{\mathbf{u}}_p, \tilde{\mathbf{u}}_s)$:

$$a_f(\mathbf{u}_f, \tilde{\mathbf{u}}_f) + a_p^d(\mathbf{u}_p, \tilde{\mathbf{u}}_p) + a_{BJS}(\mathbf{u}_f, \mathbf{u}_s; \tilde{\mathbf{u}}_f, \tilde{\mathbf{u}}_s) + b_f(\tilde{\mathbf{u}}_f, p_f) + b_p(\tilde{\mathbf{u}}_p, p_p)$$
$$+ \alpha_p b_p(\tilde{\mathbf{u}}_s, p_p) + b_s(\tilde{\mathbf{u}}_s, \boldsymbol{\sigma}_e) + b_\Gamma(\tilde{\mathbf{u}}_f, \tilde{\mathbf{u}}_p, \tilde{\mathbf{u}}_s; \lambda) = (\mathbf{f}_f, \tilde{\mathbf{u}}_f)_{\Omega_f} + (\mathbf{f}_p, \tilde{\mathbf{u}}_s)_{\Omega_p}.$$

Choosing $w_f = p_f$ and $\mu = \lambda$ in (3.3.43)–(3.3.44), we conclude that

$$-b_f(\tilde{\mathbf{u}}_f, p_f) - b_\Gamma(\tilde{\mathbf{u}}_f, \tilde{\mathbf{u}}_p, \tilde{\mathbf{u}}_s; \lambda) = (q_f, p_f)_{\Omega_f},$$

which implies that

$$a_f(\mathbf{u}_f, \tilde{\mathbf{u}}_f) + a_p^d(\mathbf{u}_p, \tilde{\mathbf{u}}_p) + a_{BJS}(\mathbf{u}_f, \mathbf{u}_s; \tilde{\mathbf{u}}_f, \tilde{\mathbf{u}}_s) + b_p(\tilde{\mathbf{u}}_p, p_p) + \alpha_p b_p(\tilde{\mathbf{u}}_s, p_p) + b_s(\tilde{\mathbf{u}}_s, \boldsymbol{\sigma}_e) = (\mathbf{f}_f, \tilde{\mathbf{u}}_f)_{\Omega_f} + (\mathbf{f}_p, \tilde{\mathbf{u}}_s)_{\Omega_p} + (q_f, p_f)_{\Omega_f}. \tag{3.3.47}$$

Similarly,

$$a_f(\tilde{\mathbf{u}}_f, \mathbf{u}_f) + a_p^d(\tilde{\mathbf{u}}_p, \mathbf{u}_p) + a_{BJS}(\tilde{\mathbf{u}}_f, \tilde{\mathbf{u}}_s; \mathbf{u}_f, \mathbf{u}_s) + b_p(\mathbf{u}_p, \tilde{p}_p) + \alpha_p b_p(\mathbf{u}_s, \tilde{p}_p) + b_s(\mathbf{u}_s, \tilde{\boldsymbol{\sigma}}_e) = (\mathbf{f}_f, \mathbf{u}_f)_{\Omega_f} + (\mathbf{f}_p, \mathbf{u}_s)_{\Omega_p} + (q_f, \tilde{p}_f)_{\Omega_f}. \tag{3.3.48}$$

Manipulating (3.3.45)–(3.3.48), we finally obtain

$$\begin{aligned}
\left(L \begin{pmatrix} p_p \\ \boldsymbol{\sigma}_e \end{pmatrix} - L \begin{pmatrix} \tilde{p}_p \\ \tilde{\boldsymbol{\sigma}}_e \end{pmatrix}, \begin{pmatrix} p_p - \tilde{p}_p \\ \boldsymbol{\sigma}_e - \tilde{\boldsymbol{\sigma}}_e \end{pmatrix} \right)_{S_2} &= a_f(\mathbf{u}_f, \mathbf{u}_f) + a_p^d(\mathbf{u}_p, \mathbf{u}_p) + a_{BJS}(\mathbf{u}_f, \mathbf{u}_s; \mathbf{u}_f, \mathbf{u}_s) \\
&\quad - a_f(\tilde{\mathbf{u}}_f, \mathbf{u}_f) - a_p^d(\tilde{\mathbf{u}}_p, \mathbf{u}_p) - a_{BJS}(\tilde{\mathbf{u}}_f, \tilde{\mathbf{u}}_s; \mathbf{u}_f, \mathbf{u}_s) - a_f(\mathbf{u}_f, \tilde{\mathbf{u}}_f) - a_p^d(\mathbf{u}_p, \tilde{\mathbf{u}}_p) \\
&\quad - a_{BJS}(\mathbf{u}_f, \mathbf{u}_s; \tilde{\mathbf{u}}_f, \tilde{\mathbf{u}}_s) + a_f(\tilde{\mathbf{u}}_f, \tilde{\mathbf{u}}_f) + a_p^d(\tilde{\mathbf{u}}_p, \tilde{\mathbf{u}}_p) + a_{BJS}(\tilde{\mathbf{u}}_f, \tilde{\mathbf{u}}_s; \tilde{\mathbf{u}}_f, \tilde{\mathbf{u}}_s) \\
&\quad = a_f(\mathbf{u}_f, \mathbf{u}_f - \tilde{\mathbf{u}}_f) + a_p^d(\mathbf{u}_p, \mathbf{u}_p - \tilde{\mathbf{u}}_p) + a_{BJS}(\mathbf{u}_f, \mathbf{u}_s; \mathbf{u}_f - \tilde{\mathbf{u}}_f, \mathbf{u}_s - \tilde{\mathbf{u}}_s) \\
&\quad - a_f(\tilde{\mathbf{u}}_f, \mathbf{u}_f - \tilde{\mathbf{u}}_f) - a_p^d(\tilde{\mathbf{u}}_p, \mathbf{u}_p - \tilde{\mathbf{u}}_p) - a_{BJS}(\tilde{\mathbf{u}}_f, \tilde{\mathbf{u}}_s; \mathbf{u}_f - \tilde{\mathbf{u}}_f, \mathbf{u}_s - \tilde{\mathbf{u}}_s) \geq 0,
\end{aligned}$$

due to the monotonicity of $a_f(\cdot,\cdot)$, $a_p^d(\cdot,\cdot)$ and $a_{BJS}(\cdot,\cdot;\cdot,\cdot)$.

□

Lemma 3.3.8. *For each $h_p \in W^{1,1}(0,T;W'_{p,2})$, $h_e \in W^{1,1}(0,T;\boldsymbol{\Sigma}'_{e,2})$, and $p_p(0) \in W_p$, $\boldsymbol{\sigma}_e(0) \in \boldsymbol{\Sigma}_e$, there exists a solution to (3.3.14) with $p_p \in W^{1,\infty}(0,T;W_p)$ and $\boldsymbol{\sigma}_e \in W^{1,\infty}(0,T;\boldsymbol{\Sigma}_e)$.*

Proof. Applying Theorem 3.3.1 with $\mathcal{N} = I$, $\mathcal{M} = L$, $E = W_{p,2} \times \boldsymbol{\Sigma}_{e,2}$, $E'_b = W'_{p,2} \times \boldsymbol{\Sigma}'_{e,2}$, and using Lemma 3.3.7 and Corollary 3.3.1, we obtain existence of a solution to (3.3.14). □

3.3.1.3 Step 3: The original problem (3.2.17)–(3.2.19) is a special case of (3.3.14)

Finally, we establish the existence of a solution to (3.2.17)–(3.2.19) as a corollary of Lemma 3.3.8.

Lemma 3.3.9. *If* $(p_p(t), \boldsymbol{\sigma}_e(t)) \in D$ *solves* (3.3.14) *with data* $\begin{pmatrix} s_0^{-1} q_p \\ 0 \end{pmatrix}$, *then it also solves* (3.2.17)–(3.2.19).

Proof. Let $(p_p(t), \boldsymbol{\sigma}_e(t)) \in D$ solve (3.3.14) with data $\begin{pmatrix} s_0^{-1} q_p \\ 0 \end{pmatrix}$. Note that (3.3.9) and (3.3.11) from the definition of the domain D directly imply (3.2.17) and (3.2.19). Also, (3.3.10) and (3.2.18) are the same when tested only with w_f. Thus it remains to show (3.2.18) with $w_f = 0$. From (3.3.14) with data $\begin{pmatrix} s_0^{-1} q_p \\ 0 \end{pmatrix}$ we have

$$\left(\frac{d}{dt} \begin{pmatrix} p_p \\ \boldsymbol{\sigma}_e \end{pmatrix}, \begin{pmatrix} w_p \\ \boldsymbol{\tau}_e \end{pmatrix} \right)_{S_2} + \left(L \begin{pmatrix} p_p \\ \boldsymbol{\sigma}_e \end{pmatrix}, \begin{pmatrix} w_p \\ \boldsymbol{\tau}_e \end{pmatrix} \right)_{S_2} = (q_p, w_p). \tag{3.3.49}$$

Since from (3.3.13) and (3.3.10) with $w_f = 0$ we have

$$\left(L \begin{pmatrix} p_p \\ \boldsymbol{\sigma}_e \end{pmatrix}, \begin{pmatrix} w_p \\ \boldsymbol{\tau}_e \end{pmatrix} \right)_{S_2} = -\alpha_p b_p (\mathbf{u}_s, w_p) - b_p(\mathbf{u}_p, w_p) - b_s(\mathbf{u}_s, \boldsymbol{\tau}_e),$$

we can write (3.3.49) equivalently as

$$(s_0 \partial_t p_p, w_p) + a_p^s(\partial_t \boldsymbol{\sigma}_e, \boldsymbol{\tau}_e) - \alpha_p b_p (\mathbf{u}_s, w_p) - b_p(\mathbf{u}_p, w_p) - b_s(\mathbf{u}_s, \boldsymbol{\tau}_e) = (q_p, w_p),$$

which is (3.2.18) with $w_f = 0$. □

Proof of Theorem 3.3.2. The statement of the theorem follows from Lemma 3.3.8 and Lemma 3.3.9. □

3.3.2 Existence and uniqueness of solution of the original formulation

In this subsection we discuss how the well-posedness of the original formulation (3.2.5)–(3.2.7) follows from the existence of a solution of the alternative formulation (3.2.17)–(3.2.19). Recall that $\mathbf{u}_s$ is the structure velocity, so the displacement solution can be recovered from

$$\boldsymbol{\eta}_p(t) = \boldsymbol{\eta}_{p,0} + \int_0^t \mathbf{u}_s(s)\, ds, \qquad \forall t \in (0,T]. \tag{3.3.50}$$

Since $\mathbf{u}_s(t) \in L^\infty(0,T;\mathbf{X}_p)$, then $\boldsymbol{\eta}_p(t) \in W^{1,\infty}(0,T;\mathbf{X}_p)$ for any $\boldsymbol{\eta}_{p,0} \in \mathbf{X}_p$. By construction, $\mathbf{u}_s = \partial_t \boldsymbol{\eta}_p$ and $\boldsymbol{\eta}_p(0) = \boldsymbol{\eta}_{p,0}$.

Theorem 3.3.3. *For each* $\mathbf{f}_f \in W^{1,1}(0,T;\mathbf{V}_f')$, $\mathbf{f}_p \in W^{1,1}(0,T;\mathbf{X}_p')$, $q_f \in W^{1,1}(0,T;W_f')$, $q_p \in W^{1,1}(0,T;W_p')$, *and* $p_p(0) = p_{p,0} \in W_p$, $\boldsymbol{\eta}_p(0) = \boldsymbol{\eta}_{p,0} \in \mathbf{X}_p$, *there exists a unique solution* $(\mathbf{u}_f(t), p_f(t), \mathbf{u}_p(t), p_p(t), \boldsymbol{\eta}_p(t), \lambda(t)) \in L^\infty(0,T;\mathbf{V}_f) \times L^\infty(0,T;W_f) \times L^\infty(0,T;\mathbf{V}_p) \times W^{1,\infty}(0,T;W_p) \times W^{1,\infty}(0,T;\mathbf{X}_p) \times L^\infty(0,T;\Lambda)$ *of* (3.2.5)–(3.2.7).

Proof. We begin by using the existence of a solution of the alternative formulation (3.2.17)–(3.2.19) to establish solvability of the original formulation (3.2.5)–(3.2.7). Let ($\mathbf{u}_f$, p_f, $\mathbf{u}_p$, p_p, $\mathbf{u}_s$, $\boldsymbol{\sigma}_e$, λ) be a solution to (3.2.17)–(3.2.19). Let $\boldsymbol{\eta}_p$ be defined in (3.3.50), so $\mathbf{u}_s = \partial_t \boldsymbol{\eta}_p$. Then (3.2.18) with $\boldsymbol{\tau}_e = \mathbf{0}$ implies (3.2.6) and (3.2.19) implies (3.2.7). We further note that (3.2.5) and (3.2.17) differ only in their respective terms $a_p^e(\boldsymbol{\eta}_p, \boldsymbol{\xi}_p)$ and $b_s(\mathbf{v}_s, \boldsymbol{\sigma}_e)$. Testing (3.2.18) with $\boldsymbol{\tau}_e \in \boldsymbol{\Sigma}_e$ gives $(\partial_t(A\boldsymbol{\sigma}_e - \mathbf{D}(\boldsymbol{\eta}_p)), \boldsymbol{\tau}_e)_{\Omega_p} = 0$, which, using that $\mathbf{D}(\mathbf{X}_p) \subset \boldsymbol{\Sigma}_e$, implies that $\partial_t(A\boldsymbol{\sigma}_e - \mathbf{D}(\boldsymbol{\eta}_p)) = \mathbf{0}$. Integrating from 0 to $t \in (0,T]$ and using that $\boldsymbol{\sigma}_e(0) = A^{-1}\mathbf{D}(\boldsymbol{\eta}_p(0))$ implies that $\boldsymbol{\sigma}_e(t) = A^{-1}\mathbf{D}(\boldsymbol{\eta}_p(t))$. Therefore, with (3.2.9),

$$b_s(\mathbf{v}_s, \boldsymbol{\sigma}_e) = (\boldsymbol{\sigma}_e, \mathbf{D}(\mathbf{v}_s))_{\Omega_p} = (A^{-1}\mathbf{D}(\boldsymbol{\eta}_p), \mathbf{D}(\mathbf{v}_s))_{\Omega_p} = a_p^e(\boldsymbol{\eta}_p, \mathbf{v}_s).$$

Therefore (3.2.17) implies (3.2.5), which establishes that $(\mathbf{u}_f, p_f, \mathbf{u}_p, p_p, \boldsymbol{\eta}_{p,0} + \int_0^t \mathbf{u}_s(s)\, ds, \lambda)$ is a solution to (3.2.5)–(3.2.7).

Now, assume that the solution of (3.2.5)–(3.2.7) is not unique. Let $(\mathbf{u}_f^i, p_f^i, \mathbf{u}_p^i, p_p^i, \boldsymbol{\eta}_p^i, \lambda^i)$, $i = 1, 2$, be two solutions corresponding to the same data. Using the monotonicity property (3.1.6) with $G(\mathbf{x}) = \nu(\mathbf{x})\mathbf{x}$, $\mathbf{s} = \mathbf{D}(\mathbf{u}_f^1)$ and $\mathbf{t} = \mathbf{D}(\mathbf{u}_f^2)$, we have

$$C\frac{\|\mathbf{D}(\mathbf{u}_f^1) - \mathbf{D}(\mathbf{u}_f^2)\|_{L^r(\Omega_f)}^2}{c + \|\mathbf{D}(\mathbf{u}_f^1)\|_{L^r(\Omega_f)}^{2-r} + \|\mathbf{D}(\mathbf{u}_f^2)\|_{L^r(\Omega_f)}^{2-r}}$$

$$\leq \left(2\nu(\mathbf{D}(\mathbf{u}_f^1))\mathbf{D}(\mathbf{u}_f^1) - 2\nu(\mathbf{D}(\mathbf{u}_f^2))\mathbf{D}(\mathbf{u}_f^2), \mathbf{D}(\mathbf{u}_f^1) - \mathbf{D}(\mathbf{u}_f^2)\right)_{\Omega_f}$$
$$= \left(a_f(\mathbf{u}_f^1, \mathbf{u}_f^1 - \mathbf{u}_f^2) - a_f(\mathbf{u}_f^2, \mathbf{u}_f^1 - \mathbf{u}_f^2)\right) =: I_1. \tag{3.3.51}$$

Similarly, we use (3.1.6) with $G(\mathbf{x}) = \nu_{eff}(\mathbf{x})\mathbf{x}$, $\mathbf{s} = \mathbf{u}_p^1$ and $\mathbf{t} = \mathbf{u}_p^2$, to obtain

$$C\frac{\|\mathbf{u}_p^1 - \mathbf{u}_p^2\|^2_{L^r(\Omega_p)}}{c + \|\mathbf{u}_p^1\|^{2-r}_{L^r(\Omega_p)} + \|\mathbf{u}_p^2\|^{2-r}_{L^r(\Omega_p)}} \leq (\kappa^{-1}(\nu_{eff}(\mathbf{u}_p^1)\mathbf{u}_p^1 - \nu_{eff}(\mathbf{u}_p^2)\mathbf{u}_p^2), \mathbf{u}_p^1 - \mathbf{u}_p^2)_{\Omega_p}$$
$$= a_p^d(\mathbf{u}_f^1, \mathbf{u}_f^1 - \mathbf{u}_f^2) - a_p^d(\mathbf{u}_f^2, \mathbf{u}_f^1 - \mathbf{u}_f^2) =: I_2. \tag{3.3.52}$$

We apply (3.1.6) one more time to bound the terms coming from BJS condition. Set $G(\mathbf{x}) = \nu_I(\mathbf{x})\mathbf{x}$, $\mathbf{s} = ((\mathbf{u}_f^1 - \partial_t\boldsymbol{\eta}_p^1)\cdot\mathbf{t}_{f,j})\mathbf{t}_{f,j}$ and $\mathbf{t} = ((\mathbf{u}_f^2 - \partial_t\boldsymbol{\eta}_p^2)\cdot\mathbf{t}_{f,j})\mathbf{t}_{f,j}$, then

$$\alpha_{BJS}C\sum_{j=1}^{d-1}\frac{\|(\mathbf{u}_f^1 - \partial_t\boldsymbol{\eta}_p^1)\cdot\mathbf{t}_{f,j} - (\mathbf{u}_f^2 - \partial_t\boldsymbol{\eta}_p^2)\cdot\mathbf{t}_{f,j}\|^2_{L^r(\Gamma_{fp})}}{c + \|(\mathbf{u}_f^1 - \partial_t\boldsymbol{\eta}_p^1)\cdot\mathbf{t}_{f,j}\|^{2-r}_{L^r(\Gamma_{fp})} + \|(\mathbf{u}_f^2 - \partial_t\boldsymbol{\eta}_p^2)\cdot\mathbf{t}_{f,j}\|^{2-r}_{\Gamma_{fp}}}$$
$$\leq a_{BJS}(\mathbf{u}_f^1, \partial_t\boldsymbol{\eta}_p^1; \mathbf{u}_f^1 - \mathbf{u}_f^2, \partial_t\boldsymbol{\eta}_p^1 - \partial_t\boldsymbol{\eta}_p^2) - a_{BJS}(\mathbf{u}_f^2, \partial_t\boldsymbol{\eta}_p^2; \mathbf{u}_f^1 - \mathbf{u}_f^2, \partial_t\boldsymbol{\eta}_p^1 - \partial_t\boldsymbol{\eta}_p^2) =: I_3. \tag{3.3.53}$$

From (3.2.5) we have

$$I_1 + I_2 + I_3 + a_p^e(\boldsymbol{\eta}_p^1 - \boldsymbol{\eta}_p^2, \partial_t\boldsymbol{\eta}_p^1 - \partial_t\boldsymbol{\eta}_p^2) = -b_f(\mathbf{u}_f^1 - \mathbf{u}_f^2, p_f^1 - p_f^2) - b_p(\mathbf{u}_p^1 - \mathbf{u}_p^2, p_p^1 - p_p^2)$$
$$-\alpha_p b_p(\partial_t\boldsymbol{\eta}_p^1 - \partial_t\boldsymbol{\eta}_p^2, p_p^1 - p_p^2) - b_\Gamma(\mathbf{u}_f^1 - \mathbf{u}_f^2, \mathbf{u}_p^1 - \mathbf{u}_p^2, \partial_t\boldsymbol{\eta}_p^1 - \partial_t\boldsymbol{\eta}_p^2; \lambda^1 - \lambda^2). \tag{3.3.54}$$

On the other hand, it follows from (3.2.6) and (3.2.7), with $w_f = p_f^1 - p_f^2$, $w_p = p_p^1 - p_p^2$, $\mu = \lambda^1 - \lambda^2$, that

$$(s_0\,\partial_t\left(p_p^1 - p_p^2\right), p_p^1 - p_p^2) - \alpha_p b_p(\partial_t\left(\boldsymbol{\eta}_p^1 - \boldsymbol{\eta}_p^2\right), p_p^1 - p_p^2) - b_p(\mathbf{u}_p^1 - \mathbf{u}_p^2, p_p^1 - p_p^2)$$
$$-b_f(\mathbf{u}_f^1 - \mathbf{u}_f^2, p_f^1 - p_f^2) - b_\Gamma(\mathbf{u}_f^1 - \mathbf{u}_f^2, \mathbf{u}_p^1 - \mathbf{u}_p^2, \partial_t\left(\boldsymbol{\eta}_p^1 - \boldsymbol{\eta}_p^2\right); \lambda^1 - \lambda^2) = 0\,. \tag{3.3.55}$$

Combining (3.3.54) and (3.3.55), we obtain

$$I_1 + I_2 + I_3 + a_p^e(\boldsymbol{\eta}_p^1 - \boldsymbol{\eta}_p^2, \partial_t\boldsymbol{\eta}_p^1 - \partial_t\boldsymbol{\eta}_p^2) = -(s_0\,\partial_t\left(p_p^1 - p_p^2\right), p_p^1 - p_p^2),$$

which implies

$$\frac{1}{2}\partial_t\left(a_p^e(\boldsymbol{\eta}_p^1 - \boldsymbol{\eta}_p^2, \boldsymbol{\eta}_p^1 - \boldsymbol{\eta}_p^2) + s_0\|p_p^1 - p_p^2\|^2_{L^2(\Omega_p)}\right) + I_1 + I_2 + I_3 = 0.$$

Integrating in time from 0 to $t \in (0,T]$, and using $p_p^1(0) = p_p^2(0),\ \boldsymbol{\eta}_p^1(0) = \boldsymbol{\eta}_p^2(0)$, we obtain

$$\frac{1}{2}\left(a_p^e(\boldsymbol{\eta}_p^1(t) - \boldsymbol{\eta}_p^2(t), \boldsymbol{\eta}_p^1(t) - \boldsymbol{\eta}_p^2(t)) + s_0\|p_p^1(t) - p_p^2(t)\|^2_{L^2(\Omega_p)}\right) + \int_0^t (I_1 + I_2 + I_3)\, ds = 0.$$

Hence, using (3.3.51)–(3.3.53), we have

$$\begin{aligned}
&\frac{1}{2}\left(a_p^e(\boldsymbol{\eta}_p^1(t) - \boldsymbol{\eta}_p^2(t), \boldsymbol{\eta}_p^1(t) - \boldsymbol{\eta}_p^2(t)) + s_0\|p_p^1(t) - p_p^2(t)\|^2_{L^2(\Omega_p)}\right) \\
&\quad + C\int_0^t \left(\frac{\|\mathbf{D}(\mathbf{u}_f^1) - \mathbf{D}(\mathbf{u}_f^2)\|^2_{L^2(\Omega_f)}}{c + \|\mathbf{D}(\mathbf{u}_f^1)\|^{2-r}_{L^r(\Omega_f)} + \|\mathbf{D}(\mathbf{u}_f^2)\|^{2-r}_{L^r(\Omega_f)}} + \frac{\|\mathbf{u}_p^1 - \mathbf{u}_p^2\|^2_{L^r(\Omega_p)}}{c + \|\mathbf{u}_p^1\|^{2-r}_{L^r(\Omega_p)} + \|\mathbf{u}_p^2\|^{2-r}_{L^r(\Omega_p)}}\right) ds \leq 0.
\end{aligned} \tag{3.3.56}$$

We note that $a_p^e(\cdot,\cdot)$ satisfies the bounds, for some $c_e,\ C_e > 0$, for all $\boldsymbol{\eta}_p,\ \boldsymbol{\xi}_p \in \mathbf{X}_p$,

$$c_e\|\boldsymbol{\xi}_p\|^2_{H^1(\Omega_p)} \leq a_p^e(\boldsymbol{\xi}_p, \boldsymbol{\xi}_p), \quad a_p^e(\boldsymbol{\eta}_p, \boldsymbol{\xi}_p) \leq C_e\|\boldsymbol{\eta}_p\|_{H^1(\Omega_p)}\|\boldsymbol{\xi}_p\|_{H^1(\Omega_p)}, \tag{3.3.57}$$

where the coercivity bound follows from Korn's inequality (1.3.4). Therefore, it follows from (3.3.56) that $\mathbf{u}_f^1(t) = \mathbf{u}_f^2(t), \mathbf{u}_p^1(t) = \mathbf{u}_p^2, \boldsymbol{\eta}^1(t) = \boldsymbol{\eta}_p^2,\ \forall t \in (0,T]$. Finally, we use the inf-sup condition (3.3.2) for $p_f^1 - p_f^2, p_p^1 - p_p^2, \lambda^1 - \lambda^2$ together with (3.2.5) to obtain

$$\begin{aligned}
&\|(p_f^1 - p_f^2, p_p^1 - p_p^2, \lambda^1 - \lambda^2)\|_{W\times\Lambda} \\
&\quad \leq C \sup_{(\mathbf{v}_f,\mathbf{v}_p)\in\mathbf{V}_f\times\mathbf{V}_p} \frac{b_f(\mathbf{v}_f, p_f^1 - p_f^2) + b_p(\mathbf{v}_p, p_p^1 - p^2) + b_\Gamma(\mathbf{v}_f, \mathbf{v}_p, \mathbf{0}; \lambda^1 - \lambda^2)}{\|(\mathbf{v}_f, \mathbf{v}_p)\|_{\mathbf{V}_f\times\mathbf{V}_p}} \\
&\quad = C \sup_{(\mathbf{v}_f,\mathbf{v}_p)\in\mathbf{V}_f\times\mathbf{V}_p} \Big(\frac{a_f(\mathbf{u}_f^2, \mathbf{v}_f) - a_f(\mathbf{u}_f^1, \mathbf{v}_f) + a_p^d(\mathbf{u}_p^2, \mathbf{v}_p) - a_p^d(\mathbf{u}_p^1, \mathbf{v}_p)}{\|(\mathbf{v}_f, \mathbf{v}_p)\|_{\mathbf{V}_f\times\mathbf{V}_p}} \\
&\qquad\qquad + \frac{a_{BJS}(\mathbf{u}_f^2, \partial_t\boldsymbol{\eta}_p^2; \mathbf{v}_f, \mathbf{0}) - a_{BJS}(\mathbf{u}_f^1, \partial_t\boldsymbol{\eta}_p^1; \mathbf{v}_f, \mathbf{0})}{\|(\mathbf{v}_f, \mathbf{v}_p)\|_{\mathbf{V}_f\times\mathbf{V}_p}}\Big) = 0.
\end{aligned}$$

Therefore, for all $t \in (0,T]$, $p_f^1 = p_f^2,\ p_p^1 = p_p^2,\ \lambda^1 = \lambda^2$, and we can conclude that (3.2.5)–(3.2.7) has a unique solution. □

We conclude with a stability bound for the solution of (3.2.5)–(3.2.7).

Theorem 3.3.4. *For the solution of (3.2.5)–(3.2.7), assuming sufficient regularity of the data, there exists $C > 0$ such that*

$$\begin{aligned}
&\|\mathbf{u}_f\|^r_{L^r(0,T;W^{1,r}(\Omega_f))} + \|\mathbf{u}_p\|^r_{L^r(0,T;L^r(\Omega_p))} + |\mathbf{u}_f - \partial_t\boldsymbol{\eta}_p|^r_{BJS} + \|p_f\|^{r'}_{L^{r'}(0,T;L^{r'}(\Omega_f))} \\
&\quad + \|p_p\|^{r'}_{L^{r'}(0,T;L^{r'}(\Omega_p))} + \|\lambda\|^{r'}_{L^{r'}(0,T;W^{1/r,r'}(\Gamma_{fp}))} + \|\boldsymbol{\eta}_p\|^2_{L^\infty(0,T;H^1(\Omega_p))} + s_0\|p_p\|^2_{L^\infty(0,T;L^2(\Omega_p))} \\
&\leq C\exp(T)\Big(\|\mathbf{f}_p\|^2_{L^\infty(0,T;H^{-1}(\Omega_p))} + \|\boldsymbol{\eta}_p(0)\|^2_{H^1(\Omega_p)} + s_0\|p_p(0)\|^2_{L_2(\Omega_p)} + \|\partial_t\mathbf{f}_p\|^2_{L^2(0,T;H^{-1}(\Omega_p))} \\
&\quad + \|\mathbf{f}_f\|^{r'}_{L^{r'}(0,T;W^{-1,r'}(\Omega_f))} + \|q_f\|^r_{L^r(0,T;L^r(\Omega_f))} + \|q_p\|^r_{L^r(0,T;L^r(\Omega_f))} + c(\bar{c}_f + \bar{c}_p + \bar{c}_I)\Big).
\end{aligned}$$

Proof. We first note that the term $c(\bar{c}_f + \bar{c}_p + \bar{c}_I)$ appears due to the use of the coercivity bounds in (3.3.3)–(3.3.5) in the general case $c > 0$. For simplicity, we present the proof for $c = 0$, noting that the extra term appears in (3.3.59) and the last inequality in the proof. We choose $(\mathbf{v}_f, w_f, \mathbf{v}_p, w_p, \boldsymbol{\xi}_p, \mu) = (\mathbf{u}_f, p_f, \mathbf{u}_p, p_p, \partial_t\boldsymbol{\eta}_p, \lambda)$ in (3.2.5)–(3.2.7) to get

$$\begin{aligned}
&\frac{1}{2}\partial_t\left[(s_0p_p, p_p)_{\Omega_p} + a^e_p(\boldsymbol{\eta}_p, \boldsymbol{\eta}_p)\right] + a_f(\mathbf{u}_f, \mathbf{u}_f) + a^d_p(\mathbf{u}_p, \mathbf{u}_p) + a_{BJS}(\mathbf{u}_f, \partial_t\boldsymbol{\eta}_p; \mathbf{u}_f, \partial_t\boldsymbol{\eta}_p) \\
&\qquad = (\mathbf{f}_f, \mathbf{u}_f)_{\Omega_f} + (\mathbf{f}_p, \partial_t\boldsymbol{\eta}_p)_{\Omega_p} + (q_f, p_f)_{\Omega_f} + (q_p, p_p)_{\Omega_p}. \qquad (3.3.58)
\end{aligned}$$

Next, we integrate (3.3.58) from 0 to $t \in (0, T]$ and use the coercivity bounds in (3.3.3)–(3.3.5) and (3.3.57):

$$\begin{aligned}
&s_0\|p_p(t)\|^2_{L^2(\Omega_p)} + \|\boldsymbol{\eta}_p(t)\|^2_{H^1(\Omega_p)} + \int_0^t \left(\|\mathbf{u}_f\|^r_{W^{1,r}(\Omega_f)} + \|\mathbf{u}_p\|^r_{L^r(\Omega_p)} + |\mathbf{u}_f - \partial_t\boldsymbol{\eta}_p|^r_{BJS}\right) ds \\
&\quad \leq C\Big(\int_0^t (\mathbf{f}_f, \mathbf{u}_f)_{\Omega_f}\, ds + (\mathbf{f}_p(t), \boldsymbol{\eta}_p(t))_{\Omega_p} - (\mathbf{f}_p(0), \boldsymbol{\eta}_p(0))_{\Omega_p} - \int_0^t (\partial_t\mathbf{f}_p, \boldsymbol{\eta}_p)_{\Omega_p}\, ds \\
&\qquad + \int_0^t \left((q_f, p_f)_{\Omega_f} + (q_p, p_p)_{\Omega_p}\right) ds + s_0\|p_p(0)\|^2_{L_2(\Omega_p)} + \|\boldsymbol{\eta}_p(0)\|^2_{H^1(\Omega_p)}\Big) \\
&\quad \leq C\left(\|\mathbf{f}_p(0)\|^2_{H^{-1}(\Omega_p)} + \|\boldsymbol{\eta}_p(0)\|^2_{H^1(\Omega_p)} + s_0\|p_p(0)\|^2_{L_2(\Omega_p)} + \|\mathbf{f}_p(t)\|^2_{H^{-1}(\Omega_p)}\right) \\
&\qquad + C\int_0^t \left(\|\mathbf{f}_f\|^{r'}_{W^{-1,r'}(\Omega_f)} + \|\partial_t\mathbf{f}_p\|^2_{H^{-1}(\Omega_p)} + \|\boldsymbol{\eta}_p\|^2_{H^1(\Omega_p)} + \|q_f\|^r_{L^r(\Omega_f)} + \|q_p\|^r_{L^r(\Omega_p)}\right) ds \\
&\qquad + \epsilon_1\|\boldsymbol{\eta}_p(t)\|^2_{H^1(\Omega_p)} + \epsilon_1\int_0^t \left(\|\mathbf{u}_f\|^r_{W^{1,r}(\Omega_f)} + \|p_f\|^{r'}_{L^{r'}(\Omega_f)} + \|p_p\|^{r'}_{L^{r'}(\Omega_p)}\right) ds, \qquad (3.3.59)
\end{aligned}$$

using Young's inequality (1.3.6) for the last inequality. We next apply the inf-sup condition (3.3.2) for (p_f, p_p, λ) to obtain

$$\|(p_f, p_p, \lambda)\|_{W\times\Lambda} \leq C \sup_{(\mathbf{v}_f,\mathbf{v}_p)\in\mathbf{V}_f\times\mathbf{V}_p} \frac{b_f(\mathbf{v}_f, p_f) + b_p(\mathbf{v}_p, p_p) + b_\Gamma(\mathbf{v}_f, \mathbf{v}_p, 0; \lambda)}{\|(\mathbf{v}_f, \mathbf{v}_p)\|_{\mathbf{V}_f\times\mathbf{V}_p}}$$

$$= C \sup_{(\mathbf{v}_f,\mathbf{v}_p)\in \mathbf{V}_f\times\mathbf{V}_p} \frac{-a_f(\mathbf{u}_f,\mathbf{v}_f) - a_p^d(\mathbf{u}_p,\mathbf{v}_p) - a_{BJS}(\mathbf{u}_f,\partial_t\boldsymbol{\eta}_p;\mathbf{v}_f,0) + (\mathbf{f}_f,\mathbf{v}_f)_{\Omega_f}}{\|(\mathbf{v}_f,\mathbf{v}_p)\|_{\mathbf{V}_f\times\mathbf{V}_p}}. \tag{3.3.60}$$

Using the continuity bounds in (3.3.3)–(3.3.5), we have from (3.3.60),

$$\|(p_f,p_p,\lambda)\|_{W\times\Lambda} \le C\left(\|\mathbf{f}_f\|_{W^{-1,r'}(\Omega_f)} + \|\mathbf{u}_f\|^{r/r'}_{W^{1,r}(\Omega_f)} + \|\mathbf{u}_p\|^{r/r'}_{L^r(\Omega_p)} + |\mathbf{u}_f - \partial_t\boldsymbol{\eta}_p|^{r/r'}_{BJS}\right),$$

implying

$$\begin{aligned}
&\epsilon_2 \int_0^t \left(\|p_f\|^{r'}_{L^{r'}(\Omega_f)} + \|p_p\|^{r'}_{L^{r'}(\Omega_p)} + \|\lambda\|^{r'}_{W^{1/r,r'}(\Gamma_{fp})}\right) ds \\
&\qquad \le C\epsilon_2 \int_0^t \left(\|\mathbf{f}_f\|^{r'}_{W^{-1,r'}(\Omega_f)} + \|\mathbf{u}_f\|^{r}_{W^{1,r}(\Omega_f)} + \|\mathbf{u}_p\|^{r}_{L^r(\Omega_p)} + |\mathbf{u}_f - \partial_t\boldsymbol{\eta}_p|^{r}_{BJS}\right) ds.
\end{aligned} \tag{3.3.61}$$

Adding (3.3.59) and (3.3.61) and choosing ϵ_2 small enough, and then ϵ_1 small enough, implies

$$\begin{aligned}
&s_0\|p_p(t)\|^2_{L^2(\Omega_p)} + \|\boldsymbol{\eta}_p(t)\|^2_{H^1(\Omega_p)} + \int_0^t \left(\|\mathbf{u}_f\|^{r}_{W^{1,r}(\Omega_f)} + \|\mathbf{u}_p\|^{r}_{L^r(\Omega_p)} + |\mathbf{u}_f - \partial_t\boldsymbol{\eta}_p|^{r}_{BJS}\right) ds \\
&\qquad + \int_0^t \left(\|p_f\|^{r'}_{L^{r'}(\Omega_f)} + \|p_p\|^{r'}_{L^{r'}(\Omega_p)} + \|\lambda\|^{r'}_{W^{1/r,r'}(\Gamma_{fp})}\right) ds \\
&\qquad \le C\Big(\|\mathbf{f}_p(t)\|^2_{H^{-1}(\Omega_p)} + \|\mathbf{f}_p(0)\|^2_{H^{-1}(\Omega_p)} + \|\boldsymbol{\eta}_p(0)\|^2_{H^1(\Omega_p)} + s_0\|p_p(0)\|^2_{L_2(\Omega_p)} \\
&+ \int_0^t \|\boldsymbol{\eta}_p\|^2_{H^1(\Omega_p)}\, ds + \int_0^t \left(\|\mathbf{f}_f\|^{r'}_{W^{-1,r'}(\Omega_f)} + \|\partial_t\mathbf{f}_p\|^2_{H^{-1}(\Omega_p)} + \|q_f\|^{r}_{L^r(\Omega_f)} + \|q_p\|^{r}_{L^r(\Omega_p)}\right) ds\Big).
\end{aligned}$$

The assertion of the theorem now follows from applying Gronwall's inequality (1.3.7). □

Remark 3.3.2. *The formulation* (3.2.5)-(3.2.7) *is straightforward to implement, but the presence of time derivative of displacement in non-coercive terms significantly complicates the analysis. On the other hand, the numerical method based on formulation* (3.2.17) -(3.2.19) *is rather difficult to implement and expensive to use, since the stress space is required to consist of symmetric matrices [18]. Therefore, we follow the same approach: we use* (3.2.17)-(3.2.19) *to resolve the solvability question, and* (3.2.5)-(3.2.7) *to obtain the actual numerical method.*

3.4 SEMI-DISCRETE FORMULATION

The setup for the nonlinear semi-discrete problem follows closely the one from Chapter 2. We consider a shape-regular and quasi-uniform simplicial partitions $\mathcal{T}_h^f$ and $\mathcal{T}_h^p$ of Ω_f and Ω_p, respectively, that may be non-matching along the interface Γ_{fp}. We assume that $\mathbf{V}_{f,h}$, $W_{f,h}$ is any inf-sup stable pair and we choose $\mathbf{V}_{p,h}$, $W_{p,h}$ to be any of well-known inf-sup stable mixed finite element spaces. The global spaces are

$$\mathbf{V}_h = \{\mathbf{v}_h = (\mathbf{v}_{f,h}, \mathbf{v}_{p,h}) \in \mathbf{V}_{f,h} \times \mathbf{V}_{p,h}\}, \quad W_h = \{w_h = (w_{f,h}, w_{p,h}) \in W_{f,h} \times W_{p,h}\}.$$

We employ a conforming Lagrangian finite element spaces $\mathbf{X}_{p,h} \subset \mathbf{X}_p$ to approximate the structure displacement, and we choose a nonconforming approximation for the Lagrange multiplier:

$$\Lambda_h = \mathbf{V}_{p,h} \cdot \mathbf{n}_p|_{\Gamma_{fp}}.$$

We equip Λ_h with a discrete version of the $W^{1/r,r'}(\Gamma_{fp})$ norm:

$$\|\mu_h\|_{\Lambda_h} = \|\mu_h\|_{L^2(\Gamma_{fp})} + |\mu_h|_{\Lambda_h},$$

with the semi-norm defined as $|\mu_h|_{\Lambda_h}^{r'} = (|\mathbf{u}_{p,h}^*(\mu_h)|^{r-2}\mathbf{u}_{p,h}^*(\mu_h), \mathbf{u}_{p,h}^*(\mu_h))_{\Omega_p}$, where $(\mathbf{u}_h^*(\mu_h)$, $p_h^*(\mu_h)) \in \mathbf{V}_{p,h} \times W_{p,h}$ is the mixed finite element solution to the nonlinear mixed Poisson problem with Dirichlet data μ_h on Γ_{fp}:

$$\begin{aligned}
&(|\mathbf{u}_{p,h}^*(\mu_h)|^{r-2}\mathbf{u}_{p,h}^*(\mu_h), \mathbf{v}_{p,h})_{\Omega_p} + b_p(\mathbf{v}_{p,h}, p_h^*(\mu_h)) = \langle \mathbf{v}_{p,h} \cdot \mathbf{n}_p, \mu_h\rangle_{\Gamma_{fp}}, \quad \forall\, \mathbf{v}_{p,h} \in \mathbf{V}_{p,h},\\
&b_p(\mathbf{u}_{p,h}^*(\mu_h), w_{p,h}) = 0, \qquad\qquad \forall\, w_{p,h} \in W_{p,h}. \quad (3.4.1)
\end{aligned}$$

In case of bounded viscosity functions we define the semi-norm through the velocity solution of linear problem, $|\mu_h|_{\Lambda_h}^2 = (\mathbf{u}_{p,h}^*(\mu_h), \mathbf{u}_{p,h}^*(\mu_h))_{\Omega_p}$.

The semi-discrete continuous-in-time problem reads: for $t \in (0,T]$, find $(\mathbf{u}_{f,h}(t)$, $p_{f,h}(t)$, $\mathbf{u}_{p,h}(t)$, $p_{p,h}(t)$, $\boldsymbol{\eta}_{p,h}(t), \lambda_h(t)) \in L^\infty(0,T;\mathbf{V}_{f,h}) \times L^\infty(0,T;W_{f,h}) \times L^\infty(0,T;\mathbf{V}_{p,h}) \times W^{1,\infty}(0,T;W_{p,h}) \times W^{1,\infty}(0,T;\mathbf{X}_{p,h}) \times L^\infty(0,T;\Lambda_h)$, such that for all $\mathbf{v}_{f,h} \in \mathbf{V}_{f,h}$, $w_{f,h} \in W_{f,h}$, $\mathbf{v}_{p,h} \in \mathbf{V}_{p,h}$, $w_{p,h} \in W_{p,h}$, $\boldsymbol{\xi}_{p,h} \in \mathbf{X}_p$, and $\mu_h \in \Lambda_h$,

$$a_f(\mathbf{u}_{f,h}, \mathbf{v}_{f,h}) + a_p^d(\mathbf{u}_{p,h}, \mathbf{v}_{p,h}) + a_{BJS}(\mathbf{u}_{f,h}, \partial_t\boldsymbol{\eta}_{p,h}; \mathbf{v}_{f,h}, \boldsymbol{\xi}_{p,h}) + a_p^e(\boldsymbol{\eta}_{p,h}, \boldsymbol{\xi}_{p,h}) + b_f(\mathbf{v}_{f,h}, p_{f,h})$$

$$+b_p(\mathbf{v}_{p,h},p_{p,h})+\alpha b_p(\boldsymbol{\xi}_{p,h},p_{p,h})+b_\Gamma(\mathbf{v}_{f,h},\mathbf{v}_{p,h},\boldsymbol{\xi}_{p,h};\lambda_h)$$
$$=(\mathbf{f}_f,\mathbf{v}_{f,h})_{\Omega_f}+(\mathbf{f}_p,\boldsymbol{\xi}_{p,h})_{\Omega_p}, \tag{3.4.2}$$

$$(s_0\partial_t p_{p,h},w_{p,h})_{\Omega_p}-\alpha b_p(\partial_t\boldsymbol{\eta}_{p,h},w_{p,h})-b_p(\mathbf{u}_{p,h},w_{p,h})-b_f(\mathbf{u}_{f,h},w_{f,h})$$
$$=(q_{f,h},w_{f,h})_{\Omega_f}+(q_{p,h},w_{p,h})_{\Omega_p}, \tag{3.4.3}$$

$$b_\Gamma(\mathbf{u}_{f,h},\mathbf{u}_{p,h},\partial_t\boldsymbol{\eta}_{p,h};\mu_h)=0. \tag{3.4.4}$$

We assume that the initial conditions for the semi-discrete problem (2.2.1)-(2.2.3) are chosen as suitable approximations of $p_{p,0}$ and $\boldsymbol{\eta}_{p,0}$.

In order to prove that the semi-discrete formulation (3.4.2) -(3.4.4) is well-posed, we will follow the same strategy as in the fully continuous case. *For the analysis purposes only*, we consider a conforming discretization of the weak formulation (3.2.17)-(3.2.19). Let the spaces $\mathbf{V}_h$, W_h, $\mathbf{X}_{p,h}$ and Λ_h be as described above. Let $\mathbf{X}_{p,h}$ consist of polynomials of degree at most k_s, then we introduce the stress space $\boldsymbol{\Sigma}_{e,h}\subset\boldsymbol{\Sigma}_e$ as discontinuous symmetric polynomials of degree at most k_{s-1}:

$$\boldsymbol{\Sigma}_{e,h}=\{\boldsymbol{\sigma}_e\in\boldsymbol{\Sigma}_e\big|\quad \boldsymbol{\sigma}_e|_{T\in\mathcal{T}_h^p}\in\mathcal{P}^{\mathrm{sym}}_{k_s-1}(T)\}$$

Then the corresponding semi-discrete formulation is: for $t\in(0,T]$, find $(\mathbf{u}_{f,h}(t),\ p_{f,h}(t),$ $\mathbf{u}_{p,h}(t),\ p_{p,h}(t),\ \mathbf{u}_{s,h}(t),\boldsymbol{\sigma}_{e,h}(t),\lambda_h(t))\in L^\infty(0,T;\mathbf{V}_{f,h})\times L^\infty(0,T;W_{f,h})\times L^\infty(0,T;\mathbf{V}_{p,h})\times W^{1,\infty}(0,T;W_{p,h})\times L^\infty(0,T;\mathbf{X}_{p,h})\times W^{1,\infty}(0,T;\boldsymbol{\Sigma}_{e,h})\times L^\infty(0,T;\Lambda_h)$, such that for all $\mathbf{v}_{f,h}\in\mathbf{V}_{f,h}$, $w_{f,h}\in W_{f,h}$, $\mathbf{v}_{p,h}\in\mathbf{V}_{p,h}$, $w_{p,h}\in W_{p,h}$, $\mathbf{v}_{s,h}\in\mathbf{X}_{p,h}$, $\boldsymbol{\tau}_{e,h}\in\boldsymbol{\Sigma}_{e,h}$, and $\mu_h\in\Lambda_h$,

$$a_f(\mathbf{u}_{f,h},\mathbf{v}_{f,h})+a_p^d(\mathbf{u}_{p,h},\mathbf{v}_{p,h})+a_{BJS}(\mathbf{u}_{f,h},\mathbf{u}_{s,h};\mathbf{v}_{f,h},\mathbf{v}_{s,h})+b_f(\mathbf{v}_{f,h},p_{f,h})+b_p(\mathbf{v}_{p,h},p_{p,h})$$
$$+\alpha_p b_p(\mathbf{v}_{s,h},p_{p,h})+b_s(\mathbf{v}_{s,h},\boldsymbol{\sigma}_{e,h})+b_\Gamma(\mathbf{v}_{f,h},\mathbf{v}_{p,h},\mathbf{v}_{s,h};\lambda_h)=(\mathbf{f}_f,\mathbf{v}_{f,h})_{\Omega_f}+(\mathbf{f}_p,\mathbf{v}_{s,h})_{\Omega_p}, \tag{3.4.5}$$

$$(s_0\partial_t p_{p,h},w_{p,h})_{\Omega_p}+a_p^s(\partial_t\boldsymbol{\sigma}_{e,h},\boldsymbol{\tau}_{e,h})-\alpha_p b_p\left(\mathbf{u}_{s,h},w_{p,h}\right)-b_p(\mathbf{u}_{p,h},w_{p,h})-b_s(\mathbf{u}_{s,h},\boldsymbol{\tau}_{e,h})$$
$$-b_f(\mathbf{u}_{f,h},w_{f,h})=(q_f,w_{f,h})_{\Omega_f}+(q_p,w_{p,h})_{\Omega_p}, \tag{3.4.6}$$

$$b_\Gamma\left(\mathbf{u}_{f,h},\mathbf{u}_{p,h},\mathbf{u}_{s,h};\mu_h\right)=0. \tag{3.4.7}$$

We define the spaces of generalized velocities and pressures, $\mathcal{Q}_h=\mathbf{V}_{p,h}\times\mathbf{X}_{p,h}\times\mathbf{V}_{f,h}$ and $S_h=W_{p,h}\times\boldsymbol{\Sigma}_{e,h}\times W_{f,h}\times\Lambda_h$, respectively, equipped with the corresponding norms:

$$\|\mathbf{q}_h\|_{\mathcal{Q}_h}=\|\mathbf{q}_h\|_Q,\quad \|s_h\|_{S_h}=\|w_{p,h}\|_{L^{r'}(\Omega_p)}+\|\boldsymbol{\tau}_{e,h}\|_{L^2(\Omega_p)}+\|w_{f,h}\|_{L^{r'}(\Omega_f)}+\|\mu_h\|_{\Lambda_h}.$$

3.4.1 Well-posedness of the semi-discrete problem

3.4.1.1 The inf-sup condition We first recall the following LBB condition for the mixed Stokes-Darcy problem [42, 44, 64] .

Lemma 3.4.1. *There exists a constant $C_{1,h} > 0$ independent of h such that*

$$\inf_{0\neq(w_{p,h},0,w_{f,h},0)\in S_h} \sup_{\mathbf{0}\neq\mathbf{q_h}\in\mathcal{Q_h}} \frac{b_f(\mathbf{v}_{f,h}; w_{f,h}) + b_p(\mathbf{v}_{p,h}; w_{p,h})}{\|(\mathbf{v}_{p,h}, 0, \mathbf{v}_{f,h})\|_{\mathcal{Q}}\|(w_{p,h}, 0, w_{f,h}, 0)\|_{S_h}} \geq C_{1,h}. \tag{3.4.8}$$

We will next prove the inf-sup condition between spaces $\mathcal{Q}_h$ and Λ_h, as well as $\Sigma_{e,h}$ and $\mathbf{X}_{p,h}$. Let us define $\Lambda_h^0 \subset \Lambda_h$ and $\mathcal{Q}_h^0 \subset \mathcal{Q}_h$ as follows:

$$\Lambda_h^0 = \left\{ \mu_h \in \Lambda_h : \int_{\Gamma_{fp}} \mu_h = 0 \right\},$$
$$\mathcal{Q}_h^0 = \left\{ (\mathbf{v}_{p,h}, \mathbf{v}_{s,h}, \mathbf{v}_{f,h}) \in \mathcal{Q}_h : \nabla\cdot\mathbf{v}_{p,h} = \nabla\cdot\mathbf{v}_{s,h} = \nabla\cdot\mathbf{v}_{f,h} = 0 \right\}.$$

We note that $|\mu_h|_{\Lambda_h}$ is a norm for any $\mu_h \in \Lambda_h^0$. Indeed, let $\mu_h \in \Lambda_h^0$ such that $|\mu_h|_{\Lambda_h} = 0$ be given we have

$$\|\mathbf{u}_{p,h}^*(\mu_h)\|_{L^r(\Omega_p)}^r \geq C(|\mathbf{u}_{p,h}^*(\mu_h)|^{r-2}\mathbf{u}_{p,h}^*(\mu_h), \mathbf{u}_{p,h}^*)_{\Omega_p} = C|\mu_h|_{\Lambda_h}^{r'} = 0$$

Moreover, choose a test function $\mathbf{v}_{p,h}$ in (3.4.1) such that $\mathbf{v}_{p,h}\cdot\mathbf{n}_p|_{\Gamma_{fp}} = \mu_h$ and $b_p(\mathbf{v}_{p,h}, w_{p,h}) = 0$, $\forall w_{p,h} \in W_{p,h}$. Then

$$\|\mu_h\|_{L^2(\Gamma_{fp})}^2 = \langle \mathbf{v}_{p,h}\cdot\mathbf{n}_p, \mu_h\rangle_{\Gamma_{fp}} = a_d^p(\mathbf{u}_{p,h}^*(\mu_h), \mathbf{v}_{p,h})_{\Omega_p} + b_p(\mathbf{v}_{p,h}, w_{p,h}) = 0.$$

Hence, $|\mu_h|_{\Lambda_h} = 0$ implies that $\mu_h = 0$ and since the opposite is also true, $|\cdot|_{\Lambda_h}$ is a norm on Λ_h^0. We obtain the following result.

Lemma 3.4.2. *There exists a constant $C_{2,h} > 0$ independent of h such that*

$$\inf_{0\neq\mu_h\in\Lambda_h^0} \sup_{\mathbf{0}\neq\mathbf{q_h}\in\mathcal{Q}_\mathbf{h}^\mathbf{0}} \frac{b_\Gamma(\mathbf{v}_{f,h}, \mathbf{v}_{p,h}, \mathbf{v}_{s,h}; \mu_h)}{\|\mathbf{q}_h\|_{\mathcal{Q}}\|\mu_h\|_{\Lambda_h}} \geq C_{2,h}. \tag{3.4.9}$$

Proof. Let $\mu_h \in \Lambda_h^0$ be given, let $\mathbf{u}_{p,h}^*(\mu_h)$ be the solution of (3.4.1). Choosing $w_{p,h} = \nabla \cdot \mathbf{u}_{p,h}^*(\mu_h)$ in the second equation of (3.4.1), we obtain that $\nabla \cdot \mathbf{u}_{p,h}^*(\mu_h) = 0$. So, we choose $\mathbf{q}_h = (\mathbf{u}_{p,h}^*(\mu_h), 0, 0) \in \mathcal{Q}_h^0$, then

$$\frac{b_\Gamma(0, \mathbf{u}_{p,h}^*(\mu_h), 0; \mu_h)}{\|(\mathbf{u}_{p,h}^*(\mu_h), 0, 0)\|_{\mathcal{Q}_h}} = \frac{\langle \mathbf{u}_{p,h}^*(\mu_h) \cdot \mathbf{n}_p, \mu_h \rangle_{\Gamma_{fp}}}{\|\mathbf{u}_{p,h}^*(\mu_h)\|_{L^r(\Omega_p)}} = \frac{a_d^p(\mathbf{u}_{p,h}^*(\mu_h), \mathbf{u}_{p,h}^*(\mu_h))}{\|\mathbf{u}_{p,h}^*(\mu_h)\|_{L^r(\Omega_p)}}.$$

In the case of Power Law or Carreau/Cross models with $\nu_\infty = 0$,

$$\|\mathbf{u}_{p,h}^*(\mu_h)\|_{L^r(\Omega_p)}^r \leq C(|\mathbf{u}_{p,h}^*(\mu_h)|^{r-2}\mathbf{u}_{p,h}^*(\mu_h), \mathbf{u}_{p,h})_{\Omega_p} = C|\mu_h|_{\Lambda_h}^{r'} \leq C\|\mu_h\|_{\Lambda_h}^{r'}.$$

Thus, we have:

$$\frac{b_\Gamma(0, \mathbf{u}_{p,h}^*(\mu_h), 0; \mu_h)}{\|(\mathbf{u}_{p,h}^*(\mu_h), 0, 0)\|_{\mathcal{Q}}} \geq C\frac{|\mu_h|_{\Lambda_h}^{r'}}{|\mu_h|_{\Lambda_h}^{r'/r}} = C|\mu_h|_{\Lambda_h}^{r'-r'/r} = C|\mu_h|_{\Lambda_h} \geq C\|\mu_h\|_{\Lambda_h}.$$

□

Using these results, we prove the inf-sup condition for the formulation (3.4.5)-(3.4.7).

Theorem 3.4.1. *There exist constants β_1, $\beta_2 > 0$ independent of h such that*

$$\inf_{0 \neq (w_{p,h}, 0, w_{f,h}, \mu_h) \in S_h} \sup_{\mathbf{0} \neq \mathbf{q_h} \in \mathcal{Q_h}} \frac{b(\mathbf{q}_h; s_h) + b_\Gamma(\mathbf{q}_h; s_h)}{\|\mathbf{q}_h\|_{\mathcal{Q}} \|(w_{p,h}, 0, w_{f,h}, \mu_h)\|_{S_h}} \geq \beta_1, \tag{3.4.10}$$

$$\inf_{\mathbf{0} \neq (\mathbf{0}, \mathbf{v}_{s,h}, \mathbf{0}) \in \mathcal{Q}_h} \sup_{0 \neq (0, \boldsymbol{\tau}_{e,h}, 0, 0) \in S_h} \frac{b_s(\mathbf{v}_{s,h}, \boldsymbol{\tau}_{e,h})}{\|(\mathbf{0}, \mathbf{v}_{s,h}, \mathbf{0})\|_{\mathcal{Q}} \|(0, \boldsymbol{\tau}_{e,h}, 0, 0)\|_{S_h}} \geq \beta_2, \tag{3.4.11}$$

where

$$b(\mathbf{q}_h; s_h) = b_f(\mathbf{v}_{f,h}, w_{f,h}) + b_p(\mathbf{v}_{p,h}, w_{p,h}) + \alpha b_p(\mathbf{v}_{s,h}, w_{p,h}),$$
$$b_\Gamma(\mathbf{q}_h; s_h) = b_\Gamma(\mathbf{v}_{f,h}, \mathbf{v}_{p,h}, \mathbf{v}_{s,h}; \mu_h).$$

Proof. Let $s_h = (w_{p,h}, 0, w_{f,h}, \mu_h) \in S_h$ be given. We write $\mu_h = \mu_h^1 + \bar{\mu}_h$, where $\mu_h^1 \in \Lambda_h^0$. Let further $s_h^1 = (w_{p,h}, 0, w_{f,h}, \mu_h^1)$ and let $\mathbf{q}_h^1 = (\mathbf{v}_{p,h}^1, 0, \mathbf{v}_{f,h}^1) \in \mathcal{Q}_h$ and $\mathbf{q}_h^2 = (\mathbf{v}_{p,h}^2, 0, 0) \in \mathcal{Q}_h$ be such that (3.4.8) and (3.4.9) are achieved for s_h^1.

We note that for any $\tilde{\mu}_h \in \Lambda_h \cap C(\Gamma_{fp})$, the seminorms $|\cdot|_{\Lambda_h}$ and $|\cdot|_{W^{1/r,r'}(\Gamma_{fp})}$ are equivalent. Therefore, in this case the following continuity result holds

$$b_\Gamma(\mathbf{q}_h; \tilde{s}_h) \leq C_\Gamma \|\mathbf{q}_h\|_{\mathcal{Q}} \|\tilde{\mu}_h\|_{\Lambda_h}, \quad \forall \mathbf{q}_h \in \mathcal{Q}_h.$$

Moreover, due to assumption $|\Gamma_P^D| > 0$, we can restrict $\mathbf{v}_{p,h}^1 \cdot \mathbf{n}_p\Big|_{\Gamma_{fp}} = 0$. Then, choosing C_Γ large enough, we obtain

$$\begin{aligned} b_\Gamma(\mathbf{q}_h^1; s_h) &= \langle \mathbf{v}_{f,h}^1 \cdot \mathbf{n}_f + \mathbf{v}_{p,h}^1 \cdot \mathbf{n}_p, \mu_h \rangle_{\Gamma_{fp}} = \langle \mathbf{v}_{f,h}^1 \cdot \mathbf{n}_f, \mu_h \rangle_{\Gamma_{fp}} \leq C \|\mathbf{v}_{f,h}^1\|_{L^2(\Gamma_{fp})} \|\mu_h\|_{L^2(\Gamma_{fp})} \\ &\leq C \|\mathbf{v}_{f,h}^1\|_{W^{1-1/r,r}(\partial\Omega_f)} \|\mu_h\|_{L^2(\Gamma_{fp})} \leq C_\Gamma \|\mathbf{q}_h^1\|_{\mathcal{Q}} \|\mu_h\|_{\Lambda_h}. \end{aligned}$$

We set $\mathbf{r}_h = \mathbf{q}_h^1 + \mathbf{q}_h^2(1 + C_\Gamma C_{2,h}^{-1} \|\mathbf{q}_h^1\|_{\mathcal{Q}} / \|\mathbf{q}_h^2\|_{\mathcal{Q}})$ and compute:

$$\begin{aligned} b(\mathbf{r}_h; s_h^1) &= b_f(\mathbf{v}_{f,h}^1; w_{f,h}) + b_p(\mathbf{v}_{p,h}^1; w_{f,h}) + \left(1 + C_\Gamma C_{2,h}^{-1} \frac{\|\mathbf{q}_h^1\|_{\mathcal{Q}}}{\|\mathbf{q}_h^2\|_{\mathcal{Q}}}\right) b_p(\mathbf{v}_{p,h}^2; w_{f,h}) \\ &= b_f(\mathbf{v}_{f,h}^1; w_{f,h}) + b_p(\mathbf{v}_{p,h}^1; w_{f,h}) \geq C_{1,h} \|(w_{p,h}, 0, w_{f,h}, 0)\|_{S_h} \|\mathbf{q}_h^1\|_{\mathcal{Q}}, \\ b_\Gamma(\mathbf{r}_h; s_h^1) &= b_\Gamma(\mathbf{q}_h^1; s_h^1) + \left(1 + C_\Gamma C_{2,h}^{-1} \frac{\|\mathbf{q}_h^1\|_{\mathcal{Q}}}{\|\mathbf{q}_h^2\|_{\mathcal{Q}}}\right) b_\Gamma(\mathbf{q}_h^2; s_h^1) \\ &\geq C_{2,h} \left(1 + C_\Gamma C_{2,h}^{-1} \frac{\|\mathbf{q}_h^1\|_{\mathcal{Q}}}{\|\mathbf{q}_h^2\|_{\mathcal{Q}}}\right) \|\mu_h^1\|_{\Lambda_h} \|\mathbf{q}_h^2\|_{\mathcal{Q}} - C_\Gamma \|\mathbf{q}_h^1\|_{\mathcal{Q}} \|\mu_h^1\|_{\Lambda_h} \geq C_{2,h} \|\mu_h^1\|_{\Lambda_h} \|\mathbf{q}_h^2\|_{\mathcal{Q}}. \end{aligned}$$

Hence, we obtain

$$b(\mathbf{r}_h; s_h^1) + b_\Gamma(\mathbf{r}_h; s_h^1) \geq C_1 \|\mathbf{r}_h\|_{\mathcal{Q}} \|s_h^1\|_{S_h}. \tag{3.4.12}$$

If $\bar{\mu}_h \neq 0$, we choose $\bar{\mathbf{v}}_{p,h} = \frac{1}{|\Gamma_{fp}|}$, so that

$$\|\bar{\mathbf{v}}_{p,h}\|_{L^r\Omega_p} \leq C(|\Omega_p|, |\Gamma_{fp}|), \quad \text{and } b_p(\bar{\mathbf{v}}_{p,h}, w_{p,h}) = 0, \ \forall w_{p,h} \in W_{p,h}. \tag{3.4.13}$$

We further define $\mathbf{q}_h = \mathbf{r}_h + 2C_\Gamma \|\mathbf{r}_h\|_{\mathcal{Q}} \frac{\bar{\mu}_h}{|\bar{\mu}_h|} |\Gamma_{fp}|^{1/2} (\bar{\mathbf{v}}_{p,h}, 0, 0)$. Then

$$\|\mathbf{q}_h\|_{\mathcal{Q}} \leq \|\mathbf{r}_h\|_{\mathcal{Q}} \left(1 + 2C_\Gamma |\Gamma_{fp}|^{1/2} \|\bar{\mathbf{v}}_{p,h}\|_{\mathbf{v}_p}\right) \leq C \|\mathbf{r}_h\|_{\mathcal{Q}},$$

and we also have

$$\begin{aligned} b_\Gamma(\mathbf{q}_h; s_h) &= b_\Gamma(\mathbf{r}_h; \mu_h) + 2C_\Gamma \|\mathbf{r}_h\|_{\mathcal{Q}} \frac{\bar{\mu}_h}{|\bar{\mu}_h|} |\Gamma_{fp}|^{1/2} b_\Gamma((\bar{\mathbf{v}}_{p,h}, 0, 0); \mu_h) \\ &= b_\Gamma(\mathbf{r}_h; \mu_h^1) + b_\Gamma(\mathbf{r}_h; \bar{\mu}_h) + 2C_\Gamma \|\mathbf{r}_h\|_{\mathcal{Q}} \frac{\bar{\mu}_h}{|\bar{\mu}_h|} |\Gamma_{fp}|^{1/2} b_\Gamma((\bar{\mathbf{v}}_{p,h}, 0, 0); \bar{\mu}_h) \\ &\geq b_\Gamma(\mathbf{r}_h; \mu_h^1) - C_\Gamma \|\mathbf{r}_h\|_{\mathcal{Q}} |\Gamma_{fp}|^{1/2} |\bar{\mu}_h| + 2C_\Gamma \|\mathbf{r}_h\|_{\mathcal{Q}} |\Gamma_{fp}|^{1/2} |\bar{\mu}_h| \\ &\geq b_\Gamma(\mathbf{r}_h; \mu_h^1) + C_\Gamma \|\mathbf{r}_h\|_{\mathcal{Q}} |\Gamma_{fp}|^{1/2} |\bar{\mu}_h|. \end{aligned} \tag{3.4.14}$$

Moreover,

$$b(\mathbf{q}_h; s_h) = b(\mathbf{r}_h; s_h) + 2C_\Gamma \|\mathbf{r}_h\|_{\mathcal{Q}} |\Gamma_{fp}|^{1/2} \frac{\bar{\mu}_h}{|\bar{\mu}_h|} b_p(\bar{\mathbf{v}}_{p,h}, w_{p,h}) = b(\mathbf{r}_h; s_h). \tag{3.4.15}$$

Combining (3.4.14), (3.4.15) and (3.4.12), we obtain

$$\begin{aligned} b(\mathbf{q}_h; s_h) + b_\Gamma(\mathbf{q}_h; s_h) &\geq b(\mathbf{r}_h; s_h^1) + b_\Gamma(\mathbf{r}_h; s_h^1) + C_\Gamma \|\mathbf{r}_h\|_{\mathcal{Q}} |\Gamma_{fp}|^{1/2} |\bar{\mu}_h| \\ &\geq C_1 \|\mathbf{r}_h\|_{\mathcal{Q}} \left(\|s_h^1\|_{S_h} + C_\Gamma |\Gamma_{fp}|^{1/2} |\bar{\mu}_h| \right) \geq C \|\mathbf{q}_h\|_{\mathcal{Q}} \|s_h\|_{S_h}. \end{aligned}$$

Finally, let $\mathbf{0} \neq (\mathbf{0}, \mathbf{v}_{s,h}, \mathbf{0}) \in \mathcal{Q}_h$ be given. We choose $\boldsymbol{\tau}_{e,h} = \mathbf{D}(\mathbf{v}_{s,h})$ and, using Korn's inequality (1.3.4), we obtain

$$\frac{b_s(\mathbf{v}_{s,h}, \boldsymbol{\tau}_{e,h})}{\|\boldsymbol{\tau}_{e,h}\|_{L^2(\Omega_p)}} = \frac{\|\mathbf{D}(\mathbf{v}_{s,h})\|^2_{L^2(\Omega_p)}}{\|\mathbf{D}(\mathbf{v}_{s,h})\|_{L^2(\Omega_p)}} = \|\mathbf{D}(\mathbf{v}_{s,h})\|_{L^2(\Omega_p)} \geq C_2 \|\mathbf{v}_{s,h}\|_{H^1(\Omega_p)}.$$

Therefore, (3.4.11) holds. □

3.4.1.2 Existence and uniqueness of the solution In order to show well-posedness of (3.4.5)-(3.4.7), and consequently (3.4.2)-(3.4.4), we proceed as in the case of continuous problem. We introduce $W^h_{p,2}$ and $\mathbf{\Sigma}^h_{e,2}$ as the closure of the spaces $W_{p,h}$ and $\mathbf{\Sigma}_{e,h}$ with the norms

$$\|w_{p,h}\|^2_{W^h_{p,2}} := (s_0 w_{p,h}, w_{p,h})_{L^2(\Omega_p)}, \quad \|\boldsymbol{\tau}_{e,h}\|^2_{\mathbf{\Sigma}^h_{e,2}} := (A\boldsymbol{\tau}_{e,h}, \boldsymbol{\tau}_{e,h})_{L^2(\Omega_p)},$$

and set $S^h_2 = W^h_{p,2} \times \mathbf{\Sigma}^h_{e,2}$.

Define the domain

$$\begin{aligned}
D_h := \Big\{ & (p_{p,h}, \boldsymbol{\sigma}_{e,h}) \in W_{p,h} \times \mathbf{\Sigma}_{e,h} : \text{ for given } (\mathbf{f}_f, \mathbf{f}_p, q_f) \in W^{-1,r'}(\Omega_f) \times H^{-1}(\Omega_p) \times L^r(\Omega_f) \\
& \exists\, (\mathbf{q}_h, p_{f,h}, \lambda_h) \in \mathcal{Q}_h \times W_{f,h} \times \Lambda_h \text{ such that:} \\
& a_f(\mathbf{u}_{f,h}, \mathbf{v}_{f,h}) + a^d_p(\mathbf{u}_{p,h}, \mathbf{v}_{p,h}) + a_{BJS}(\mathbf{u}_{f,h}, \mathbf{u}_{s,h}; \mathbf{v}_{f,h}, \mathbf{v}_{s,h}) + b_f(\mathbf{v}_{f,h}, p_{f,h}) \\
& \quad + b_p(\mathbf{v}_{p,h}, p_{p,h}) + \alpha_p b_p(\mathbf{v}_{s,h}, p_{p,h}) + b_s(\mathbf{v}_{s,h}, \boldsymbol{\sigma}_{e,h}) + b_\Gamma(\mathbf{v}_{f,h}, \mathbf{v}_{p,h}, \mathbf{v}_{s,h}; \lambda_h) \\
& \quad = (\mathbf{f}_{f,h}, \mathbf{v}_{f,h})_{\Omega_f} + (\mathbf{f}_{p,h}, \mathbf{v}_{s,h})_{\Omega_p}, \qquad (3.4.16) \\
& (s_0 p_{p,h}, w_{p,h})_{\Omega_p} + a^s_p(\boldsymbol{\sigma}_{e,h}, \boldsymbol{\tau}_{e,h}) - \alpha_p b_p\,(\mathbf{u}_{s,h}, w_{p,h}) - b_p(\mathbf{u}_{p,h}, w_{p,h}) - b_s(\mathbf{u}_{s,h}, \boldsymbol{\tau}_{e,h}) \\
& \quad - b_f(\mathbf{u}_{f,h}, w_{f,h}) = (q_f, w_{f,h})_{\Omega_f} + (s_0 \bar{g}_p, w_{p,h})_{\Omega_p} + (A\bar{g}_e, \boldsymbol{\tau}_{e,h})_{\Omega_p}, \qquad (3.4.17) \\
& b_\Gamma\,(\mathbf{u}_{f,h}, \mathbf{u}_{p,h}, \mathbf{u}_{s,h}; \mu_h) = 0. \qquad (3.4.18) \\
& \quad \text{for some } (\bar{g}_p, \bar{g}_e) \in \left(W^h_{p,2}\right)' \times \left(\mathbf{\Sigma}^h_{e,2}\right)' \Big\} \subset W^h_{p,2} \times \mathbf{\Sigma}^h_{e,2}\,. \qquad (3.4.19)
\end{aligned}$$

Next, define operator L_h, $L_h : D_h \longrightarrow \left(W^h_{p,2}\right)' \times \left(\Sigma^h_{e,2}\right)'$, as

$$L_h \begin{pmatrix} p_{p,h} \\ \boldsymbol{\sigma}_{e,h} \end{pmatrix} = \begin{pmatrix} \bar{g}_p \\ \bar{g}_e \end{pmatrix} - \begin{pmatrix} p_{p,h} \\ \boldsymbol{\sigma}_{e,h} \end{pmatrix}, \qquad (3.4.20)$$

and consider the following problem:

$$\frac{d}{dt} \begin{pmatrix} p_{p,h}(t) \\ \boldsymbol{\sigma}_{e,h}(t) \end{pmatrix} + L \begin{pmatrix} p_{p,h}(t) \\ \boldsymbol{\sigma}_{e,h}(t) \end{pmatrix} = \begin{pmatrix} \bar{g}_p(t) \\ \bar{g}_e(t) \end{pmatrix}. \qquad (3.4.21)$$

As before, a key result we use to establish the existence of a solution to (3.4.5)-(3.4.7) is Theorem 3.3.1, using which we can prove the following theorem.

Theorem 3.4.2. *For each* $\mathbf{f}_f \in W^{1,1}(0,T;\mathbf{V}_f')$, $\mathbf{f}_p \in W^{1,1}(0,T;\mathbf{X}_p')$, $q_f \in W^{1,1}(0,T;W_f')$, $q_p \in W^{1,1}(0,T;W_p')$, *and* $p_{p,h}(0) \in W_p$, $\boldsymbol{\sigma}_{e,h}(0) = A^{-1}\mathbf{D}(\boldsymbol{\eta}_{p,h}(0)) \in \boldsymbol{\Sigma}_{e,h}$, *there exists a solution of* (3.4.5)–(3.4.7) *with* $(\mathbf{u}_{f,h},\ p_{f,h},\ \mathbf{u}_{p,h},\ p_{p,h},\ \mathbf{u}_{s,h},\ \boldsymbol{\sigma}_{e,h},\ \lambda_h) \in L^\infty(0,T;\mathbf{V}_{f,h}) \times L^\infty(0,T;W_{f,h}) \times L^\infty(0,T;\mathbf{V}_{p,h}) \times W^{1,\infty}(0,T;W_{p,h}) \times L^\infty(0,T;\mathbf{X}_{p,h}) \times W^{1,\infty}(0,T;\boldsymbol{\Sigma}_{e,h}) \times L^\infty(0,T;\Lambda_h)$.

We note that the proof of Theorem 3.4.2 can be split into the following steps:

Step 1. Establish that the domain D_h given by (3.4.19) is well-defined.

Step 2. Show solvability of parabolic problem (3.4.21).

Step 3. Show that the initial problem (3.4.5)-(3.4.7) is a special case of (3.4.21).

The proofs of Step 2 and Step 3 in the discrete setting are identical to the continuous case and the proof of Step 1 is very similar as well. The only difference is in the definition of operator $\mathcal{L}$, which is corrected in accordance with the discrete norm $\|\cdot\|_{\Lambda_h}$ for the Lagrange multiplier variable. More precisely, to prove that the domain D_h is well-defined, one needs to verify that $L_\Gamma : \Lambda_h \to \Lambda_h'$ defined as $L_\Gamma(\mu_{h,1})(\mu_{h,2}) := \langle \mu_{h,1}, \mu_{h,2}\rangle_{\Gamma_{fp}} + (|\mathbf{u}^*_{p,h}(\mu_{h,1})|^{r-2}\mathbf{u}^*_{p,h}(\mu_{h,1}), \mathbf{u}^*_{p,h}(\mu_{h,2}))_{\Omega_p}$ is a bounded, continuous, coercive and monotone operator. The desired properties follow immediately from Lemma 3.3.2 and the fact that $(L_\Gamma(\mu_h)(\mu_h))^{1/r'}$ defines a norm on Λ_h.

As an immediate corollary of Theorem 3.4.2, we obtain the well-posedness result for the semi-discrete problem (3.4.2)-(3.4.4).

Theorem 3.4.3. *For each* $\mathbf{f}_f \in W^{1,1}(0,T;\mathbf{V}_f')$, $\mathbf{f}_p \in W^{1,1}(0,T;\mathbf{X}_p')$, $q_f \in W^{1,1}(0,T;W_f')$, $q_p \in W^{1,1}(0,T;W_p')$, *and* $p_{p,h}(0) \in W_{p,h}$, $\boldsymbol{\eta}_{p,h}(0) \in \mathbf{X}_{p,h}$, *there exists a unique solution* $(\mathbf{u}_{f,h}(t), p_{f,h}(t),\ \mathbf{u}_{p,h}(t), p_{p,h}(t), \boldsymbol{\eta}_{p,h}(t), \lambda_h(t)) \in L^\infty(0,T;\mathbf{V}_{f,h}) \times L^\infty(0,T;W_{f,h})$
$\times L^\infty(0,T;\mathbf{V}_{p,h}) \times W^{1,\infty}(0,T;W_{p,h}) \times W^{1,\infty}(0,T;\mathbf{X}_{p,h}) \times L^\infty(0,T;\Lambda_h)$ *of* (3.4.2)–(3.4.4).

We also note that one can obtain a stability estimate for the solution of (3.4.2)–(3.4.4) in a similar way, as it was done for the continuous formulation (3.2.5)-(3.2.7).

3.4.2 Error analysis

3.4.2.1 Preliminaries As in the analysis for the linear problem, in order to derive the error estimate for (3.4.2)–(3.4.4), we would like to use an interpolant, satisfying (2.2.27)–(2.2.28). Following the steps from Section 2.2.3.1, we can verify that such interpolant indeed can be constructed and it also satisfies approximation properties, similar to (2.2.33)–(2.2.35), which we present below for the sake of completeness. However we omit the details to avoid duplication.

Lemma 3.4.3. *For all sufficiently smooth* $\mathbf{v}_f$, $\mathbf{v}_p$, *and* $\boldsymbol{\xi}_p$,

$$\|\mathbf{v}_f - I_{f,h}\mathbf{v}_f\|_{W^{1,r}(\Omega_f)} \leq Ch^{r_{k_f}}\|\mathbf{v}_f\|_{W^{r_{k_f}+1,1}(\Omega_f)}, \quad 0 \leq r_{k_f} \leq k_f, \tag{3.4.22}$$

$$\|\boldsymbol{\xi}_p - I_h^s\boldsymbol{\xi}_p\|_{L^2(\Omega_p)} + h|\boldsymbol{\xi}_p - I_h^s\boldsymbol{\xi}_p|_{H^1(\Omega_p)} \leq Ch^{r_{k_s}}\|\boldsymbol{\xi}_p\|_{H^{r_{k_s}}(\Omega_p)}, \quad 1 \leq r_{k_s} \leq k_s + 1, \tag{3.4.23}$$

$$\|\mathbf{v}_p - I_{p,h}\mathbf{v}_p\|_{L^r(\Omega_p)} \leq C\left(h^{r_{k_p}}\|\mathbf{v}_p\|_{W^{r_{k_p},1}(\Omega_p)} + h^{r_{k_f}}\|\mathbf{v}_f\|_{W^{r_{k_f}+1,1}(\Omega_f)} + h^{r_{k_s}}\|\boldsymbol{\xi}_p\|_{H^{r_{k_s}+1}(\Omega_p)}\right),$$
$$1 \leq r_{k_p} \leq k_p + 1,\ 0 \leq r_{k_f} \leq k_f,\ 0 \leq r_{k_s} \leq k_s. \tag{3.4.24}$$

To analyze the error in Lagrange multiplier variable we use the L^2-projection operator onto Λ_h, satisfying

$$\|\lambda - Q_{\lambda,h}\lambda\|_{L^{r'}(\Gamma_{fp})} \leq Ch^{\tilde{r}_{k_p}}\|\lambda\|_{W^{\tilde{r}_{k_p},r'}(\Gamma_{fp})}, 0 \leq \tilde{r}_{k_p} \leq k_p + 1. \tag{3.4.25}$$

Finally, we introduce the following notations. For $\mathbf{u} = (\mathbf{u}_f, \mathbf{u}_p, \boldsymbol{\eta}_p)$ and $\mathbf{u}_h = (\mathbf{u}_{f,h}, \mathbf{u}_{p,h}, \boldsymbol{\eta}_{p,h})$, let's define

$$\begin{aligned}
\mathcal{E}(\mathbf{u}, \mathbf{u}_h) = &\left\|\frac{|\mathbf{D}(\mathbf{u}_f) - \mathbf{D}(\mathbf{u}_{f,h})|}{c + |\mathbf{D}(\mathbf{u}_f)| + |\mathbf{D}(\mathbf{u}_{f,h})|}\right\|_{L^\infty(\Omega_f)}^{\frac{2-r}{r}} + \left\|\frac{|\mathbf{u}_p - \mathbf{u}_{p,h}|}{c + |\mathbf{u}_p| + |\mathbf{u}_{p,h}|}\right\|_{L^\infty(\Omega_p)}^{\frac{2-r}{r}} \\
&+ \sum_{j=1}^{d-1}\left\|\frac{|(\mathbf{u}_f - \partial_t\boldsymbol{\eta}_p)\cdot\mathbf{t}_{f,j} - (\mathbf{u}_{f,h} - \partial_t\boldsymbol{\eta}_{p,h})\cdot\mathbf{t}_{f,j}|}{c + |(\mathbf{u}_f - \partial_t\boldsymbol{\eta}_p)\cdot\mathbf{t}_{f,j}| + |(\mathbf{u}_{f,h} - \partial_t\boldsymbol{\eta}_{p,h})\cdot\mathbf{t}_{f,j}|}\right\|_{L^\infty(\Gamma_{fp})}^{\frac{2-r}{r}} \quad \text{and} \\
\mathcal{G}(\mathbf{u}, \mathbf{u}_h) = &\int_{\Omega_f} |\nu(\mathbf{D}(\mathbf{u}_f))\mathbf{D}(\mathbf{u}_f) - \nu(\mathbf{D}(\mathbf{u}_{f,h}))\mathbf{D}(\mathbf{u}_{f,h})||\mathbf{D}(\mathbf{u}_f) - \mathbf{D}(\mathbf{u}_{f,h})|dA \\
&+ \int_{\Omega_p} (1/k_M)|\nu_{eff}(\mathbf{u}_p)\mathbf{u}_p - \nu_{eff}(\mathbf{u}_{p,h})\mathbf{u}_{p,h}||\mathbf{u}_p - \mathbf{u}_{p,h}|dA \\
&+ \int_{\Gamma_{fp}} \sum_{j=1}^{d-1} \frac{a_{BJS}}{k_M^{1/2}}|\nu_I(((\mathbf{u}_f - \partial_t\boldsymbol{\eta}_p)\cdot\mathbf{t}_{f,j})\mathbf{t}_{f,j}((\mathbf{u}_f - \partial_t\boldsymbol{\eta}_p)\cdot\mathbf{t}_{f,j})\mathbf{t}_{f,j}
\end{aligned}$$

$$- \nu_I(((\mathbf{u}_{f,h} - \partial_t \boldsymbol{\eta}_{p,h}) \cdot \mathbf{t}_{f,j})\mathbf{t}_{f,j})((\mathbf{u}_{f,h} - \partial_t \boldsymbol{\eta}_{p,h}) \cdot \mathbf{t}_{f,j})\mathbf{t}_{f,j}|$$
$$\cdot |((\mathbf{u}_f - \partial_t \boldsymbol{\eta}_p) \cdot \mathbf{t}_{f,j})\mathbf{t}_{f,j} - ((\mathbf{u}_{f,h} - \partial_t \boldsymbol{\eta}_{p,h}) \cdot \mathbf{t}_{f,j})\mathbf{t}_{f,j}| ds, \tag{3.4.26}$$

where k_M is the largest eigenvalue of K.

3.4.2.2 Error estimates

Theorem 3.4.4. *Let $(\mathbf{u}_f, \mathbf{u}_p, \boldsymbol{\eta}_p, p_f, p_p, \lambda)$ be the solution of (3.2.5)-(3.2.7) and $(\mathbf{u}_{f,h}, \mathbf{u}_{p,h}, \boldsymbol{\eta}_{p,h}, p_{f,h}, p_{p,h}, \lambda_h)$ be the solution of (3.4.2)-(3.4.4). Under the assumption of sufficient smoothness for the solution of the continuous problem, the following estimate holds*

$$\begin{aligned}
&\|\mathbf{u}_f - \mathbf{u}_{f,h}\|^2_{L^2(0,T;W^{1,r}(\Omega_f))} + \|\mathbf{u}_p - \mathbf{u}_{p,h}\|^2_{L^2(0,T;L^r(\Omega_p))} + \|\mathbf{u}_f - \partial_t \boldsymbol{\eta}_p - (\mathbf{u}_{f,h} - \partial_t \boldsymbol{\eta}_{p,h})\|^2_{L^2(0,T;BJS)} \\
&+ \|p_f - p_{f,h}\|^{r'}_{L^{r'}(0,T;L^{r'}(\Omega_f))} + \|p_p - p_{p,h}\|^{r'}_{L^{r'}(0,T;L^{r'}(\Omega_p))} + \|Q_{\lambda,h}\lambda - \lambda_h\|^{r'}_{L^{r'}(0,T;L^{r'}(\Gamma_{fp}))} \\
&+ \|\boldsymbol{\eta}_p - \boldsymbol{\eta}_{p,h}\|^2_{L^\infty(0,T;H^1(\Omega_p))} + s_0\|p_p - p_{p,h}\|^2_{L^\infty(0,T;L^2(\Omega_p))} + \|\mathcal{G}(\mathbf{u}, \mathbf{u}_h)\|_{L^1(0,T)} \\
&\leq C\exp(T)\Big[h^{2k_f}\|\mathbf{u}_f\|^2_{L^2(0,T;W^{k_f+1,r}(\Omega_f))} + h^{rk_f}\|\mathbf{u}_f\|^r_{L^r(0,T;W^{k_f+1,r}(\Omega_f))} \\
&+ h^{2(s_f+1)}\|p_f\|^2_{L^2(0,T;W^{s_f+1,r'}(\Omega_f))} + h^{r'(s_f+1)}\|p_f\|^{r'}_{L^{r'}(0,T;W^{s_f+1,r'}(\Omega_f))} \\
&+ h^{r(k_p+1)}\|\mathbf{u}_p\|^r_{L^r(0,T;W^{k_p+1,r}(\Omega_p))} + h^{r'(s_p+1)}\|p_p\|^{r'}_{L^{r'}(0,T;W^{s_p+1,r'}(\Omega_p))} \\
&+ h^{2(s_p+1)}\left(\|\partial_t p_p\|^2_{L^2(0,T;W^{s_p+1,r'}(\Omega_p))} + \|p_p\|^2_{L^\infty(0,T;W^{s_p+1,r'}(\Omega_p))}\right) \\
&+ h^{2k_s}\left(\|\boldsymbol{\eta}_p\|^2_{L^2(0,T;H^{k_s+1}(\Omega_p))} + \|\partial_t\boldsymbol{\eta}_p\|^2_{L^2(0,T;H^{k_s+1}(\Omega_p))} + \|\boldsymbol{\eta}_p\|^2_{L^\infty(0,T;H^{k_s+1}(\Omega_p))}\right) \\
&+ h^{rk_s}\|\partial_t\boldsymbol{\eta}_p\|^r_{L^r(0,T;H^{k_s+1}(\Omega_p))} + h^{r'(k_p+1)}\|\lambda\|^{r'}_{L^{r'}(0,T;W^{k_p+1,r'}(\Gamma_{fp}))} \\
&+ h^{2(k_p+1)}\left(\|\lambda\|^2_{L^2(0,T;W^{k_p+1,r'}(\Gamma_{fp}))} + \|\partial_t\lambda\|^2_{L^2(0,T;W^{k_p+1,r'}(\Gamma_{fp}))} + \|\lambda\|^2_{L^\infty(0,T;W^{k_p+1,r'}(\Gamma_{fp}))}\right)\Big].
\end{aligned} \tag{3.4.27}$$

Proof. We start by using (3.1.6) with $G(\mathbf{u}) = \nu(\mathbf{u})\mathbf{u}$, $\mathbf{s} = \mathbf{D}(\mathbf{u}_f)$ and $\mathbf{t} = \mathbf{D}(\mathbf{u}_{f,h})$:

$$\begin{aligned}
&\frac{\|\mathbf{D}(\mathbf{u}_f) - \mathbf{D}(\mathbf{u}_{f,h})\|^2_{L^r(\Omega_f)}}{c + \|\mathbf{D}(\mathbf{u}_f)\|^{2-r}_{L^r(\Omega_f)} + \|\mathbf{D}(\mathbf{u}_{f,h})\|^{2-r}_{L^r(\Omega_f)}} \\
&\qquad + \int_{\Omega_f} |\nu(\mathbf{D}(\mathbf{u}_f))\mathbf{D}(\mathbf{u}_f) - \nu(\mathbf{D}(\mathbf{u}_{f,h})\mathbf{D}(\mathbf{u}_{f,h}))||\mathbf{D}(\mathbf{u}_f) - \mathbf{D}(\mathbf{u}_{f,h})| dA \\
&\qquad \leq C\int_{\Omega_f} (\nu(\mathbf{D}(\mathbf{u}_f))\mathbf{D}(\mathbf{u}_f) - \nu(\mathbf{D}(\mathbf{u}_{f,h}))\mathbf{D}(\mathbf{u}_{f,h})) : (\mathbf{D}(\mathbf{u}_f) - \mathbf{D}(\mathbf{u}_{f,h}))\, dA
\end{aligned}$$

$$= C \int_{\Omega_f} (\nu(\mathbf{D}(\mathbf{u}_f))\mathbf{D}(\mathbf{u}_f) - \nu(\mathbf{D}(\mathbf{u}_{f,h}))\mathbf{D}(\mathbf{u}_{f,h})) : (\mathbf{D}(\mathbf{u}_f) - \mathbf{D}(\mathbf{v}_{f,h}))\, dA$$
$$+ C \int_{\Omega_f} (\nu(\mathbf{D}(\mathbf{u}_f))\mathbf{D}(\mathbf{u}_f) - \nu(\mathbf{D}(\mathbf{u}_{f,h}))\mathbf{D}(\mathbf{u}_{f,h})) : (\mathbf{D}(\mathbf{v}_{f,h}) - \mathbf{D}(\mathbf{u}_{f,h}))\, dA$$
$$= C(I_1 + I_2), \qquad \forall \mathbf{v}_{f,h} \in \mathbf{V}_{f,h}. \quad (3.4.28)$$

The term I_1 can be estimated using (3.1.7) with $\mathbf{s} = \mathbf{D}(\mathbf{u}_f)$, $\mathbf{t} = \mathbf{D}(\mathbf{u}_{f,h})$, $\mathbf{w} = \mathbf{D}(\mathbf{u}_f) - \mathbf{D}(\mathbf{v}_{f,h})$, $\forall \mathbf{v}_{f,h} \in \mathbf{V}_{f,h}$, and Young's inequality (1.3.6):

$$\int_{\Omega_f} (\nu(\mathbf{D}(\mathbf{u}_f))\mathbf{D}(\mathbf{u}_f) - \nu(\mathbf{D}(\mathbf{u}_{f,h}))\mathbf{D}(\mathbf{u}_{f,h})) : (\mathbf{D}(\mathbf{u}_f) - \mathbf{D}(\mathbf{v}_{f,h}))\, dA$$
$$\leq C \left(\int_{\Omega_f} |\nu(\mathbf{D}(\mathbf{u}_f))\mathbf{D}(\mathbf{u}_f) - \nu(\mathbf{D}(u_{f,h}))\mathbf{D}(\mathbf{u}_{f,h})||\mathbf{D}(\mathbf{u}_f) - \mathbf{D}(\mathbf{u}_{f,h})| dA \right)^{1/r'}$$
$$\times \left\| \frac{|\mathbf{D}(\mathbf{u}_f) - \mathbf{D}(\mathbf{u}_{f,h})|}{c + |\mathbf{D}(\mathbf{u}_f)| + |\mathbf{D}(\mathbf{u}_{f,h})|} \right\|_\infty^{\frac{2-r}{r}} \|\mathbf{D}(\mathbf{u}_f) - \mathbf{D}(\mathbf{v}_{f,h})\|_{L^r(\Omega_f)}$$
$$\leq \epsilon \int_{\Omega_f} |\nu(\mathbf{D}(\mathbf{u}_f))\mathbf{D}(\mathbf{u}_f) - \nu(\mathbf{D}(\mathbf{u}_{f,h}))\mathbf{D}(\mathbf{u}_{f,h})|\, |\mathbf{D}(\mathbf{u}_f) - \mathbf{D}(\mathbf{u}_{f,h})|\, dA$$
$$+ C \left\| \frac{|\mathbf{D}(\mathbf{u}_f) - \mathbf{D}(\mathbf{u}_{f,h})|}{c + |\mathbf{D}(\mathbf{u}_f)| + |\mathbf{D}(\mathbf{u}_{f,h})|} \right\|_\infty^{2-r} \|\mathbf{D}(\mathbf{u}_f) - \mathbf{D}(\mathbf{v}_{f,h})\|_{L^r(\Omega_f)}^r. \quad (3.4.29)$$

We choose ϵ small enough and combine (3.4.28)-(3.4.29):

$$\frac{\|\mathbf{D}(\mathbf{u}_f) - \mathbf{D}(\mathbf{u}_{f,h})\|_{L^r(\Omega_f)}^2}{c + \|\mathbf{D}(\mathbf{u}_f)\|_{L^r(\Omega_f)}^{2-r} + \|\mathbf{D}(\mathbf{u}_{f,h})\|_{L^r(\Omega_f)}^{2-r}}$$
$$+ \int_{\Omega_f} |\nu(\mathbf{D}(\mathbf{u}_f))\mathbf{D}(\mathbf{u}_f) - \nu(\mathbf{D}(\mathbf{u}_{f,h}))\mathbf{D}(\mathbf{u}_{f,h})||\mathbf{D}(\mathbf{u}_f) - \mathbf{D}(\mathbf{u}_{f,h})| dA$$
$$\leq C \left(\left\| \frac{|\mathbf{D}(\mathbf{u}_f) - \mathbf{D}(\mathbf{u}_{f,h})|}{c + |\mathbf{D}(\mathbf{u}_f)| + |\mathbf{D}(\mathbf{u}_{f,h})|} \right\|_\infty^{2-r} \|\mathbf{D}(\mathbf{u}_f) - \mathbf{D}(\mathbf{v}_{f,h})\|_{L^r(\Omega_f)}^r + I_2 \right) \quad (3.4.30)$$

Similarly, to bound the error in Darcy velocity we use (3.1.6) and (3.1.7) with $G(\mathbf{u}) = K^{-1}\nu_{eff}(\mathbf{u})\mathbf{u}$, $\mathbf{s} = \mathbf{u}_p$, $\mathbf{t} = \mathbf{u}_{p,h}$ and $\mathbf{w} = \mathbf{u}_p - \mathbf{v}_{p,h}$, $\mathbf{v}_{p,h} \in \mathbf{V}_{p,h}$, together with Young's inequality (1.3.6) to we obtain:

$$\frac{\|\mathbf{u}_p - \mathbf{u}_{p,h}\|_{L^r(\Omega_p)}^2}{c + \|\mathbf{u}_p\|_{L^r(\Omega_p)}^{2-r} + \|\mathbf{u}_{p,h}\|_{L^r(\Omega_p)}^{2-r}} + \int_{\Omega_p} (1/k_M)|\nu_{eff}(\mathbf{u}_p)\mathbf{u}_p - \nu_{eff}(\mathbf{u}_{p,h})\mathbf{u}_{p,h}||\mathbf{u}_p - \mathbf{u}_{p,h}| dA$$
$$\leq C \left(\left\| \frac{|\mathbf{u}_p - \mathbf{u}_{p,h}|}{c + |\mathbf{u}_p| + |\mathbf{u}_{p,h}|} \right\|_\infty^{2-r} \|\mathbf{u}_p - \mathbf{v}_{p,h}\|_{L^r(\Omega_p)}^r + I_4 \right), \quad (3.4.31)$$

where

$$I_4 := \int_{\Omega_p} K^{-1}(\nu_{eff}(\mathbf{u}_p)\mathbf{u}_p - \nu_{eff}(\mathbf{u}_{p,h})\mathbf{u}_{p,h}) \cdot (\mathbf{v}_{p,h} - \mathbf{u}_{p,h}) dA.$$

We apply (3.1.6) and (3.1.7) one more time to bound the terms coming from BJS condition. Set $G(\mathbf{u}) = \alpha_{BJS} K_j^{-1/2} \nu_I(\mathbf{u})\mathbf{u}$, $\mathbf{s} = ((\mathbf{u}_f - \partial_t \boldsymbol{\eta}_p) \cdot \mathbf{t}_{f,j})\mathbf{t}_{f,j}$, $\mathbf{t} = ((\mathbf{u}_{f,h} - \partial_t \boldsymbol{\eta}_{p,h}) \cdot \mathbf{t}_{f,j})\mathbf{t}_{f,j}$ and $\mathbf{w} = ((\mathbf{u}_f - \partial_t \boldsymbol{\eta}_p) \cdot \mathbf{t}_{f,j})\mathbf{t}_{f,j} - ((\mathbf{v}_{f,h} - \boldsymbol{\xi}_{p,h}) \cdot \mathbf{t}_{f,j})\mathbf{t}_{f,j}$, $\mathbf{v}_{f,h} \in \mathbf{V}_{f,h}$, $\boldsymbol{\xi}_{p,h} \in \mathbf{X}_{p,h}$, then

$$\begin{aligned}
&\sum_{j=1}^{d-1} \frac{\|(\mathbf{u}_f - \partial_t \boldsymbol{\eta}_p) \cdot \mathbf{t}_{f,j} - (\mathbf{u}_{f,h} - \partial_t \boldsymbol{\eta}_{p,h}) \cdot \mathbf{t}_{f,j}\|^2_{L^r(\Gamma_{fp})}}{c + \|(\mathbf{u}_f - \partial_t \boldsymbol{\eta}_p) \cdot \mathbf{t}_{f,j}\|^{2-r}_{L^r(\Gamma_{fp})} + \|(\mathbf{u}_{f,h} - \partial_t \boldsymbol{\eta}_{p,h}) \cdot \mathbf{t}_{f,j}\|^{2-r}_{\Gamma_{fp}}} \\
&\qquad + \sum_{j=1}^{d-1} \int_{\Gamma_{fp}} \frac{\alpha_{BJS}}{k_M^{1/2}} |\nu_I(((\mathbf{u}_f - \partial_t \boldsymbol{\eta}_p) \cdot \mathbf{t}_{f,j})\mathbf{t}_{f,j})((\mathbf{u}_f - \partial_t \boldsymbol{\eta}_p) \cdot \mathbf{t}_{f,j})\mathbf{t}_{f,j} \\
&\qquad\quad - \nu_I(((\mathbf{u}_{f,h} - \partial_t \boldsymbol{\eta}_{p,h}) \cdot \mathbf{t}_{f,j})\mathbf{t}_{f,j})((\mathbf{u}_{f,h} - \partial_t \boldsymbol{\eta}_{p,h}) \cdot \mathbf{t}_{f,j})\mathbf{t}_{f,j}| \\
&\qquad\qquad \cdot |((\mathbf{u}_f - \partial_t \boldsymbol{\eta}_p) \cdot \mathbf{t}_{f,j})\mathbf{t}_{f,j} - ((\mathbf{u}_{f,h} - \partial_t \boldsymbol{\eta}_{p,h}) \cdot \mathbf{t}_{f,j})\mathbf{t}_{f,j}| ds \\
&\qquad \le C \sum_{j=1}^{d-1} \left\| \frac{|(\mathbf{u}_f - \partial_t \boldsymbol{\eta}_p) \cdot \mathbf{t}_{f,j} - (\mathbf{u}_{f,h} - \partial_t \boldsymbol{\eta}_{p,h}) \cdot \mathbf{t}_{f,j}|}{c + |(\mathbf{u}_f - \partial_t \boldsymbol{\eta}_p) \cdot \mathbf{t}_{f,j}| + |(\mathbf{u}_{f,h} - \partial_t \boldsymbol{\eta}_{p,h}) \cdot \mathbf{t}_{f,j}|} \right\|^{2-r}_{\infty} \\
&\qquad\qquad \times \|(\mathbf{u}_f - \partial_t \boldsymbol{\eta}_p) \cdot \mathbf{t}_{f,j} - (\mathbf{v}_{f,h} - \boldsymbol{\xi}_{p,h}) \cdot \mathbf{t}_{f,j}\|^r_{L^r(\Gamma_{fp})} + C I_6, \quad (3.4.32)
\end{aligned}$$

where

$$\begin{aligned}
I_6 &:= \sum_{j=1}^{d-1} \int_{\Gamma_{fp}} \alpha_{BJS}(\nu_I(((\mathbf{u}_f - \partial_t \boldsymbol{\eta}_p) \cdot \mathbf{t}_{f,j})\mathbf{t}_{f,j})(\mathbf{u}_f - \partial_t \boldsymbol{\eta}_p) \cdot \mathbf{t}_{f,j} \\
&- \nu_I(((\mathbf{u}_{f,h} - \partial_t \boldsymbol{\eta}_{p,h}) \cdot \mathbf{t}_{f,j})\mathbf{t}_{f,j})(\mathbf{u}_{f,h} - \partial_t \boldsymbol{\eta}_{p,h}) \cdot \mathbf{t}_{f,j})((\mathbf{v}_{f,h} - \boldsymbol{\xi}_{p,h}) \cdot \mathbf{t}_{f,j} - (\mathbf{u}_{f,h} - \partial_t \boldsymbol{\eta}_{p,h}) \cdot \mathbf{t}_{f,j}).
\end{aligned}$$

Note that

$$\begin{aligned}
&I_2 = a_f(\mathbf{u}_f, \mathbf{v}_{f,h} - \mathbf{u}_{f,h}) - a_f(\mathbf{u}_{f,h}, \mathbf{v}_{f,h} - \mathbf{u}_{f,h}),\ I_4 = a_p^d(\mathbf{u}_p, \mathbf{v}_{p,h} - \mathbf{u}_{p,h}) - a_p^d(\mathbf{u}_{p,h}, \mathbf{v}_{p,h} - \mathbf{u}_{p,h}) \\
&I_6 = a_{BJS}(\mathbf{u}_f, \partial_t \boldsymbol{\eta}_p; \mathbf{v}_{f,h} - \mathbf{u}_{f,h}, \boldsymbol{\xi}_{p,h} - \partial_t \boldsymbol{\eta}_{p,h}) - a_{BJS}(\mathbf{u}_{f,h}, \partial_t \boldsymbol{\eta}_{p,h}; \mathbf{v}_{f,h} - \mathbf{u}_{f,h}, \boldsymbol{\xi}_{p,h} - \partial_t \boldsymbol{\eta}_{p,h}).
\end{aligned}$$

We subtract (3.4.2) from (3.2.5) and choose to test this difference with $(\mathbf{v}_{f,h} - \mathbf{u}_{f,h}, \mathbf{v}_{p,h} - \mathbf{u}_{p,h}, \boldsymbol{\xi}_{p,h} - \partial_t \boldsymbol{\eta}_{p,h})$, $\mathbf{v}_{f,h} \in \mathbf{V}_{f,h}$, $\mathbf{v}_{p,h} \in \mathbf{V}_{p,h}$, $\boldsymbol{\xi}_{p,h} \in \mathbf{X}_{p,h}$:

$$\begin{aligned}
&a_f(\mathbf{u}_f, \mathbf{v}_{f,h} - \mathbf{u}_{f,h}) + a_p^d(\mathbf{u}_p, \mathbf{v}_{p,h} - \mathbf{u}_{p,h}) + a_p^e(\boldsymbol{\eta}_p, \boldsymbol{\xi}_{p,h} - \partial_t \boldsymbol{\eta}_{p,h}) \\
&\quad + a_{BJS}(\mathbf{u}_f, \partial_t \boldsymbol{\eta}_p; \mathbf{v}_{f,h} - \mathbf{u}_{f,h}, \boldsymbol{\xi}_{p,h} - \partial_t \boldsymbol{\eta}_{p,h}) + b_f(\mathbf{v}_{f,h} - \mathbf{u}_{f,h}, p_f) + b_p(\mathbf{v}_{p,h} - \mathbf{u}_{p,h}, p_p) \\
&\qquad + \alpha b_p(\boldsymbol{\xi}_{p,h} - \partial_t \boldsymbol{\eta}_{p,h}, p_p) + b_\Gamma(\mathbf{v}_{f,h} - \mathbf{u}_{f,h}, \mathbf{v}_{p,h} - \mathbf{u}_{p,h}, \boldsymbol{\xi}_{p,h} - \partial_t \boldsymbol{\eta}_{p,h}; \lambda)
\end{aligned}$$

$$- a_f(\mathbf{u}_{f,h}, \mathbf{v}_{f,h} - \mathbf{u}_{f,h}) - a_p^d(\mathbf{u}_{p,h}, \mathbf{v}_{p,h} - \mathbf{u}_{p,h}) - a_p^e(\boldsymbol{\eta}_{p,h}, \boldsymbol{\xi}_{p,h} - \partial_t \boldsymbol{\eta}_{p,h})$$
$$- a_{BJS}(\mathbf{u}_{f,h}, \partial_t \boldsymbol{\eta}_{p,h}; \mathbf{v}_{f,h} - \mathbf{u}_{f,h}, \boldsymbol{\xi}_{p,h} - \partial_t \boldsymbol{\eta}_{p,h}) + b_f(\mathbf{v}_{f,h} - \mathbf{u}_{f,h}, p_{f,h}) + b_p(\mathbf{v}_{p,h} - \mathbf{u}_{p,h}, p_{p,h})$$
$$- \alpha b_p(\boldsymbol{\xi}_{p,h} - \partial_t \boldsymbol{\eta}_{p,h}, p_{p,h}) + b_\Gamma(\mathbf{v}_{f,h} - \mathbf{u}_{f,h}, \mathbf{v}_{p,h} - \mathbf{u}_{p,h}, \boldsymbol{\xi}_{p,h} - \partial_t \boldsymbol{\eta}_{p,h}; \lambda_h) = 0.$$

Then, we have:

$$\begin{aligned}
I_2 + I_4 + I_6 &= a_p^e(\boldsymbol{\eta}_{p,h} - \boldsymbol{\eta}_p, \boldsymbol{\xi}_{p,h} - \partial_t \boldsymbol{\eta}_{p,h}) + b_f(\mathbf{v}_{f,h} - \mathbf{u}_{f,h}, p_{f,h} - p_f) + \alpha b_p(\boldsymbol{\xi}_{p,h} - \partial_t \boldsymbol{\eta}_{p,h}, p_{p,h} - p_p) \\
&\quad + b_p(\mathbf{v}_{p,h} - \mathbf{u}_{p,h}, p_{p,h} - p_p) + b_\Gamma(\mathbf{v}_{f,h} - \mathbf{u}_{f,h}, \mathbf{v}_{p,h} - \mathbf{u}_{p,h}, \boldsymbol{\xi}_{p,h} - \partial_t \boldsymbol{\eta}_{p,h}; \lambda_h - \lambda) \\
&= a_p^e(\boldsymbol{\eta}_{p,h} - \boldsymbol{\eta}_p, \boldsymbol{\xi}_{p,h} - \partial_t \boldsymbol{\eta}_p) + a_p^e(\boldsymbol{\eta}_{p,h} - \boldsymbol{\eta}_p, \partial_t \boldsymbol{\eta}_p - \partial_t \boldsymbol{\eta}_{p,h}) + b_f(\mathbf{v}_{f,h} - \mathbf{u}_{f,h}, p_{f,h} - Q_{f,h} p_f) \\
&\quad + b_f(\mathbf{v}_{f,h} - \mathbf{u}_{f,h}, Q_{f,h} p_f - p_f) + \alpha b_p(\boldsymbol{\xi}_{p,h} - \partial_t \boldsymbol{\eta}_{p,h}, p_{p,h} - Q_{p,h} p_p) + \alpha b_p(\boldsymbol{\xi}_{p,h} - \partial_t \boldsymbol{\eta}_{p,h}, Q_{p,h} p_p - p_p) \\
&\quad + b_p(\mathbf{v}_{p,h} - \mathbf{u}_{p,h}, p_{p,h} - Q_{p,h} p_p) + b_p(\mathbf{v}_{p,h} - \mathbf{u}_{p,h}, Q_{p,h} p_p - p_p) \\
&\quad + b_\Gamma(\mathbf{v}_{f,h} - \mathbf{u}_{f,h}, \mathbf{v}_{p,h} - \mathbf{u}_{p,h}, \boldsymbol{\xi}_{p,h} - \partial_t \boldsymbol{\eta}_{p,h}; \lambda_h - Q_{\lambda,h} \lambda) \\
&\quad + b_\Gamma(\mathbf{v}_{f,h} - \mathbf{u}_{f,h}, \mathbf{v}_{p,h} - \mathbf{u}_{p,h}, \boldsymbol{\xi}_{p,h} - \partial_t \boldsymbol{\eta}_{p,h}; Q_{\lambda,h} \lambda - \lambda). \quad (3.4.33)
\end{aligned}$$

Since $\nabla \cdot \mathbf{V}_{p,h} = W_{p,h}$, $\mathbf{V}_{p,h} \cdot \mathbf{n}_p|_{\Gamma_{fp}} = \Lambda_h$ and (1.3.17), (2.2.24), the following terms cancel:

$$b_p(\mathbf{v}_{p,h} - \mathbf{u}_{p,h}, Q_{p,h} p_p - p_p) = b_\Gamma(0, \mathbf{v}_{p,h} - \mathbf{u}_{p,h}, 0; Q_{\lambda,h} \lambda - \lambda) = 0.$$

Note that the calculations above are valid for any $\mathbf{v}_{f,h} \in \mathbf{V}_{f,h}$, $\mathbf{v}_{p,h} \in \mathbf{V}_{p,h}$, $\boldsymbol{\xi}_{p,h} \in \mathbf{X}_{p,h}$. Now we would like to make a specific choice:

$$(\mathbf{v}_{f,h}, \mathbf{v}_{p,h}, \boldsymbol{\xi}_{p,h}) = (I_{f,h} \mathbf{u}_f, I_{p,h} \mathbf{u}_p, I_{s,h} \partial_t \boldsymbol{\eta}_p).$$

Then (3.4.33) can be written as follows:

$$\begin{aligned}
&I_2 + I_4 + I_6 + a_p^e(\boldsymbol{\eta}_{p,h} - \boldsymbol{\eta}_p, \partial_t \boldsymbol{\eta}_{p,h} - \partial_t \boldsymbol{\eta}_p) = a_p^e(\boldsymbol{\eta}_{p,h} - \boldsymbol{\eta}_p, I_{s,h} \partial_t \boldsymbol{\eta}_p - \partial_t \boldsymbol{\eta}_p) \\
&+ b_f(I_{f,h} \mathbf{u}_f - \mathbf{u}_{f,h}, p_{f,h} - Q_{f,h} p_f) + b_f(I_{f,h} \mathbf{u}_f - \mathbf{u}_{f,h}, Q_{f,h} p_f - p_f) + b_p(I_{p,h} \mathbf{u}_p - \mathbf{u}_{p,h}, p_{p,h} - Q_{p,h} p_p) \\
&\quad + \alpha b_p(I_{s,h} \partial_t \boldsymbol{\eta}_p - \partial_t \boldsymbol{\eta}_{p,h}, p_{p,h} - Q_{p,h} p_p) + \alpha b_p(I_{s,h} \partial_t \boldsymbol{\eta}_p - \partial_t \boldsymbol{\eta}_{p,h}, Q_{p,h} p_p - p_p) \\
&\quad + b_\Gamma(I_{f,h} \mathbf{u}_f - \mathbf{u}_{f,h}, I_{p,h} \mathbf{u}_p - \mathbf{u}_{p,h}, I_{s,h} \partial_t \boldsymbol{\eta}_p - \partial_t \boldsymbol{\eta}_{p,h}; \lambda_h - Q_{\lambda,h} \lambda) \\
&\quad + b_\Gamma(I_{f,h} \mathbf{u}_f - \mathbf{u}_{f,h}, 0, I_{s,h} \partial_t \boldsymbol{\eta}_p - \partial_t \boldsymbol{\eta}_{p,h}; Q_{\lambda,h} \lambda - \lambda). \quad (3.4.34)
\end{aligned}$$

Note that due to (3.4.4) and (2.2.27), we have:

$$b_\Gamma(I_{f,h}\mathbf{u}_f-\mathbf{u}_{f,h},I_{p,h}\mathbf{u}_p-\mathbf{u}_{p,h},I_{s,h}\partial_t\boldsymbol{\eta}_p-\partial_t\boldsymbol{\eta}_{p,h};\lambda_h-Q_{\lambda,h}\lambda)$$
$$=b_\Gamma(I_{f,h}\mathbf{u}_f,I_{p,h}\mathbf{u}_p,I_{s,h}\partial_t\boldsymbol{\eta}_p;\lambda_h-Q_{\lambda,h}\lambda)-b_\Gamma(\mathbf{u}_{f,h},\mathbf{u}_{p,h},\partial_t\boldsymbol{\eta}_{p,h};\lambda_h-Q_{\lambda,h}\lambda)=0. \quad (3.4.35)$$

We subtract (3.4.3) from (3.2.6) with the choice $(w_{f,h},w_{p,h})=(Q_{f,h}p_f-p_{f,h},Q_{p,h}p_p-p_{p,h})$:

$$\begin{aligned}&s_0(\partial_t p_p-Q_{p,h}\partial_t p_p,Q_{p,h}p_p-p_{p,h})_{\Omega_p}+s_0(Q_{p,h}\partial_t p_p-\partial_t p_{p,h},Q_{p,h}p_p-p_{p,h})_{\Omega_p}\\&-\alpha b_p(\partial_t\boldsymbol{\eta}_p-I_{s,h}\partial_t\boldsymbol{\eta}_p,Q_{p,h}p_p-p_{p,h})-\alpha b_p(I_{s,h}\partial_t\boldsymbol{\eta}_p-\partial_t\boldsymbol{\eta}_{p,h},Q_{p,h}p_p-p_{p,h})\\&-b_p(\mathbf{u}_p-I_{p,h}\mathbf{u}_p,Q_{p,h}p_p-p_{p,h})-b_p(I_{p,h}\mathbf{u}_p-\mathbf{u}_{p,h},Q_{p,h}p_p-p_{p,h})\\&-b_f(\mathbf{u}_f-I_{f,h}\mathbf{u}_f,Q_{f,h}p_f-p_{f,h})-b_f(I_{f,h}\mathbf{u}_f-\mathbf{u}_{f,h},Q_{f,h}p_f-p_{f,h})=0. \quad (3.4.36)\end{aligned}$$

By (1.3.17) and (2.2.28), we have

$$s_0(\partial_t p_p-Q_{p,h}\partial_t p_p,Q_{p,h}p_p-p_{p,h})_{\Omega_p}=b_p(\mathbf{u}_p-I_{p,h}\mathbf{u}_p,Q_{p,h}p_p-p_{p,h})=0.$$

Then (3.4.36) becomes:

$$\begin{aligned}&s_0(Q_{p,h}\partial_t p_p-\partial_t p_{p,h},Q_{p,h}p_p-p_{p,h})_{\Omega_p}\\&=\alpha b_p(\partial_t\boldsymbol{\eta}_p-I_{s,h}\partial_t\boldsymbol{\eta}_p,Q_{p,h}p_p-p_{p,h})+\alpha b_p(I_{s,h}\partial_t\boldsymbol{\eta}_p-\partial_t\boldsymbol{\eta}_{p,h},Q_{p,h}p_p-p_{p,h})\\&+b_p(I_{p,h}\mathbf{u}_p-\mathbf{u}_{p,h},Q_{p,h}p_p-p_{p,h})+b_f(\mathbf{u}_f-I_{f,h}\mathbf{u}_f,Q_{f,h}p_f-p_{f,h})+b_f(I_{f,h}\mathbf{u}_f-\mathbf{u}_{f,h},Q_{f,h}p_f-p_{f,h}).\end{aligned} \quad (3.4.37)$$

Next we combine (3.4.34),(3.4.35) and (3.4.37):

$$\begin{aligned}&I_2+I_4+I_6+a_p^e(\boldsymbol{\eta}_{p,h}-\boldsymbol{\eta}_p,\partial_t\boldsymbol{\eta}_{p,h}-\partial_t\boldsymbol{\eta}_p)+s_0(Q_{p,h}\partial_t p_p-\partial_t p_{p,h},Q_{p,h}p_p-p_{p,h})_{\Omega_p}\\&=a_p^e(\boldsymbol{\eta}_{p,h}-\boldsymbol{\eta}_p,I_{s,h}\partial_t\boldsymbol{\eta}_p-\partial_t\boldsymbol{\eta}_p)+b_f(\mathbf{u}_f-I_{f,h}\mathbf{u}_f,Q_{f,h}p_f-p_{f,h})+b_f(I_{f,h}\mathbf{u}_f-\mathbf{u}_{f,h},Q_{f,h}p_f-p_f)\\&+\alpha b_p(I_{s,h}\partial_t\boldsymbol{\eta}_p-\partial_t\boldsymbol{\eta}_p,Q_{p,h}p_p-p_{p,h})+\alpha b_p(I_{s,h}\partial_t\boldsymbol{\eta}_p-\partial_t\boldsymbol{\eta}_{p,h},Q_{p,h}p_p-p_p)\\&+b_\Gamma(I_{f,h}\mathbf{u}_f-\mathbf{u}_{f,h},0,I_{s,h}\partial_t\boldsymbol{\eta}_p-\partial_t\boldsymbol{\eta}_{p,h};Q_{\lambda,h}\lambda-\lambda). \quad (3.4.38)\end{aligned}$$

We bound the first four terms of the right hand side, using Hölder's and Young's inequalities (1.3.2), (1.3.6):

$$\begin{aligned}&a_p^e(\boldsymbol{\eta}_{p,h}-\boldsymbol{\eta}_p,I_{s,h}\partial_t\boldsymbol{\eta}_p-\partial_t\boldsymbol{\eta}_p)+b_f(\mathbf{u}_f-I_{f,h}\mathbf{u}_f,Q_{f,h}p_f-p_{f,h})+b_f(I_{f,h}\mathbf{u}_f-\mathbf{u}_{f,h},Q_{f,h}p_f-p_f)\\&+\alpha b_p(I_{s,h}\partial_t\boldsymbol{\eta}_p-\partial_t\boldsymbol{\eta}_p,Q_{p,h}p_p-p_{p,h})\le\epsilon_1\left(\|\mathbf{u}_f-\mathbf{u}_{f,h}\|^2_{W^{1,r}(\Omega_f)}+\|p_{f,h}-Q_{f,h}p_f\|^{r'}_{L^{r'}(\Omega_f)}\right)\end{aligned}$$

$$+\epsilon_2\|p_{p,h}-Q_{p,h}p_p\|^{r'}_{L^{r'}(\Omega_p)}+C\left(\|Q_{f,h}p_f-p_f\|^2_{L^{r'}(\Omega_f)}+\|I_{f,h}\mathbf{u}_f-\mathbf{u}_f\|^2_{W^{1,r}(\Omega_f)}\right.$$
$$\left.+\|I_{f,h}\mathbf{u}_f-\mathbf{u}_f\|^r_{W^{1,r}(\Omega_f)}\right)+C\left(\|\boldsymbol{\eta}_{p,h}-\boldsymbol{\eta}_p\|^2_{H^1(\Omega_p)}+\|I_{s,h}\partial_t\boldsymbol{\eta}_p-\partial_t\boldsymbol{\eta}_p\|^2_{H^1(\Omega_p)}\right.$$
$$\left.+\|I_{s,h}\partial_t\boldsymbol{\eta}_p-\partial_t\boldsymbol{\eta}_p\|^r_{H^1(\Omega_p)}\right). \tag{3.4.39}$$

We combine (3.4.38) and (3.4.39) :

$$\begin{aligned}
&I_2+I_4+I_6+a^e_p(\boldsymbol{\eta}_p-\boldsymbol{\eta}_{p,h},\partial_t(\boldsymbol{\eta}_p-\boldsymbol{\eta}_{p,h}))+s_0(Q_{p,h}\partial_t p_p-\partial_t p_{p,h},Q_{p,h}p_p-p_{p,h})_{\Omega_p}\\
&\quad\le\epsilon_1\left(\|p_{f,h}-Q_{f,h}p_f\|^{r'}_{L^{r'}(\Omega_f)}+\|p_{p,h}-Q_{p,h}p_p\|^{r'}_{L^{r'}(\Omega_p)}\right)+\epsilon_2\|\mathbf{u}_f-\mathbf{u}_{f,h}\|^2_{W^{1,r}(\Omega_f)}\\
&\quad+\alpha b_p(I_{s,h}\partial_t\boldsymbol{\eta}_p-\partial_t\boldsymbol{\eta}_{p,h},Q_{p,h}p_p-p_p)+b_\Gamma(I_{f,h}\mathbf{u}_f-\mathbf{u}_{f,h},0,I_{s,h}\partial_t\boldsymbol{\eta}_p-\partial_t\boldsymbol{\eta}_{p,h};Q_{\lambda,h}\lambda-\lambda)\\
&\quad+C\Big(\|\boldsymbol{\eta}_{p,h}-\boldsymbol{\eta}_p\|^2_{H^1(\Omega_p)}+\|I_{s,h}\partial_t\boldsymbol{\eta}_p-\partial_t\boldsymbol{\eta}_p\|^2_{H^1(\Omega_p)}+\|I_{s,h}\partial_t\boldsymbol{\eta}_p-\partial_t\boldsymbol{\eta}_p\|^r_{H^1(\Omega_p)}\\
&\quad+\|Q_{f,h}p_f-p_f\|^2_{L^{r'}(\Omega_f)}+\|I_{f,h}\mathbf{u}_f-\mathbf{u}_f\|^2_{W^{1,r}(\Omega_f)}+\|I_{f,h}\mathbf{u}_f-\mathbf{u}_f\|^r_{W^{1,r}(\Omega_f)}\Big).
\end{aligned}\tag{3.4.40}$$

Next we integrate (3.4.40) in time from 0 to $t\in(0,T]$:

$$\begin{aligned}
&\frac{1}{2}\left(a^e_p(\boldsymbol{\eta}_p(t)-\boldsymbol{\eta}_{p,h}(t),\boldsymbol{\eta}_p(t)-\boldsymbol{\eta}_{p,h}(t))+s_0\|Q_{p,h}p_p(t)-p_{p,h}(t)\|^2_{L^2(\Omega_p)}\right)+\int_0^t(I_2+I_4+I_6)\,ds\\
&\quad\le\int_0^t\left(\epsilon_1\left(\|p_{f,h}-Q_{f,h}p_f\|^{r'}_{L^{r'}(\Omega_f)}+\|p_{p,h}-Q_{p,h}p_p\|^{r'}_{L^{r'}(\Omega_p)}\right)+\epsilon_2\|\mathbf{u}_f-\mathbf{u}_{f,h}\|^2_{W^{1,r}(\Omega_f)}\right),ds\\
&\qquad+\frac{1}{2}\left(a^e_p(\boldsymbol{\eta}_p(0)-\boldsymbol{\eta}_{p,h}(0),\boldsymbol{\eta}_p(0)-\boldsymbol{\eta}_{p,h}(0))+s_0\|Q_{p,h}p_p(0)-p_{p,h}(0)\|^2_{L^2(\Omega_p)}\right)\\
&+\int_0^t\left(\alpha b_p(I_{s,h}\partial_t\boldsymbol{\eta}_p-\partial_t\boldsymbol{\eta}_{p,h},Q_{p,h}p_p-p_p)+b_\Gamma(I_{f,h}\mathbf{u}_f-\mathbf{u}_{f,h},0,I_{s,h}\partial_t\boldsymbol{\eta}_p-\partial_t\boldsymbol{\eta}_{p,h};Q_{\lambda,h}\lambda-\lambda)\right)ds\\
&\qquad+\int_0^t C\Big(\|\boldsymbol{\eta}_{p,h}-\boldsymbol{\eta}_p\|^2_{H^1(\Omega_p)}+\|I_{s,h}\partial_t\boldsymbol{\eta}_p-\partial_t\boldsymbol{\eta}_p\|^2_{H^1(\Omega_p)}+\|I_{s,h}\partial_t\boldsymbol{\eta}_p-\partial_t\boldsymbol{\eta}_p\|^r_{H^1(\Omega_p)}\\
&\qquad+\|Q_{f,h}p_f-p_f\|^2_{L^{r'}(\Omega_f)}+\|I_{f,h}\mathbf{u}_f-\mathbf{u}_f\|^2_{W^{1,r}(\Omega_f)}+\|I_{f,h}\mathbf{u}_f-\mathbf{u}_f\|^r_{W^{1,r}(\Omega_f)}\Big)\,ds.
\end{aligned}\tag{3.4.41}$$

We bound the remaining terms on the right hand side using integration by parts, (1.3.2), (1.3.3) and (1.3.6):

$$\begin{aligned}
&\int_0^t\left(\alpha b_p(I_{s,h}\partial_t\boldsymbol{\eta}_p-\partial_t\boldsymbol{\eta}_{p,h},Q_{p,h}p_p-p_p)+b_\Gamma(I_{f,h}\mathbf{u}_f-\mathbf{u}_{f,h},0,I_{s,h}\partial_t\boldsymbol{\eta}_p-\partial_t\boldsymbol{\eta}_{p,h};Q_{\lambda,h}\lambda-\lambda)\right)ds\\
&\qquad=\alpha b_p(I_{s,h}\boldsymbol{\eta}_p-\boldsymbol{\eta}_{p,h},Q_{p,h}p_p-p_p)\Big|_{s=0}^{s=t}+b_\Gamma(0,0,I_{s,h}\boldsymbol{\eta}_p-\boldsymbol{\eta}_{p,h};Q_{\lambda,h}\lambda-\lambda)\Big|_{s=0}^{s=t}\\
&\qquad-\int_0^t\left(\alpha b_p(I_{s,h}\boldsymbol{\eta}_p-\boldsymbol{\eta}_{p,h},Q_{p,h}\partial_t p_p-\partial_t p_p)+b_\Gamma(0,0,I_{s,h}\boldsymbol{\eta}_p-\boldsymbol{\eta}_{p,h};Q_{\lambda,h}\partial_t\lambda-\partial_t\lambda)\right)ds
\end{aligned}$$

$$
\begin{aligned}
&+\int_0^t b_\Gamma(I_{f,h}\mathbf{u}_f-\mathbf{u}_{f,h},0,0;Q_{\lambda,h}\lambda-\lambda)\,ds\\
&\le \epsilon_2\left(\|I_{s,h}\boldsymbol{\eta}_p(t)-\boldsymbol{\eta}_{p,h}(t)\|^2_{H^1(\Omega_p)}+\int_0^t\left(\|I_{f,h}\mathbf{u}_f-\mathbf{u}_{f,h}\|^2_{W^{1,r}(\Omega_f)}+\|I_{s,h}\boldsymbol{\eta}_p-\boldsymbol{\eta}_{p,h}\|^2_{H^1(\Omega_p)}\right)\,ds\right)\\
&\qquad+C\left(\|Q_{p,h}p_p(t)-p_p(t)\|^2_{L^{r'}(\Omega_p)}+\|Q_{\lambda,h}\lambda(t)-\lambda(t)\|^2_{L^{r'}(\Gamma_{fp})}\right)\\
&\quad+C\left(\|Q_{\lambda,h}\lambda(0)-\lambda(0)\|^2_{L^{r'}(\Gamma_{fp})}+\|Q_{p,h}p_p(0)-p_p(0)\|^2_{L^{r'}(\Omega_p)}+\|I_{s,h}\boldsymbol{\eta}_p(0)-\boldsymbol{\eta}_{p,h}(0)\|^2_{H^1(\Omega_p)}\right)\\
&\qquad+\int_0^t C\left(\|Q_{p,h}\partial_t p_p-\partial_t p_p\|^2_{L^{r'}(\Omega_p)}+\|Q_{\lambda,h}\partial_t\lambda-\partial_t\lambda\|^2_{L^{r'}(\Gamma_{fp})}+\|Q_{\lambda,h}\lambda-\lambda\|^2_{L^{r'}(\Gamma_{fp})}\right)\,ds\\
&\qquad\le \epsilon_2\left(\|\boldsymbol{\eta}_p(t)-\boldsymbol{\eta}_{p,h}(t)\|^2_{H^1(\Omega_p)}+\int_0^t\left(\|\mathbf{u}_f-\mathbf{u}_{f,h}\|^2_{W^{1,r}(\Omega_f)}+\|\boldsymbol{\eta}_p-\boldsymbol{\eta}_{p,h}\|^2_{H^1(\Omega_p)}\right)\,ds\right)\\
&\quad+C\left(\|\boldsymbol{\eta}_p(t)-I_{s,h}\boldsymbol{\eta}_p(t)\|^2_{H^1(\Omega_p)}+\|Q_{p,h}p_p(t)-p_p(t)\|^2_{L^{r'}(\Omega_p)}+\|Q_{\lambda,h}\lambda(t)-\lambda(t)\|^2_{L^{r'}(\Gamma_{fp})}\right)\\
&\quad+C\left(\|Q_{p,h}p_p(0)-p_p(0)\|^2_{L^{r'}(\Omega_p)}+\|I_{s,h}\boldsymbol{\eta}_p(0)-\boldsymbol{\eta}_{p,h}(0)\|^2_{H^1(\Omega_p)}+\|Q_{\lambda,h}\lambda(0)-\lambda(0)\|^2_{L^{r'}(\Gamma_{fp})}\right)\\
&\qquad+\int_0^t C\left(\|\boldsymbol{\eta}_p-I_{s,h}\boldsymbol{\eta}_p\|^2_{H^1(\Omega_p)}+\|\mathbf{u}_f-I_{f,h}\mathbf{u}_f\|^2_{W^{1,r}(\Omega_f)}+\|Q_{\lambda,h}\lambda-\lambda\|^2_{L^{r'}(\Gamma_{fp})}\right)\,ds\\
&\qquad+\int_0^t C\left(\|Q_{p,h}\partial_t p_p-\partial_t p_p\|^2_{L^{r'}(\Omega_p)}+\|Q_{\lambda,h}\partial_t\lambda-\partial_t\lambda\|^2_{L^{r'}(\Gamma_{fp})}\right)\,ds.
\end{aligned}
\tag{3.4.42}
$$

We choose $p_{p,h}(0)=Q_{p,h}p_p(0)$, $\boldsymbol{\eta}_{p,h}(0)=I_{s,h}\boldsymbol{\eta}_p(0)$, then using coercivity of $a_p^e(\cdot,\cdot)$ form, (2.2.6), we obtain:

$$
\begin{aligned}
&\|\boldsymbol{\eta}_p(t)-\boldsymbol{\eta}_{p,h}(t)\|^2_{H^1(\Omega_p)}+s_0\|Q_{p,h}p_p(t)-p_{p,h}(t)\|^2_{L^2(\Omega_p)}+\int_0^t(I_2+I_4+I_6)\,ds\\
&\qquad\le \epsilon_2\left(\|\boldsymbol{\eta}_p(t)-\boldsymbol{\eta}_{p,h}(t)\|^2_{H^1(\Omega_p)}+\int_0^t\|\mathbf{u}_f-\mathbf{u}_{f,h}\|^2_{W^{1,r}(\Omega_f)}\,ds\right)\\
&\qquad+\epsilon_1\int_0^t\left(\|p_{f,h}-Q_{f,h}p_f\|^{r'}_{L^{r'}(\Omega_f)}+\|p_{p,h}-Q_{p,h}p_p\|^{r'}_{L^{r'}(\Omega_p)}\right)\,ds\\
&\quad+C\left(\|Q_{p,h}p_p(0)-p(0)\|^2_{L^{r'}(\Omega_p)}+\|\boldsymbol{\eta}_p(0)-I_{s,h}\boldsymbol{\eta}_p(0)\|^2_{H^1(\Omega_p)}+\|Q_{\lambda,h}\lambda(0)-\lambda(0)\|^2_{L^{r'}(\Gamma_{fp})}\right)\\
&\qquad+\int_0^t C\Big(\|\boldsymbol{\eta}_{p,h}-\boldsymbol{\eta}_p\|^2_{H^1(\Omega_p)}+\|I_{s,h}\partial_t\boldsymbol{\eta}_p-\partial_t\boldsymbol{\eta}_p\|^2_{H^1(\Omega_p)}+\|I_{s,h}\partial_t\boldsymbol{\eta}_p-\partial_t\boldsymbol{\eta}_p\|^r_{H^1(\Omega_p)}\\
&+\|\boldsymbol{\eta}_p-I_{s,h}\boldsymbol{\eta}_p\|^2_{H^1(\Omega_p)}+\|Q_{\lambda,h}\lambda-\lambda\|^2_{L^{r'}(\Gamma_{fp})}+\|Q_{p,h}\partial_t p_p-\partial_t p_p\|^2_{L^{r'}(\Omega_p)}+\|Q_{\lambda,h}\partial_t\lambda-\partial_t\lambda\|^2_{L^{r'}(\Gamma_{fp})}\\
&\qquad+\|Q_{f,h}p_f-p_f\|^2_{L^{r'}(\Omega_f)}+\|I_{f,h}\mathbf{u}_f-\mathbf{u}_f\|^2_{W^{1,r}(\Omega_f)}+\|I_{f,h}\mathbf{u}_f-\mathbf{u}_f\|^r_{W^{1,r}(\Omega_f)}\Big)\,ds\\
&\quad+C\left(\|\boldsymbol{\eta}_p(t)-I_{s,h}\boldsymbol{\eta}_p(t)\|^2_{H^1(\Omega_p)}+\|Q_{p,h}p_p(t)-p_p(t)\|^2_{L^{r'}(\Omega_p)}+\|Q_{\lambda,h}\lambda(t)-\lambda(t)\|^2_{L^{r'}(\Gamma_{fp})}\right).
\end{aligned}
\tag{3.4.43}
$$

We combine (3.4.30), (3.4.31), (3.4.32) and (3.4.43):

$$\begin{aligned}
&\int_0^t \Big(\mathcal{G}(\mathbf{u},\mathbf{u}_h) + \frac{\|\mathbf{D}(\mathbf{u}_f)-\mathbf{D}(\mathbf{u}_{f,h})\|^2_{L^r(\Omega_f)}}{c+\|\mathbf{D}(\mathbf{u}_f)\|^{2-r}_{L^r(\Omega_f)}+\|\mathbf{D}(\mathbf{u}_{f,h})\|^{2-r}_{L^r(\Omega_f)}} + \frac{\|\mathbf{u}_p-\mathbf{u}_{p,h}\|^2_{L^r(\Omega_p)}}{c+\|\mathbf{u}_p\|^{2-r}_{L^r(\Omega_p)}+\|\mathbf{u}_{p,h}\|^{2-r}_{L^r(\Omega_p)}} \\
&\qquad + \frac{\|\mathbf{u}_f-\partial_t\boldsymbol{\eta}_p-(\mathbf{u}_{f,h}-\partial_t\boldsymbol{\eta}_{p,h})\|^2_{L^r(\Gamma_{fp})}}{c+\|\mathbf{u}_f-\partial_t\boldsymbol{\eta}_p\|^{2-r}_{L^r(\Gamma_{fp})}+\|\mathbf{u}_{f,h}-\partial_t\boldsymbol{\eta}_{p,h}\|^{2-r}_{\Gamma_{fp}}}\Big)\,ds \\
&\qquad + \|\boldsymbol{\eta}_p(t)-\boldsymbol{\eta}_{p,h}(t)\|^2_{H^1(\Omega_p)} + s_0\|Q_{p,h}p_p(t)-p_p(t)\|^2_{L^2(\Omega_p)} \\
&\quad \le C\int_0^t \mathcal{E}(\mathbf{u},\mathbf{u}_h)^r\left(\|\mathbf{D}(\mathbf{u}_f)-\mathbf{D}(I_{f,h}\mathbf{u}_f)\|^r_{L^r(\Omega_f)}+\|\mathbf{u}_p-I_{p,h}\mathbf{u}_p\|^r_{L^r(\Omega_p)}\right)ds \\
&+C\int_0^t \mathcal{E}(\mathbf{u},\mathbf{u}_h)^r\|\mathbf{u}_f-\partial_t\boldsymbol{\eta}_p-(I_{f,h}\mathbf{u}_f-I_{s,h}\partial_t\boldsymbol{\eta}_p)\|^r_{L^r(\Gamma_{fp})}\,ds+\epsilon_2\|\boldsymbol{\eta}_p(t)-\boldsymbol{\eta}_{p,h}(t)\|^2_{H^1(\Omega_p)} \\
&+\epsilon_2\int_0^t\|\mathbf{u}_f-\mathbf{u}_{f,h}\|^2_{W^{1,r}(\Omega_f)}\,ds+\epsilon_1\int_0^t\left(\|p_{f,h}-Q_{f,h}p_f\|^{r'}_{L^{r'}(\Omega_f)}+\|p_{p,h}-Q_{p,h}p_p\|^{r'}_{L^{r'}(\Omega_p)}\right)ds \\
&+C\left(\|Q_{p,h}p_p(0)-p(0)\|^2_{L^{r'}(\Omega_p)}+\|\boldsymbol{\eta}_p(0)-I_{s,h}\boldsymbol{\eta}_p(0)\|^2_{H^1(\Omega_p)}+\|Q_{\lambda,h}\lambda(0)-\lambda(0)\|^2_{L^{r'}(\Gamma_{fp})}\right) \\
&\quad+\int_0^t C\Big(\|\boldsymbol{\eta}_{p,h}-\boldsymbol{\eta}_p\|^2_{H^1(\Omega_p)}+\|I_{s,h}\partial_t\boldsymbol{\eta}_p-\partial_t\boldsymbol{\eta}_p\|^2_{H^1(\Omega_p)}+\|I_{s,h}\partial_t\boldsymbol{\eta}_p-\partial_t\boldsymbol{\eta}_p\|^r_{H^1(\Omega_p)} \\
&+\|\boldsymbol{\eta}_p-I_{s,h}\boldsymbol{\eta}_p\|^2_{H^1(\Omega_p)}+\|Q_{\lambda,h}\lambda-\lambda\|^2_{L^{r'}(\Gamma_{fp})}+\|Q_{p,h}\partial_t p_p-\partial_t p_p\|^2_{L^{r'}(\Omega_p)}+\|Q_{\lambda,h}\partial_t\lambda-\partial_t\lambda\|^2_{L^{r'}(\Gamma_{fp})} \\
&\quad+\|Q_{f,h}p_f-p_f\|^2_{L^{r'}(\Omega_f)}+\|I_{f,h}\mathbf{u}_f-\mathbf{u}_f\|^2_{W^{1,r}(\Omega_f)}+\|I_{f,h}\mathbf{u}_f-\mathbf{u}_f\|^r_{W^{1,r}(\Omega_f)}\Big)\,ds \\
&+C\left(\|\boldsymbol{\eta}_p(t)-I_{s,h}\boldsymbol{\eta}_p(t)\|^2_{H^1(\Omega_p)}+\|Q_{p,h}p_p(t)-p_p(t)\|^2_{L^{r'}(\Omega_p)}+\|Q_{\lambda,h}\lambda(t)-\lambda(t)\|^2_{L^{r'}(\Gamma_{fp})}\right).
\end{aligned} \tag{3.4.44}$$

Using (3.4.10), we obtain the bound for the pressure variables:

$$\begin{aligned}
&\|((p_{f,h}-Q_{f,h}p_f,p_{p,h}-Q_{p,h}p_p),\lambda_h-Q_{\lambda,h}\lambda)\|_{W\times\Lambda_h} \\
&\le \sup_{\mathbf{v}_h\in\mathbf{V}_h}\frac{b_f(\mathbf{v}_{f,h},p_{f,h}-Q_{f,h}p_f)+b_p(\mathbf{v}_{p,h},p_{p,h}-Q_{p,h}p_p)+b_\Gamma(\mathbf{v}_{f,h},\mathbf{v}_{p,h},\mathbf{0};\lambda_h-Q_{\lambda,h}\lambda)}{\|\mathbf{v}_h\|_{\mathbf{V}}} \\
&\qquad\le \sup_{\mathbf{v}_h\in\mathbf{V}_h}\Big[\frac{a_f(\mathbf{u}_{f,h}\mathbf{v}_{f,h})-a_f(\mathbf{u}_f,\mathbf{v}_{f,h})}{\|\mathbf{v}_h\|_{\mathbf{V}}}+\frac{a_p^d(\mathbf{u}_{p,h},\mathbf{v}_{p,h})-a_p^d(\mathbf{u}_p,\mathbf{v}_{p,h})}{\|\mathbf{v}_h\|_{\mathbf{V}}} \\
&\qquad\qquad\frac{a_{BJS}(\mathbf{u}_{f,h},\partial_t\boldsymbol{\eta}_{p,h};\mathbf{v}_{f,h},\mathbf{0})-a_{BJS}(\mathbf{u}_f,\partial_t\boldsymbol{\eta}_p;\mathbf{v}_{f,h},\mathbf{0})}{\|\mathbf{v}_h\|_{\mathbf{V}}} \\
&\qquad+\frac{b_f(\mathbf{v}_{f,h},Q_{f,h}p_f-p_f)+b_p(\mathbf{v}_{p,h},Q_{p,h}p_p-p_p)+b_\Gamma(\mathbf{v}_{f,h},\mathbf{v}_{p,h},\mathbf{0};Q_{\lambda,h}\lambda-\lambda)}{\|\mathbf{v}_h\|_{\mathbf{V}}}\Big] \\
&\qquad\le C\Big(\mathcal{E}(\mathbf{u},\mathbf{u}_h)\mathcal{G}(\mathbf{u},\mathbf{u}_h)^{1/r'}+\|Q_{f,h}p_f-p_f\|_{L^{r'}(\Omega_f)}+\|Q_{p,h}p_p-p_p\|_{L^{r'}(\Omega_p)} \\
&\qquad\qquad+\|Q_{\lambda,h}\lambda-\lambda\|_{L^{r'}(\Gamma_{fp})}\Big).
\end{aligned} \tag{3.4.45}$$

Hence,

$$\epsilon_1 \int_0^t \left(\|p_{p,h} - Q_{p,h}p_p\|^{r'}_{L^{r'}(\Omega_p)} + \ \|p_{f,h} - Q_{f,h}p_f\|^{r'}_{L^{r'}(\Omega_f)} + \|\lambda_h - Q_{\lambda,h}\lambda\|^{r'}_{L^{r'}(\Gamma_{fp})} \right) ds$$
$$\leq \epsilon_1 C \int_0^t \mathcal{E}(\mathbf{u}, \mathbf{u}_h)^{r'} \mathcal{G}(\mathbf{u}, \mathbf{u}_h)\, ds$$
$$+ \epsilon_1 C \int_0^t \left(\|Q_{f,h}p_f - p_f\|^{r'}_{L^{r'}(\Omega_f)} + \|Q_{p,h}p_p - p_p\|^{r'}_{L^{r'}(\Omega_p)} + \|Q_{\lambda,h}\lambda - \lambda\|^{r'}_{L^{r'}(\Gamma_{fp})} \right) ds. \quad (3.4.46)$$

Using stability of both continuous and semi-continuous solutions, we combine (3.4.44) and (3.4.46) and apply Gronwall's Lemma (1.3.7) to obtain:

$$\|\mathbf{u}_f - \mathbf{u}_{f,h}\|^2_{L^2(0,T;W^{1,r}(\Omega_f))} + \|\mathbf{u}_p - \mathbf{u}_{p,h}\|^2_{L^2(0,T;L^r(\Omega_p))} + \|\mathbf{u}_f - \partial_t \boldsymbol{\eta}_p - (\mathbf{u}_{f,h} - \partial_t \boldsymbol{\eta}_{p,h})\|^2_{L^2(0,T;BJS)}$$
$$+ \|p_f - p_{f,h}\|^{r'}_{L^{r'}(0,T;L^{r'}(\Omega_f))} + \|p_p - p_{p,h}\|^{r'}_{L^{r'}(0,T;L^{r'}(\Omega_p))} + \|\lambda - \lambda_h\|^{r'}_{L^{r'}(0,T;L^{r'}(\Gamma_{fp}))}$$
$$+ \|\boldsymbol{\eta}_p - \boldsymbol{\eta}_{p,h}\|^2_{L^\infty(0,T;H^1(\Omega_p))} + s_0 \|Q_{p,h}p_p - p_p\|^2_{L^\infty(0,T;L^2(\Omega_p))} + \|\mathcal{G}(\mathbf{u}, \mathbf{u}_h)\|_{L^1(0,T)}$$
$$\leq C \exp(T) \Big[\|\mathbf{u}_f - I_{f,h}\mathbf{u}_f\|^2_{L^2(0,T;W^{1,r}(\Omega_f))} + \|\mathbf{u}_f - I_{f,h}\mathbf{u}_f\|^r_{L^r(0,T;W^{1,r}(\Omega_f))}$$
$$+ \|\boldsymbol{\eta}_p - I_{s,h}\boldsymbol{\eta}_p\|^2_{L^2(0,T;H^1(\Omega_p))} + \|\mathbf{u}_p - I_{p,h}\mathbf{u}_p\|^r_{L^r(0,T;L^r(\Omega_p))} + \|\partial_t \boldsymbol{\eta}_p - I_{s,h}\partial_t \boldsymbol{\eta}_p\|^r_{L^r(0,T;H^1(\Omega_p))}$$
$$+ \|\partial_t \boldsymbol{\eta}_p - I_{s,h}\partial_t \boldsymbol{\eta}_p\|^2_{L^2(0,T;H^1(\Omega_p))} + \|Q_{f,h}p_f - p_f\|^2_{L^2(0,T;L^{r'}(\Omega_f))} + \|Q_{\lambda,h}\lambda - \lambda\|^2_{L^2(0,T;L^{r'}(\Gamma_{fp}))}$$
$$+ \|Q_{p,h}\partial_t p_p - \partial_t p_p\|^2_{L^2(0,T;L^{r'}(\Omega_p))} + \|Q_{\lambda,h}\partial_t \lambda - \partial_t \lambda\|^2_{L^2(0,T;L^{r'}(\Gamma_{fp}))} + \|\boldsymbol{\eta}_p - I_{s,h}\boldsymbol{\eta}_p\|^2_{L^\infty(0,T;H^1(\Omega_p))}$$
$$+ \|Q_{p,h}p_p - p_p\|^2_{L^\infty(0,T;L^{r'}(\Omega_p))} + \|Q_{\lambda,h}\lambda - \lambda\|^2_{L^\infty(0,T;L^{r'}(\Gamma_{fp}))} + \|Q_{f,h}p_f - p_f\|^{r'}_{L^{r'}(0,T;L^{r'}(\Omega_f))}$$
$$+ \|Q_{p,h}p_p - p_p\|^{r'}_{L^{r'}(0,T;L^{r'}(\Omega_p))} + \|Q_{\lambda,h}\lambda - \lambda\|^{r'}_{L^{r'}(0,T;L^{r'}(\Gamma_{fp}))} \Big]. \quad (3.4.47)$$

Then the error estimate (3.4.27) follows from (3.4.47) and (1.3.18)-(1.3.19), (3.4.22)-(3.4.24).

□

3.5 NUMERICAL RESULTS

3.5.1 Convergence test

In this subsection we discuss numerical results that verify the theoretical bound (3.4.27).

We discretize the problem (3.4.2)-(3.4.4) in time using backward Euler method. Let T denote the final time and τ the length of time step, then for each $n = 1, \ldots, N$ the n-th time step is $t_n = n\tau$. To approximate the time derivatives we use:

$$d_\tau \phi = \frac{\phi^n - \phi^{n-1}}{\tau}, \qquad n = 1, \ldots, N.$$

For the spacial discretization in fluid domain we will use $\mathcal{P}_1 b - \mathcal{P}_1 b$ MINI elements, we will also use $\mathcal{RT}_0 - \mathcal{P}_0$ for $\mathbf{V}_{p,h} \times W_{p,h}$, continuous piecewise linears $\mathcal{P}_1$ for $\mathbf{X}_{p,h}$ and piecewise constants $\mathcal{P}_0$ for Λ_h. We handle nonlinearity in Stokes and Darcy terms using Picard iterations and we assume that the constant in the Beavers-Joseph-Saffman condition (1.2.9) does not depend on fluid viscosity.

We consider a computational domain $\Omega = [0, 2] \times [0, 1]$, where $\Omega_f = [0, 1] \times [0, 1]$ represents the fluid region and $\Omega_p = [1, 2] \times [0, 1]$ – the solid region. The flow is driven by the pressure drop: on the left boundary of Ω_f we set $p_{in} = 1$ kPa and on the right boundary of Ω_p $p_{out} = 0$ kPa, which is also chosen as initial condition for Darcy pressure. Along the top and bottom boundaries, we impose a no-slip boundary condition for the Stokes flow and a no-flow boundary condition for the Darcy flow. We also set zero displacement boundary condition on top, bottom and right parts of boundary of structure subdomain, as well as zero initial condition for the displacement. We set $\lambda_p = \mu_p = s_0 = \alpha = \alpha_{BJS} = 1.0$ and $K = \mathbf{I}$.

We assume that the fluid viscosity in Stokes region satisfies the Cross model:

$$\nu_f(|D(\mathbf{u}_f)|) = \nu_{f,\infty} + \frac{\nu_{f,0} - \nu_{f,\infty}}{1 + K_f |D(\mathbf{u}_f)|^{2-r_f}}.$$

And the effective viscosity in Darcy region also satisfies the Cross model:

$$\nu_p(|\mathbf{u}_p|) = \nu_{p,\infty} + \frac{\nu_{p,0} - \nu_{p,\infty}}{1 + K_p |\mathbf{u}_p|^{2-r_p}},$$

where the parameters are chosen as follows: $K_f = K_p = 1$, $\nu_{f,\infty} = \nu_{p,\infty} = 1$, $\nu_{f,0} = \nu_{p,0} = 10$, $r_f = r_p = 1.35$. The simulation time is $T = 1.0$ s and the time step $\Delta t = 0.01$ s. To verify the convergence estimate (3.4.27), we compute a reference solution, obtained on the mesh with characteristic size $h = 1/320$. Table 5 shows the relative errors and rates of convergence for the solutions computed with discretization steps $h = 1/20, 1/40, 1/80$ and $1/160$ for the case of lowest order elements. Since we use bounded functions to model viscosity in both regions, we compute the norms of the errors using $r = r' = 2$. As we can see, the results agree with theory, i.e. we observe at least first convergence rate for all variables.

$\mathcal{P}_1^b - \mathcal{P}_1$, $\mathcal{RT}_0 - \mathcal{P}_0$, $\mathcal{P}_1$, and $\mathcal{P}_0$.										
	$\|\mathbf{e}_f\|_{l^2(H^1(\Omega_f))}$		$\|e_{fp}\|_{l^2(L^2(\Omega_f))}$		$\|\mathbf{e}_p\|_{l^2(L^2(\Omega_p))}$		$\|e_{pp}\|_{l^\infty(L^2(\Omega_p))}$		$\|\mathbf{e}_s\|_{l^\infty(H^1(\Omega_p))}$	
h	error	rate	error	rate	error	rate	error	rate	error	rate
1/20	4.83E-03	–	2.75E-02	–	1.55E-01	–	1.15E-01	–	4.98E-02	–
1/40	2.31E-03	1.06	1.03E-02	1.41	8.63E-02	0.85	5.28E-02	1.12	2.88E-02	0.79
1/80	1.04E-03	1.16	4.62E-03	1.16	4.08E-02	1.08	2.25E-02	1.23	1.61E-02	0.84
1/160	3.94E-04	1.40	2.14E-04	1.11	2.07E-02	0.98	7.48E-03	1.59	6.59E-03	1.29

Table 5: Example 1: relative numerical errors and convergence rates.

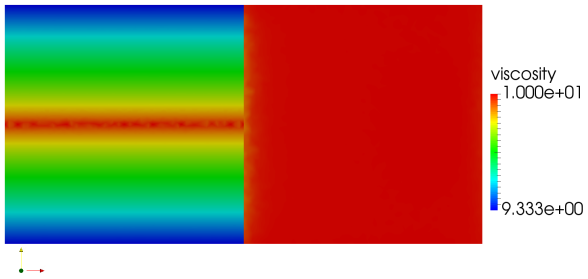

(a) Viscosity at $t = 0.01s$

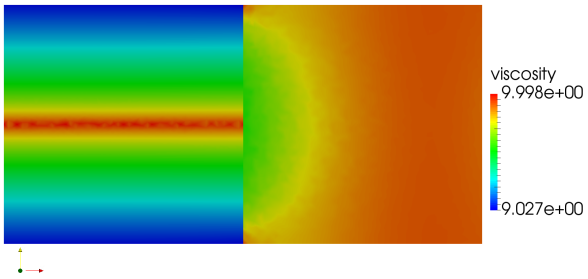

(b) Viscosity at $t = 1s$

Figure 7: Example 1: nonlinear viscosity computed at $t = 0.01s$ (left) and at $t = 1s$ (right).

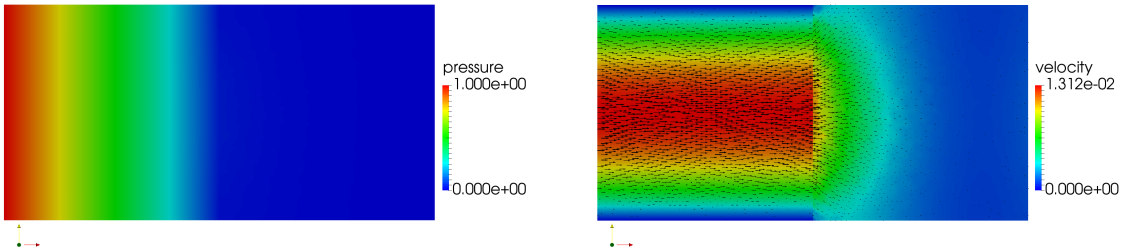

(a) Pressure solution (b) Velocity solution

Figure 8: Example 1: pressure (left) and velocity (right) solutions at time $t = 1s$.

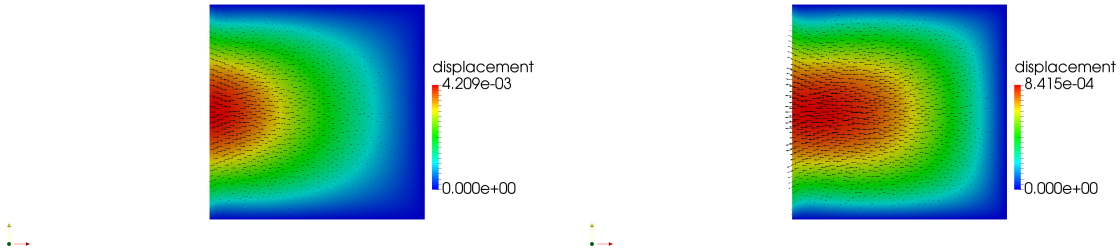

(a) Nonlinear solution (b) Difference

Figure 9: Example 1: displacement solution (left) and difference (right) at time $t = 1s$.

We also investigate the behavior of solution visually and compare it to the solution of the linear method (2.3.1)-(2.3.3). For visualization we use the solutions corresponding to the mesh size $h = 1/40$. All plots are presented at the first and final time steps. For a fair comparison between models, we calculate the viscosity in linear case as $\nu_f^{lin} = \nu_f\big|_{r_f=2} = 5.5$ and $\nu_p^{lin} = \nu_p\big|_{r_p=2} = 5.5$. Figures with difference between velocity and displacement solutions are obtained by plotting $\mathbf{u}_{f,h}^{nonlin} - \mathbf{u}_{f,h}^{lin}$, $\mathbf{u}_{p,h}^{nonlin} - \mathbf{u}_{p,h}^{lin}$ and $\boldsymbol{\eta}_{p,h}^{nonlin} - \boldsymbol{\eta}_{p,h}^{lin}$, where colors represent the magnitude of the corresponding difference and arrows represent the direction.

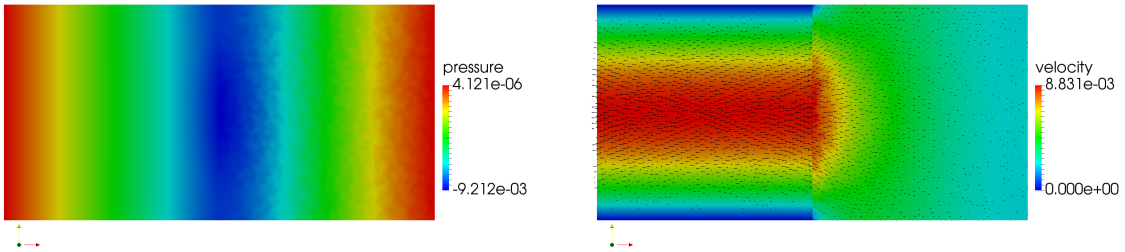

(a) Difference in pressure

(b) Difference in velocity

Figure 10: Example 1: difference between non-Newtonian and Newtonian solutions at time $t = 1$.

As we can see from Figure 7, in nonlinear case the viscosity is high in the middle of the fluid domain and it decreases towards the boundary, which is due to the fact that the strain rate increases towards the boundary. On the other hand, the viscosity does not vary as much in the solid domain due to almost uniform velocity profile (see Figure 7). We note that these observations agree with conclusions in [45]. Moreover, use of non-Newtonian model results in lower Stokes velocity, as shown on Figure 10(b), which in turn entails lower displacement, Figure 9(b).

3.5.2 Towards bloodflow applications

The focus of our method is on the non-Newtonian fluids, which exhibit the so-called shear thinning properties, which is typical for blood. Therefore, in this subsection we present a preliminary 2d test case, in which we consider blood flow in idealized artery, shown in Figure 11. The geometry of the domain is as follows:

$$d_{inflow} = 1cm, \quad d_{outflow} \approx 0.5cm, \quad d_{wall} \approx 0.1cm, \quad , l_{total} = 6cm, \quad l_{single} \approx 1.6cm.$$

where l_{single} is a distance from inflow to the splitting point of the fluid region.

We prescribe zero initial condition and the following boundary conditions:

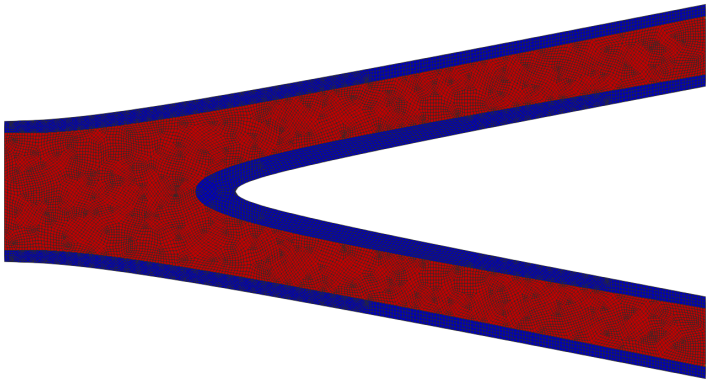

Figure 11: Example 2: computational grid, where red region corresponds to free fluid, blue - to the medium.

$$
\begin{aligned}
&u_f \cdot \tau = 0 && \text{on } \Gamma_{f,inflow}, \cup \Gamma_{f,outflow},\\
&u_p \cdot n = 0, && \text{on } \Gamma_{p,inflow} \cup \Gamma_{p,outflow},\\
&\eta = 0, && \text{on } \Gamma_{p,inflow} \cup \Gamma_{p,outflow},\\
&\eta \cdot \tau = 0, && \text{on } \Gamma_p \setminus (\Gamma_{p,inflow} \cup \Gamma_{p,outflow}),\\
&(\sigma_f\, n) \cdot n = g(x,y), && \text{on } \Gamma_{f,inflow},\\
&(\sigma_f\, n) \cdot n = 0, && \text{on } \Gamma_{f,outflow}.
\end{aligned}
$$

Here, the inflow part of the boundary corresponds to $x = 0$, while the outflow part – to $x = 6$.

Except for the geometry of the domain, the setup in this test case follows closely the one in [58]. In particular, for the sake of more realistic simulations, we consider the Navier–Stokes equations for the flow in the fluid region. We also follow [19, 57] and add a spring term $\xi\boldsymbol{\eta}$ to the governing equation for elastic skeleton (1.2.5) in order to keep the top and bottom structure displacements connected. We allow for the motion of the domain due to the deformation of the solid region, which we deal with by adopting the Arbitrary Lagrangian–Eulerian (ALE) approach [41, 60].

For the viscosity in the fluid region we use Carreau-Yasuda model [27]

$$\nu(x,y,t) = \nu_\infty + (\nu_0 - \nu_\infty)(1 + (\lambda\dot{\gamma}(x,y,t)^a)^{\frac{n-1}{a}}),$$

where $\dot{\gamma}(x,y,t) = \sqrt{\frac{1}{2}D(u_f) : D(u_f)}$. We adopt the same nonlinearity law with the same parameters for the Darcy region, but with $\dot{\gamma}(x,y,t) = \sqrt{u_p \cdot u_p}$. The values of the parameters that define this model are chosen as $\lambda = 1.902s$, $n = 0.22$, $a = 1.25$, $\nu_0 = 0.56$ Poi and $\nu_\infty = 0.035$ Poi.

The function that drives the flow in the fluid region (simulating the heart pulse) is given by

$$g(x,y) = \begin{cases} 6667[1 - \cos(\frac{2\pi t}{0.003})], & \text{if } t \leq 0.003, \\ 0, & \text{otherwise.} \end{cases}$$

The rest of the parameters are given in Table 6.

Parameter	Symbol	Units	Values
Fluid density	ρ_f	(g/cm^3)	1
Lamé coefficient	λ_p	(dyne/cm^2)	4.28×10^6
Lamé coefficient	μ_p	(dyne/cm^2)	1.07×10^6
Permeability	K	(cm^2)	$diag(0.035, 0.035) \times 10^{-9}$
Mass storativity	s_0	(cm^2/dyne)	5×10^{-6}
Spring coeff.	ξ	(dyne/cm^4)	5×10^7
Total time	T	(ms)	6
Time step	Δt	(ms)	0.01

Table 6: Example 2: poroelasticity and fluid parameters.

The results presented in Figures 12–14. For the illustration purposes, we show the pictures with the deformation magnified by a factor of 50. We do not present Darcy pressure and velocity as there is very little flow observed in this region.

As a result of this simulation, we observe the flow following the geometry of the vessel, with slightly pronounced bifurcation region at the splitting point of the domain (see Figure 13). The velocity solution agrees with the pulse-nature of the injection, namely we see

the wave-like region of higher velocity traveling across the domain. This is coherent with our expectation of an idealized simulated heart beat driven flow. While it is not visually obvious that the fluid exhibits shear–thinning properties, the realization of the viscosity field indicates that it is indeed the case. We note how the viscosity in the fluid region is being affected by the variation in the velocity field - we see that the viscosity next to the artery wall is hardly different from the initially specified coefficient, while it exhibits more variation further from the walls(see Figure 12). It is also worth seeing that the regions of higher viscosity propagate with the higher velocity front, the effect one expects to see in modeling of shear–thinning fluids.

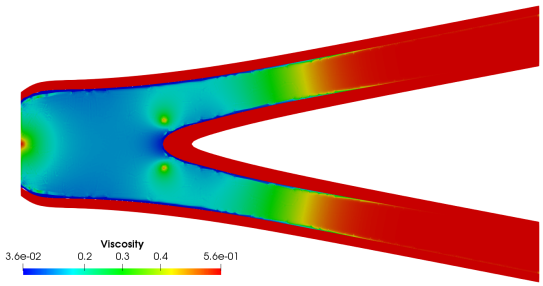

(a) Fluid viscosity, $t = 1.5ms$

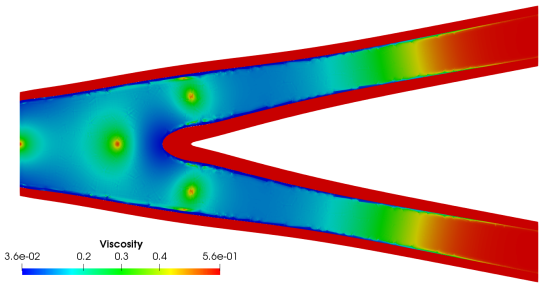

(b) Fluid viscosity, $t = 2.5ms$

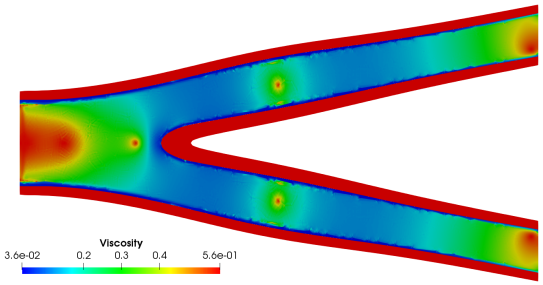

(c) Fluid viscosity, $t = 3.5ms$

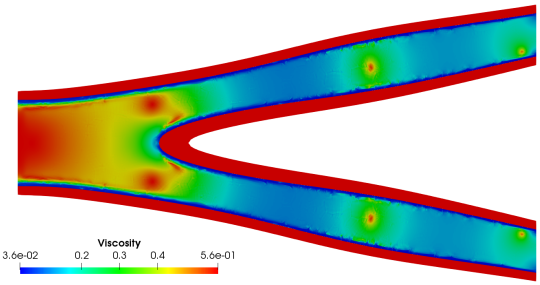

(d) Fluid viscosity, $t = 4.5ms$

Figure 12: Example 2: viscosity solution at different time.

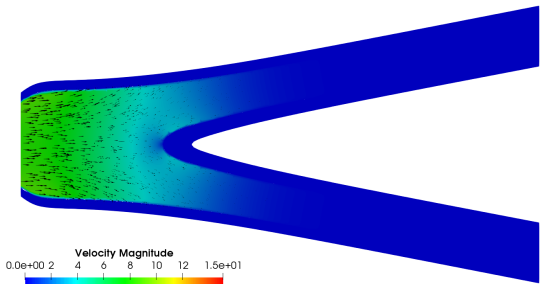

(a) Fluid velocity, $t = 1.5ms$

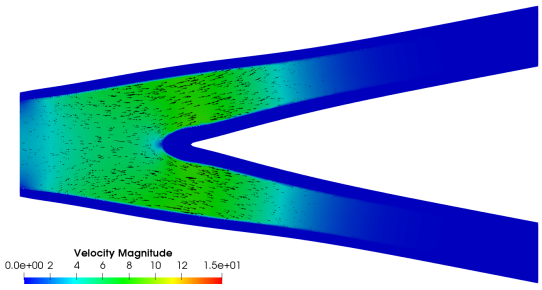

(b) Fluid velocity, $t = 2.5ms$

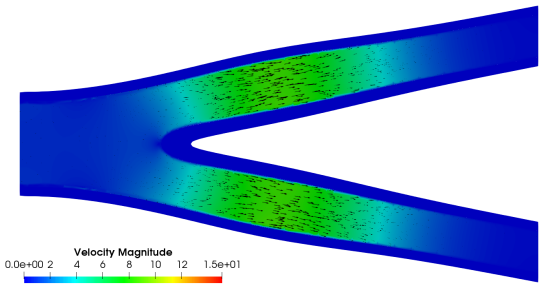

(c) Fluid velocity, $t = 3.5ms$

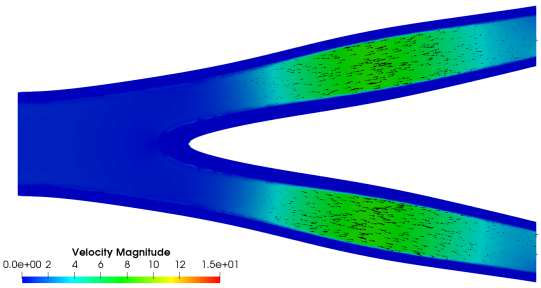

(d) Fluid velocity, $t = 4.5ms$

Figure 13: Example 2: velocity solution at different time.

We also present the displacement solution on Figure 14. As expected, higher values are observed near the regions of high fluid velocity in the flow region. We note that we do not see any singularities near the bifurcation area, which can be explained by smoothness of the computational domain. However, we do expect to see singularities in stress, which can be recovered from the displacement solution, using (1.2.4).

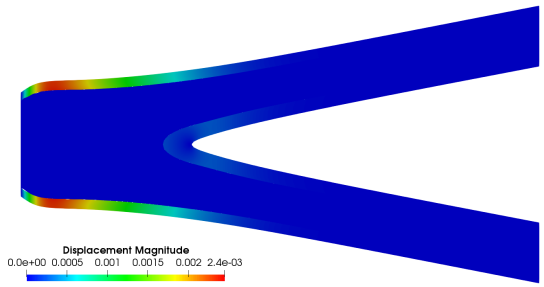

(a) Structure displacement, $t = 1.5ms$

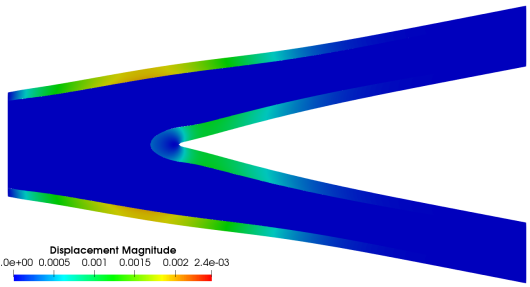

(b) Structure displacement, $t = 2.5ms$

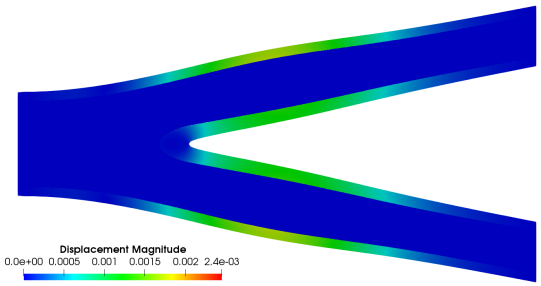

(c) Structure displacement, $t = 3.5ms$

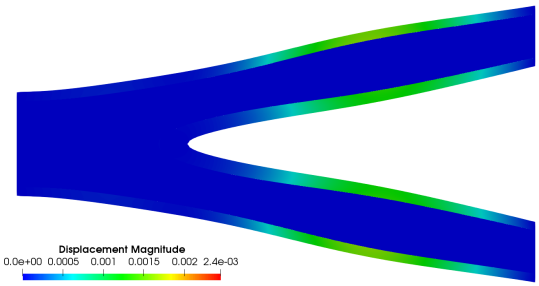

(d) Structure displacement, $t = 4.5ms$

Figure 14: Example 2: structure displacement solution at different time.

This is a proof-of-concept numerical example with an idealized geometry of a blood vessel. However, our future work is in extending this simulation towards a real X-ray scan based artery geometries, involving ones with severe stenosis and/or constricted areas.

4.0 TRANSPORT SIMULATION IN FLUID-POROELASTIC STRUCTURE INTERACTION

4.1 TRANSPORT PROBLEM

In this chapter we consider coupling of the Stokes–Biot problem with the transport equation on $\Omega = \Omega_f \cup \Omega_p$:

$$\phi c_t + \nabla \cdot (c\mathbf{u}(t) - \mathbf{D}\nabla c) = qc^*, \quad \text{in } \Omega \times (0, T], \tag{4.1.1}$$

where $c(\mathbf{x}, t)$ is the concentration of some chemical component, $0 < \phi_* \leq \phi(\mathbf{x}) \leq \phi^*$ is the porosity of the medium in Ω_p (it is set to 1 in Ω_f), $\mathbf{u}(t)$ is the velocity field over Ω, defined as $\mathbf{u}(t)|_{\Omega_f} = \mathbf{u}_f(t), \mathbf{u}(t)|_{\Omega_p} = \mathbf{u}_p(t)$, q is the source term given by $q\big|_{\Omega_f} = q_f$ and $q\big|_{\Omega_p} = q_p$, and

$$c^* = \begin{cases} \text{injected concentration } c_w, & q > 0, \\ \text{resident concentration } c, & q < 0. \end{cases}$$

We assume that the diffusion/dispersion tensor $\mathbf{D}$ is a nonlinear function of the velocity, given by

$$\mathbf{D}(\mathbf{u}) = d_m \mathbf{I} + |\mathbf{u}|\{\alpha_l \mathbf{E} + \alpha_t(\mathbf{I} - \mathbf{E})\}, \tag{4.1.2}$$

where $d_m = \phi\tau D_m$, τ is the tortuosity coefficient, D_m is the molecular diffusivity, $\mathbf{E}(\mathbf{u})$ is the tensor that projects onto the $\mathbf{u}$ direction with $(\mathbf{E}(\mathbf{u}))_{ij} = \frac{u_i u_j}{|\mathbf{u}|^2}$, and α_l, α_t are the longitudinal and transverse dispersion, respectively.

The model is complemented by the initial condition

$$c(\mathbf{x}, 0) = c_0(\mathbf{x}), \quad \text{in } \Omega, \tag{4.1.3}$$

and the boundary conditions

$$(c\mathbf{u} - \mathbf{D}\nabla c) \cdot \mathbf{n} = (c_{in}\mathbf{u}) \cdot \mathbf{n}, \qquad \text{on } \Gamma_{in} \times (0,T], \tag{4.1.4}$$

$$(\mathbf{D}\nabla c) \cdot \mathbf{n} = 0, \qquad \text{on } \Gamma_{out} \times (0,T], \tag{4.1.5}$$

where $\Gamma_{in} := \{\mathbf{x} \in \partial\Omega : \mathbf{u} \cdot \mathbf{n} < 0\}$, $\Gamma_{out} := \{\mathbf{x} \in \partial\Omega : \mathbf{u} \cdot \mathbf{n} \geq 0\}$ and $\mathbf{n}$ is the unit outward normal vector to $\partial\Omega$.

4.2 SEMI-DISCRETE FORMULATION

We consider a shape-regular and quasi-uniform partitions of Ω, denoted by $\mathcal{T}_h$. We note that $\mathcal{T}_h$ may be different from $\mathcal{T}_h^f$ and $\mathcal{T}_h^p$. We denote by E_h the set of all interior edges(faces) of $\mathcal{T}_h$ and on each edge(face) we arbitrarily fix a unit normal vector $\mathbf{n}_e$. We further denote E_h^{out} and E_h^{in} the set of edges(faces) on Γ_{out} and Γ_{in}, for which $\mathbf{n}_e$ coincides with the outward unit normal vector.

Since the details of the discretization of the flow problem were presented in Chapter 2, we focus only on derivation of the numerical method for the transport problem. Following [92], we adopt the discontinuous Galerkin scheme, known as Non-symmetric Interior Penalty Galerkin (NIPG) [79].

For $s \geq 0$, we define the space

$$H^s(\mathcal{T}_h) = \{\phi \in L^2(\Omega) : \phi \in H^s(E), E \in \mathcal{T}_h\},$$

equipped with the norm

$$|||\phi|||_{s,\Omega} = \left(\sum_{E \in \mathcal{T}_h} \|\phi\|^2_{H^s(E)} \right)^{1/2}.$$

We now define the jump and average for $\phi \in H^s(\mathcal{T}_h), s > 1/2$ as follows. Let $E_i, E_j \in \mathcal{T}_h$ and $e = \partial E_i \cap \partial E_j \in E_h$, with $\mathbf{n}_e$ exterior to E_i. We denote

$$[\phi] = (\phi|_{E_i})|_e - (\phi|_{E_j})|_e, \tag{4.2.1}$$

$$\{\phi\} = \frac{(\phi|_{E_i})|_e + (\phi|_{E_j})|_e}{2}. \tag{4.2.2}$$

We consider the finite element space

$$\mathcal{D}_r(\mathcal{T}_h) = \{\phi \in L^2(\Omega) : \phi|_E \in \mathcal{P}_r(E),\, E \in \mathcal{T}_h\},$$

where $\mathcal{P}_r(E)$ denotes the space of polynomials of degree less than or equal to r on E.

Let the bilinear form $B_{\mathbf{u}_h}(c_h, \psi_h)$ and the linear functional $L_h(\psi_h)$ be defined as follows:

$$\begin{aligned} B_{\mathbf{u}_h}(c_h, \psi_h) &= \sum_{E\in\mathcal{T}_h} \int_E (\mathbf{D}(\mathbf{u}_h)\nabla c_h - c_h\mathbf{u}_h)\cdot\nabla\psi_h - \sum_{e\in E_h}\int_e \{\mathbf{D}(\mathbf{u}_h)\nabla c_h\cdot\mathbf{n}_e\}[\psi_h] \\ &+ \sum_{e\in E_h}\int_e \{\mathbf{D}(\mathbf{u}_h)\nabla\psi_h\cdot\mathbf{n}_e\}[c_h] + \sum_{e\in E_h}\int_e c_h^*\mathbf{u}_h\cdot\mathbf{n}_e[\psi_h] \\ &+ \sum_{e\in E_h^{out}}\int_e c_h\mathbf{u}_h\cdot\mathbf{n}_e\psi_h - \int_\Omega c_h q^-\psi_h + J_0^{\sigma,\beta}(c_h,\psi_h), \\ L_h(\psi_h) &= \int_\Omega c_w q^+\psi_h - \sum_{e\in E_h^{in}}\int_e c_{in}\mathbf{u}_h\cdot\mathbf{n}_e\psi_h. \end{aligned} \tag{4.2.3}$$

Here $q^+ = \max(q,0)$ is the injection part of source term and $q^- = \min(q,0)$ is the extraction part of source term, $c_h^*|_e$ is the upwind value of concentration, defined as

$$c_h^*|_e = \begin{cases} c_h|_{E_1} \text{ if } \mathbf{u}_h\cdot\mathbf{n}_e > 0, \\ c_h|_{E_2} \text{ if } \mathbf{u}_h\cdot\mathbf{n}_e < 0, \end{cases} \tag{4.2.4}$$

and $J_0^{\sigma,\beta}(c_h,\psi_h)$ is the interior penalty term

$$J_0^{\sigma,\beta}(c_h,\psi_h) = \sum_{e\in E_h}\frac{\sigma_e}{h_e^\beta}\int_e [c_h][\psi_h], \tag{4.2.5}$$

where, σ is a discrete positive function that takes constant value σ_e on the edge and is bounded below by $\sigma_* > 0$ and above σ^*, h_e is the side of edge(face) e and $\beta \geq 0$ is a real number. It was shown in [92], that the optimal choice for β is $\beta^* = 1$.

The continuous-in-time DG scheme for the transport problem reads as follows: find $c_h(t) \in \mathcal{D}_r(\mathcal{T}_h)$ such that $\forall\psi_h \in \mathcal{D}_r(\mathcal{T}_h)$

$$(\phi\partial_t c_h, \psi_h) + B_{\mathbf{u}_h}(c_h,\psi_h) = L_h(\psi_h) \tag{4.2.6}$$

and the initial condition $c_h(0)$ is a suitable approximation of c_0.

4.3 ANALYSIS OF SEMI-DISCRETE PROBLEM

In this section we discuss the stability and error estimates for the transport problem (4.2.6). We note that a similar scheme has been used and analyzed in details in [92]. The main difference and improvement in this work is the fact that the numerically computed velocity field $\mathbf{u}_h$ is directly incorporated into the scheme for transport (4.2.6), while in [92] the authors used a special "cut-off" operator in order to ensure optimal properties of the method.

In next lemma, we present the main ingredient required for the analysis – the point-wise stability of the flow solution.

Lemma 4.3.1. *Let the solution of (2.1.11)-(2.1.13) be regular enough. Then there exists a positive constant* $C = C(\mathbf{u}_f,\, p_f,\, \mathbf{u}_p,\, p_p,\, \boldsymbol{\eta}_p,\, \lambda)$ *such that*

$$\|\mathbf{u}_f - \mathbf{u}_{f,h}\|_{L^\infty(0,T;H^1(\Omega_f))} + \|\mathbf{u}_p - \mathbf{u}_{p,h}\|_{L^\infty(0,T;L^2(\Omega_p))} \leq C\sqrt{\exp(T)}h^{\min\{k_f,\, s_f+1,\, k_p+1,\, s_p+1,\, k_s\}}. \tag{4.3.1}$$

Proof. We differentiate (2.1.11) and (2.2.1) in time, and then subtract (2.2.1)–(2.2.2) from (2.1.11)–(2.1.12) to form the error equation

$$\begin{aligned} &a_f(\partial_t \mathbf{e}_f, \mathbf{v}_{f,h}) + a_p^d(\partial_t \mathbf{e}_p, \mathbf{v}_{p,h}) + a_p^e(\partial_t \mathbf{e}_s, \boldsymbol{\xi}_{p,h}) + a_{BJS}(\partial_t \mathbf{e}_f, \partial_{tt}\mathbf{e}_s; \mathbf{v}_{f,h}, \boldsymbol{\xi}_{p,h}) + b_f(\mathbf{v}_{f,h}, \partial_t e_{fp}) \\ &\quad + b_p(\mathbf{v}_{p,h}, \partial_t e_{pp}) + \alpha b_p(\boldsymbol{\xi}_{p,h}, \partial_t e_{pp}) + b_\Gamma(\mathbf{v}_{f,h}, \mathbf{v}_{p,h}, \boldsymbol{\xi}_{p,h}; \partial_t e_\lambda) + (s_0\, \partial_t e_{pp}, w_{p,h}) \\ &\quad - \alpha b_p(\partial_t e_s, w_{p,h}) - b_p(\mathbf{e}_p, w_{p,h}) - b_f(\mathbf{e}_f, w_{f,h}) = 0, \end{aligned} \tag{4.3.2}$$

Setting $\mathbf{v}_{f,h} = \boldsymbol{\phi}_{f,h}, \mathbf{v}_{p,h} = \boldsymbol{\phi}_{p,h}, \boldsymbol{\xi}_{p,h} = \partial_t \boldsymbol{\phi}_{s,h}, w_{f,h} = \partial_t \phi_{fp,h}$, and $w_{p,h} = \partial_t \phi_{pp,h}$, we have

$$\begin{aligned} &a_f(\partial_t \boldsymbol{\chi}_f, \boldsymbol{\phi}_{f,h}) + a_f(\partial_t \boldsymbol{\phi}_{f,h}, \boldsymbol{\phi}_{f,h}) + a_p^d(\partial_t \boldsymbol{\chi}_p, \boldsymbol{\phi}_{p,h}) + a_p^d(\partial_t \boldsymbol{\phi}_{p,h}, \boldsymbol{\phi}_{p,h}) + a_p^e\left(\partial_t \boldsymbol{\chi}_s, \partial_t \boldsymbol{\phi}_{s,h}\right) \\ &\quad + a_p^e\left(\partial_t \boldsymbol{\phi}_{s,h}, \partial_t \boldsymbol{\phi}_{s,h}\right) + a_{BJS}\left(\partial_t \boldsymbol{\chi}_f, \partial_{tt}\boldsymbol{\chi}_s; \boldsymbol{\phi}_{f,h}, \partial_t \boldsymbol{\phi}_{s,h}\right) + a_{BJS}\left(\partial_t \boldsymbol{\phi}_{f,h}, \partial_{tt}\boldsymbol{\phi}_{s,h}; \boldsymbol{\phi}_{f,h}, \partial_t \boldsymbol{\phi}_{s,h}\right) \\ &\quad + b_f(\boldsymbol{\phi}_{f,h}, \partial_t \chi_{fp}) + b_f(\boldsymbol{\phi}_{f,h}, \partial_t \phi_{fp,h}) + b_p(\boldsymbol{\phi}_{p,h}, \partial_t \chi_{pp}) + b_p(\boldsymbol{\phi}_{p,h}, \partial_t \phi_{pp,h}) + \alpha b_p\left(\partial_t \boldsymbol{\phi}_{s,h}, \partial_t \chi_{pp}\right) \\ &\quad + \alpha b_p\left(\partial_t \boldsymbol{\phi}_{s,h}, \partial_t \phi_{pp,h}\right) + b_\Gamma\left(\boldsymbol{\phi}_{f,h}, \boldsymbol{\phi}_{p,h}, \partial_t \boldsymbol{\phi}_{s,h}; \partial_t \chi_\lambda\right) + b_\Gamma\left(\boldsymbol{\phi}_{f,h}, \boldsymbol{\phi}_{p,h}, \partial_t \boldsymbol{\phi}_{s,h}; \partial_t \phi_{\lambda,h}\right) \\ &\quad + (s_0\, \partial_t \chi_{pp}, \partial_t \phi_{pp,h}) + (s_0\, \partial_t \phi_{pp,h}, \partial_t \phi_{pp,h}) - \alpha b_p\left(\partial_t \boldsymbol{\chi}_s, \partial_t \phi_{pp,h}\right) - \alpha b_p\left(\partial_t \boldsymbol{\phi}_{s,h}, \partial_t \phi_{pp,h}\right) \\ &\quad - b_p(\boldsymbol{\chi}_p, \partial_t \phi_{pp,h}) - b_p(\boldsymbol{\phi}_{p,h}, \partial_t \phi_{pp,h}) - b_f(\boldsymbol{\chi}_f, \partial_t \phi_{fp,h}) - b_f(\boldsymbol{\phi}_{f,h}, \partial_t \phi_{fp,h}) = 0. \end{aligned} \tag{4.3.3}$$

The following terms simplify, due to the properties of projection operators (1.3.17),(2.2.24) and (2.2.28):

$$b_p(\boldsymbol{\chi}_p, \partial_t \phi_{pp,h}) = b_p(\boldsymbol{\phi}_{p,h}, \partial_t \chi_{pp}) = 0, \quad (s_0\, \partial_t \chi_{pp}, \partial_t \phi_{pp,h}) = \langle \boldsymbol{\phi}_{p,h} \cdot \mathbf{n}_p, \partial_t \chi_\lambda \rangle_{\Gamma_{fp}} = 0, \quad (4.3.4)$$

where we also used that $\Lambda_h = \mathbf{V}_{p,h} \cdot \mathbf{n}_p|_{\Gamma_{fp}}$ for the last equality. We also have

$$b_\Gamma\left(\boldsymbol{\phi}_{f,h}, \boldsymbol{\phi}_{p,h}, \partial_t \boldsymbol{\phi}_{s,h}; \partial_t \phi_{\lambda,h}\right) = 0, \quad b_\Gamma\left(\boldsymbol{\phi}_{f,h}, \boldsymbol{\phi}_{p,h}, \partial_t \boldsymbol{\phi}_{s,h}; \partial_t \chi_\lambda\right) = \left\langle \boldsymbol{\phi}_{f,h} \cdot \mathbf{n}_f + \partial_t \boldsymbol{\phi}_{s,h} \cdot \mathbf{n}_p, \partial_t \chi_\lambda \right\rangle_{\Gamma_{fp}},$$

where we have used (2.2.27) and (2.2.3) for the first equality and the last equality in (4.3.4) for the second equality. Rearranging terms and using the results above, the error equation (4.3.3) becomes

$$\begin{aligned}
&\frac{1}{2}\partial_t \left(a_f(\boldsymbol{\phi}_{f,h}, \boldsymbol{\phi}_{f,h}) + a_p^d(\boldsymbol{\phi}_{p,h}, \boldsymbol{\phi}_{p,h}) + \left|\boldsymbol{\phi}_{f,h} - \partial_t \boldsymbol{\phi}_{s,h}\right|^2_{a_{BJS}} \right) + a_p^e(\partial_t \boldsymbol{\phi}_{s,h}, \partial_t \boldsymbol{\phi}_{s,h}) + s_0 \|\partial_t \phi_{pp,h}\|^2_{L^2(\Omega_p)} \\
&\quad = a_f(\partial_t \boldsymbol{\chi}_f, \boldsymbol{\phi}_{f,h}) + a_p^d(\partial_t \boldsymbol{\chi}_p, \boldsymbol{\phi}_{p,h}) + a_p^e\left(\partial_t \boldsymbol{\chi}_s, \partial_t \boldsymbol{\phi}_{s,h}\right) + b_f(\boldsymbol{\chi}_f, \partial_t \phi_{fp,h}) \\
&\quad + \sum_{j=1}^{d-1} \left\langle \nu \alpha_{BJS} \sqrt{K_j^{-1}} \partial_t (\boldsymbol{\chi}_f - \partial_t \boldsymbol{\chi}_s) \cdot \boldsymbol{\tau}_{f,j}, (\boldsymbol{\phi}_{f,h} - \partial_t \boldsymbol{\phi}_{s,h}) \cdot \boldsymbol{\tau}_{f,j} \right\rangle_{\Gamma_{fp}} - b_f(\boldsymbol{\phi}_{f,h}, \partial_t \chi_{fp}) \\
&\quad - \alpha b_p(\partial_t \boldsymbol{\phi}_{s,h}, \partial_t \chi_{pp}) + \alpha b_p(\partial_t \boldsymbol{\chi}_s, \partial_t \phi_{pp,h}) - \langle \boldsymbol{\phi}_{f,h} \cdot \mathbf{n}_f + \partial_t \boldsymbol{\phi}_{s,h} \cdot \mathbf{n}_p, \partial_t \chi_\lambda \rangle_{\Gamma_{fp}}. \qquad (4.3.5)
\end{aligned}$$

Using Cauchy-Schwartz (1.3.2), Young's (1.3.6) and trace (1.3.3) inequalities, we bound the right-hand side of (4.3.5) as follows

$$\begin{aligned}
&a_f(\partial_t \boldsymbol{\chi}_f, \boldsymbol{\phi}_{f,h}) + a_p^d(\partial_t \boldsymbol{\chi}_p, \boldsymbol{\phi}_{p,h}) + a_p^e\left(\partial_t \boldsymbol{\chi}_s, \partial_t \boldsymbol{\phi}_{s,h}\right) \\
&\quad + \sum_{j=1}^{d-1} \left\langle \nu \alpha_{BJS} \sqrt{K_j^{-1}} \partial_t (\boldsymbol{\chi}_f - \partial_t \boldsymbol{\chi}_s) \cdot \boldsymbol{\tau}_{f,j}, (\boldsymbol{\phi}_{f,h} - \partial_t \boldsymbol{\phi}_{s,h}) \cdot \boldsymbol{\tau}_{f,j} \right\rangle_{\Gamma_{fp}} - b_f(\boldsymbol{\phi}_{f,h}, \partial_t \chi_{fp}) \\
&\quad - \alpha b_p(\partial_t \boldsymbol{\phi}_{s,h}, \partial_t \chi_{pp}) + \alpha b_p(\partial_t \boldsymbol{\chi}_s, \partial_t \phi_{pp,h}) - \langle \boldsymbol{\phi}_{f,h} \cdot \mathbf{n}_f + \partial_t \boldsymbol{\phi}_{s,h} \cdot \mathbf{n}_p, \partial_t \chi_\lambda \rangle_{\Gamma_{fp}} \\
&\leq \epsilon \left(\|\boldsymbol{\phi}_{f,h}\|^2_{H^1(\Omega_f)} + \|\boldsymbol{\phi}_{p,h}\|^2_{L^2(\Omega_p)} + \|\partial_t \boldsymbol{\phi}_{s,h}\|^2_{H^1(\Omega_p)} + \left|\boldsymbol{\phi}_{f,h} - \partial_t \boldsymbol{\phi}_{s,h}\right|^2_{a_{BJS}} \right) \\
&+ C \left(\|\partial_t \boldsymbol{\chi}_f\|^2_{H^1(\Omega_f)} + \|\partial_t \boldsymbol{\chi}_p\|^2_{L^2(\Omega_p)} + \|\partial_t \boldsymbol{\chi}_s\|^2_{H^1(\Omega_p)} + \|\partial_{tt} \boldsymbol{\chi}_s\|^2_{H^1(\Omega_p)} \right. \\
&\left. -\alpha b_p(\partial_t \boldsymbol{\phi}_{s,h}, \partial_t \chi_{pp}) + \|\partial_t \chi_{pp}\|^2_{L^2(\Omega_p)} + \|\partial_t \chi_\lambda\|^2_{L^2(\Gamma_{fp})} \right). \qquad (4.3.6)
\end{aligned}$$

We combine (4.3.5)–(4.3.6) and integrate the result in time from 0 to an arbitrary $t \in (0, T]$:

$$a_f(\boldsymbol{\phi}_{f,h}(t), \boldsymbol{\phi}_{f,h}(t)) + a_p^d(\boldsymbol{\phi}_{p,h}(t), \boldsymbol{\phi}_{p,h}(t)) + \left|\boldsymbol{\phi}_{f,h}(t) - \partial_t \boldsymbol{\phi}_{s,h}(t)\right|^2_{a_{BJS}}$$

$$
\begin{aligned}
&+\int_0^t \left(a_p^e(\partial_t \boldsymbol{\phi}_{s,h}, \partial_t \boldsymbol{\phi}_{s,h}) + s_0 \|\partial_t \phi_{pp,h}\|^2_{L^2(\Omega_p)}\right) ds \\
&\leq a_f(\boldsymbol{\phi}_{f,h}(0), \boldsymbol{\phi}_{f,h}(0)) + a_p^d(\boldsymbol{\phi}_{p,h}(0), \boldsymbol{\phi}_{p,h}(0)) + \left|\boldsymbol{\phi}_{f,h}(0) - \partial_t \boldsymbol{\phi}_{s,h}(0)\right|^2_{a_{BJS}} \\
&+\epsilon \int_0^t \left(\|\boldsymbol{\phi}_{f,h}\|^2_{H^1(\Omega_f)} + \|\boldsymbol{\phi}_{p,h}\|^2_{L^2(\Omega_p)} + \|\partial_t \boldsymbol{\phi}_{s,h}\|^2_{H^1(\Omega_p)} + \left|\boldsymbol{\phi}_{f,h} - \partial_t \boldsymbol{\phi}_{s,h}\right|^2_{a_{BJS}}\right) ds \\
&+C \int_0^t \Big(\|\partial_t \boldsymbol{\chi}_f\|^2_{H^1(\Omega_f)} + \|\partial_t \boldsymbol{\chi}_p\|^2_{L^2(\Omega_p)} + \|\partial_t \boldsymbol{\chi}_s\|^2_{H^1(\Omega_p)} + \|\partial_{tt} \boldsymbol{\chi}_s\|^2_{H^1(\Omega_p)} + \|\partial_t \chi_{fp}\|^2_{L^2(\Omega_f)} \\
&+\|\partial_t \chi_{pp}\|^2_{L^2(\Omega_p)} + \|\partial_t \chi_\lambda\|^2_{L^2(\Gamma_{fp})} + \alpha b_p(\partial_t \boldsymbol{\chi}_s, \partial_t \phi_{pp,h}) + b_f(\boldsymbol{\chi}_f, \partial_t \phi_{fp,h})\Big) ds. \qquad (4.3.7)
\end{aligned}
$$

Using integration by parts, we get

$$
\begin{aligned}
\int_0^t \left(\alpha b_p(\partial_t \boldsymbol{\chi}_s, \partial_t \phi_{pp,h}) + b_f(\boldsymbol{\chi}_f, \partial_t \phi_{fp,h})\right) ds &= \alpha b_p(\partial_t \boldsymbol{\chi}_s(t), \phi_{pp,h}(t)) - \alpha b_p(\partial_t \boldsymbol{\chi}_s(0), \phi_{pp,h}(0)) \\
+b_f(\boldsymbol{\chi}_f(t), \phi_{fp,h}(t)) - b_f(\boldsymbol{\chi}_f(0), \phi_{fp,h}(0)) &- \int_0^t \left(\alpha b_p(\partial_{tt} \boldsymbol{\chi}_{s,h}, \phi_{pp}) + b_f(\partial_t \boldsymbol{\chi}_f, \phi_{fp,h})\right) ds \\
&\leq \epsilon \left(\|\phi_{pp}(t)\|^2_{L^2(\Omega_p)} + \|\phi_{fp}(t)\|^2_{L^2(\Omega_f)} + \int_0^t \left(\|\phi_{pp}\|^2_{L^2(\Omega_p)} + \|\phi_{fp}\|^2_{L^2(\Omega_f)}\right) ds\right) \\
+C \Big(\|\phi_{pp}(0)\|^2_{L^2(\Omega_p)} + \|\phi_{fp}(0)\|^2_{L^2(\Omega_f)} + \|\partial_t \boldsymbol{\chi}_s(t)\|^2_{H^1(\Omega_p)} + \|\boldsymbol{\chi}_f(t)\|^2_{H^1(\Omega_f)} + \|\partial_t \boldsymbol{\chi}_s(0)\|^2_{H^1(\Omega_p)} & \\
+\|\boldsymbol{\chi}_f(0)\|^2_{H^1(\Omega_f)} + \int_0^t \left(\|\partial_{tt} \boldsymbol{\chi}_s\|^2_{H^1(\Omega_p)} + \|\partial_t \boldsymbol{\chi}_f\|^2_{H^1(\Omega_f)}\right) ds\Big) &
\end{aligned} \qquad (4.3.8)
$$

We assume that at the initial moment $t = 0$ both the medium and the fluid are at rest, i.e., $\mathbf{u}_f(0) = \mathbf{u}_p(0) = \partial_t \boldsymbol{\eta}(0) = 0$ with constant $p_f(0)$ and $p_p(0)$, which implies

$$
\begin{aligned}
\|\boldsymbol{\phi}_{f,h}(0)\|^2_{H^1(\Omega_f)} + \|\boldsymbol{\phi}_{p,h}(0)\|^2_{L^2(\Omega_p)} + \left|\boldsymbol{\phi}_{f,h}(0) - \partial_t \boldsymbol{\phi}_{s,h}(0)\right|^2_{a_{BJS}} + \|\partial_t \boldsymbol{\chi}_s(0)\|^2_{H^1(\Omega_p)} & \\
+\|\boldsymbol{\chi}_f(0)\|^2_{H^1(\Omega_f)} + \|\phi_{pp}(0)\|^2_{L^2(\Omega_p)} + \|\phi_{fp}(0)\|^2_{L^2(\Omega_f)} = 0. \qquad (4.3.9)
\end{aligned}
$$

We use coercivity of bilinear forms $a_f(\cdot,\cdot)$, $a_p^d(\cdot,\cdot)$ and $a_p^e(\cdot,\cdot)$ and choose ϵ small enough to obtain:

$$
\begin{aligned}
&\|\boldsymbol{\phi}_{f,h}(t)\|^2_{H^1(\Omega_f)} + \|\boldsymbol{\phi}_{p,h}(t)\|^2_{L^2(\Omega_p)} + \left|\boldsymbol{\phi}_{f,h}(t) - \partial_t \boldsymbol{\phi}_{s,h}(t)\right|^2_{a_{BJS}} \\
&+\int_0^t \left(\|\partial_t \boldsymbol{\phi}_{s,h}, \partial_t \boldsymbol{\phi}_{s,h}\|^2_{H^1(\Omega_p)} + s_0 \|\partial_t \phi_{pp,h}\|^2_{L^2(\Omega_p)}\right) ds \\
&\leq \epsilon \int_0^t \left(\|\boldsymbol{\phi}_{f,h}\|^2_{H^1(\Omega_f)} + \|\boldsymbol{\phi}_{p,h}\|^2_{L^2(\Omega_p)} + \left|\boldsymbol{\phi}_{f,h} - \partial_t \boldsymbol{\phi}_{s,h}\right|^2_{a_{BJS}} + \|\phi_{fp,h}\|^2_{L^2(\Omega_f)} + \|\phi_{pp,h}\|^2_{L^2(\Omega_p)}\right) ds
\end{aligned}
$$

$$+\epsilon(\|\phi_{pp,h}(t)\|^2_{L^2(\Omega_p)}+\|\phi_{fp,h}(t)\|^2_{L^2(\Omega_f)})+C\int_0^t\Big(\|\partial_t\boldsymbol{\chi}_f\|^2_{H^1(\Omega_f)}+\|\partial_t\boldsymbol{\chi}_p\|^2_{L^2(\Omega_p)}+\|\partial_t\boldsymbol{\chi}_s\|^2_{H^1(\Omega_p)}$$
$$+\|\partial_{tt}\boldsymbol{\chi}_s\|^2_{H^1(\Omega_p)}+\|\partial_t\chi_{fp}\|^2_{L^2(\Omega_f)}+\|\partial_t\chi_{pp}\|^2_{L^2(\Omega_p)}+\|\partial_t\chi_\lambda\|^2_{L^2(\Gamma_{fp})}\Big)\,ds$$
$$+C\left(\|\partial_t\boldsymbol{\chi}_s(t)\|^2_{H^1(\Omega_p)}+\|\boldsymbol{\chi}_f(t)\|^2_{H^1(\Omega_f)}\right). \tag{4.3.10}$$

Next, we use the inf-sup condition (2.2.9) with the choice $(w_h,\mu_h)=((\phi_{fp,h},\phi_{pp,h}),\phi_{\lambda,h})$ and the error equation obtained by subtracting (2.2.1) from (2.1.11):

$$\|((\phi_{fp,h},\phi_{pp,h}),\phi_{\lambda,h})\|_{W\times\Lambda_h}$$
$$\le C\sup_{(\mathbf{v}_h,\boldsymbol{\xi}_{p,h})\in\mathbf{V}_h\times\mathbf{X}_{p,h}}\frac{b_f(\mathbf{v}_{f,h},\phi_{fp,h})+b_p(\mathbf{v}_{p,h},\phi_{pp,h})+\alpha b_p(\boldsymbol{\xi}_{p,h},\phi_{pp,h})+b_\Gamma(\mathbf{v}_{f,h},\mathbf{v}_{p,h},\boldsymbol{\xi}_{p,h};\phi_{\lambda,h})}{\|(\mathbf{v}_h,\boldsymbol{\xi}_{p,h})\|_{\mathbf{V}\times\mathbf{X}_p}}$$
$$=\sup_{(\mathbf{v}_h,\boldsymbol{\xi}_{p,h})\in\mathbf{V}_h\times\mathbf{X}_{p,h}}\Bigg(\frac{-a_f(\mathbf{e}_f,\mathbf{v}_{f,h})-a^d_p(\mathbf{e}_p,\mathbf{v}_{p,h})-a^e_p(\mathbf{e}_s,\boldsymbol{\xi}_{p,h})-a_{BJS}(\mathbf{e}_f,\partial_t\mathbf{e}_s;\mathbf{v}_{f,h},\boldsymbol{\xi}_{p,h})}{\|(\mathbf{v}_h,\boldsymbol{\xi}_{p,h})\|_{\mathbf{V}\times\mathbf{X}_p}}$$
$$+\frac{-b_f(\mathbf{v}_{f,h},\chi_{fp})-b_p(\mathbf{v}_{p,h},\chi_{pp})-\alpha b_p(\boldsymbol{\xi}_{p,h},\chi_{pp})-b_\Gamma(\mathbf{v}_{f,h},\mathbf{v}_{p,h},\boldsymbol{\xi}_{p,h};\chi_\lambda)}{\|(\mathbf{v}_h,\boldsymbol{\xi}_{p,h})\|_{\mathbf{V}\times\mathbf{X}_p}}\Bigg).$$

We have $b_p(\mathbf{v}_{p,h},\chi_{pp})=\langle\mathbf{v}_{p,h}\cdot\mathbf{n}_p,\chi_\lambda\rangle_{\Gamma_{fp}}=0$. Then, using the continuity of the bilinear forms and the trace inequality, we get

$$\epsilon(\|\phi_{fp,h}\|^2_{L^\infty(0,t;L^2(\Omega_f))}+\|\phi_{pp,h}\|^2_{L^\infty(0,t;L^2(\Omega_p))}+\|\phi_{\lambda,h}\|^2_{L^\infty(0,t;L^2(\Gamma_{fp}))})$$
$$\le C\epsilon\Big(\|\boldsymbol{\phi}_{f,h}\|^2_{L^\infty(0,t;H^1(\Omega_f))}+\|\boldsymbol{\phi}_{p,h}\|^2_{L^\infty(0,t;L^2(\Omega_p))}+\|\boldsymbol{\phi}_{s,h}\|^2_{L^\infty(0,t;H^1(\Omega_p))}+\big|\boldsymbol{\phi}_{f,h}-\partial_t\boldsymbol{\phi}_{s,h}\big|^2_{L^\infty(0,t;a_{BJS})}$$
$$+\|\boldsymbol{\chi}_f\|^2_{L^\infty(0,t;H^1(\Omega_f))}+\|\boldsymbol{\chi}_p\|^2_{L^\infty(0,t;L^2(\Omega_p))}+\|\boldsymbol{\chi}_s\|^2_{L^\infty(0,t;H^1(\Omega_p))}+\|\partial_t\boldsymbol{\chi}_s\|^2_{L^\infty(0,t;H^1(\Omega_p))}$$
$$+\|\chi_{fp}\|^2_{L^\infty(0,t;L^2(\Omega_f))}+\|\chi_{pp}\|^2_{L^\infty(0,t;L^2(\Omega_p))}+\|\chi_\lambda\|_{L^\infty(0,t;L^2(\Gamma_{fp}))}\Big). \tag{4.3.11}$$

It follows from (4.3.10), (4.3.11) and Lemma 2.2.3 that

$$\|\mathbf{u}_f-\mathbf{u}_{f,h}\|_{L^\infty(0,T;H^1(\Omega_f))}+\|\mathbf{u}_p-\mathbf{u}_{p,h}\|_{L^\infty(0,T;L^2(\Omega_p))}$$
$$\le C\sqrt{\exp(T)}\Big[h^{k_f}\left(\|\mathbf{u}_f\|_{L^2(0,T;H^{k_f+1}(\Omega_f))}+\|\mathbf{u}_f\|_{L^\infty(0,T;H^{k_f+1}(\Omega_f))}+\|\partial_t\mathbf{u}_f\|_{L^2(0,T;H^{k_f+1}(\Omega_f))}\right)$$
$$+h^{s_f+1}\left(\|p_f\|_{L^2(0,T;H^{s_f+1}(\Omega_f))}+\|p_f\|_{L^\infty(0,T;H^{s_f+1}(\Omega_f))}+\|\partial_t p_f\|_{L^2(0,T;H^{s_f+1}(\Omega_f))}\right)$$
$$+h^{k_p+1}\Big(\|\mathbf{u}_p\|_{L^2(0,T;H^{k_p+1}(\Omega_p))}+\|\mathbf{u}_p\|_{L^\infty(0,T;H^{k_p+1}(\Omega_p))}+\|\partial_t\mathbf{u}_p\|_{L^2(0,T;H^{k_p+1}(\Omega_p))}$$
$$+\|\lambda\|_{L^2(0,T;H^{k_p+1}(\Gamma_{fp}))}+\|\lambda\|_{L^\infty(0,T;H^{k_p+1}(\Gamma_{fp}))}+\|\partial_t\lambda\|_{L^2(0,T;H^{k_p+1}(\Gamma_{fp}))}\Big)$$
$$+h^{s_p+1}\left(\|p_p\|_{L^\infty(0,T;H^{s_p+1}(\Omega_p))}+\|p_p\|_{L^2(0,T;H^{s_p+1}(\Omega_p))}+\|\partial_t p_p\|_{L^2(0,T;H^{s_p+1}(\Omega_p))}\right)$$

$$+ h^{k_s} \Big(\|\boldsymbol{\eta}_p\|_{L^\infty(0,T;H^{k_s+1}(\Omega_p))} + \|\boldsymbol{\eta}_p\|_{L^2(0,T;H^{k_s+1}(\Omega_p))} + \|\partial_t \boldsymbol{\eta}_p\|_{L^2(0,T;H^{k_s+1}(\Omega_p))} \\ + \|\partial_t \boldsymbol{\eta}_p\|_{L^\infty(0,T;H^{k_s+1}(\Omega_p))} + \|\partial_{tt} \boldsymbol{\eta}_p\|_{L^2(0,T;H^{k_s+1}(\Omega_p))} \Big) \Big],$$

which implies (4.3.1). □

Lemma 4.3.2. *Under the assumptions of Lemma 4.3.1, there exists a positive constant* $M = M(\mathbf{u}_f, p_f, \mathbf{u}_p, p_p, \boldsymbol{\eta}_p, \lambda)$, *such that the solution* $\mathbf{u}_h$ *of* (2.2.1)–(2.2.3) *satisfies*

$$\|\mathbf{u}_h\|_{L^\infty(0,T;L^\infty(\Omega))} \leq M(h^{k_p+1-d/2} + h^{s_p+1-d/2}). \tag{4.3.12}$$

Proof. We recall that by definition

$$\mathbf{u}_h = \begin{cases} \mathbf{u}_{f,h} & \text{in } \Omega_f, \\ \mathbf{u}_{p,h} & \text{in } \Omega_p. \end{cases}$$

Therefore, we prove (4.3.12) separately for $\mathbf{u}_{f,h}$ in the fluid domain and for $\mathbf{u}_{p,h}$ in the solid domain. Let $S_{f,h}$ be the Scott-Zhang interpolant onto $\mathbf{V}_{f,h}$ [86], satisfying

$$\|S_{f,h}\mathbf{v}_f\|_{L^\infty(\Omega_f)} \leq C(\|\mathbf{v}_f\|_{L^\infty(\Omega_f)} + h\|\nabla \mathbf{v}_f\|_{L^\infty(\Omega_f)}), \qquad \forall \mathbf{v}_f \in W^{1,\infty}(\Omega_f), \tag{4.3.13}$$

$$\|\mathbf{v}_f - S_{f,h}\mathbf{v}_f\|_{L^2(\Omega_f)} + h|\mathbf{v}_f - S_{f,h}\mathbf{v}_f|_{H^1(\Omega_f)} \leq Ch^{k_f+1}\|\mathbf{v}_f\|_{H^{k_f+1}(\Omega_f)}, \quad \forall \mathbf{v}_f \in H^{k_f+1}(\Omega_f). \tag{4.3.14}$$

We further write

$$\|\mathbf{u}_{f,h}\|_{L^\infty(0,T;L^\infty(\Omega_f))} \leq \|\mathbf{u}_{f,h} - S_{f,h}\mathbf{u}_f\|_{L^\infty(0,T;L^\infty(\Omega_f))} + \|S_{f,h}\mathbf{u}_f\|_{L^\infty(0,T;L^\infty(\Omega_f))}. \tag{4.3.15}$$

To obtain a bound on $\|\mathbf{u}_{f,h} - S_{f,h}\mathbf{u}_f\|_{L^\infty(0,T;L^\infty(\Omega_f))}$, we recall that the Jacobian matrix of the finite element mapping and its determinant satisfy

$$\|J_E\|_{L^\infty(\hat{E})} \sim h^d, \quad \|DF_E\|_{L^\infty(\hat{E})} \sim h, \quad \forall E \in \mathcal{T}_h^f. \tag{4.3.16}$$

Therefore, since the space $\mathbf{V}_{f,h}$ is defined through the change of variables, we get for any $E \in \mathcal{T}_h^f$

$$\|\mathbf{u}_{f,h} - S_{f,h}\mathbf{u}_f\|_{L^\infty(E)} \leq \|\hat{\mathbf{u}}_{f,h} - \hat{S}_{f,h}\hat{\mathbf{u}}_f\|_{L^\infty(\hat{E})} \leq \|\hat{\mathbf{u}}_{f,h} - \hat{S}_{f,h}\hat{\mathbf{u}}_f\|_{H^1(\hat{E})}$$

$$\leq Ch^{1-d/2}\|\mathbf{u}_{f,h} - S_{f,h}\mathbf{u}_f\|_{H^1(E)} \leq Ch^{1-d/2}\|\mathbf{u}_{f,h} - \mathbf{u}_f\|_{H^1(E)} + Ch^{1-d/2}\|\mathbf{u}_f - S_{f,h}\mathbf{u}_f\|_{H^1(E)}. \tag{4.3.17}$$

Combining (4.3.15), (4.3.13), (4.3.14), (4.3.17) and (4.3.1), we obtain

$$\begin{aligned}\|\mathbf{u}_{f,h}\|_{L^\infty(0,T;L^\infty(\Omega_f))} &\leq C(\|\mathbf{u}_f\|_{L^\infty(0,T;L^\infty(\Omega_f))} + h\|\nabla\mathbf{u}_f\|_{L^\infty(0,T;L^\infty(\Omega_f))}) \\ &+ Ch^{1-d/2+k_f}\|\mathbf{u}_f\|_{L^\infty(0,T;H^{k_f+1}(\Omega_f))} + C\sqrt{\exp(T)}h^{\min\{k_f,\, s_f+1,\, k_p+1,\, s_p+1,\, k_s\}} \leq M_1,\end{aligned} \tag{4.3.18}$$

where $M_1 = M_1(\mathbf{u}_f,\, p_f,\, \mathbf{u}_p,\, p_p,\, \boldsymbol{\eta}_p,\, \lambda)$.

Next we consider the MFE interpolant $\Pi_{p,h}$ onto $\mathbf{V}_{p,h}$ that satisfies [1]

$$\|\Pi\mathbf{v}_p\|_{L^\infty(\Omega_p)} \leq C\left(\|\mathbf{v}_p\|_{L^\infty(\Omega_p)} + h\|\nabla\mathbf{v}_p\|_{L^\infty(\Omega_p)}\right), \qquad \forall\mathbf{v}_p \in W^{1,\infty}(\Omega_p), \tag{4.3.19}$$

$$\|\mathbf{v}_p - \Pi_{p,h}\mathbf{v}_p\|_{L^2(\Omega_p)} \leq Ch^{k_p+1}\|\mathbf{v}_p\|_{H^{k_p+1}(\Omega_p)}, \qquad \forall\mathbf{v}_p \in H^{k_p+1}(\Omega_p). \tag{4.3.20}$$

As in (4.3.15), we split the norm of $\mathbf{u}_p$ into two parts

$$\|\mathbf{u}_{p,h}\|_{L^\infty(0,T;L^\infty(\Omega_p))} \leq \|\mathbf{u}_{p,h} - \Pi\mathbf{u}_p\|_{L^\infty(0,T;L^\infty(\Omega_p))} + \|\Pi\mathbf{u}_p\|_{L^\infty(0,T;L^\infty(\Omega_p))}, \tag{4.3.21}$$

where the first term on the right-hand side can be bounded element-wise, using (4.3.16) and the fact that the space $\mathbf{V}_{p,h}$ is constructed using the Piola transformation,

$$\begin{aligned}\|\mathbf{u}_{p,h} - \Pi_{p,h}\mathbf{u}_p\|_{L^\infty(E)} &\leq h^{1-d}\|\hat{\mathbf{u}}_{p,h} - \hat{\Pi}_{p,h}\hat{\mathbf{u}}_p\|_{L^\infty(\hat{E})} \leq h^{1-d}\|\hat{\mathbf{u}}_{p,h} - \hat{\Pi}_{p,h}\hat{\mathbf{u}}_p\|_{L^2(\hat{E})} \\ \leq Ch^{-d/2}\|\mathbf{u}_{p,h} - \Pi_{p,h}\mathbf{u}_f\|_{L^2(E)} &\leq Ch^{-d/2}\|\mathbf{u}_{p,h} - \mathbf{u}_p\|_{L^2(E)} + Ch^{-d/2}\|\mathbf{u}_p - \Pi_{p,h}\mathbf{u}_p\|_{L^2(E)}.\end{aligned} \tag{4.3.22}$$

Combining (4.3.21), (4.3.19), (4.3.20), (4.3.22) and (4.3.1), we obtain

$$\begin{aligned}\|\mathbf{u}_{p,h}\|_{L^\infty(0,T;L^\infty(\Omega_p))} &\leq C(\|\mathbf{u}_p\|_{L^\infty(0,T;L^\infty(\Omega_p))} + h\|\nabla\mathbf{u}_p\|_{L^\infty(0,T;L^\infty(\Omega_p))}) \\ &+Ch^{-d/2+k_p+1}\|\mathbf{u}_p\|_{L^\infty(0,T;H^{k_p+1}(\Omega_p))} + C\sqrt{\exp(T)}h^{-d/2}h^{\min\{k_f,\, s_f+1,\, k_p+1,\, s_p+1,\, k_s\}} \\ &\leq M_2(h^{k_p+1-d/2} + h^{s_p+1-d/2}),\end{aligned} \tag{4.3.23}$$

where $M_2 = M_2(\mathbf{u}_f,\, p_f,\, \mathbf{u}_p,\, p_p,\, \boldsymbol{\eta}_p,\, \lambda)$.

The final result (4.3.12) follows from combining (4.3.18) and (4.3.23). □

Remark 4.3.1. *The estimate* (4.3.12) *implies that* $\|\mathbf{u}_h\|_{L^2(0,T;L^\infty(\Omega))} \leq M$ *when* $d = 2$ *for any choice of stable spaces for the flow problem and when* $d = 3$ *with* $k_p \geq 1$, $s_p \geq 1$. *In the lowest order case,* $k_p = s_p = 0$ *in three dimensions,* $\|\mathbf{u}_h\|_{L^2(0,T;L^\infty(\Omega))} \leq Mh^{-1/2}$. *For the rest of the paper we will restrict* $k_p \geq 1$, $s_p \geq 1$ *in case* $d = 3$.

We state several properties of dispersion/diffusion tensor, which are needed to derive the stability and error estimates for the transport problem. For the proof of Lemmas 4.3.3 - 4.3.4, the reader is referred to [92].

Lemma 4.3.3. *Let* $\mathbf{D}(\mathbf{u})$ *defined as in equation* (4.1.2), *where,* $d_m(x) \geq 0, \alpha_l(x) \geq 0$ *and* $\alpha_t(x) \geq 0$ *are nonnegative functions of* $x \in \Omega$. *Then*

$$\mathbf{D}(\mathbf{u})\nabla c \cdot \nabla c \geq (d_m + \min(\alpha_l, \alpha_t)|\mathbf{u}|)|\nabla c|^2. \tag{4.3.24}$$

In particular, if $d_m(x) \geq d_{m,*} > 0$ *uniformly in the domain* Ω, *then* $\mathbf{D}(\mathbf{u})$ *is uniformly positive definite and for all* $\mathbf{x} \in \Omega$, *we have,*

$$\mathbf{D}(\mathbf{u})\nabla c \cdot \nabla c \geq d_{m,*}|\nabla c|^2. \tag{4.3.25}$$

Lemma 4.3.4. *Let* $\mathbf{D}(\mathbf{u})$ *be defined as in equation* (4.1.2), *where,* $d_m(x) \geq 0, \alpha_l(x) \geq 0$ *and* $\alpha_t(x) \geq 0$ *are nonnegative functions of* $x \in \Omega$, *and the dispersivities* α_l *and* α_t *are uniformly bounded, i.e.* $\alpha_l(x) \leq \alpha_l^*$ *and* $\alpha_t(x) \leq \alpha_t^*$.
Then

$$\|\mathbf{D}(\mathbf{u}) - \mathbf{D}(\mathbf{v})\|_{L^2(\Omega)} \leq k_D\|\mathbf{u} - \mathbf{v}\|_{L^2(\Omega)} \tag{4.3.26}$$

where, $k_D = (4\alpha_t^* + 3\alpha_l^*)d^{3/2}$ *is a fixed number (*$d = 2$ *or* 3 *is the dimension of domain* Ω.*)*

With the solution of the flow problem satisfying (4.3.12) and the uniformly positive definite dispersion tensor (4.3.25), we can prove the following Gårding's inequality for the bilinear form $B_{\mathbf{u}_h}(\cdot,\cdot)$.

Lemma 4.3.5. *The bilinear form* $B_{\mathbf{u}_h}(\cdot,\cdot)$ *defined as in* (4.2.3), *satisfies*

$$B_{\mathbf{u}_h}(\psi_h, \psi_h) \geq C\left(|||\nabla\psi_h|||_{0,\Omega}^2 - |||\psi_h|||_{0,\Omega}^2\right), \qquad \forall \psi_h \in \mathcal{D}_f(\mathcal{T}_h). \tag{4.3.27}$$

Proof. For any $\psi_h \in \mathcal{D}_f(\mathcal{T}_h)$ we have

$$\begin{aligned} B_{\mathbf{u}_h}(\psi_h,\psi_h) &= \sum_{E\in\mathcal{T}_h}\int_E (\mathbf{D}(\mathbf{u}_h)\nabla\psi_h - \psi_h\mathbf{u}_h)\cdot\nabla\psi_h - \sum_{e\in E_h}\int_e \{\mathbf{D}(\mathbf{u}_h)\nabla\psi_h\cdot\mathbf{n}_e\}[\psi_h] \\ &+ \sum_{e\in E_h}\int_e \{\mathbf{D}(\mathbf{u}_h)\nabla\psi_h\cdot\mathbf{n}_e\}[\psi_h] + \sum_{e\in E_h}\int_e \psi_h^*\mathbf{u}_h\cdot\mathbf{n}_e[\psi_h] \\ &+ \sum_{e\in E_h^{out}}\int_e \psi_h\mathbf{u}_h\cdot\mathbf{n}_e\psi_h - \int_\Omega \psi_h q^-\psi_h + J_0^{\sigma,\beta}(\psi_h,\psi_h). \end{aligned} \tag{4.3.28}$$

Next we introduce the following notations

$$\begin{aligned} J_1 &:= \sum_{E\in\mathcal{T}_h}\int_E (\mathbf{D}(\mathbf{u}_h)\nabla\psi_h - \psi_h\mathbf{u}_h)\cdot\nabla\psi_h, \quad J_2 := \sum_{e\in E_h}\int_e \psi_h^*[\psi_h]\mathbf{u}_h\cdot\mathbf{n}_e, \\ J_3 &:= \sum_{e\in E_h^{out}}\int_e \psi_h^2\mathbf{u}_h\cdot\mathbf{n}_e - \int_\Omega q^-\psi_h^2 + J_0^{\sigma,\beta}(\psi_h,\psi_h) \end{aligned} \tag{4.3.29}$$

With (4.3.29), we can rewrite (4.3.28) as

$$B_{\mathbf{u}_h}(\psi_h,\psi_h) = J_1 + J_2 + J_3. \tag{4.3.30}$$

Using (4.3.12), Remark 4.3.1 and (4.3.25), we bound J_1 term as follows

$$\begin{aligned} J_1 &= \sum_{E\in\mathcal{T}_h}\int_E \mathbf{D}(\mathbf{u}_h)\nabla\psi_h\cdot\nabla\psi_h - \sum_{E\in\mathcal{T}_h}\int_E \psi_h\mathbf{u}_h\cdot\nabla\psi_h \geq d_{m,*}|||\nabla\psi_h|||_{0,\Omega}^2 \\ &- M\sum_{E\in\mathcal{T}_h}\|\psi_h\|_{L^2(E)}\|\nabla\psi_h\|_{L^2(E)} \geq d_{m,*}|||\nabla\psi_h|||_{0,\Omega}^2 - C\epsilon^{-1}|||\psi_h|||_{0,\Omega}^2 - \epsilon|||\nabla\psi_h|||_{0,\Omega}^2. \end{aligned} \tag{4.3.31}$$

For the second term we have:

$$\begin{aligned} J_2 &= \sum_{e\in E_h}\int_e \psi_h^*[\psi_h]\mathbf{u}_h\cdot\mathbf{n}_e \geq -M\left|\sum_{e\in E_h}\int_e \psi_h^*[\psi_h]\right| \geq -M\sum_{e\in E_h}\|\psi_h^*\|_{L^2(e)}\|[\psi_h]\|_{L^2(e)} \\ &\geq -\sum_{e\in E_h}\left(\frac{\epsilon\sigma_e}{h_e^\beta}\|[\psi_h]\|_{L^2(e)}^2 + \frac{Ch_e^\beta}{\epsilon}\|\psi_h^*\|_{L^2(e)}^2\right) \geq -\epsilon J^{\sigma,\beta}(\psi_h,\psi_h) - \frac{Ch^\beta}{\epsilon}\sum_{E\in\mathcal{T}_h} h^{-1}\|\psi_h\|_{L^2(E)}^2 \\ &\geq -\epsilon J^{\sigma,\beta}(\psi_h,\psi_h) - C\epsilon^{-1}|||\psi_h|||_{0,\Omega}, \end{aligned} \tag{4.3.32}$$

provided β is chosen in such a way that $h^{\beta-1} \leq C$.

We rewrite J_3, using (4.2.5) and the definitions of q^-, Γ_{in} and Γ_{out}:

$$J_3 := \sum_{e\in E_h^{out}} \int_e \psi_h^2 \mathbf{u}_h \cdot \mathbf{n}_e - \int_\Omega q^- \psi_h^2 + J_0^{\sigma,\beta}(\psi_h,\psi_h) \geq J_0^{\sigma,\beta}(\psi_h,\psi_h). \tag{4.3.33}$$

Finally, we combine (4.3.30)-(4.3.33):

$$B_{\mathbf{u}_h}(\psi_h,\psi_h) \geq (d_{m,*}-\epsilon)|||\nabla\psi_h|||_{0,\Omega}^2 - C\epsilon^{-1}|||\psi_h|||_{0,\Omega}^2 + (1-\epsilon)J^{\sigma,\beta}(\psi_h,\psi_h).$$

Choosing ϵ small enough, we obtain

$$B_{\mathbf{u}_h}(\psi_h,\psi_h) \geq C\left(|||\nabla\psi_h|||_{0,\Omega}^2 - |||\psi_h|||_{0,\Omega}^2 + J^{\sigma,\beta}(\psi_h,\psi_h)\right) \geq C\left(|||\nabla\psi_h|||_{0,\Omega}^2 - |||\psi_h|||_{0,\Omega}^2\right),$$

as desired. □

Theorem 4.3.1. *The solution $c_h(t) \in L^\infty(0,T;\mathcal{D}_r(\mathcal{T}_h))$ of (4.2.6) satisfies*

$$\begin{aligned}&\|c_h\|_{L^\infty(0,T;L^2(\Omega))} + |||\nabla c_h|||_{L^2(0,T;H^0(\mathcal{T}_h))} \\ &\qquad \leq C\sqrt{\exp(T)}\left(\|c_h(0)\|_{L^2(\Omega)} + \|c_w q^+\|_{L^2(0,T;L^2(\Omega))} + \|c_{in}\|_{L^2(0,T;L^2(E_h^{int}))}\right).\end{aligned} \tag{4.3.34}$$

Proof. With the choice $\psi_h = c_h$, (4.2.6) reads

$$\int_\Omega \phi c_h \partial_t c_h + B_{\mathbf{u}_h}(c_h,c_h) = L_h(c_h). \tag{4.3.35}$$

Using (4.3.27), (2.2.16) and the definition of L_h, (4.2.3), we obtain

$$\begin{aligned}\phi\frac{1}{2}\partial_t\|c_h\|_{L^2(\Omega)}^2 + C\left(|||\nabla c_h|||_{0,\Omega}^2 - |||c_h|||_{0,\Omega}^2\right) &\leq C\|c_h\|_{L^2(\Omega)}^2 + L_h(c_h) \\ &= C\|c_h\|_{L^2(\Omega)}^2 + \int_\Omega c_w q^+ c_h - \sum_{e\in E_h^{in}}\int_e c_{in}\mathbf{u}_h\cdot\mathbf{n}_e c_h.\end{aligned} \tag{4.3.36}$$

We integrate (4.3.36) in time from $s=0$ to $s=t$ for $0<t\leq T$ and use Cauchy-Schwarz (1.3.2) and Young's (1.3.6) inequalities

$$\begin{aligned}&\|c_h(t)\|_{L^2(\Omega)}^2 + \int_0^t |||\nabla c_h(s)|||_{0,\Omega}^2\,ds \leq C\|c_h(0)\|_{L^2(\Omega)}^2 + C\int_0^t |||c_h(s)|||_{0,\Omega}^2\,ds \\ &+ C\int_0^t\left(\int_\Omega c_w(s)q^+(s)c_h(s) - \sum_{e\in E_h^{in}}\int_e c_{in}(s)c_h(s)\mathbf{u}_h(s)\cdot\mathbf{n}_e\right)ds \leq C\left(\|c_h(0)\|_{L^2(\Omega)}^2\right. \\ &\left.+\int_0^t\|c_h(s)\|_{L^2(\Omega)}^2\,ds + \int_0^t\left[\|c_w(s)q^+(s)\|_{L^2(\Omega)}^2 + \|c_{in}(s)\|_{L^2(E_h^{int})}^2\right]ds\right).\end{aligned} \tag{4.3.37}$$

The final result then follows from (4.3.37) and Gronwall's lemma (1.3.7). □

In the next theorem we state the error estimate for the transport problem (4.2.6). Derivation of the bound follows the steps in Theorem 4.3.1 and the analysis in [92], using the estimate (4.3.12), rather than a boundedness property of the "cut-off" operator. For the sake of space, we omit the proof and the reader is referred to [92] for the details.

Theorem 4.3.2. *Let the assumptions of Lemma (4.3.2) hold and assume that only Neumann boundary condition is imposed for the flow problem. Let further* $c \in L^\infty(0,T;W^{1,\infty}(\Omega)) \cap L^2(0,T;H^{r+1}(\Omega))$ *be the solution of (4.1.1), (4.1.3), (4.1.4)-(4.1.5). Then for any* $h \leq \left(\frac{\sigma_*}{3M}\right)^{1/\beta}$ *there exists a positive constant* C *such that*

$$|||c - c_h|||_{L^\infty(0,T,L^2(\Omega))} + |||\nabla(c - c_h)|||_{L^2(0,T,L^2(\Omega))} \leq C\sqrt{\exp(T)}h^{\min\{k_f,s_f+1,k_p+1,s_p+1,k_s,r\}}. \tag{4.3.38}$$

4.4 NUMERICAL RESULTS

In this section, we present results from several computational experiments in two dimensions. The fully discrete method has been implemented using the finite element package FreeFem++ [59]. The first test confirms the theoretical convergence rates for the problem using an analytical solution, while the rest of the experiments show the applicability of the method to modeling fluid flow in an irregularly shaped fractured reservoir with physical parameters.

4.4.1 Convergence test

In the first example we study the convergence of the spatial discretization using an analytical solution. We build this test case upon the convergence test for the flow problem, described in Section 2.4.1. The total simulation time for this test case is $T = 10^{-3}$s and the time step is $\Delta t = 10^{-4}$s. The time step is sufficiently small, so that the time discretization error does not affect the convergence rates.

The transport solution is chosen such that

$$c = t\left(\cos(\pi x) + \cos(\pi y)\right)/\pi,$$

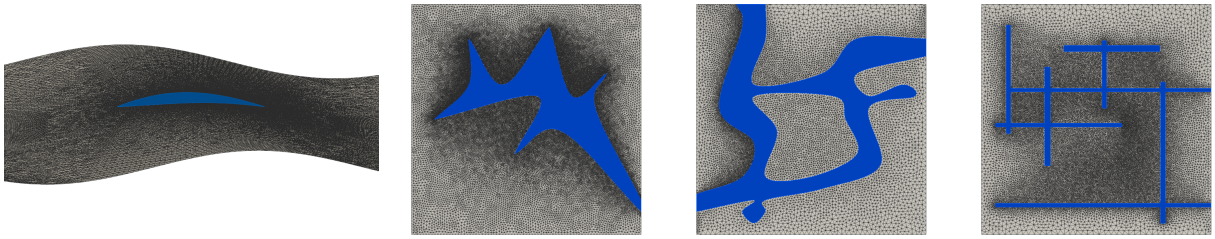

(a) Example 1 (b) Example 2 (c) Example 3 (d) Example 4

Figure 15: Computational domains.

with diffusivity tensor chosen as $\mathbf{D} = 10^{-3}\mathbf{I}$ and effective porosity $\phi = 1$.

We study the convergence with the lowest order choice for the flow problem:the MINI elements $\mathcal{P}_1^b - \mathcal{P}_1$ for Stokes, the Raviart-Thomas $\mathcal{RT}_0 - \mathcal{P}_0$ and continuous Lagrangian $\mathcal{P}_1$ elements for the Biot system, and piecewise constant Lagrange multiplier $\mathcal{P}_0$. The transport problem is further discretized using discontinuous piecewise linears, $\mathcal{P}_1^{dc}$. Theorem 4.3.2 predicts first order of convergence in both L^2 and H^1-type norms of the concentration solution and the computed errors and rates shown in the Table 7, verify this.

$\mathcal{P}_1^b - \mathcal{P}_1$, $\mathcal{RT}_0 - \mathcal{P}_0$, $\mathcal{P}_1$, $\mathcal{P}_0$ and $\mathcal{P}_1^{dc}$				
	$\|\|\|e_c\|\|\|_{l^2(H^1(\Omega))}$		$\|\|\|e_c\|\|\|_{l^\infty(L^2(\Omega))}$	
h	error	rate	error	rate
1/4	2.24E-01	–	2.52E-02	–
1/8	1.14E-01	1.0	6.17E-03	2.0
1/16	5.71E-02	1.0	1.56E-03	2.0
1/32	2.87E-02	1.0	3.96E-04	2.0
1/64	1.44E-02	1.0	1.00E-04	2.0

Table 7: Example 1: relative numerical errors and convergence rates.

4.4.2 Application to coupling of transport with flow through fractured media

4.4.2.1 Example 1: Application to flow through fractured reservoirs This example follows the one from Section 2.4.2, namely it is focused on modeling the interaction between a stationary fracture filled with fluid and the surrounding poroelastic reservoir.

We first introduce the reference domain $\hat{\Omega}$ given by a square $[-1,1]m \times [-1,1]m$. A fracture, representing the reference fluid domain $\hat{\Omega}_f$, is then described by its top and bottom boundaries, as follows

$$\hat{y}^2 = 8^2(\hat{x}-0.35)^2(\hat{x}+0.35)^2, \quad \hat{x} \in [-0.35, 0.35].$$

The physical domain (see Figure 15) is further obtained from the reference one $\hat{\Omega}$ via the smooth mapping of the form

$$\begin{bmatrix} x \\ y \end{bmatrix} = \begin{bmatrix} \hat{x} \\ 8\left(\cos(\frac{\pi\hat{x}+\hat{y}}{100}) + \frac{\hat{y}}{4}\right) \end{bmatrix}.$$

The external boundary of Ω_p is split into $\Gamma_{p,\star}$, where $\star \in \{left, right, top, bottom\}$.

We are interested in the solution on the physical domain Ω. The physical units are meters for length, seconds for time, and KPa for pressure. The boundary conditions are chosen to be

Pressure:	$p_p = 1000$ KPa/s	on Γ_p,
Clamped boundaries:	$\boldsymbol{\eta}_p \cdot \mathbf{n}_p = 0$ m	on Γ_p.

The flow is driven by the injection of the fluid into the fracture with the constant rate $g = 5 \cdot 10^{-3}$ kg/s. The fluid is injected into a region of radius 0.017m in the center of the reference fracture $\hat{\Omega}_f$. The contaminant species are injected in this same region, continuously over the entire simulation period, i.e. $c_w = 1$ in the circular region specified above. Other physical parameters are the same as in the Table 3.

The initial conditions are set accordingly to $\boldsymbol{\eta}_p(0) = 0$ m, $p_p(0) = 10^3$ KPa and initial concentration $c(0) = 0$. The total simulation time is $T = 100$ s with the time step of size $\Delta t = 1$s.

The diffusion tensor is chosen to be $\mathbf{D}_{\Omega_f} = 10^{-6}\mathbf{I}$ in the Stokes region and

$$\mathbf{D}(\mathbf{u}) = d_m\mathbf{I} + |\mathbf{u}|\{\alpha_l\mathbf{E} + \alpha_t(\mathbf{I} - \mathbf{E})\}$$

in poroelastic stucture region, as shown in (4.1.2). For this and all further examples, we choose the molecular diffusion d_m, together with longitudinal and transverse dispersion to be equal to 10^{-4}. The effective porosity was set to be $\phi = 0.4$ for this and forthcoming examples.

This and the following test cases use the Taylor-Hood $\mathcal{P}_2 - \mathcal{P}_1$ [93] elements for the fluid velocity and pressure in the fracture region, the Raviart-Thomas $\mathcal{RT}_1 - \mathcal{P}_1^{dc}$ elements for the Darcy velocity and pressure, the continuous Lagrangian $\mathcal{P}_1$ elements for the displacement, and the $\mathcal{P}_1^{dc}$ elements for the Lagrange multiplier. We use discontinuous piecewise linears $\mathcal{P}_1^{dc}$ for the transport equation.

Figure 16 shows the computed velocity field in the reservoir and fracture at the final time $T = 100$ s. We observe channel-like flow in the fracture region, which concentrates at the tips. There is also noticeable leak-off into the reservoir. Furthermore, Figure 17 shows the solution we obtained for the concentration at various time moments. We see the concentration of interested species propagates in accordance with the velocity field, preferring to move in horizontal directions towards the tips of the fracture. This example demonstrates the ability of the proposed method to handle irregularly shaped domains with a computationally challenging set of parameters.

Qualitatively, the solution of the transport equation agrees with the flow. We see how the interested species tend to propagate in horizontal direction at earlier time steps following the velocity field of the Stokes flow. However, even with small permeability as in this example, the contaminant reaches the outer poroelastic structure, and is further transported/diffused in it.

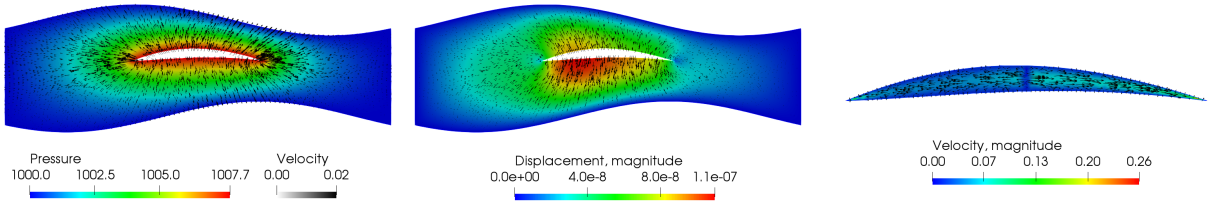

(a) Velocity over pressure (b) Displacement (c) Stokes velocity field

Figure 16: Example 1, computed velocity and pressure fields.

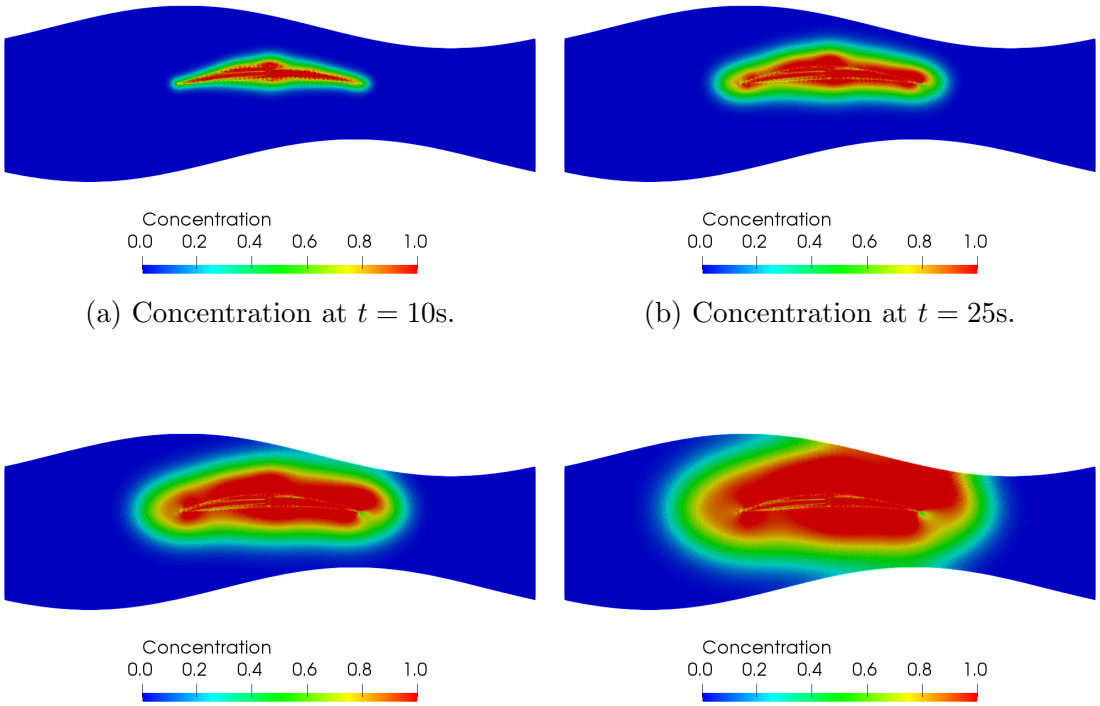

(a) Concentration at $t = 10$s. (b) Concentration at $t = 25$s.

(c) Concentration at $t = 50$s. (d) Concentration at $t = 100$s.

Figure 17: Example 1, computed concentration solution.

4.4.2.2 Example 2: flow through fractured reservoir with heterogeneous permeability

This example continues the idea of the previous test case, while we furthermore illustrate the ability of the method to handle heterogeneous permeability and Youngs modulus. For this simulation we use the domain Ω that is given by the rectangle $[0,1]m \times [-1,1]m$. A fracture, which represents the fluid domain Ω_f is then positioned in the middle of the rectangle, with the boundaries defined by

$$x^2 = 200(0.05 - y)(0.05 + y), \quad y \in [-0.05, 0.05].$$

The same boundary and initial conditions as in the previous test case are specified, and the same physical parameters from Table 3 are used, except for the permeability K, the Youngs modulus E and smaller diffusivity coefficients $d_m = \alpha_l = \alpha_t = 10^{-5}$ which would allow to see the contaminant propagating closer to the regions of higher permeability. The permeability and porosity data is taken from a two-dimensional cross-section of the data provided by the Society of Petroleum Engineers (SPE) Comparative Solution Project 1.

The computed velocity and displacement solution at the last time step are shown in Figure 18a and 18b, respectively. Five snapshots of the concentration solution at various time steps are given in Figure 19. At the early time moments we see how the interested species tend to stay within the channel-like regions of high permeability, with the contaminant following the velocity field and escaping the fracture at the tip and two higher permeable regions near the middle top and bottom of it. At the later times, we see more diffusion occurring in the poroelastic region, however the overall profile of the contaminant front roughly resembles the underlying permeability field.

4.4.2.3 Example 3: irregularly shaped fluid-filled cavity

Our next two examples study the behavior of the method on grids that represent poroelastic media with irregularly shaped fractures filled with free fluid. The boundary conditions are chosen to better represent the physical setting of the experiment, namely

$$\begin{aligned} &\text{Pressure drop:} && p_p = 1 && \text{on } \Gamma_{p,left}, \\ & && p_p = 0 && \text{on } \Gamma_{p,right}, \end{aligned}$$

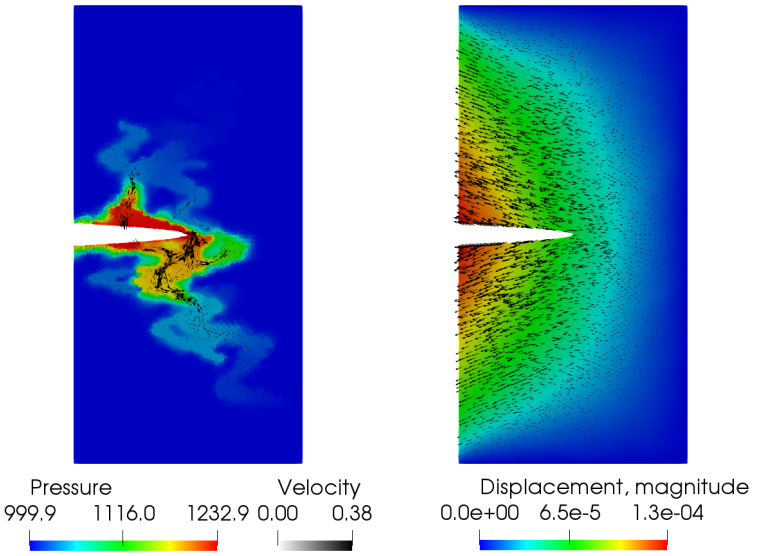

(a) Velocity over pressure (b) Displacement field

Figure 18: Example 6, computed velocity and pressure fields.

No flux:	$\mathbf{u}_p \cdot \mathbf{n}_p = 0$	on $\Gamma_{p,top} \cup \Gamma_{p,bottom}$,
Clamped boundaries:	$\boldsymbol{\eta}_p \cdot \mathbf{n}_p = 0$	on $\Gamma_{p,right}$,
No normal stress:	$\boldsymbol{\sigma}_p \, \mathbf{n}_p = 0$	on $\Gamma_{p,left}$,
No tangential displacement:	$\boldsymbol{\eta}_p \cdot \tau_p = 0$	on $\Gamma_{p,top} \cup \Gamma_{p,bottom}$,
No normal stress:	$(\boldsymbol{\sigma}_f \, \mathbf{n}_f) \cdot \mathbf{n}_f = 0$	on $\Gamma_{f,right}$,
	$\mathbf{u}_f \cdot \tau_f = 0$	on $\Gamma_{f,right}$.

The boundary condition for the transport equation $c_{in} = 1$ along the left boundary $\Gamma_{p,left}$. The physical parameters for this test case are chosen as in the previous example, except for the permeability, which in this case is $K = 10^{-8}\mathbf{I}$. The total simulation time is 10 s, with time step size $\Delta t = 0.1$ s.

The velocity fields in both poroelastic structure and fracture regions are shown in Figures 20a, 20c while the structure displacement can be seen in Figure 20b. Four snapshots of the

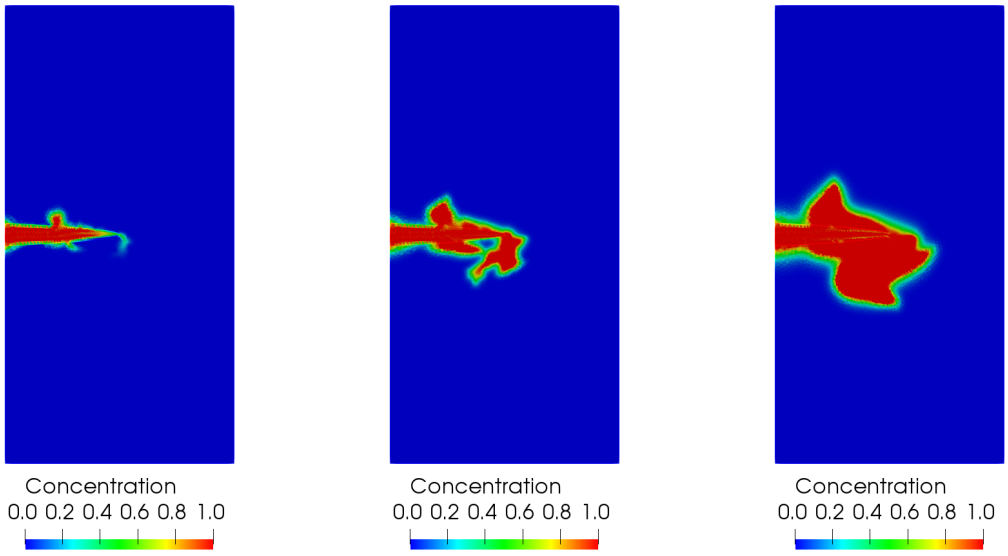

(a) Concentration at $t = 0.5$s. (b) Concentration at $t = 1$s. (c) Concentration at $t = 2.5$s.

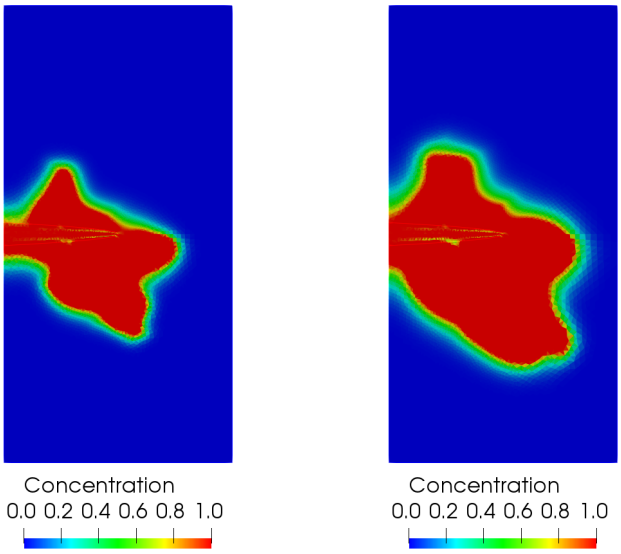

(d) Concentration at $t = 5$s. (e) Concentration at $t = 10$s.

Figure 19: Example 6, computed concentration solution.

concentration solution at different time moments are shown in Figure 21. As one would expect, the contaminant follows the flow, and tends to get into the free fluid region through

the nearest fracture tip. After that, it is transported towards the opening in the right boundary, following the Stokes velocity profile and with little diffusion happening, which agrees with the parameters we set for the transport equation.

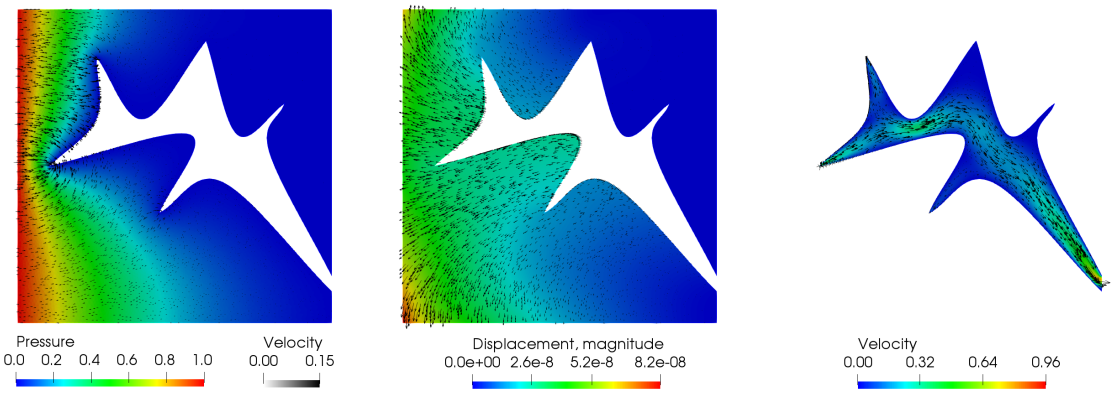

(a) Velocity over pressure (b) Displacement (c) Stokes velocity field

Figure 20: Example 2, computed velocity and pressure fields.

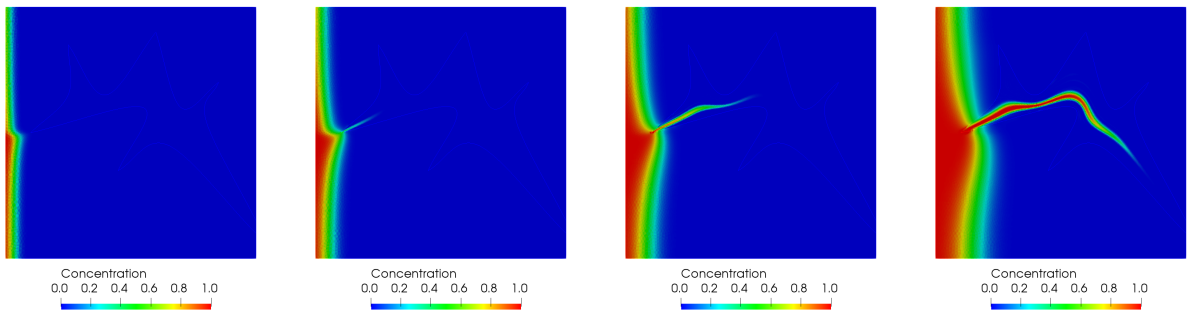

(a) Concentration at $t = 1$s. (b) Concentration at $t = 2.5$s. (c) Concentration at $t = 5$s. (d) Concentration at $t = 10$s.

Figure 21: Example 2, computed concentration solution.

4.4.2.4 Example 4: flow through poroelastic media with channel network This example follows the setup from Example 3, in particular the physical parameters and appropriate boundary conditions are the chosen to be the same, except for the boundaries of the

Stokes region - now they satisfy the following constraints

No normal stress:	$(\boldsymbol{\sigma}_f \mathbf{n}_f) \cdot \mathbf{n}_f = 0$	on $\Gamma_{f,right}$,
	$\mathbf{u}_f \cdot \tau_f = 0$	on $\Gamma_{f,right} \cup \Gamma_{f,top}$,
Injection:	$\mathbf{u}_f \cdot \mathbf{n}_f = 0.2$	on $\Gamma_{f,left}$,
	$\mathbf{u}_f \cdot \tau_f = 0$	on $\Gamma_{f,left}$.

The rest of the controls is the same as in Example 3, including initial data, physical parameters and the boundary conditions for the transport equation. In this case, the boundary condition for the contaminant is set over the entire left boundary, including the fluid region, namely $c_{in} = 1$ on $\Gamma_{f,left} \cup \Gamma_{p,left}$.

We present the computed velocity fields in poroelastic structure and fracture regions in Figures 22a, 22c and the structure displacement - in Figure 22b. Similarly as before, four snapshots of the concentration solution at different time moments are shown in Figure 23. The concentration solution depicts how the interested species are being transported both in porous medium and in fracture. Due to the significant difference in the velocities, we observe how the concentration solution propagates along the fluid region, being driven by the Stokes flow towards the outflow boundaries. It is also important to notice, that some species appear in the fluid region by tunneling through the interface, and being further quickly transported towards the outflow. Smaller diffusivity in the fractures, lead to the contaminant front being much more expressed, to the point where we see two coexisting streams of species in close proximity to each other being transported by the free fluid (see upper outflow at time $t = 5$s).

4.4.2.5 Example 5: flow through poroelastic media with fracture network Our final example how a network of fractures in the porous media affects the flow and concentration of interested species. The setting for this test case matches the one from the Example 3, namely we have a pressure drop from left to right, no flow on top and bottom boundaries, the right boundary is clamped and the outflow regions of the fracture network have no normal stress boundary conditions specified on them. The physical parameters, initial data and the transport equation boundary conditions are chosen as in the previous two examples.

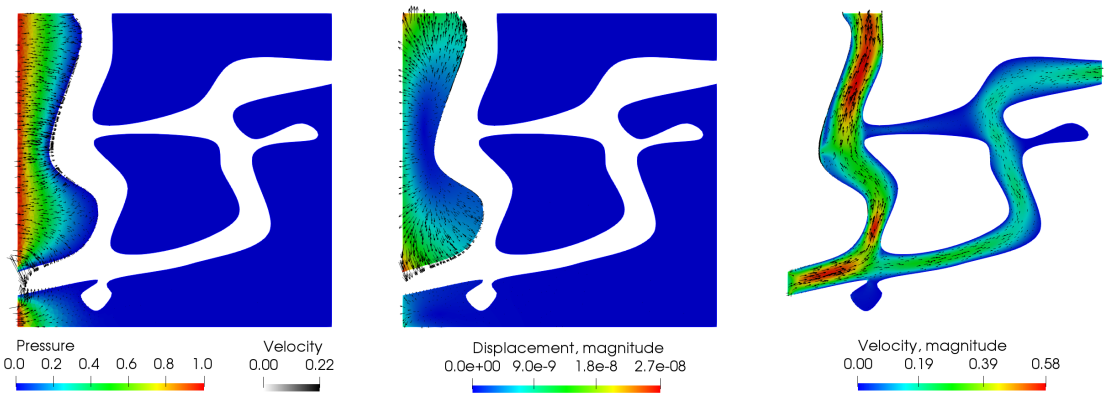

(a) Velocity over pressure (b) Displacement (c) Stokes velocity field

Figure 22: Example 3, computed velocity and pressure fields.

The solution of the velocity fields in structure and fracture network regions are visualized in Figures 24a and 24c, while the displacement of the porous media skeleton is shown in Figure 24b. We see much higher velocity in the free fluid regions, as one would expect, since the permeability is chosen to be small in the case and the natural behavior for the fluid would be to flow through the fractures towards the openings in the right boundary. The concentration solution at various time moments agrees with the flow solution in a sense that the contaminant is quickly transported towards the outflow regions by the means of free fluid. However, due to relatively small size of outflow boundaries, the concentration builds up in the fracture region and starts to propagate outside of it, this can be seen at the later times near the right boundary of the domain.

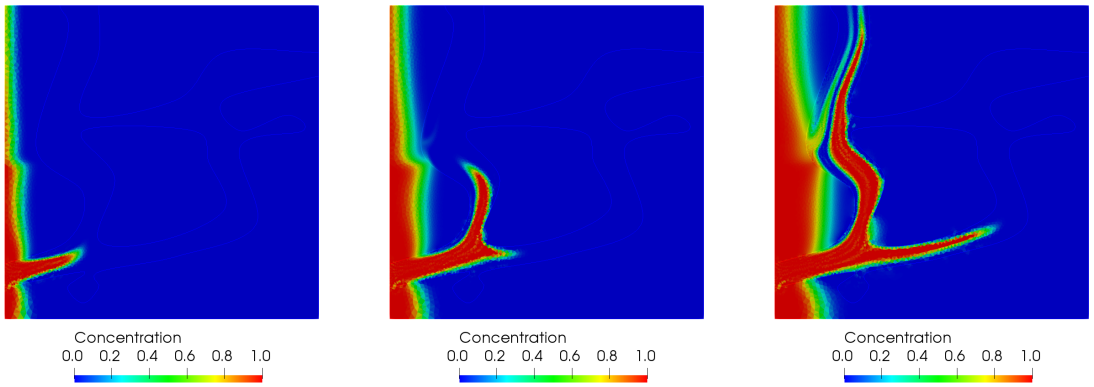

(a) Concentration at $t = 1$s. (b) Concentration at $t = 2.5$s. (c) Concentration at $t = 5$s.

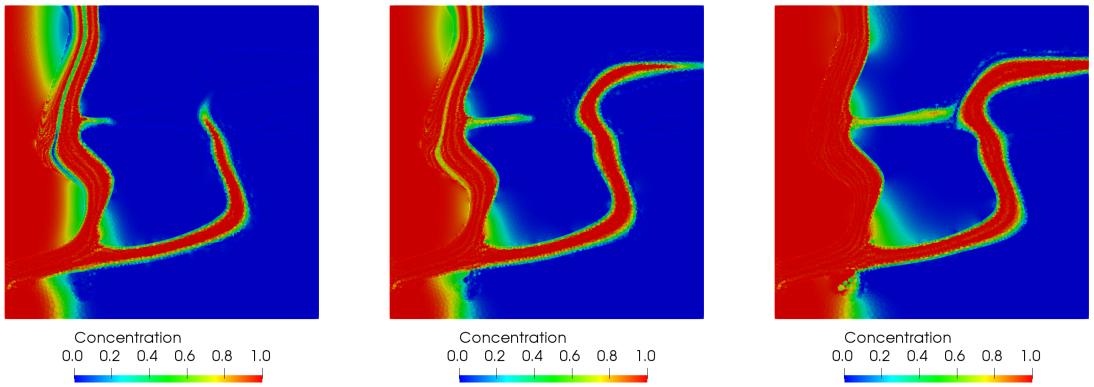

(d) Concentration at $t = 10$s. (e) Concentration at $t = 15$s. (f) Concentration at $t = 25$s.

Figure 23: Example 3, computed concentration solution.

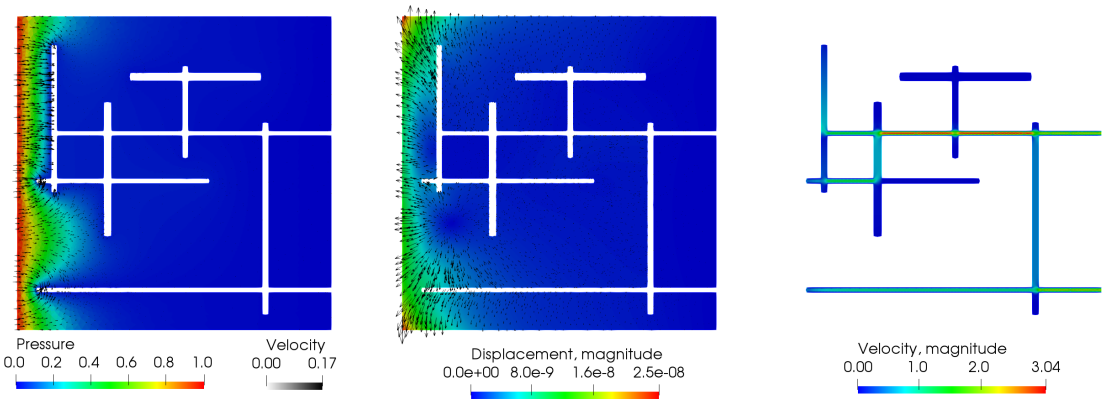

(a) Velocity over pressure (b) Velocity over pressure (c) Stokes velocity field

Figure 24: Example 5, computed velocity and pressure fields.

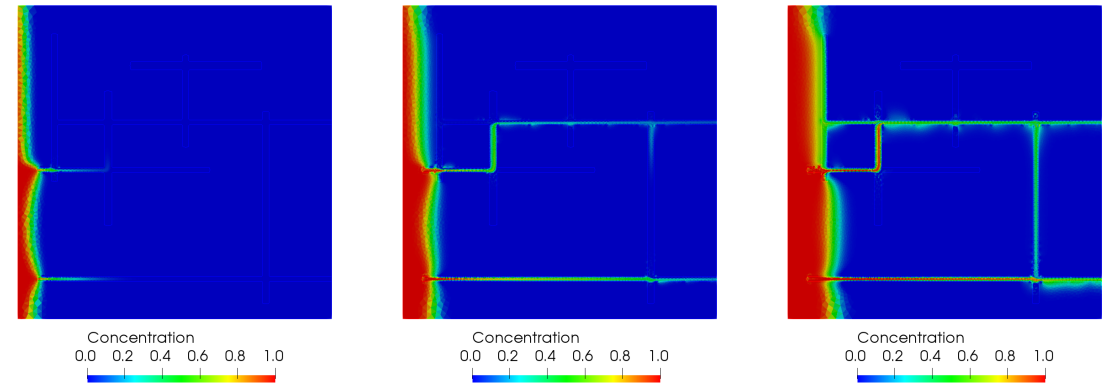

(a) Concentration at $t = 1$s. (b) Concentration at $t = 2.5$s. (c) Concentration at $t = 5$s.

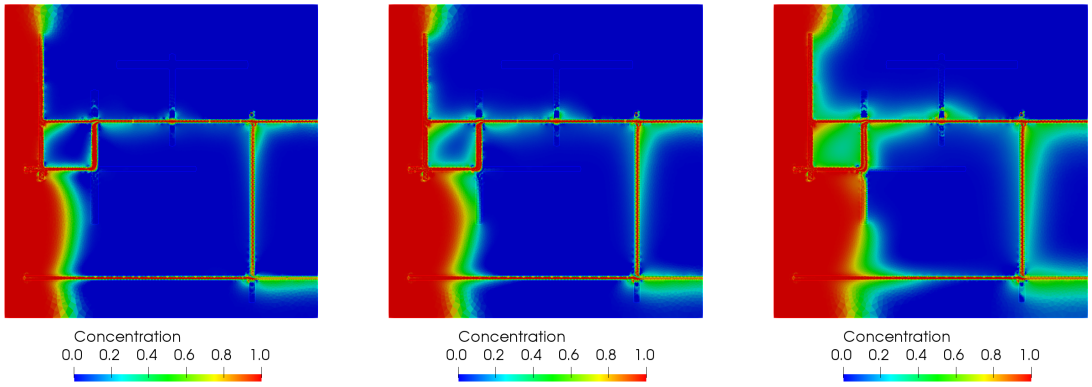

(d) Concentration at $t = 10$s. (e) Concentration at $t = 15$s. (f) Concentration at $t = 25$s.

Figure 25: Example 5, computed concentration solution.

5.0 CONCLUSIONS

In this thesis we have studied the interaction of a free fluid with a fluid within a poroelastic medium. Motivated by a broad range of applications, we developed and analyzed several new mathematical modeling approaches allowing for robust and efficient numerical simulation of phenomena arising in FPSI problems. We further coupled the proposed methods with the transport equation, in order to address such applications as modeling subsurface waste repositories or underground water contamination.

First, we derived the method for the Stokes-Biot model, in which we used a Lagrange multiplier to weakly impose the continuity of normal velocity interface condition, which is of essesntial type in the mixed Darcy formulation. We then showed that the method is stable and convergent, with optimal order of convergence expected in all variables, even in the case of non-matching grids across the interface. Computational experiments illustrate that this method is an effective and robust approach for simulating fluid-poroelastic structure interaction with a wide range of physical parameters, including cases of heterogeneous permeability and Young's modulus.

Second, we extended the method to the case of quasi-Newtonian fluids, that possess the so-called shear-thinning property. The method assumes either unbounded viscosity models, such as the Power law, or bounded models, such as the Cross and Carreau models. An alternative formulation was used in order to prove the method's well-posedness in both fully continuous and semi-discrete continuous-in-time settings, followed by the justification of the equivalence of two formulations. We performed convergence studies both theoretically and numerically, and compared the numerical solution of linear and nonlinear versions of the method. A realistic test case, which illustrates the application of the method for the cardiovascular simulations, was also presented.

Finally, we presented the framework for a coupled FPSI-transport problem, in which the transport subproblem was solved using the non-symmetric interior penalty (NIPG) Galerkin method. We performed the analysis of the semi-discrete continuous-in-time formulation, in which we showed how to obtain the desired stability and convergence properties without introducing an artificial cut-off operator. This allowed us to use the unmodified computed velocity field directly in the numerical scheme for transport. We concluded with a range of computational examples, including the convergence study as well as the realistic cases simulating flow and concentration of the interested species in the porous and deformable medium. The latter cases consider the fractured domains, heterogeneous permeability fields and fracture networks within the poroelastic media.

The potential extensions of this work include a development of parallel non-overlapping domain decomposition methods and algorithms, as well as multiscale approximations via coarse mortar spaces. This together with an incorporation of adaptive space–time discretization, is believed to lead to a flexible and efficient FPSI framework for complex 3d physical experiments simulation. After this command, chapters will be formatted as appendices. For example:

APPENDIX

FREEFEM++ CODE

We first present FreeFem++ code that was used to obtain convergence results for FPSI model coupled with transport.

Listing A.0.1: FreeFem++ code for coupled FPSI–transport problem

```
1  // Load extra files
2  load "Element_Mixte"
3  load "MUMPS"
4  load "iovtk"
5
6  // Macros
7  macro div(ax,ay)         (dx(ax)+dy(ay))//
8  macro cdot(ax,ay,bx,by) (ax*bx+ay*by)//
9  macro tgx(ax,ay)         (ax-cdot(ax,ay,N.x,N.y)*N.x)//
10 macro tgy(ax,ay)         (ay-cdot(ax,ay,N.x,N.y)*N.y)//
11
12 macro Dxx(ax,ay)  (diffc)//
13 macro Dxy(ax,ay)  (0.0)//
14 macro Dyx(ax,ay)  (0.0)//
15 macro Dyy(ax,ay)  (diffc)//
16
17 int Ttx = -1;
18 int Tty =  0;
19
20 // Time parameters
21 real T    = 0.0001;
22 real delt = 0.00001;
23 int  pr   = 1;
24 real t    = 0;
25 func NN   = T/delt;
26
27 // Flags
28 // true for debuging, mesh plots etc.
29 bool debug     = false;
30 // true for making .vtk files
31 bool plotflag  = true;
32 // true for convergence test (output made in reverse order, from finer mesh to coarser)
33 bool converg   = true;
34 // true for interface residual (output made in reverse order, from finer mesh to coarser)
35 bool intresid  = false;
36 // true for time dependent Stokes
37 bool timedep   = false;
38 // true if extra plots are needed
```

```
39  bool extraplot = false;
40
41  // Mesh parameters
42  int m,n,l;
43
44  if(converg){
45      m = 32 ;
46      l = 4;
47  }
48  else {
49      m = 16;
50      l = m;
51  }
52
53  int number = log(real(m/l))/log(2.0) + 1;
54  cout << "Number of refinement cycles: " << number << endl;
55
56  int count   = 0;
57  int nMeshes = number;
58
59  // initialize arrays for errors
60  real[int] error1(nMeshes);
61  real[int] error2(nMeshes);
62  real[int] error3(nMeshes);
63  real[int] error4(nMeshes);
64  real[int] error5(nMeshes);
65  real[int] error6(nMeshes);
66  real[int] error7(nMeshes);
67  real[int] error81(nMeshes);
68  real[int] error82(nMeshes);
69
70  error1 = 0;
71  error2 = 0;
72  error3 = 0;
73  error4 = 0;
74  error5 = 0;
75  error6 = 0;
76  error7 = 0;
77
78  real[int] abs1 (nMeshes);
79  real[int] abs4 (nMeshes);
80  real[int] abs6 (nMeshes);
81  real[int] abs7 (nMeshes);
82  real[int] abs81(nMeshes);
83
84  abs1 = 0;
85  abs4 = 0;
86  abs6 = 0;
87  abs7 = 0;
88
89  real[int] error2tmp (NN);
90  real[int] error3tmp (NN);
91  real[int] error5tmp (NN);
92  real[int] error82tmp(NN);
93
94  error2tmp  = 0;
95  error3tmp  = 0;
96  error5tmp  = 0;
97  error82tmp = 0;
98
99  real[int] cond13left (nMeshes);
100 real[int] cond13right(nMeshes);
101 real[int] displright (nMeshes);
102
103 // h-TEST LOOP
104 for(int n=l;n<=m;n*=2)
105 {
106     t=0;
```

```
107
108     string namefluid  = "./paraview"+string(n)+"/fluid";
109     string namesolid1 = "./paraview"+string(n)+"/structure1_";
110     string nameq1     = "./paraview"+string(n)+"/Darcy1_";
111     string namesolid2 = "./paraview"+string(n)+"/structure2_";
112     string nameq2     = "./paraview"+string(n)+"/Darcy2_";
113
114     int[int] labelF = [11,12,13,14];
115     int[int] labelS = [21,22,23,24];
116
117     // Fluid and structure regions
118     mesh ThF = square(n,n,flags=3,label=labelF);
119     mesh ThS = square(n,n,flags=3,label=labelS);
120     ThF      = change(ThF, fregion=1);
121     ThS      = change(movemesh(ThS, [x,y-1]),fregion=2);
122
123     // Global mesh for transport solution
124     mesh ThG  = square(n,2*n,flags=3);
125     ThG       = movemesh(ThG,[x,2*y-1]);
126
127     // Mesh for the Lagrange multiplier
128     mesh ThL = emptymesh(ThS);
129
130     // Finite Element spaces
131     // Free fluid:
132     fespace VFh(ThF,[P2,P2,P1]);
133     // Porous media flow:
134     fespace VMh(ThS,[RT1,P1dc]);
135     // Mechanics
136     fespace VSh(ThS,[P2,P2]);
137     // Lagrange:
138     fespace LLh (ThL, P1dc);
139
140     VFh [uFx,uFy,pF], [vFx,vFy,wF], [uFoldx,uFoldy,pFold];
141     VMh [uPx,uPy,pP], [vPx,vPy,wP], [uPoldx,uPoldy,pPold], [dummyX, dummyY, dummyP];
142     VSh [etax,etay], [ksix,ksiy], [etaoldx,etaoldy];
143     LLh LAMBDA, MU, LAMBDAold;
144
145     // Physical parameters
146     // Mechanics
147     func rohS    = 1.0;
148     func ES      = 1.0;
149     func sigmaS  = 1.0;
150     func lambdaS = 1.0;
151     func muS     = 1.0;
152
153     // Stokes region
154     func rohF     = 1.0;
155     real muF      = 1.0;
156
157     // Darcy region
158     real alfa    = 1.0;
159     real alfabjs = 1.0;
160     real s0      = 1.0;
161     real Kxx     = 1.0;
162     real Kyy     = 1.0;
163     real kappaxx = muF/Kxx;
164     real kappayy = muF/Kyy;
165
166     // Interface BJS coefficient
167     real bjs = alfabjs*muF*sqrt(2)/sqrt(Kxx+Kyy);
168
169     // Analytical solution and data
170     // Stokes velocity and its gradient
171     func ufx0   = pi*cos(pi*t)*(-3*x+cos(y));
172     func ufy0   = pi*cos(pi*t)*(y+1);
173     func duf11  = pi*cos(pi*t)*(-3);
174     func duf12  = pi*cos(pi*t)*(-sin(y));
```

```
175     func duf21  = 0;
176     func duf22  = pi*cos(pi*t);
177
178     // Stokes pressure
179     func upx0   = -exp(t)*pi*cos(pi*x)*cos(pi*y/2);
180     func upy0   = exp(t)*pi/2*sin(pi*x)*sin(pi*y/2);
181
182     // Darcy velocity divergence
183     func divup  = 1.25*pi*pi*exp(t)*sin(pi*x)*cos(pi*y/2);
184
185     // Displacement and its gradient
186     func etax0  = sin(pi*t)*(-3*x+cos(y));
187     func etay0  = sin(pi*t)*(y+1);
188     func deta11 = sin(pi*t)*(-3);
189     func deta12 = sin(pi*t)*(-sin(y));
190     func deta21 = 0;
191     func deta22 = sin(pi*t);
192
193     // Darcy and Stokes pressures
194     func pp0sol = exp(t)*sin(pi*x)*cos(pi*y/2);
195     func pf0sol = pp0sol + 2*pi*cos(pi*t);
196
197     // Elasticity RHS
198     func ffx    = pi*cos(pi*t)*cos(y) + pi*exp(t)*cos(pi*x)*cos((pi*y)/2);
199     func ffy    = -(pi*exp(t)*sin(pi*x)*sin((pi*y)/2))/2;
200
201     // Stokes RHS
202     func qf     = -2*pi*cos(pi*t);
203     func fpx    = sin(pi*t)*cos(y) + pi*exp(t)*cos(pi*x)*cos((pi*y)/2);
204     func fpy    = -(pi*exp(t)*sin(pi*x)*sin((pi*y)/2))/2;
205
206     // Darcy RHS
207     func qp     = exp(t)*cos((pi*y)/2)*sin(pi*x) - 2*pi*cos(pi*t)
208                   + (5*pi^2*exp(t)*cos((pi*y)/2)*sin(pi*x))/4;
209
210     // Functions to switch between solutions for transport
211     func real divug(real x, real y){
212         if (y > 0)
213             return (pi*cos(pi*t)*(-3) + pi*cos(pi*t));
214         else
215             return 1.25*pi*pi*exp(t)*sin(pi*x)*cos(pi*y/2);
216     }
217
218     func real ugx(real x, real y){
219         if (y > 0)
220             return pi*cos(pi*t)*(-3*x+cos(y));
221         else
222             return -exp(t)*pi*cos(pi*x)*cos(pi*y/2);
223     }
224
225     func real ugy(real x, real y){
226         if (y > 0)
227             return pi*cos(pi*t)*(y+1);
228         else
229             return exp(t)*pi/2*sin(pi*x)*sin(pi*y/2);
230     }
231
232     // Diffusivity coefficient
233     real diffc = 1e-4;
234
235     // Transport solution and RHS
236     func cf0    = t*(cos(pi*x)+cos(pi*y))/pi;
237     func rc0    = (1/pi)*(1+t*divug(x,y)+t*pi*pi*diffc)*(cos(pi*x)+cos(pi*y))
238                   - t*(ugx(x,y)*sin(pi*x) + ugy(x,y)*sin(pi*y));
239
240     // Concentration gradient
241     func gcf0x = -t*sin(pi*x);
242     func gcf0y = -t*sin(pi*y);
```

```
243
244     /*
245      * Matrix assembly, Stokes region
246      */
247     varf BCin([uFx,uFy,pF],[vFx,vFy,wF],init=1)
248         = int2d(ThF)(ffx*vFx + ffy*vFy) + int2d(ThF)(qf*wF)
249         + on(12,13,14,uFx=ufx0, uFy=ufy0);
250
251     varf MASSFsum([uFx,uFy,pF],[vFx,vFy,wF],init=1)
252         = int2d(ThF)((timedep*rohF/delt)*cdot(uFx,uFy,vFx,vFy))
253         + on(12,13,14,uFx=ufx0, uFy=ufy0);
254     matrix MASSF = MASSFsum(VFh,VFh);
255
256     varf AFsum([uFx,uFy,pF],[vFx,vFy,wF],init=1)
257         = int2d(ThF)(2.0*muF*(dx(uFx)*dx(vFx) + dy(uFy)*dy(vFy)))
258         + int2d(ThF)(muF*((dy(uFx)+dx(uFy))*dy(vFx) + (dy(uFx)+dx(uFy))*dx(vFy)));
259     matrix AF = AFsum(VFh,VFh);
260
261     varf ABJS1sum([uFx,uFy,pF],[vFx,vFy,wF],init=1)
262         = int1d(ThF,11)(bjs*(cdot( uFx,uFy,Ttx,Tty)*cdot(vFx,vFy,Ttx,Tty)));
263     matrix ABJS1 = ABJS1sum(VFh,VFh);
264
265     varf BPFTsum([uFx,uFy,pF],[vFx,vFy,wF],init=1)
266         = - int2d(ThF)(pF*div(vFx,vFy));
267     matrix BPFT = BPFTsum(VFh,VFh);
268
269     varf BPFsum([uFx,uFy,pF],[vFx,vFy,wF],init=1)
270         = int2d(ThF)(wF*div(uFx,uFy));
271     matrix BPF = BPFsum(VFh,VFh);
272
273     matrix FF = ABJS1+AF+BPF+BPFT+MASSF;
274
275     /*
276      * Matrix assembly, Stokes-Biot communication
277      */
278     varf ABJS2Tsum([etax,etay],[vFx,vFy,wF],init=1)
279         = - int1d(ThF,11)(bjs*(1.0/delt)*cdot(etax,etay,Ttx,Tty) * cdot(vFx,vFy,Ttx,Tty));
280     matrix ABJS2T = ABJS2Tsum(VSh,VFh);
281
282     varf BG1Tsum([LAMBDA],[vFx,vFy,wF],init=1)
283         = -int1d(ThL,23)(LAMBDA*cdot(vFx,vFy,N.x,N.y));
284     matrix BG1T = BG1Tsum(LLh,VFh);
285
286     matrix FS = [[ABJS2T, BG1T]];
287
288     /*
289      * Matrix assembly, Darcy terms
290      */
291     varf BCinM([uPx,uPy,pP],[vPx,vPy,wP],solver=UMFPACK,init=1)
292         = int2d(ThS)(qp*wP)
293         - int1d(ThS,21,22,24)(cdot(pp0sol,pp0sol,vPx*N.x,vPy*N.y));
294
295     varf AQsum([uPx,uPy,pP],[vPx,vPy,wP],init=1)
296         = int2d(ThS)(cdot(kappaxx*uPx,kappayy*uPy,vPx,vPy))
297         + int2d(ThS)(1.e-8*pP*wP);
298     matrix AQ = AQsum(VMh,VMh);
299
300     varf BPQTsum([uPx,uPy,pP],[vPx,vPy,wP],init=1)
301         = -int2d(ThS)(1*pP*div(vPx,vPy));
302     matrix BPQT = BPQTsum(VMh,VMh);
303
304     varf BPQsum([uPx,uPy,pP],[vPx,vPy,wP],init=1)
305         = int2d(ThS)(1*wP*div(uPx,uPy));
306     matrix BPQ = BPQsum(VMh,VMh);
307
308     varf MASSPsum([uPx,uPy,pP],[vPx,vPy,wP],init=1)
309         = int2d(ThS)((s0/delt)*(wP*pP));
310     matrix MASSP = MASSPsum(VMh,VMh);
```

```
311
312     matrix MM = AQ + BPQT + BPQ + MASSP;
313
314     /*
315      * Matrix assembly, Darcy-Biot communication
316      */
317     varf BSPTsum([etax,etay],[vPx,vPy,wP],init=1)
318         = int2d(ThS)((alfa/delt)*wP*div(etax,etay));
319     matrix BSPT = BSPTsum(VSh,VMh);
320
321     varf BG2Tsum([LAMBDA],[vPx,vPy,wP],init=1)
322         = int1d(ThL,23)(LAMBDA*cdot(vPx,vPy,N.x,N.y));
323     matrix BG2T = BG2Tsum(LLh,VMh);
324
325     matrix MS = [[BSPT, BG2T]];
326
327     /*
328      * Matrix assembly, Biot-Stokes communication
329      */
330     varf ABJS2sum([uFx,uFy,pF],[ksix,ksiy],init=1)
331         = -int1d(ThS,23)(bjs*cdot(uFx,uFy,Ttx,Tty)*cdot(ksix,ksiy,Ttx,Tty));
332     matrix ABJS2 = ABJS2sum(VFh,VSh);
333
334     varf BG1sum([uFx,uFy,pF],[MU],init=1)
335         = -int1d(ThL,23)(MU*cdot(uFx,uFy,N.x,N.y));
336     matrix BG1 = BG1sum(VFh,LLh);
337
338     matrix SF = [[ABJS2],[BG1]];
339
340     /*
341      * Matrix assembly, Biot-Darcy communication
342      */
343     varf BSPsum([uPx,uPy,pP],[ksix,ksiy],init=1)
344         = -int2d(ThS)(alfa*pP*div(ksix,ksiy));
345     matrix BSP = BSPsum(VMh,VSh);
346
347     varf BG2sum([uPx,uPy,pP],[MU],init=1)
348         = int1d(ThL,23)(MU*cdot(uPx,uPy,N.x,N.y));
349     matrix BG2 = BG2sum(VMh,LLh);
350
351     matrix SM = [[BSP],[BG2]];
352
353     /*
354      * Matrix assembly, Biot terms
355      */
356     varf BCinS([etax,etay],[ksix,ksiy],solver=UMFPACK,init=1)
357         = int2d(ThS)(fpx*ksix + fpy*ksiy) + on(21,22,24,etax=etax0, etay=etay0);
358
359     varf ASsum([etax,etay],[ksix,ksiy],init=1)
360         = int2d(ThS)(2.0*muS*(dx(etax)*dx(ksix) + dy(etay)*dy(ksiy)))
361         + int2d(ThS)(muS*((dy(etax) + dx(etay))*dy(ksix)
362         + (dy(etax) + dx(etay))*dx(ksiy) ))
363         + int2d(ThS)((lambdaS)*(dx(ksix)*dx(etax)+dy(ksiy)*dx(etax)
364         + dx(ksix)*dy(etay)+dy(ksiy)*dy(etay))) + on(21,22,24,etax=etax0, etay=etay0);
365     matrix AS = ASsum(VSh,VSh);
366
367     varf ABJS3sum([etax,etay],[ksix,ksiy],init=1)
368         = int1d(ThS,23)(bjs*(1.0/delt)*cdot(etax,etay,Ttx,Tty)*cdot(ksix,ksiy,Ttx,Tty));
369     matrix ABJS3 = ABJS3sum(VSh,VSh);
370
371     varf BG3Tsum([LAMBDA],[ksix,ksiy],init=1)
372         = int1d(ThL,23)(LAMBDA*cdot(ksix,ksiy,N.x,N.y));
373     matrix BG3T = BG3Tsum(LLh,VSh);
374
375     varf BG3sum([etax,etay],[MU],init=1)
376         = int1d(ThL,23)(MU*(1/delt)*cdot(etax,etay,N.x,N.y));
377     matrix BG3 = BG3sum(VSh,LLh);
378
```

```
379     // Technical stabilization term due to implementation of ThL
380     varf TECHsum([LAMBDA],[MU],init=1)
381         = int2d(ThL)(1.e-13*LAMBDA*MU) + int1d(ThL,22,21,24)(1.e-13*LAMBDA*MU);
382     matrix TECH = TECHsum(LLh,LLh);
383     matrix tmp10 = AS + ABJS3;
384
385     matrix SS=[
386         [tmp10, BG3T],
387         [BG3   , TECH]];
388
389     /*
390      * "Old" matrices, to speedup the time loop
391      */
392     ////////////////////////////////////////////////////////////////////////////////
393     varf MASSFsumold([uFoldx,uFoldy,pFold],[vFx,vFy,wF],init=1)
394         = int2d(ThF)((timedep*rohF/delt)*cdot(uFoldx,uFoldy,vFx,vFy));
395     matrix MASSFold = MASSFsumold(VFh,VFh);
396     matrix FFold = MASSFold;
397
398     varf ABJS2Tsumold([etaoldx,etaoldy],[vFx,vFy,wF],init=1)
399         = -int1d(ThF,11)(bjs*(1.0/delt)*cdot(etaoldx,etaoldy,Ttx,Tty)*cdot(vFx,vFy,Ttx,Tty));
400     matrix ABJS2Told = ABJS2Tsumold(VSh,VFh);
401     matrix tmp2 = 0*BG1T;
402     matrix FSold = [[ABJS2Told, tmp2]];
403
404     varf MASSPsumold([uPoldx,uPoldy,pPold],[vPx,vPy,wP],init=1)
405         = int2d(ThS)((s0/delt)*(wP*pPold));
406     matrix MASSPold = MASSPsumold(VMh,VMh);
407
408     matrix MMold = MASSPold;
409
410     varf BSPTsumold([etaoldx,etaoldy],[vPx,vPy,wP],init=1)
411         = int2d(ThS)((alfa/delt)*wP*div(etaoldx,etaoldy));
412     matrix BSPTold = BSPTsumold(VSh,VMh);
413
414     matrix tmp3 = 0*BG2T;
415
416     matrix MSold = [[BSPTold, tmp3]];
417     matrix MSmonoold = [[BSPTold, tmp3]];
418
419     varf ABJS3sumold([etaoldx,etaoldy],[ksix,ksiy],init=1)
420         = int1d(ThS,23)(bjs*(1.0/delt)*cdot(etaoldx,etaoldy,Ttx,Tty)*cdot(ksix,ksiy,Ttx,Tty));
421     matrix ABJS3old = ABJS3sumold(VSh,VSh);
422
423     varf BG3sumold([etaoldx,etaoldy],[MU],init=1)
424         = int1d(ThL,23)(MU*(1/delt)*cdot(etaoldx,etaoldy,N.x,N.y));
425     matrix BG3old = BG3sumold(VSh,LLh);
426     matrix tmp4 = 0*BG3T;
427
428     matrix SSold=[[ABJS3old, tmp4],
429                   [BG3old   , 0    ]];
430
431     /*
432      * System matrices
433      */
434     matrix mono=[
435     [ SS, SM, SF],
436     [ MS, MM, 0  ],
437     [ FS, 0   , FF ]
438     ];
439
440     matrix monoold=[
441     [ SSold, 0      , 0     ],
442     [ MSold, MMold, 0     ],
443     [ FSold, 0      , FFold]
444     ];
445
446     /*
```

```
447         * Initialize solution and RHS vectors
448         */
449        real[int] xxf(FF.n),xxfold(FF.n);
450        real[int] xxm1(MM.n),xxm1old(MMold.n);
451        real[int] xxs1(AS.n),xxs1old(AS.n);
452        real[int] xxl1(TECH.n),xxl1old(TECH.n),xxl1mono(TECH.n);
453        real[int] pfakel(TECH.n);
454        pfakel  = 0;
455
456        /*
457         * Assemble RHS
458         */
459        varf l   (unused,VFh)  = BCin;
460        varf lM(unused,VMh) = BCinM;
461        varf lS(unused,VSh) = BCinS;
462
463        // Counter to plot each br-th time step
464        int br = 1;
465
466        [uFx,uFy,pF] = [ufx0,ufy0,pf0sol];
467        [uPx,uPy,pP] = [upx0,upy0,pp0sol];
468        [etax,etay]  = [etax0,etay0];
469       LAMBDA        = pp0sol;
470
471        // Plot parameters (vector/scalar)
472        int[int] fforder1 = [1,0];
473        int[int] fforder2 = [1,0,1];
474
475        // Initialization and initial conditions
476        xxf     = 0;
477        xxm1    = 0;
478        xxs1    = 0;
479        xxfold  = uFx[];
480        xxm1old = uPx[];
481        xxs1old = etax[];
482        xxl1old = LAMBDA[];
483
484        // The solution is a block vector (Elasticity-Lambda-Darcy-Stokes)
485        real[int] xx    = [xxs1,xxl1,xxm1,xxf];
486        real[int] xxold = [xxs1old,xxl1old,xxm1old,xxfold];
487        xx = 0.0;
488
489        // Initialize error vectors
490        error4[count]  = 0;
491        error1[count]  = 0;
492        error5[count]  = 0;
493        error81[count] = 0;
494        error82[count] = 0;
495
496
497        /*
498         * Transport problem setup and assembly
499         */
500        // Global space for velocities and concentration
501        mesh inTh = ThF + ThS;
502        mesh Th   = ThG;
503
504        fespace VGh   (Th, [P2dc, P2dc]);
505        fespace inVGh (inTh, [P2dc, P2dc]);
506        VGh   [uTx,uTy], [vTx, vTy];
507        inVGh [inuTx,inuTy], [invTx, invTy];
508
509        // Project the sum of Stokes and Darcy velocities onto the global space VGh
510        problem proj([inuTx,inuTy], [invTx,invTy], solver=CG)
511            = int2d(inTh)(cdot(inuTx,inuTy,invTx,invTy))
512            - int2d(inTh,2)(cdot(uPx,uPy,invTx,invTy))
513            - int2d(inTh,1)(cdot(uFx,uFy,invTx,invTy))
514            + on(21,22,24, inuTx=uPx, inuTy=uPy)
```

```
515         + on(12,13,14, inuTx=uFx, inuTy=uFy);
516
517     // Transport FE spaces
518     fespace CFh(ThF, P2dc);
519     fespace CSh(ThS, P2dc);
520     CFh cF,wFF,cFold;
521     CSh cS,wS,cSold;
522
523     // Physical parameters for transport
524     func s      = 0.0;
525     func sigmae = 10000.0;
526     real beta   = 1.0;
527     real tau    = 1.0;
528     real Dm     = 1.0;
529     real alphal = Dm;
530     real alphat = Dm;
531     real qq     = 0;
532
533     func real Cin(real x, real y){
534         return cf0;
535     }
536
537     func real phi(real x, real y){
538         return 1;
539     }
540
541     func real C0(real x, real y){
542         return cf0;
543     }
544
545     cFold = C0(x,y);
546     cSold = C0(x,y);
547     real magnitude = sqrt(uTx^2 + uTy^2);
548
549     /*
550      * Transport problem
551      */
552     problem concentrationDGFluid (cF,wFF,solver=sparsesolver) =
553         int2d(ThF)((1/delt)*phi(x,y)*cF*wFF ) - int2d(ThF)((1/delt)*phi(x,y)*cFold*wFF)
554         - int2d(ThF)(rc0*wFF) + int2d(ThF)(((Dxx(uFx,uFy)*dx(cF) + Dxy(uFx,uFy)*dy(cF)
555             -cF*uFx)*dx(wFF) + (Dyx(uFx,uFy)*dx(cF) + Dyy(uFx,uFy)*dy(cF) - cF*uFy)*dy(wFF)))
556         - intalledges(ThF)(((1 - nTonEdge)*mean((Dxx(uFx,uFy)*dx(cF)
557             + Dxy(uFx,uFy)*dy(cF))*N.x + (Dyx(uFx,uFy)*dx(cF)
558             + Dyy(uFx,uFy)*dy(cF))*N.y)*jump(wFF)))
559         + intalledges(ThF)(((1 - nTonEdge)*mean((Dxx(uFx,uFy)*dx(wFF)
560             + Dxy(uFx,uFy)*dy(wFF))*N.x
561             + (Dyx(uFx,uFy)*dx(wFF) + Dyy(uFx,uFy)*dy(wFF))*N.y)*jump(cF)))
562         + intalledges(ThF)((1 - nTonEdge)*(uFx*N.x + uFy*N.y)*jump(wFF)
563             *((0 < (uFx*N.x + uFy*N.y))*(mean(cF) - 0.5*jump(cF))))
564         + intalledges(ThF)((1 - nTonEdge)*(uFx*N.x+uFy*N.y)*jump(wFF)
565             *((0 > (uFx*N.x + uFy*N.y))*(mean(cF) + 0.5*jump(cF))))
566         + intalledges(ThF)((1 - nTonEdge)*(sigmae/hTriangle^beta)*jump(cF)*jump(wFF))
567         + int1d(ThF)(((N.x*uFx + N.y*uFy) < 0)*Cin(x,y)*(uFx*N.x + uFy*N.y)*wFF)
568         + int1d(ThF)(((N.x*uFx + N.y*uFy) > 0)*(uFx*N.x + uFy*N.y)*cF*wFF);
569
570     problem concentrationDGStruct (cS,wS,solver=sparsesolver) =
571     int2d(ThS)((1/delt)*phi(x,y)*cS*wS) - int2d(ThS)((1/delt)*phi(x,y)*cSold*wS)
572     - int2d(ThS) (rc0 * wS) + int2d(ThS)(((Dxx(uPx,uPy)*dx(cS) + Dxy(uPx,uPy)*dy(cS)
573         - cS*uPx)*dx(wS) + (Dyx(uPx,uPy)*dx(cS) + Dyy(uPx,uPy)*dy(cS) - cS*uPy)*dy(wS)))
574     - intalledges(ThS)(((1 - nTonEdge)*mean((Dxx(uPx,uPy)*dx(cS)
575         + Dxy(uPx,uPy)*dy(cS))*N.x + (Dyx(uPx,uPy)*dx(cS)
576         + Dyy(uPx,uPy)*dy(cS))*N.y)*jump(wS)))
577     + intalledges(ThS)(((1 - nTonEdge)*mean((Dxx(uPx,uPy)*dx(wS)
578         + Dxy(uPx,uPy)*dy(wS))*N.x
579         + (Dyx(uPx,uPy)*dx(wS) + Dyy(uPx,uPy)*dy(wS))*N.y)*jump(cS)))
580     + intalledges(ThS)((1 - nTonEdge)*(uPx*N.x + uPy*N.y)*jump(wS)
581         *((0 < (uPx*N.x + uPy*N.y))*(mean(cS) - 0.5*jump(cS))))
582     + intalledges(ThS)((1 - nTonEdge)*(uPx*N.x + uPy*N.y)*jump (wS)
```

```
583         *((0 > (uPx*N.x + uPy*N.y))*(mean(cS) + 0.5*jump(cS))))
584     + intalledges(ThS)((1 - nTonEdge)*(sigmae/hTriangle^beta)*jump(cS)*jump(wS))
585     + int1d(ThS)(((N.x*uPx + N.y*uPy) < 0)*Cin(x,y)*(uPx*N.x + uPy*N.y)*wS)
586     + int1d(ThS)(((N.x*uPx + N.y*uPy) > 0)*(uPx*N.x + uPy*N.y)*cS*wS);
587
588     /*
589      * Time loop
590      */
591     for (int k=1;k<=NN;++k){
592         t=t+delt;
593
594         // Initial values
595         real[int] Pinvec  = l(0,VFh);
596         real[int] PinvecM = lM(0,VMh);
597         real[int] PinvecS = lS(0,VSh);
598
599         // Right-hand side
600         real[int] b = [PinvecS,pfakel,PinvecM,Pinvec];
601         b += (monoold*xxold);
602         [dummyX,dummyY,dummyP] = [uFx,uFy,pF];
603
604         etaoldx[] = etax[];
605
606         // Solve flow problem
607         set(mono,solver=sparsesolver);
608         xx = mono^-1 * b;
609
610         xxold = xx;
611         [xxs1,xxl1,xxm1,xxf] = xx;
612
613
614         uFx[]     = xxf;
615         uPx[]     = xxm1;
616         etax[]    = xxs1;
617         LAMBDA[] = xxl1;
618
619         // Solve transport problem
620         concentrationDGFluid;
621         concentrationDGStruct;
622
623         cFold[] = cF[];
624         cSold[] = cS[];
625
626         // Continuity of flux (residual)
627         if(k == NN){
628             cond13left[count] = int1d(ThF,1)((1/delt)*cdot(etax,etay,N.x,N.y)
629                                 -(1/delt)*cdot(etaoldx,etaoldy,N.x,N.y));
630         }
631
632
633         fespace Vh1(ThF,P1);
634         fespace VhS(ThS,P1);
635
636         Vh1  pf;
637         pf = pF;
638         VhS pp1;
639         pp1 = pP;
640
641         if(k % 10 == 0)
642             cout << k << " iterations out of " << NN << endl;
643
644         // Output .vtk files
645         if(k%pr == 0&&plotflag){
646             br=br+1;
647
648             savevtk("paraview/fracture"+string(n)+"_"+string(br)+".vtk",
649                     ThF, [uFx,uFy,0],pF,order=fforder1,dataname="Velocity Pressure");
650             savevtk("paraview/TrueTransport"+string(n)+"_"+string(br)+".vtk",
```

```
651                 Th, [uTx,uTy,0],cf0,order=fforder1,dataname="Velocity Concentration");
652         savevtk("paraview/structure"+string(n)+"_"+string(br)+".vtk",
653                 ThS, [uPx,uPy,0],pP,[etax,etay,0], order=fforder2,
654                 dataname="Velocity Pressure Displacement");
655     }
656
657     // Error functions
658     VFh [ttx,tty,ttp]   = [ufx0,ufy0,pf0sol];
659
660     VFh [eufx,eufy,epf] = [ufx0 - uFx, ufy0 - uFy, pf0sol - pF];
661     VFh [rufx,rufy,rpf] = [ufx0, ufy0, pf0sol];
662
663     VMh [eup1x,eup1y,ep1] = [upx0 - uPx, upy0 - uPy, pp0sol - pP];
664     VMh [rup1x,rup1y,rp1] = [upx0, upy0, pp0sol];
665
666     VSh [deta11x,deta12y]     = [dx(etax),dy(etax)];
667     VSh [deta21x,deta22y] = [dy(etax),dy(etay)];
668
669     VSh [eetax,eetay] = [etax0 - etax, etay0 - etay];
670     VSh [retax,retay] = [etax0, etay0];
671
672     // Output .vtk files with errors
673     if (extraplot){
674         savevtk("GradDispl"+string(n)+"_"+string(br)+".vtk", ThS,
675             [deta11x,deta12y,0],pP,[deta21x,deta22y,0],order=fforder2,
676             dataname="Grad1 P Grad2");
677         savevtk("GradDisplTrue"+string(n)+"_"+string(br)+".vtk", ThS,
678             [deta11,deta12,0],pP,[deta21,deta22,0],
679             order=fforder2,dataname="Grad1 P Grad2");
680         savevtk("ErrorDispl"+string(n)+"_"+string(br)+".vtk", ThS,
681             [eetax,eetay,0],pP,
682             order=fforder1,dataname="Error P ");
683         savevtk("ErrorStokes"+string(n)+"_"+string(br)+".vtk", ThF,
684             [eufx,eufy,0],epf,order=fforder1,dataname="ErrorVel ErrorPres ");
685         savevtk("ErrorDarcy"+string(n)+"_"+string(br)+".vtk", ThS,
686             [eup1x,eup1y,0],ep1,order=fforder1,dataname="ErrorVel ErrorPres ");
687     }
688
689     LLh elambda = 1.0;
690     LLh rlambda = 1.0;
691
692
693     // Compute L2 in time errors and absolute values
694     error1[count]   += int2d(ThF)( (dx(uFx) - duf11)^2 + (dy(uFy) - duf22)^2
695                     + (dx(uFy) - duf21)^2 + (dy(uFx) - duf12)^2 );
696     abs1[count]     += int2d(ThF)( duf11^2 + duf12^2 + duf21^2 + duf22^2 );
697
698     error4[count]   += int2d(ThS)( (uPx - upx0)^2 + (uPy - upy0)^2 );
699     abs4[count]     += int2d(ThS)( upx0^2 + upy0^2 );
700
701     error6[count]   += int2d(ThL)( 1.0 );
702     abs6[count]     += int2d(ThL)( 1.0 );
703
704     error7[count]   += int2d(ThF)( (pF - pf0sol)^2 );
705     abs7[count]     += int2d(ThF)( pf0sol^2 );
706
707     error81[count]  += int2d(ThF)( (dx(cF)-gcf0x)^2 + (dy(cF)-gcf0y)^2 )
708                     + int2d(ThS)( (dx(cS)-gcf0x)^2 + (dy(cS)-gcf0y)^2 );
709     abs81[count]    += int2d(ThF)( gcf0x^2 + gcf0y^2 )
710                     + int2d(ThS)( gcf0x^2 + gcf0y^2);
711
712     error2tmp[k-1]  = (int2d(ThS)( (pp0sol - pP)^2 )) / (int2d(ThS)( pp0sol^2 ));
713     error5tmp[k-1]  = (int2d(ThF)( (ufx0 - uFx)^2 + (ufy0 - uFy)^2 ))
714                     / (int2d(ThF)( ufx0^2 + ufy0^2 ));
715
716     error3tmp[k-1]  = (int2d(ThS)( (dx(etax) - deta11)^2 + (dy(etay) - deta22)^2
717                     + (dx(etay) - deta21)^2 + (dy(etax) - deta12)^2 )) /
718     (int2d(ThS)( deta11^2 + deta22^2 + deta12^2 + deta21^2 ));
```

```
719
720         error82tmp[k-1] = (int2d(ThF) ( (cf0 - cF)^2 ) + int2d(ThS) ( (cf0 - cS)^2 ))
721                         / (int2d(ThF)( cf0^2 ) + int2d(ThS)( cf0^2 ));
722     }
723
724     error2[count]  = error2tmp.max;
725     error3[count]  = error3tmp.max;
726     error5[count]  = error5tmp.max;
727     error82[count] = error82tmp.max;
728
729     count += 1;
730 }
731
732 // Errors to output
733 real[int] err1(nMeshes);
734 real[int] err2(nMeshes);
735 real[int] err3(nMeshes);
736 real[int] err4(nMeshes);
737 real[int] err5(nMeshes);
738 real[int] err6(nMeshes);
739 real[int] err7(nMeshes);
740 real[int] err81(nMeshes);
741 real[int] err82(nMeshes);
742 // initialize rate arrays
743 real[int] rate1(nMeshes);
744 real[int] rate2(nMeshes);
745 real[int] rate3(nMeshes);
746 real[int] rate4(nMeshes);
747 real[int] rate5(nMeshes);
748 real[int] rate6(nMeshes);
749 real[int] rate7(nMeshes);
750 real[int] rate81(nMeshes);
751 real[int] rate82(nMeshes);
752
753
754 for (int k=0; k<error1.n; ++k){
755     cout.precision(8);
756     cout.scientific << error1(k) << " " << error4(k) << " " << error7(k) << endl;
757 }
758
759
760 cout << nMeshes << "  " << error1.n << endl;
761
762 for (int k=0; k<error1.n; ++k){
763     // Fluid velocity H1 in space L2 in time
764     err1(k) = sqrt(error1(k)/abs1(k));
765     // Fluid pressure L2 is space L2 in time
766     err7(k) = sqrt(error7(k)/abs7(k));
767     // Darcy velocity L2 in space L2 in time
768     err4(k) = sqrt(error4(k)/abs4(k));
769     // Darcy pressure L2 in space l-infinity in time
770     err2(k) = sqrt(error2(k));
771     // Displacement H1 in space l-infinity
772     err3(k) = sqrt(error3(k));
773     // Fluid velocity L2 in space l-infinity in time
774     err5(k) = sqrt(error5(k));
775     // Transport errors
776     err81(k) = sqrt(error81(k)/abs81(k));
777     err82(k) = sqrt(error82(k));
778
779     //   If non-relative errors are needed
780     //  err1(k) = sqrt(error1(k)/1.0);
781     //   Darcy pressure L2 in space l-infinity in time
782     //  err2(k) = sqrt(error2(k));
783     //   Displacement H1 in space l-infinity
784     //  err3(k) = sqrt(error3(k)/1.0);
785     //   Darcy velocity L2 in space L2 in time
786     //  err4(k) = sqrt(error4(k)/1.0);
```

```
787     //   Fluid pressure L2 is space L2 in time
788     //  err7(k) = sqrt(error7(k)/1.0);
789     //   Fluid velocity L2 in space l-infinity in time
790     //  err5(k) = sqrt(error5(k));
791
792     //   Lagrange mult
793     //  err6(k) = sqrt(error6(nMeshes-k-1));
794
795     if (k == 0){
796         rate1(k) = 0.0;
797         rate2(k) = 0.0;
798         rate3(k) = 0.0;
799         rate4(k) = 0.0;
800         rate5(k) = 0.0;
801         rate7(k) = 0.0;
802         rate81(k) = 0.0;
803         rate82(k) = 0.0;
804     }
805     else{
806         rate1(k) = log(err1(k-1)/err1(k))/log(2.0);
807         rate2(k) = log(err2(k-1)/err2(k))/log(2.0);
808         rate3(k) = log(err3(k-1)/err3(k))/log(2.0);
809         rate4(k) = log(err4(k-1)/err4(k))/log(2.0);
810         rate5(k) = log(err5(k-1)/err5(k))/log(2.0);
811         rate7(k) = log(err7(k-1)/err7(k))/log(2.0);
812         rate81(k) = log(err81(k-1)/err81(k))/log(2.0);
813         rate82(k) = log(err82(k-1)/err82(k))/log(2.0);
814     }
815 }
816
817 // Output errors
818 if(converg){
819     matrix errors=[[(err1), (rate1), (err2), (rate2), (err3), (rate3), (err4), (rate4),
820                     (err5), (rate5), (err7), (rate7)]];
821     {
822         ofstream errOut("errorsrates.txt");
823         errOut<<errors;
824     }
825     matrix errors1=[[(error1), (error2), (error3), (error4), (error5), (error7)]];
826     {
827         ofstream errout("errors.txt");
828         errout << errors1;
829     }
830 }
831
832 // Output interface residuals:
833 if(intresid){
834     matrix flux=[[cond13left]];
835     {
836         ofstream fluxOut("flux.txt");
837         fluxOut<<flux;
838     }
839 }
840
841 // Print results
842 cout << "=============================================================================" << endl;
843 cout << "Errors and rates" << endl;
844 cout << "|u_f(H1)|" << "    rate    "
845 << "|p_f(L2)|" << " rate    "
846 << "|u_p(L2)|" << " rate    "
847 << "|p_p(L2)|" << " rate    "
848 << "|eta(H1)|" << " rate    "
849 << endl;
850 for (int i=0; i<err1.n; i++){
851     // Stokes velocity
852     cout.precision(3);
853     cout.scientific << err1[i] << " ";
854     cout.precision(1);
```

```
855     cout.fixed << rate1[i] << " ";
856     // Stokes pressure
857     cout.precision(3);
858     cout.scientific << err7[i] << " ";
859     cout.precision(1);
860     cout.fixed << rate7[i] << " ";
861     // Darcy velocity
862     cout.precision(3);
863     cout.scientific << err4[i] << " ";
864     cout.precision(1);
865     cout.fixed << rate4[i] << " ";
866     // Darcy pressure
867     cout.precision(3);
868     cout.scientific << err2[i] << " ";
869     cout.precision(1);
870     cout.fixed << rate2[i] << " ";
871     // Displacement
872     cout.precision(3);
873     cout.scientific << err3[i] << " ";
874     cout.precision(1);
875     cout.fixed << rate3[i] << " ";
876     // Transport L2-L2
877     cout.precision(3);
878     cout.scientific << err81[i] << "    ";
879     cout.precision(1);
880     cout.fixed << rate81[i] << "    ";
881     // Transport L8-L2
882     cout.precision(3);
883     cout.scientific << err82[i] << "    ";
884     cout.precision(1);
885     cout.fixed << rate82[i] << "    ";
886     cout << endl;
887 }
```

We also briefly discuss how to modify the code to model non-Newtonian flow. To avoid duplication, we only focus on the part of the code corresponding to the time loop, where we now assemble the nonlinear terms and use Picard iterations. The setup is as in the convergence studies for the non-Newtonian model.

Listing A.0.2: Part of FreeFem++ code to account for nonlinear viscosity

```
1  //Macro for Cross model in both regions
2  macro nuF(ax,ay) (nuFinf + (nuF0-nuFinf)/(1+Kf*sqrt(dx(ax)^2 + dy(ay)^2
3                      +0.5*(dy(ax)+dx(ay))^2))) //
4  macro nuP(ax,ay) (nuPinf + (nuP0-nuPinf)/(1+Kp*sqrt(ax^2 + ay^2))) //
5
6  // Viscosity parameters
7  func nuF0   = 10.0;
8  func nuFinf = 1.0;
9  func Kf     = 1.0;
10
11 func nuP0   = 10.0;
12 func nuPinf = 1.0;
13 func Kp     = 1.0;
14 func mc     = 1.0;
15
16 ..................................
17
18     /*
19     * Time loop
20     */
21     for (int k=1;k<=NN;++k){
22         ..................................
23
24         // Parameters for Picard iterations
```

```
25          real tol    = 1e-6;
26          int maxiter = 50;
27          int iter    = 0;
28          real epsln  = 10;
29
30          // Picard iterations
31          while(epsln > tol && iter < maxiter){
32              // Assemble nonlinear Stokes term
33              varf AFsum([uFx,uFy,pF],[vFx,vFy,wF])
34                          = int2d(ThF)(nuF(uFprevx,uFprevy)*(dx(uFx)*dx(vFx)
35                          + dx(uFy)*dx(vFy)+dy(uFx)*dy(vFx)+dy(uFy)*dy(vFy)));
36              matrix AF = AFsum(VFh,VFh);
37              matrix FF = ABJS1 + AF + BPF + BPFT + MASSF;
38
39              // Assemble nonlinear Darcy term
40              varf AQsum([uPx,uPy,pP],[vPx,vPy,wP]) = int2d(ThS)(nuP(uPprevx,uPprevy)
41                          *cdot(kappaxx*uPx,kappayy*uPy,vPx,vPy))
42                          + on(21,23,uPy=0,uPx=0) + on(22,uPx=1,uPy=0);
43
44              matrix AQ = AQsum(VMh,VMh);
45              matrix MM = AQ + BPQT + BPQ + MASSP;
46
47              // Assemble final matrix
48              matrix mono = [[SS, SM , SF],
49                             [ MS, MM , 0  ],
50                             [ FS, 0  , FF ]];
51
52              // Solve flow problem
53              set(mono,solver=sparsesolver);
54              xx = mono^-1 * b;
55              [xxs1mono,xxm1mono,xxfmono] = xx;
56
57              uFx[]  = xxfmono;
58              uPx[]  = xxm1mono;
59              etax[] = xxs1mono;
60
61              // Compute residual
62              epsln = int2d(ThF)((uFx -uFprevx)^2 + (uFy - uFprevy)^2)
63                    + int2d(ThS)((uPx -uPprevx)^2 + (uPy - uPprevy)^2);
64
65              xxold      = xx;
66              uFprevx[]  = uFx[];
67              uPprevx[]  = uPx[];
68
69              // Print residual
70              cout << "Epsilon: " << epsln << endl;
71          }
72      }
```

BIBLIOGRAPHY

[1] G. Acosta, T. Apel, R. Durán, and A. Lombardi. Error estimates for Raviart-Thomas interpolation of any order on anisotropic tetrahedra. *Mathematics of Computation*, 80(273):141–163, 2011.

[2] I. Ambartsumyan, E. Khattatov, I. Yotov, and P. Zunino. Simulation of flow in fractured poroelastic media: a comparison of different discretization approaches. In *Finite difference methods, theory and applications*, volume 9045 of *Lecture Notes in Comput. Sci.*, pages 3–14. Springer, Cham, 2015.

[3] T. Arbogast, G. Pencheva, M. F. Wheeler, and I. Yotov. A multiscale mortar mixed finite element method. *Multiscale Model. Simul.*, 6(1):319–346, 2007.

[4] T. Arbogast and M. F. Wheeler. A characteristics-mixed finite element method for advection-dominated transport problems. *SIAM J. Numer. Anal.*, 32(2):404–424, 1995.

[5] D. N. Arnold. An interior penalty finite element method with discontinuous elements. *SIAM J. Numer. Anal.*, 19(4):742–760, 1982.

[6] D. N. Arnold, F. Brezzi, B. Cockburn, and L. D. Marini. Unified analysis of discontinuous Galerkin methods for elliptic problems. *SIAM J. Numer. Anal.*, 39(5):1749–1779, 2001/02.

[7] S. Badia, A. Quaini, and A. Quarteroni. Coupling Biot and Navier-Stokes equations for modelling fluid-poroelastic media interaction. *J. Comput. Phys.*, 228(21):7986–8014, 2009.

[8] G. A. Baker. Finite element methods for elliptic equations using nonconforming elements. *Math. Comp.*, 31(137):45–59, 1977.

[9] S. Basting, P. Birken, E. H. Brummelen, S. Canic, C. Colciago, S. Deparis, D. Forti, R. Glowinski, J. Hoffman, D. Jodlbauer, et al. *Fluid-Structure Interaction: Modeling, Adaptive Discretisations and Solvers*, volume 20. Walter de Gruyter GmbH & Co KG, 2017.

[10] C. E. Baumann and J. T. Oden. A discontinuous *hp* finite element method for convection-diffusion problems. *Comput. Methods Appl. Mech. Engrg.*, 175(3-4):311–341, 1999.

[11] Y. Bazilevs, K. Takizawa, and T. E. Tezduyar. *Computational fluid-structure interaction: methods and applications*. John Wiley & Sons, 2013.

[12] G. S. Beavers and D. D. Joseph. Boundary conditions at a naturally impermeable wall. *J. Fluid. Mech*, 30:197–207, 1967.

[13] M. Biot. General theory of three-dimensional consolidation. *J. Appl. Phys.*, 12:155–164, 1941.

[14] R. B. Bird, R. C. Armstrong, O. Hassager, and C. F. Curtiss. *Dynamics of polymeric liquids*, volume 1. Wiley New York, 1977.

[15] D. Boffi, F. Brezzi, and M. Fortin. *Mixed finite element methods and applications*, volume 44 of *Springer Series in Computational Mathematics*. Springer, Heidelberg, 2013.

[16] D. Boffi and L. Gastaldi. Analysis of finite element approximation of evolution problems in mixed form. *SIAM J. Numer. Anal.*, 42(4):1502–1526, 2004.

[17] K. Brenan, S. Campbell, and L. Petzold. *Numerical Solution of Initial-Value Problems in Differential-Algebraic Equations*. 1995.

[18] F. Brezzi, D. Boffi, L. Demkowicz, R. G. Durán, R. S. Falk, and M. Fortin. *Mixed finite elements, compatibility conditions, and applications*. Springer, 2008.

[19] M. Bukac, I. Yotov, R. Zakerzadeh, and P. Zunino. Partitioning strategies for the interaction of a fluid with a poroelastic material based on a Nitsche's coupling approach. *Comput. Methods Appl. Mech. Engrg.*, 292:138–170, 2015.

[20] M. Bukac, I. Yotov, and P. Zunino. An operator splitting approach for the interaction between a fluid and a multilayered poroelastic structure. *Numer. Methods Partial Differential Equations*, 31(4):1054–1100, 2015.

[21] M. Bukac, I. Yotov, and P. Zunino. Dimensional model reduction for flow through fractures in poroelastic media. *ESAIM Math. Model. Numer. Anal.*, http://dx.doi.org/10.1051/m2an/2016069, 2016.

[22] H.-J. Bungartz and M. Schäfer. *Fluid-structure interaction: modelling, simulation, optimisation*, volume 53. Springer Science & Business Media, 2006.

[23] E. Burman and M. A. Fernández. Stabilization of explicit coupling in fluid-structure interaction involving fluid incompressibility. *Comput. Methods Appl. Mech. Engrg.*, 198(5-8):766–784, 2009.

[24] E. Burman and M. A. Fernández. Explicit strategies for incompressible fluid-structure interaction problems: Nitsche type mortaring versus Robin-Robin coupling. *Internat. J. Numer. Methods Engrg.*, 97(10):739–758, 2014.

[25] T. Carraro, C. Goll, A. Marciniak-Czochra, and A. Mikelić. Pressure jump interface law for the Stokes-Darcy coupling: confirmation by direct numerical simulations. *J. Fluid Mech.*, 732:510–536, 2013.

[26] S. Caucao, G. N. Gatica, R. Oyarzúa, and I. Sebestová. A fully-mixed finite element method for the Navier-Stokes/Darcy coupled problem with nonlinear viscosity. *J. Numer. Math.*, 25(2):55–88, 2017.

[27] Y. I. Cho and K. R. Kensey. Effects of the non-newtonian viscosity of blood on flows in a diseased arterial vessel. part 1: Steady flows. *Biorheology*, 28(3-4):241–262, 1991.

[28] S.-S. Chow and G. F. Carey. Numerical approximation of generalized Newtonian fluids using Powell–Sabin–Heindl elements: I. Theoretical estimates. *Internat. J. Numer. Methods Fluids*, 41(10):1085–1118, 2003.

[29] P. Ciarlet. *The finite element method for elliptic problems*, volume 4. North Holland, 1978.

[30] B. Cockburn and C. Dawson. Approximation of the velocity by coupling discontinuous Galerkin and mixed finite element methods for flow problems. *Comput. Geosci.*, 6(3-4):505–522, 2002. Locally conservative numerical methods for flow in porous media.

[31] B. Cockburn and C.-W. Shu. The local discontinuous Galerkin method for time-dependent convection-diffusion systems. *SIAM J. Numer. Anal.*, 35(6):2440–2463, 1998.

[32] C. D'Angelo and A. Scotti. A mixed finite element method for Darcy flow in fractured porous media with non-matching grids. *ESAIM: Math. Model. Numer. Anal.*, 46(2):465–489, 2012.

[33] B. L. Darlow and M. F. Wheeler. Interior penalty Galerkin procedures for miscible displacement problems in porous media. In *Computational methods in nonlinear mechanics (Proc. Second Internat. Conf., Univ. Texas, Austin, Tex., 1979)*, pages 485–506. North-Holland, Amsterdam-New York, 1980.

[34] M. Dauge. *Elliptic boundary value problems on corner domains*, volume 1341 of *Lecture Notes in Mathematics*. Springer-Verlag, Berlin, 1988. Smoothness and asymptotics of solutions.

[35] C. Dawson, S. Sun, and M. F. Wheeler. Compatible algorithms for coupled flow and transport. *Comput. Methods Appl. Mech. Engrg.*, 193(23-26):2565–2580, 2004.

[36] C. N. Dawson, T. F. Russell, and M. F. Wheeler. Some improved error estimates for the modified method of characteristics. *SIAM J. Numer. Anal.*, 26(6):1487–1512, 1989.

[37] C. N. Dawson and M. F. Wheeler. An operator-splitting method for advection-diffusion-reaction problems. In *The mathematics of finite elements and applications, VI (Uxbridge, 1987)*, pages 463–482. Academic Press, London, 1988.

[38] C. N. Dawson and M. F. Wheeler. Time-splitting methods for advection-diffusion-reaction equations arising in contaminant transport. In *ICIAM 91 (Washington, DC, 1991)*, pages 71–82. SIAM, Philadelphia, PA, 1992.

[39] M. Discacciati, E. Miglio, and A. Quarteroni. Mathematical and numerical models for coupling surface and groundwater flows. *Appl. Numer. Math.*, 43(1-2):57–74, 2002.

[40] S. Domínguez, G. N. Gatica, A. Márquez, and S. Meddahi. A primal-mixed formulation for the strong coupling of quasi-Newtonian fluids with porous media. *Adv. Comput. Math.*, 42(3):675–720, 2016.

[41] J. Donea, S. Giuliani, and J.-P. Halleux. An arbitrary lagrangian-eulerian finite element method for transient dynamic fluid-structure interactions. *Computer methods in applied mechanics and engineering*, 33(1-3):689–723, 1982.

[42] R. Durán. Error analysis in L^p, $1 \leq p \leq \infty$, for mixed finite element methods for linear and quasi-linear elliptic problems. *ESAIM: Mathematical Modelling and Numerical Analysis*, 22(3):371–387, 1988.

[43] A. Ern and J.-L. Guermond. *Theory and practice of finite elements*, volume 159 of *Applied Mathematical Sciences*. Springer-Verlag, New York, 2004.

[44] V. J. Ervin, E. W. Jenkins, and S. Sun. Coupled generalized nonlinear Stokes flow with flow through a porous medium. *SIAM J. Numer. Anal.*, 47(2):929–952, 2009.

[45] V. J. Ervin, E. W. Jenkins, and S. Sun. Coupling nonlinear Stokes and Darcy flow using mortar finite elements. *Appl. Numer. Math.*, 61(11):1198–1222, 2011.

[46] L. Formaggia, A. Quarteroni, and A. Veneziani. *Cardiovascular Mathematics: Modeling and simulation of the circulatory system*, volume 1. Springer Science & Business Media, 2010.

[47] N. Frih, V. Martin, J. E. Roberts, and A. Saada. Modeling fractures as interfaces with nonmatching grids. *Comput. Geosci.*, 16(4):1043–1060, 2012.

[48] N. Frih, J. E. Roberts, and A. Saada. Modeling fractures as interfaces: a model for Forchheimer fractures. *Comput. Geosci.*, 12(1):91–104, 2008.

[49] A. Fumagalli and A. Scotti. Numerical modelling of multiphase subsurface flow in the presence of fractures. *Commun. Appl. Ind. Math.*, 3(1):e–380, 23, 2012.

[50] G. P. Galdi. *An introduction to the mathematical theory of the Navier-Stokes equations: Steady-state problems*. Springer Science & Business Media, 2011.

[51] G. P. Galdi and R. Rannacher, editors. *Fundamental trends in fluid-structure interaction*, volume 1 of *Contemporary Challenges in Mathematical Fluid Dynamics and Its Applications*. World Scientific Publishing Co. Pte. Ltd., Hackensack, NJ, 2010.

[52] J. Galvis and M. Sarkis. Non-matching mortar discretization analysis for the coupled Stokes-Darcy equations. *Electronic Transactions on Numerical Analysis*, 26:350–384, 2007.

[53] B. Ganis and I. Yotov. Implementation of a mortar mixed finite element method using a multiscale flux basis. *Comput. Methods Appl. Mech. Engrg.*, 198(49-52):3989–3998, 2009.

[54] V. Girault and B. Rivière. DG approximation of coupled Navier-Stokes and Darcy equations by Beaver-Joseph-Saffman interface condition. *SIAM J. Numer. Anal.*, 47(3):2052–2089, 2009.

[55] V. Girault, D. Vassilev, and I. Yotov. Mortar multiscale finite element methods for Stokes-Darcy flows. *Numer. Math.*, 127(1):93–165, 2014.

[56] V. Girault, M. F. Wheeler, B. Ganis, and M. E. Mear. A lubrication fracture model in a poro-elastic medium. *Math. Models Methods Appl. Sci.*, 25(4):587–645, 2015.

[57] V. Girault, M. F. Wheeler, B. Ganis, and M. E. Mear. A lubrication fracture model in a poro-elastic medium. *Mathematical Models and Methods in Applied Sciences*, 25(04):587–645, 2015.

[58] B. Guerciotti and C. Vergara. Computational comparison between newtonian and non-newtonian blood rheologies in stenotic vessels. In *Biomedical Technology*, pages 169–183. Springer, 2018.

[59] F. Hecht. New development in FreeFem++. *J. Numer. Math.*, 20(3-4):251–265, 2012.

[60] T. J. Hughes, W. K. Liu, and T. K. Zimmermann. Lagrangian-eulerian finite element formulation for incompressible viscous flows. *Computer methods in applied mechanics and engineering*, 29(3):329–349, 1981.

[61] W. Jäger, A. Mikelić, and N. Neuss. Asymptotic analysis of the laminar viscous flow over a porous bed. *SIAM J. Sci. Comput.*, 22(6):2006–2028, 2000.

[62] J. Janela, A. Moura, and A. Sequeira. A 3D non-Newtonian fluid–structure interaction model for blood flow in arteries. *J. Comput. Appl. Math.*, 234(9):2783–2791, 2010.

[63] J. Kovacik. Correlation between Young's modulus and porosity in porous materials. *Journal of materials science letters*, 18(13):1007–1010, 1999.

[64] W. J. Layton, F. Schieweck, and I. Yotov. Coupling fluid flow with porous media flow. *SIAM J. Numer. Anal.*, 40(6):2195–2218, 2003.

[65] S. Lee, A. Mikelić, M. F. Wheeler, and T. Wick. Phase-field modeling of proppant-filled fractures in a poroelastic medium. *Comput. Methods Appl. Mech. Engrg.*, 312:509–541, 2016.

[66] M. Lesinigo, C. D'Angelo, and A. Quarteroni. A multiscale Darcy–Brinkman model for fluid flow in fractured porous media. *Numer. Math.*, 117(4):717–752, 2011.

[67] X. Lopez, P. Valvatne, and M. Blunt. Predictive network modeling of single-phase non-Newtonian flow in porous media. *Journal of colloid and interface science*, 264(1):256–265, 2003.

[68] V. Martin, J. Jaffre, and J. E. Roberts. Modeling fractures and barriers as interfaces for flow in porous media. *SIAM J. Sci. Comput.*, 26(5):1667–1691, 2005.

[69] T. P. Mathew. *Domain decomposition and iterative refinement methods for mixed finite element discretizations of elliptic problems*. PhD thesis, Courant Institute of Mathematical Sciences, New York University, 1989. Tech. Rep. 463.

[70] A. Mikelić, M. F. Wheeler, and T. Wick. Phase-field modeling of a fluid-driven fracture in a poroelastic medium. *Comput. Geosci.*, 19(6):1171–1195, 2015.

[71] F. A. Morales and R. E. Showalter. The narrow fracture approximation by channeled flow. *J. Math. Anal. Appl.*, 365(1):320–331, 2010.

[72] F. A. Morales and R. E. Showalter. A Darcy-Brinkman model of fractures in porous media. *J. Math. Anal. Appl.*, 452(2):1332–1358, 2017.

[73] J. Necas, J. Málek, M. Rokyta, and M. Ruzicka. *Weak and measure-valued solutions to evolutionary PDEs*, volume 13. CRC Press, 1996.

[74] J. T. Oden, I. Babuska, and C. E. Baumann. A discontinuous *hp* finite element method for diffusion problems. *J. Comput. Phys.*, 146(2):491–519, 1998.

[75] R. G. Owens and T. N. Phillips. *Computational rheology*, volume 14. World Scientific, 2002.

[76] J. R. A. Pearson and P. M. J. Tardy. Models for flow of non-Newtonian and complex fluids through porous media. *J. non-Newton. fluid mech.*, 102(2):447–473, 2002.

[77] M. Renardy and R. C. Rogers. *An introduction to partial differential equations*, volume 13. Springer Science & Business Media, 2006.

[78] T. Richter. *Fluid-structure Interactions: Models, Analysis and Finite Elements*, volume 118. Springer, 2017.

[79] B. Riviere. Discontinuous Galerkin methods for solving the miscible displacement problem in porous media. 2001.

[80] B. Rivière, M. F. Wheeler, and V. Girault. Improved energy estimates for interior penalty, constrained and discontinuous Galerkin methods for elliptic problems. I. *Comput. Geosci.*, 3(3-4):337–360 (2000), 1999.

[81] B. Rivière, M. F. Wheeler, and V. Girault. A priori error estimates for finite element methods based on discontinuous approximation spaces for elliptic problems. *SIAM J. Numer. Anal.*, 39(3):902–931, 2001.

[82] B. Rivière and I. Yotov. Locally conservative coupling of Stokes and Darcy flows. *SIAM J. Numer. Anal.*, 42(5):1959–1977, 2005.

[83] P. G. Saffman. On the boundary condition at the surface of a porous media. *Stud. Appl. Math., L*, (2):93–101, 1971.

[84] D. Sandri. Sur l'approximation numérique des écoulements quasi-newtoniens dont la viscosité suit la loi puissance ou la loi de Carreau. *RAIRO Modél. Math. Anal. Numér.*, 27(2):131–155, 1993.

[85] L. R. Scott and S. Zhang. Finite element interpolation of nonsmooth functions satisfying boundary conditions. *Math. Comp.*, 54(190):483–493, 1990.

[86] R. Scott and S. Zhang. Finite element interpolation of nonsmooth functions satisfying boundary conditions. *Mathematics of Computation*, 54(190):483–493, 1990.

[87] R. E. Showalter. Poroelastic filtration coupled to Stokes flow. In *Control theory of partial differential equations*, volume 242 of *Lect. Notes Pure Appl. Math.*, pages 229–241. Chapman & Hall/CRC, Boca Raton, FL, 2005.

[88] R. E. Showalter. Nonlinear degenerate evolution equations in mixed formulation. *SIAM J. Math. Anal.*, 42(5):2114–2131, 2010.

[89] R. E. Showalter. *Monotone operators in Banach space and nonlinear partial differential equations*, volume 49. American Mathematical Soc., 2013.

[90] S. Shuyu and M. F. Wheeler. Mesh adaptation strategies for discontinuous galerkin methods applied to reactive transport problems. 2004.

[91] S. Sun. *Discontinuous Galerkin methods for reactive transport in porous media*. ProQuest LLC, Ann Arbor, MI, 2003. Thesis (Ph.D.)–The University of Texas at Austin.

[92] S. Sun, B. Rivière, and M. F. Wheeler. A combined mixed finite element and discontinuous Galerkin method for miscible displacement problem in porous media. In *Recent progress in computational and applied PDEs (Zhangjiajie, 2001)*, pages 323–351. Kluwer/Plenum, New York, 2002.

[93] C. Taylor and P. Hood. A numerical solution of the Navier-Stokes equations using the finite element technique. *Computers & Fluids*, 1(1):73–100, 1973.

[94] D. Vassilev, C. Wang, and I. Yotov. Domain decomposition for coupled Stokes and Darcy flows. *Comput. Methods Appl. Mech. Engrg.*, 268:264–283, 2014.

[95] M. F. Wheeler. An elliptic collocation-finite element method with interior penalties. *SIAM J. Numer. Anal.*, 15(1):152–161, 1978.

[96] X. Xie, J. Xu, and G. Xue. Uniformly-stable finite element methods for Darcy-Stokes-Brinkman models. *J. Comput. Math.*, 26(3):437–455, 2008.

[97] S.-Y. Yi. Convergence analysis of a new mixed finite element method for Biot's consolidation model. *Numer. Methods Partial Differential Eq.*, 30(4):1189–1210, 2014.